DESIGN, SYNTHESIS, AND BIOLOGICAL INVESTIGATION OF NEW PEPTIDES AND PEPTIDOMIMETICS OF COSMECEUTICAL INTEREST

DOCTORAL DISSERTATION
Patrycja Ledwoń

Supervisors:

Prof. Rafał Latajka
Wroclaw University of Science and Technology
Faculty of Chemistry
Department of Bioorganic Chemistry

Prof. Paolo Rovero
University of Florence
Department of NEUROFARBA
Interdepartmental Research Unit of Peptide and Protein Chemistry and Biology

Thesis in cotutelle prepared in the framework of the collaboration between Wroclaw University of Science and Technology and University of Florence (XXXV Ciclo)

Politechnika Wrocławska

February 2023

Wrocław University of Science and Technology

Uniwersytet Wrocławski

WROCŁAW UNIVERSITY OF ENVIRONMENTAL AND LIFE SCIENCES

Table of contents

LIST OF ABBREVIATIONS

α-MSH	–	α-melanocyte-stimulating hormone
aa	–	Amino acid
Ac₂O	–	Acetic anhydride
ACN	–	Acetonitrile
ADAM	–	A disintegrin and metalloproteinase
ADAMTS	–	A disintegrin and metalloproteinase (ADAM) with thrombospondin motifs
APEC	–	Antibody peptide epitope conjugates
CAS	–	Chemical Abstracts Service number
CatG	–	Cathepsin G
CD	–	Circular Dichroism
CI	–	Confidence interval
COSY	–	Correlated Spectroscopy
CTLP	–	Chymotrypsin-like proteinase
DCM	–	Dichloromethane
DIPEA	–	*N,N′*-Diisopropylethylamine
DMF	–	*N,N′*-Dimethylformamide
DMSO	–	Dimethyl sulfoxide
DQ	–	Dopaquinone
EC	–	Enzyme control
ECM	–	Extracellular matrix
EDT	–	1,2-Ethanedithiol
EDTA	–	Ethylenediaminetetraacetic acid
ELISA	–	Enzyme-linked Immunosorbent Assay
eq.	–	Molar equivalent
ESI-MS	–	Electrospray Ionization Mass Spectrometry
Et	–	Ethyl
EtOH	–	Ethanol
FBS	–	Fetal bovine serum
FDA	–	Food and Drug Administration
Fmoc	–	Fluorenylmethoxycarbonyl protecting group
HBTU	–	2-(1*H*-benzotriazol-1-yl)-1,1,3,3-tetramethyluronium hexafluorophosphate, Hexafluorophosphate benzotriazole tetramethyl uronium
HES	–	Hydroxyethylstarch
HLE	–	Human leukocyte elastase
HNE	–	Human neutrophil elastase
HPLC	–	High Performance Liquid Chromatography
HSF	–	Human skin fibroblast elastase
hTYR	–	Human tyrosinase
IC	–	Inhibitor control
INCI	–	International Nomenclature Cosmetic Ingredient
IUPAC	–	International Union of Pure and Applied Chemistry
KA	–	Kojic acid
LC-MS	–	Liquid Chromatography coupled with Mass Spectrometry
L-DOPA	–	L-3,4-dihydroxyphenylalanine, levodopa
LOX	–	Lysyl oxidase
Me	–	Methyl
MeOH	–	Methanol
MM	–	Molecular Modeling
MMPs	–	Matrix metalloproteases
MS	–	Mass Spectrometry
MSACK	–	Methoxysuccinyl-Ala-Ala-Pro-Ala chloromethyl ketone

MT-MMP	–	Membrane-bound MMP
Mtt	–	4-Methyltrityl
MTT	–	3-(4,5-Dimethyl-2-thiazolyl)-2,5-diphenyl-2H- tetrazolium bromide, Thiazolyl blue tetrazolium bromide
mTYR	–	Mushroom tyrosinase
M$_W$	–	Molecular weight
n.a.	–	Data not available
n/a	–	Not applicable
NE	–	Neutrophil elastase
NEP	–	Neprilysin
NMM	–	N-Methylmorpholine
NMR	–	Nuclear Magnetic Resonance
NPLT	–	N-phenetylphosphonyl-leucyl-tryptophane
PDB	–	Protein Data Bank
PEG	–	Poly[ethylene glycol]
Ph	–	Phenyl
PPE	–	Porcine pancreas elastase
RCL	–	Reactive center loop
RP	–	Reversed-phase
RP-HPLC	–	Reversed-phase High Performance Liquid Chromatography
S-A1	–	Serpin A1
SAR	–	Structure-activity relationship
SDS	–	Sodium dodecyl sulfate
Serpin(s)	–	Serine protease inhibitor(s)
SI	–	Supplementary information section
SLS	–	Sodium lauryl sulphate
SNAP	–	Synaptosome-associated protein
SNARE	–	Soluble N-ethylmaleimide-sensitive factor activating protein receptor
SPCK	–	MeOSuc-Ala-Ala-Pro-Val-chloromethylketone, MeOSuc-AAPV-CMK
SPPS	–	Solid-phase Peptide Synthesis
tBu	–	*Tert*-butyl group
TFA	–	Trifluoroacetic acid
TIS	–	Triisopropylsilane
TOCSY	–	Total Correlation Spectroscopy
TSC(s)	–	Thiosemicarbazone(s)
UHPLC	–	Ultra-High Performance Liquid Chromatography
UV	–	Ultraviolet
VAMP	–	Vesicle-associated membrane protein

LIST OF FIGURES

LIST OF SCHEMES

LIST OF TABLES

LIST OF DISCUSSED COMPOUNDS*

A	–	4-Methylpiperidine
B	–	Pyrrolidine
C	–	Morpholine
D	–	*N*-Ethylisopropylamine
1	–	Potassium cyanohydroxyamate
2	–	*N*-hydroxy-3-(hydroxyamino)-3-iminopropanamide
3	–	4,6-dimethylisoxazolo[3,4-*b*]pyridin-3(1*H*)-one
4	–	8-carboxy-4',5,7-trimethyl-3H-2λ^5-spiro[[1,2,4]triazolo[4,3-a]pyridine-2,1'-piperidin]-2-ylium (derivative with **A**)
4a	–	Fmoc-Lys[N$^\varepsilon$**(4)**]-OH
5	–	8-carboxy-5,7-dimethyl-3*H*-2λ^5-spiro[[1,2,4]triazolo[4,3-*a*]pyridine-2,1'-pyrrolidin]-2-ylium (derivative with **B**)
5a	–	Fmoc-Lys[N$^\varepsilon$**(5)**]-OH
6	–	8-carboxy-5,7-dimethyl-3*H*-2λ^5-spiro[[1,2,4]triazolo[4,3-a]pyridine-2,4'-morpholin]-2-ylium (derivative with **C**)
6a	–	Fmoc-Lys[N$^\varepsilon$**(6)**]-OH
7	–	8-carboxy-2-ethyl-5,7-dimethyl-2-(propan-2-yl)-2*H*,3*H*-[1,2,4]triazolo[4,3-*a*]pyridin-2-ium (derivative with **D**)
7a	–	Fmoc-Lys[N$^\varepsilon$**(7)**]-OH
8	–	Ac-MGKVV-NH$_2$
9	–	Ac-PGKVV-NH$_2$
10	–	**3**-PGKVV-NH$_2$
11	–	**4**-MGKVV-NH$_2$
12	–	**5**-MGKVV-NH$_2$
13	–	**6**-MGKVV-NH$_2$
14	–	**7**-MGKVV-NH$_2$
15	–	**4**-PGKVV-NH$_2$
16	–	**5**-PGKVV-NH$_2$
17	–	**6**-PGKVV-NH$_2$
18	–	**7**-PGKVV-NH$_2$
19	–	Ac-MGK[N$^\varepsilon$**(4)**]VV-NH$_2$
20	–	Ac-MGK[N$^\varepsilon$**(5)**]VV-NH$_2$
21	–	Ac-MGK[N$^\varepsilon$**(6)**]VV-NH$_2$
22	–	Ac-MGK[N$^\varepsilon$**(7)**]VV-NH$_2$
23	–	Ac-PGK[N$^\varepsilon$**(4)**]VV-NH$_2$
24	–	Ac-PGK[N$^\varepsilon$**(5)**]VV-NH$_2$
25	–	Ac-PGK[N$^\varepsilon$**(6)**]VV-NH$_2$
26	–	Ac-PGK[N$^\varepsilon$**(7)**]VV-NH$_2$
27-42	–	16 derivatives of (2*E*)-2-[1-(4-bromophenyl)ethylidene]hydrazine-1-carbothioamide
43	–	4-[(*E*)-(2-carbamothioylhydrazinylidene)methyl]benzoic acid
44	–	2-{3-[(*E*)-(2-carbamothioylhydrazinylidene)(phenyl)methyl]phenyl}propanoic acid
45	–	4-[(1*E*)-1-(2-carbamothioylhydrazinylidene)ethyl]benzoic acid
46	–	Ac-FFY-OH
47	–	Ac-FYY-OH
48	–	Ac-FWY-OH
49	–	TSC**43**-FFY-OH
50	–	TSC**43**-FYY-OH
51	–	TSC**43**-FWY-OH
52	–	TSC**44**-FFY-OH
53	–	TSC**44**-FYY-OH
54	–	TSC**44**-FWY-OH
55	–	TSC**45**-FFY-OH
56	–	TSC**45**-FYY-OH
57	–	TSC**45**-FWY-OH

*Compounds marked with gray background were purchased (**A-D**) or provided (**27-45**).
Other compounds were synthesized and purified by the Author for the purpose of this thesis.

ABSTRACT

IN ENGLISH

Cosmeceuticals, i.e., cosmetic products with active ingredients possessing the scientifically proven and thoroughly evaluated biological activity, are becoming progressively more common on the market. Consumer awareness has prompted manufacturers to create formulas with a valuable composition, good permeability through the skin, and prolonged stability. Peptides, short chains of amino acids, are good candidates for active ingredients. Due to the ease of their modification, uncomplicated synthesis, and the possibility of giving them the desired properties, they are becoming frequent ingredients in cosmeceuticals. This doctoral dissertation discusses two enzymes contributing to the appearance of signs of skin aging – elastase, responsible for the breakdown of collagen fibers, and tyrosinase – directly affecting the synthesis of melanin and skin discoloration. Design, synthesis, biological investigation, and molecular modeling of peptides and their conjugates with small organic molecules were discussed. *In vitro* studies of these compounds indicated inhibitors of the abovementioned enzymes, some of them with micromolar activity. The correlation between the structure of obtained compounds and their activity was discussed, and special attention was paid to the role of peptide conjugates in the design of biologically active compounds.

IN POLISH

Kosmeceutyki, czyli produkty kosmetyczne zawierające składniki aktywne o udowodnionej naukowo i ściśle przebadanej aktywności biologicznej, stają się coraz bardziej powszechne na rynku. Świadomość konsumentów skłoniła producentów do tworzenia produktów o wartościowym składzie, dobrej przenikalności przez skórę i przedłużonej stabilności. Peptydy jako krótkie łańcuchy aminokwasów są dobrymi kandydatami na składniki aktywne, a z uwagi na warianty ich modyfikacji, nieskomplikowaną syntezę i możliwość nadania im pożądanych właściwości, są coraz powszechniejszymi składnikami kosmeceutyków. W niniejszej rozprawie doktorskiej omówione zostały dwa enzymy przyczyniające się do pojawienia się oznak starzenia skóry – elastaza, odpowiedzialna za rozpad włókien kolagenowych oraz tyrozynaza – bezpośrednio wpływająca na syntezę melanin i wystąpienie przebarwień skórnych. Przedstawione zostały projektowanie, synteza, badania biologiczne i modelowanie

molekularne peptydów oraz ich koniugatów z małymi cząsteczkami organicznymi. Badania *in vitro* tych związków wskazały na inhibitory wymienionych enzymów, część z nich o aktywności mikromolowej. Omówiono korelację między strukturą cząsteczek a ich aktywnością oraz zwrócono szczególną uwagę na rolę koniugatów peptydowych w projektowaniu związków biologicznie aktywnych.

IN ITALIAN

I *prodotti cosmeceutici*, che esplicano un'attività biologica scientificamente provata e ampiamente testata, stanno diventando sempre più diffusi sul mercato. La consapevolezza dei consumatori ha spinto i produttori a creare formule con una composizione pregiata, una buona permeabilità attraverso la pelle e, infine, una stabilità prolungata. I peptidi, essendo catene corte di aminoacidi, sono buoni candidati per ingredienti attivi. Grazie alla possibilità di modificarli chimicamente, alla semplice sintesi e alla capacità di conferire loro le proprietà desiderate, stanno diventando ingredienti sempre più comuni nei prodotti cosmeceutici. L'obiettivo di questa tesi di dottorato è quello di discutere due enzimi che contribuiscono alla comparsa dei segni dell'invecchiamento cutaneo – l'elastasi, responsabile della degradazione delle fibre di collagene, e la tirosinasi – che influenza direttamente la sintesi della melanina e la comparsa di discromie cutanee. Vengono in essa presentate la progettazione, la sintesi, i saggi biologici e la modellazione molecolare dei peptidi e dei loro coniugati con piccole molecole organiche. Studi *in vitro* di questi composti hanno mostrato la loro capacità di agire come inibitori di questi enzimi, alcuni dei quali con attività micromolare. È discussa la correlazione tra la struttura delle molecole e la loro attività, con particolare attenzione al ruolo dei coniugati peptidici nella progettazione di composti biologicamente attivi.

Chapter 1: Introduction

Amino acids play a pivotal role in human bodies. Longer sequences of amino acids are called *peptides*, including oligopeptides and polypeptides, and finally *proteins*. Proteins stand for a part of each cell in the human body, including internal tissues, tendons, skin, hair, nails, and enzymes. The meaning of enzymes in our organisms is beyond words, and the importance of balanced enzyme activity has been known for years.[1,2] The improper activity of enzymes is called *hypoactivity* and *hyperactivity*, or *inactivity* and *overactivity*, respectively. For this reason, enzyme deficiencies cause a string of illnesses and disabilities. They may also provoke harmless, but esthetically noticeable changes in the superficies. Two examples of the enzymes responsible for such deviations are elastase and tyrosinase.

Elastase has a recognized importance in wrinkle formation and elastic fiber degeneration.[3] It has to be underlined that in the human skin we observe at least two types of elastase, neutrophil elastase (HNE; EC 3.4.21.37), and fibroblast elastase (HSF; EC 3.4.24.11) structurally identical to neprilysin. The first one is a classic serine protease, while the HSF has been characterized as metalloproteinase. Up to 2010, the structure and amino acid sequence of HSF were not known in detail, until Morisaki *et al.* proved the hypothesis that HSF is identical to neprilysin using immunoprecipitation and transfection methods.[4] However, both of these enzymes possess the ability to degrade fibrillar collagen. Well-known inhibitors of the collagen fibers degradation process were described in the review by Ledwoń *et al*. in 2021.[5] At the beginning of the 2000s Tsukahara *et al.* underlined the relevance of elastase inhibition in cosmeceutical applications.[6]

Tyrosinase belongs to the oxygen oxidoreductase family and is a copper-containing enzyme (EC 1.14.18.1).[7] It participates in melanogenesis process, where melanins – the pigments responsible for skin color – are produced. These biopolymers are synthesized in melanocytes, cells found in the basal layer of dermis, and then are secreted to keratinocytes. The intensity of melanogenesis determines the coloration of human skin and hair.[8] Nevertheless, because melanins can absorb UV light radiation and protect the skin, the overproduction of this pigment (hence, the tyrosinase overactivity) may lead to its accumulation and hyperpigmentation diseases. Freckles, age spots, and skin blemishing are good and common examples, but also melasma and melanoma are the consequences of uncontrolled melanin production.

In recent years, the skin-care products market has grown significantly according to the *Global Wellness Economy Monitor* data from 2018. *Cosmeceuticals* lie in a grey area between cosmetics and drugs, and despite their large use, they are not recognized by the Food and Drug Administration (FDA) to date.[9] The concept of beauty is linked to the model of young-looking skin, and this has led to the large spread of peptides in the anti-aging product.[10] External agents, such as smog, together with internal ones, such as stress, affect our skin cells' oxidative damage, resulting in skin aging. To adjust the skin biological clock, it is necessary to get and maintain a good balance between structural protein synthesis and degradation, and in fact most of the products act in this way, leading to the decrease of fine and age-induced wrinkles.[11] Particular attention should be paid to the association between topical care products and food supplements in which the name "peptide" became used to call frequently not well-identified hydrolysates. People today understood the importance of reading product labels and INCI lists, they look for information regarding the active principles used in cosmeceuticals, they are attracted to scientific explanations that could demonstrate the several claims used by the cosmetic industries. It should be clearly emphasized that cosmeceuticals, beside the cosmetics, contain highly concentrated active ingredients and are supported by scientific proofs. Only at these conditions the use of active ingredients (among which peptides) in cosmetic formula is acceptable.[12]

Chapter 2: Literature review

2.1 Peptides in cosmeceutical field

Peptides have a wide range of functions, with a variety of potential applications, starting from active pharmaceutical ingredients to pioneering nanomaterials.[13] Particularly, in recent years the cosmetic industry showed the enhanced interest toward peptides application as active ingredients in cosmeceuticals.[10,14] In fact, the Global Wellness Institute statistics from 2019 confirmed that the most relevant segment of the wellness economy stands for "Personal care, beauty & anti-aging" products.

Peptides started to take part of the cosmeceutical field in 1973, when Pickart proposed the synthetic peptide GHK able to enhance the synthesis of collagen.[15] Thanks to that, plenty of peptides of cosmeceutical interest have been developed in response to the market requests. Originally, peptides in cosmeceutical applications were used as carriers for larger molecules, thus enhancing their penetration through skin layers. A good example of that is indeed the Copper tripeptide GHK-Cu, a complex of copper ions (IUPAC name: copper (2*S*)-6-amino-2-[[(2*S*)-2-(2-azanidylacetyl)azanidyl-3-(1*H*-imidazol-4-yl)propanoyl]amino]hexanoate).[16,17] Nowadays, after the further development of this sector, cosmeceutical peptides can be divided into three major categories, e.g., neurotransmitter inhibitor peptides, carrier peptides, and signal peptides (**Table 1**). They will be briefly discussed below, mentioning the most relevant peptide sequences and the mechanism of their bioactivity. Due to the important role of peptides with direct inhibitory activity against enzymes involved in skin aging processes,[18] they will be discussed further in subchapters **2.5** and **2.8**. Examples of peptides and peptidomimetics as inhibitors of elastase and tyrosinase will be reported there in details.

Table 1. Commercially available cosmeceutical peptides divided into main categories.

CLASSIFICATION	PEPTIDE	COMMERCIAL NAME	MECHANISM OF ACTION
Neurotransmitter inhibitor peptides	**Acetyl hexapeptide-3** Ac-Glu-Glu-Met-Gln-Arg-Arg-NH$_2$	Argireline	inhibition of Ca^{2+}-dependent catecholamine release through the interrupted formation of SNARE complex[19]
	Pentapeptide-3 H-Gly-Pro-Arg-Pro-Ala-NH$_2$	Vialox	an antagonist of acetylcholine receptor, disables the function of nerves[20]
	Pentapeptide-18 H-Tyr-Ala-Gly-Phe-Leu-OH	Leuphasyl®	decline of acetylcholine secretion in synaptic clefts[21]
	Tripeptide-3 β-Ala-Pro-Dab-NH-benzyl × 2·AcOH	Syn®-Ake	reversible antagonist of muscular nicotinic acetylcholine receptors, prevents acetylcholine receptor binding[22]
	Acetyl Octapeptide-1/-3 Ac-Glu-Glu-Met-Gln-Arg-Arg-Ala-Asp-NH$_2$	SNAP-8™	declined release of glutamate, due to competitive inhibitory of SNAP-8 (mimicking SNAP-25) and interrupted formation of SNARE complex[23,24]
Carrier peptides	**Copper Tripeptide-1** (Cu) H-Gly-His-Lys-OH	n.a. *[a]*	cofactor in collagen and elastase formation; reduces the activity of MMPs and collagenase[16,17]
	Manganese Tripeptide-1 (Mn) H-Gly-His-Lys-OH	n.a.	*As above*[25]
Signal peptides	**Palmitoyl hexapeptide-12** Pal-Val-Gly-Val-Ala-Pro-Gly-OH	Biopeptide EL™	upregulates the activity of metalloproteinases, decreasing the synthesis of elastin and stimulating the production of collagen[26]
	Palmitoyl pentapeptide-3 Pal-Lys-Thr-Thr-Lys-Ser-OH	Matrixyl®	stimulates feedback regulation of new collagen synthesis and ECM proteins[27]
	Palmitoyl Tripeptide-1 Pal-Gly-His-Lys-OH	Biopeptide CL™	stimulates the synthesis of collagen and glycosaminoglycan (GAG)[28]
	Palmitoyl Tripeptide-5 Pal-Lys-Val-Lys-OH	Syn®-Coll	stimulates TGF-β, a growth factor, inducing collagen biosynthesis; inhibits the activity of matrix metalloproteases[29]
	Lipospondin Elaidyl-Lys-Phe-Lys	n.a.	stimulates TGF-β, a growth factor; fatty acid moiety is possibly inhibiting matrix metalloproteases[30]
	Hexapeptide-11 or **Pentamide-6** H-Pro-Val-Ala-Pro-Phe-Pro-OH	n.a.	downregulates cellular proteins (ATM and p53), protecting fibroblasts against oxidative stress[31]
	Tripeptide-10 citrulline n.a.	Decorinyl®	regulates collagen fibers diameter, increasing the quality of the endogenous collagen, without affecting its synthesis[32]
	PKEK H-Pro-Lys-Glu-Lys-OH	n.a.	decreases the expression of interleukin-6 and -8 (IL-6 and IL-8), α-melanocyte-stimulating hormone (α-MSH), and tumor necrosis factor-α; reduces the hyperpigmentation[33]

	GEKG H-Gly-Glu-Lys-Gly-OH	n.a.	stimulates the synthesis of collagen[34,35]
	SA1-III Ac-Met-Gly-Lys-Val-Val-Asn- Pro-Thr-Gln-Lys-NH$_2$	KP1	through a molecular mechanism based on inhibition of collagen degradation by proteases, modulates skin protein turnover[36,37]

[a] *n.a. – data not available.*

Neurotransmitter inhibitor peptides. Muscle cramps are, together with other various factors, the cause of fine lines and wrinkles. This kind of movement can be provoked both consciously and unknowingly and is always strictly connected with increased release of SNARE complexes (**S**oluble **N**-ethylmaleimide-sensitive factor **A**ctivating protein **RE**ceptor). The major neurotransmitter involved in this process is called *acetylcholine*, and gets released from vesicles as a consequence of SNAP-mediated (**SyN**aptosome-**A**ssociated **P**rotein) reactions.[38] Once acetylcholine is released, it binds to the appropriate receptor and triggers muscle cramps. Peptides termed *neurotransmitter inhibitor peptides* can potentially inhibit this process, due to their similarity to the synaptic proteins.[20] SNAP with molecular weight of 25 kDa (so-called SNAP-25) is essential for the release of acetylcholine, and is a target of well-known botulinum neurotoxin type A. Other type of botulinum neurotoxin, type B, has a diverse mechanism of action. Briefly, botulinum neurotoxin type B leads to the cleavage of VAMP (**V**esicle-**A**ssociated **M**embrane **P**rotein), necessary for the acetylcholine delivery.[39] In most cases, for peptides acting as inhibitors of neurotransmission and muscle cramps, botulinum toxins are applied as a compound of reference and comparison.

Carrier peptides. Copper(II) ions are involved in various processes in human body, such as enzymatic reactions, angiogenesis, or wound healing.[40] Cu^{2+} can be stabilized or delivered to cells by peptides. From the point of view of cosmeceutical arena, copper(II) ions are relevant in the formation of collagen or elastin, since they are essential cofactors for the enzyme called lysyl oxidase (LOX). Two peptides found to be carrier peptides are *Copper Tripeptide-1* (Cu)H-Gly-His-Lys-OH and *Manganese Tripeptide-1* (Mn)H-Gly-His-Lys-OH, able to reduce the activity of MMPs (Matrix metalloproteases) and collagenase.[16,17,25] Thus, they prevent the signs of premature skin aging.[19,39]

Signal peptides. Signal peptides can moderate the turnover of skin proteins. Most of this class of cosmeceuticals is enhancing the production of collagen. The name "signal" in this case derive from the capability to mimic the signal present during the

synthesis of ECM (extracellular matrix) proteins.[20] The term *matricins* refers to the peptides released by the ECM, and promoting collagen production. One of the pioneering peptides with a similar activity is a bombesin-like neuropeptide, called gastrin-releasing peptide.[41] It stimulates the proliferation of keratinocytes, therefore promoting the wound healing. Other recently discovered and published signal peptides are summarized in **Table 1**. Among them, peptide *SA1-III* with commercial name *KP1* can be found.[36,37] Due to its important role in the research described in this thesis, this particular sequence will be elaborated further below.

2.1.1 SA1-III (*KP1*) sequence as a relevant example of signal peptide

Serpins (**ser**ine **p**rotease **in**hibitor**s**) is the gene family including peptides with similar structure but different function. Their principal function is the regulation of proteases activity.[42] One of them is serpin A1, so called S-A1, with an ability to participate in the collagen degradation process, and is highly concerned with tissue remodeling pathways. Proteolytic disruption of serpin A1 results with the cleavage of 36-long amino acid sequence, situated on the C-terminus (C-36). It was found that the bioactivity of S-A1, apart from already known Reactive Center Loop (RCL, sequence GTEAAGAMFLEAIPMSIPPEVKFNK), is served also by the C-36 fragment. For example, it was able to inhibit the catalytic activity of neutrophil elastase and cathepsin G. Moreover, C-36 contains the internal C-26 portion, adopting the β-sheet conformation in the complex of serpin A1 with antitrypsin (**Figure 1** and **Figure 2**).[43,44]
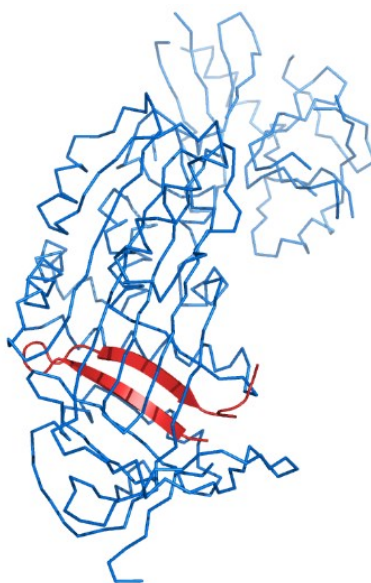
Figure 1. β-sheet domain (in red) identified in the complex of serpin A1 with antitrypsin (based on PDB ID: 1EZX structure visualized in *PyMOL*).[45,46]

```
  1   MPSSVSWGIL  LLAGLCCLVP  VSLAEDPQGD  AAQKTDTSHH  DQDHPTFNKI
 51   TPNLAEFAFS  LYRQLAHQSN  STNIFFSPVS  IATAFAMLSL  GTKADTHDEI
101   LEGLNFNLTE  IPEAQIHEGF  QELLRTLNQP  DSQLQLTTGN  GLFLSEGLKL
151   VDKFLEDVKK  LYHSEAFTVN  FGDTEEAKKQ  INDYVEKGTQ  GKIVDLVKEL
201   DRDTVFALVN  YIFFKGKWER  PFEVKDTEEE  DFHVDQVTTV  KVPMMKRLGM
251   FNIQHCKKLS  SWVLLMKYLG  NATAIFFLPD  EGKLQHLENE  LTHDIITKFL
301   ENEDRRSASL  HLPKLSITGT  YDLKSVLGQL  GITKVFSNGA  DLSGVTEEAP
351   LKLSKAVHKA  VLTIDEKGTE  AAGAMFLEAI  PMSIPPEVKF  NKPFVFLMIE
401   QNTKSPLFMG  KVVNPTQK
```

Figure 2. Sequence of serpin A1 with C-36 fragment marked in yellow, and underlined C-26 sequence adopting β-sheet conformation.[47]

Very recently in *PeptLab* at University of Florence serpin A1 analogs have been developed, starting from the potent serine proteases inhibitor activity of the native sequence. The broad performed investigation was aimed to find a reasonably short, but still active fragment of this molecule for cosmeceutical applications.[36,37,44,48] Therefore, the influence on collagen concentration of three overlapping peptides from C-terminus of S-A1 was evaluated. Sandwich ELISA (**E**nzyme-**l**inked **I**mmunosorbent **A**ssay) test demonstrated a significant role of Ac-MGKVVNPTQK-NH$_2$ peptide (namely SA1-III) in increased level of collagen, despite the presence of collagenase in the sample. In 2020, this sequence was patented as one of bioactive peptides for cosmeceutical purposes.[48] Further investigations have shown inhibition mechanism based on a Michaelis-Menten kinetics, comprising two possible pathways at the last step of complex forming reaction.[36,37,45] Already in 1975 the S-A1 deficiency was connected with skin abnormalities.[49] Pivotal role of serpins, their inhibition mechanism and peptide chain-modification prospective (e.g., decreasing or increasing of lipophilicity) allows to consider them as wound-healing agent or potential ingredient of cosmeceuticals.[10,11]

2.1.2 Enhancers of peptide bioavailability

One of the most crucial factors when dealing with peptides as active ingredients in cosmeceuticals is their stability in the final formulation. Together with the biodegradability, or difficulties with the penetration through the skin layers, peptides as bioactive components may bring some issues when designing new formulas. Indeed, various enhancers of peptide bioavailability in such products have been recently invented.[11]

Despite the fact that some of the peptides in cosmeceutical formulations undergo the pharmacological evaluation, it is relatively uncommon to find the published data claiming their bioavailability and stability after the contact with human skin.[50] Topical

applications of cosmeceutical products may lead to premature degradation of active ingredients, provoked by the enzymatic disruption.[51] Actually, the pharmaceutical use of peptide active ingredients demonstrates that there are several possibilities to enhance their bioavailability, and in some cases these approaches have been applied to cosmeceutically relevant peptides as well. [52,53]

Even though in the years 2017-2022 nearly 300 review articles dealing with cosmeceuticals appeared in PubMed database, only ten of them address in some way the problem of active ingredients skin permeation. The methods of bioavailability and stability enhancement focus on the modifications improving the penetration through the *stratum corneum*, or the peptide stability to dermal enzymes. The aspect of peptides stability as well as permeability (and thus efficacy) cannot be omitted, so the most recent modifications, summarized in **Scheme 1**, will be discussed below.
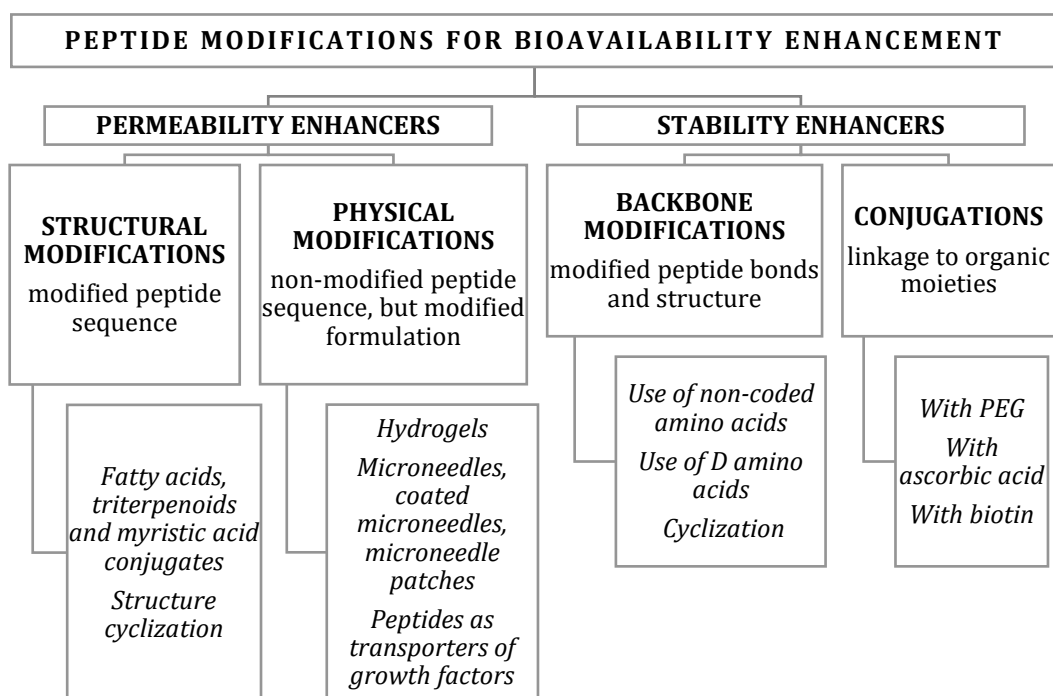
Scheme 1. Modifications of peptides applied for their bioavailability enhancement.[11,54,55]

Permeability enhancement. Due to the particular skin properties, including lipophilicity, the presence of various enzymes, and layering, bioactive molecules with possibly high permeation level should be characterized by the physicochemical features. They include a relatively low molecular weight (up to 500 Da) and melting point (up to 200ºC), balanced lipophilicity (log P between 1-3), and decent water solubility (over 1 mg/mL).[56] The transdermal delivery of macromolecules can be boosted by chemical or physical enhancers. The first group regards the conjugation with i.e., alcohols, fatty

acids, or surfactants. On the other hand, the use of physical enhancers includes ultrasonic waves, microneedles, or low electrical current. Another interesting examples applied for the purpose of skin permeability improvement are nanoparticles, nanostructured liquids, liposome enclosing, (micro)emulsions, hydrogels, techniques based on polymers or liquid nanocrystals.[57] The mechanism of action of both chemical and physical methods can be different, and mainly is based on one of the following: 1) *stratum corneum* lipid layer disrupting; 2) interfering with intercellular protein; 3) use of co-enhancers or solvents, improving the penetration of the drug into the *stratum corneum*.[58]

Chemical penetration enhancers can be divided into 10 chemical classes.[54] The most applicable in cosmeceuticals are alcohols (e.g., propylene glycol), surfactants (e.g., sodium lauryl sulphate, SLS), and fatty acids (e.g., palmitic acid). For instance, the N-terminal peptide conjugation with fatty acid is an example of the structure modification by covalent bond formation. On the other hand, chemical enhancer can facilitate the permeation without interfering with peptide structure – alcohols are solvents able to improve the permeation of poorly soluble active ingredients. Physical enhancers do not modify the peptide structure neither. They can be divided into five classes on the basis of the mechanism applied for the transdermal delivery: sono- and iontophoresis, electroporation, microneedles, and radiofrequency.[55] Widely used microneedles, perforating skin external layers, create a pathway for molecule delivery.[59] A good example of microneedles' use in cosmeceutical field are patches with microneedles, enhancing i.e., the permeation of previously mentioned Cu-GHK peptide.[60]

Stability enhancement. Physiological conditions of the skin are a crucial aspect for the use of peptides. Improving their half-life has always been and still is a big challenge. Considering the peptides for therapeutical applications, in 2016 the repository *PEPlife: A Repository of the Half-life of Peptides* was introduced.[61] Despite their mostly topical applications, cosmeceutical peptides have limited bioavailability due to their particular susceptibility to the proteases, enzymes widely spread all over the skin. This feature is a result of peptide bonds between amino acid in the sequence. Therefore, the peptide backbone is similar enough to natural substrates of various proteolytic enzymes, and peptides get degraded likewise.[5] To prevent the recognition of cosmeceutical peptides by problematic proteases, some modifications can be applied, for example: backbone modifications,[62] such as use of non-coded amino acids,[63,64] use of

D-amino acids,[65,66] cyclization,[67–72] or peptide conjugation with other molecules. Interesting examples of cosmeceutical peptide conjugates are summarized in **Table 2**.

Table 2. Examples of peptide conjugates, designed for the improvement of their stability.

ONE-LETTER CODE NAME	SEQUENCE OF AMINO ACIDS	ENHANCED STABILITY MODIFICATIONS
GHK	H-Gly-His-Lys-OH	Use of non-proteinogenic amino acids[63]
		Use of D-amino acids[65]
		Biotinylation[73–75]
KTTKS	H-Lys-Thr-Thr-Lys-Ser-OH	PEGylation[76]
		Ascorbic acid conjugation[77]
GEKG	H-Gly-Glu-Lys-Gly-OH	Ascorbic acid conjugation[75,78]

What must be underlined is the fact that some of the modifications created to improve the permeability of the final product, such as N-terminal conjugation with fatty acids, introduce additional amine bonds. They are susceptible to enzymatic degradation as well, particularly to dermal proteases standing for the part of the human degradome.[79]

2.2   Peptides conjugated with small organic molecules

Peptides conjugated with small organic molecules can act multifariously: as carriers, stabilizing agents, or active ingredients *per se*.[11,80,81] The scale of use of peptide conjugates, particularly for pharmaceutical applications, has increased to such an extent that in 2020 Balogh *et al.* introduced *ConjuPepDB*: a database of peptide-drug conjugates.[82,83] It summarizes up-to-now described organic molecules consisting of a small drug molecule, a linker, and a peptide (**Figure 3**).
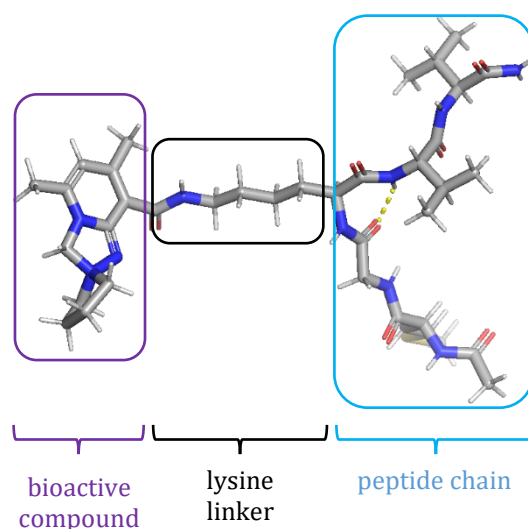
Figure 3. An example of the structure of peptide conjugate, including the lysine linker.[46] The structure presented in this figure is one of the novel compounds and will be discussed later.

Generally, the small bioactive compound has a strong pharmacological action or potential activity. Nevertheless, the reason of the conjugation is the aim to decrease the weak point(s) of the small molecule – for instance, its elevated toxicity, decreased tissue penetration, and others. In this type of conjugates the drug is mandatory for the activity, but the efficacy can be enhanced by the peptide chain, e.g., by providing an additional binding specificity.[81,84,85] *ConjuPepDB* contains essential information about the records, for example commonly used CAS (**C**hemical **A**bstracts **S**ervice) number. Moreover, each record is described by the biomedical application of the conjugate and the type of conjugation applied. In December 2022, it covered 1 645 structures from 238 references published in 95 scientific journals. To facilitate the exploration of the website, it is possible to browse it using the criteria of choice.

The new class of modified peptide conjugates stands also for antibody-peptide epitope conjugates (APEC), redirecting T-cell viral immunity against tumor cells.[86–88] The search for new peptide- and peptidomimetic-drug conjugates leads to the development of novel compounds with anticancer and antimicrobial activity[89–92] and for their diagnostic applications.[93–95] In some cases conjugation with inert polymers such as polyethylene glycol (PEGylation) and hydroxyethylstarch (HESylation), or hydrophobic molecules, e.g., fatty acids and steroids (lipidation), is used to increase *in vivo* stability of peptide therapeutics.[96] Thus, the overall biostability can be enhanced significantly, with half-life extension even from 0.1 to 33.57 h.[97] A large variety of chemical linkages are used to bind the peptide to the payload, the most frequently used being amide, sulfonamide, disulfide, glucuronide, carbamate, dipeptide, tripeptide, ether, and

ester.[82,84] Of special note is the use of the copper(I)-catalyzed alkyne-azide 1,3-dipolar Huisgen's cycloaddition, also known as *click reaction,*[98–101] that has been applied to the synthesis of a large variety of peptide-conjugates[102,103] as well as for the preparation of conformationally constrained peptides *via* side chain to side chain cyclization.[104–106]

The purpose of the conjugation applied for the compounds included in this thesis was to evaluate:

1) the influence of the lysine linker on the potential activity of conjugated small organic molecule, comparing to the small molecule alone,
2) the influence of peptide sequence conjugated with bioactive molecule, due to the potentially improved site-specificity and interaction with the active cleft of targeted enzyme.

The type of conjugation applied in the described syntheses will be discussed further and in more details in the chapter regarding the design of new compounds (**4.1**), indicating the reasonability of use of each part of the conjugate. The aim was to evaluate the inhibitory potential of such conjugates against elastase and tyrosinase. Therefore, in the following chapters the mechanisms of activity of these enzymes and the biological processes influenced by them will be described.

2.3   Collagen in the human body

Collagen structure. Collagen is one of the most essential proteins in human body and a substantial component of ECM.[107] 28 types of collagen have been classified, with a majority (around 85%) of type I and up to 15% of type III.[108,109] The most important role of collagen type I is to form the tissue fibrillar structure, while type III keeps the skin elasticity and supports the type I fibers. Approximately one-third of all proteins in human body is represented by collagen, what makes it the most plentiful protein-like component in our bodies.[110] Collagen can be classified regarding its molecular structure, e.g., fibrillar, non-fibrillar, and network-forming collagens.[111] Collagen has a helical structure, formed by three polypeptide molecules, spontaneously forming so-called *tropocollagen*. Each α-chain has the length of around 1000 residues,[112] and the helical structure is stabilized by covalent bonds together with hydrogen interactions, occurring between hydroxyproline and hydroxylysine.[108] In comparison with common proteins, the superhelix of tropocollagen is more constrained,[113] making the collagen susceptible only to a few enzymes and resistant to the most widespread proteolytic reactions.[114] Stability and resistance of the final collagen structure is

provided also by the regularity of repeated amino acid triad – Gly-Pro-hydroxyPro. It was found that the replacement of Gly by more bulky residues provokes inappropriate folding, and makes the helix less resistant to external factors, such as temperature.[113]

Collagen turnover and its role in the human body. The turnover of collagen is a complex process, consisting of repeated biosynthesis and degradation cycles. Proper degradation prevents the secretion of defective sequences and various disorders.[115] For example, the overproduction of collagen may lead to its accumulation, resulting with fibroses of bone, heart, joints, lungs, kidneys, or liver.[110,116,117] On the contrary, disrupted turnover of collagen and its enhanced degradation provokes the skin photoaging, constricted wound healing, and loss of skin firmness and elasticity.[118] Due to the complexity of collagen turnover process, a variety of review articles described it in details.[110,117,119–121] For the purpose of this thesis, the collagen degradation will be described in details below.

Collagen degradation. Collagen degradation pathways are divided into two categories: direct and indirect. Indirect pathway involves the external factors stimulating the enzymatic degradation, which is a major mechanism in the direct pathway. Direct process is coordinated by two mechanisms: extracellular and intracellular (**Scheme 2**). Extracellular mechanism is the cleavage of mature collagen, while the intracellular one degrades the procollagen chains, before their assembling into procollagen molecules.[122]
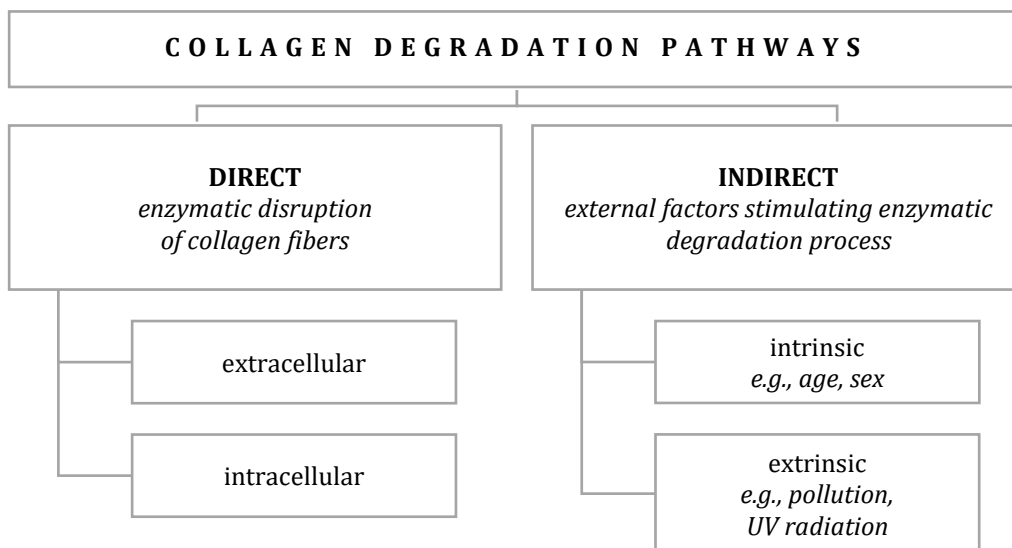
Scheme 2. Collagen degradation pathways: direct and indirect. Both have a significant influence on skin aging.

Intracellular degradation. During this mechanism, the internalization of previously and partially degraded collagen fragments is observed.[117] The intracellular degradation was found to be very rapid, and its duration depends on the tissue type. For example, there are significant differences between the kinetics of degradation between skin and heart proteins.[123,124] Collagen was found to be degraded (according to the intracellular pathway) in two cellular structures: in lysosomes and within the cisternae (endoplasmic reticulum or Golgi apparatus).

Extracellular degradation. The extracellular mechanism involves the secreted proteolytic enzymes, which are capable of collagen fibers digestion. Various classes of enzymes were identified to participate in this process, i.e., matrix metalloproteases and other diverse proteases: serine, active at neutral pH, and cysteine, aspartate, and threonine proteases, requiring mostly acidic environment.[125] MMPs activity and the target of digestion depends on the type of an enzyme. MMP-3 and MMP-10, namely stromelysins, act favorably on proteoglycans, fibronectin, and laminin.[125] Different MMPs, such as gelatinases, interact only with pre-cleaved (denaturized) collagen. ECM turnover is affected also by ADAM (**A D**isintegrin **a**nd **M**etalloproteinase) and ADAMTS (**ADAM** with **t**hrombo**s**pondin motifs) family.[125,126] Overall, the extracellular degradation and the dynamics within the ECM are complex processes, involving various complicated enzymatic pathways.[125] This thesis pays particular attention on the extracellular breakdown pathway. The most substantial enzymes involved in this process are summarized in the **Table 3**. Elastase, relevant in the discussed project, was highlighted.

Table 3. Enzymes involved in the degradation of fibrillar collagen, according to the extracellular breakdown pathway.[5]

ENZYME FAMILY	ENZYME COMMON NAME	ENZYME CLASSIFICATION OR ABBREVIATION	DEGRADED COLLAGEN TYPE	TYPE OF PREFERENTIALLY DEGRADED FIBRILLAR COLLAGEN TYPE	PREFERENTIAL CLEAVAGE SITE [c]
Matrix metalloproteinases	Collagenase-1	MMP-1	I, II, III, VII, VIII, X	I and III	Pro-*neutral amino acid*-✂-Gly-Pro
	Collagenase-2	MMP-8	I–III, V, VII, VIII, X	I	
	Collagenase-3	MMP-13	II, III	II, III	
	Gelatinase A	MMP-2	IV–VI, X	n.a. [a]	Pro-Gln-Gly-✂-Ile/Leu-Ala-Gly-Gln
	Gelatinase B	MMP-9	IV, V, VII, X, XIV	n.a.	
	Stromelysin-1	MMP-3	III	III (indirectly; by the MMP-1 activation)	Ser-✂-Met
	Stromelysin-2	MMP-10	III–V	III (indirectly; by the MMP-1 activation)	
	Matrilysin	MMP-7	IV–X	n.a.	Ser-✂-Leu Ala-✂-Leu Tyr-✂-Leu
	Metalloelastase	MMP-12	I, IV	n.a.	Pro-X-X-✂-Leu
	Matrilysin-2	MMP-26	IV	n.a.	Ser-✂-Leu
	MT-MMP-1 [b]	MMP-14	I, II, III	n.a.	Ser-✂-Leu
	MT-MMP-3	MMP-16	III	n.a.	n.a.
Serine proteases	**Elastase**	**-**	**I, III**	**I (independently and enhancing MMPs activity)**	**X-✂-Gly/Ala/Ser**
	Trypsin-2	-	I, II, III	I (independently and enhancing MMPs activity)	Lys/Arg-✂-X
Cysteine proteases	Cathepsin K	CatK	I, II	I, II	n.a.
	Cathepsin B	CatB	II	n.a.	n.a. (carboxypeptidase)
	Cathepsin L	CatL	I, II	I	Arg-✂-X
	Cathepsin S	CatS	I	I	n.a.

[a] n.a.: data not available.
[b] MT-MMP: membrane-bound MMP.
[c] ✂ - cleaved bond.

Additional factors affecting the collagen degradation. A variety of additional factors indirectly stimulating the degradation of collagen was found:[118]

1) **ultraviolet radiation**, inducing MMPs and enhancing their proteolytic activity,

2) **age** – in elder skin the overactive secretion of proteases is observed; additionally, fibroblasts are not working properly, or they are not effective enough,[108]

3) **sex**, due to the inhibitory effect of estrogen on the collagen synthesis.[127]

In 2006 and 2007 the influence of menstrual cycle on the collagen synthesis was investigated. It was demonstrated that there are no significant discrepancies between luteal and follicular phases. Nevertheless, as mentioned in the point **3)**↑, there are some differences between male and female collagen turnover (synthesis and remodeling).[128–130]

Enzymes degrading mainly fibrillar collagen led to skin aging and the loss of skin elasticity, and therefore they became a distinct cosmeceutical target. Among these enzymes, according to **Table 3**, collagenases (MMP-1, 8, and 13), elastase, and cathepsins can be found. For the purpose of this thesis, the mechanism of enzymatic digestion of collagen fibers involving elastase will be further elaborated. Examples of direct inhibitors of elastase will be mentioned, with particular attention paid to peptide-based compounds.

2.4 Elastase in collagen degradation

Term *elastase* is known since 1949, when Baló and Banga published a paper in Nature reporting that fresh pancreas extraction along with dried pancreas powder "contains a specific enzyme, called 'elastase'".[131] It was the very first scientific report describing this enzyme, which was then widely investigated. The important role of fibroblast elastase in wrinkle formation was highlighted at the beginning of 2000s.[3] In this research, Tsuji and co-workers evidenced the importance of this type of elastase in elastic fiber degradation. As mentioned in the introduction, at least two elastase types are present in the skin, i.e. neutrophil (HNE) and skin fibroblast elastase (HSF).[132] Both can degrade fibrillar collagen, but there are undoubtful differences between them.[3] Inhibitory profiles were created by comparing the efficiency of various inhibitors, including typical metalloprotease and serine protease inhibitors. Phosphoramidon, EDTA (ethylenediaminetetraacetic acid), 1,10-phenantrolin, all known as MMP inhibitors, significantly decreased the activity of fibroblast elastase. Instead, neutrophil elastase remained active in these conditions, and it was inhibited only by phenylmethyl sulfonylfluoride and elastatinal, which are the typical inhibitors of serine proteases.[3] Biological activity and functions of HNE were widely described in the literature, with examples of diverse inhibitors.[133–136]

HNE was classified Chymotrypsin-Like Proteinase (CTLP), in the family S1 consisting of over 130 structures.[137] HNE is produced in the bone marrow, and accumulates primarily in the azurophilic granules of neutrophils, where its

concentration exceeds 5 millimoles. This value depends on the maturity level of neutrophils. Released from the granule, it enters the extracellular space or binds to the outer side of the cytoplasmic membrane. In addition, this enzyme is present in monocytes, eosinophils, mast cells, epidermal and dermal cells, i.e. keratinocytes and fibroblasts.[3,138]

Structural properties of elastase. Neutrophil elastase is a small globular protein with a mass of approximately 30,000 Da. HNE consists of a polypeptide chain of 218 amino acids and two carbohydrate side chains. The stability of the structure is ensured by the presence of four disulfide bridges, as well as β-barrels built of antiparallel β-sheets.[139]

2.4.1 Mechanism of action

Catalytic triad. The proteolytic activity of elastase is related to the presence of three catalytic residues forming a *catalytic triad*: histidine (**His-57**), serine (**Ser-195**) and aspartic acid (**Asp-102**) (**Figure 4**).[140,141] Serine residue located in the active site has a strong affinity for amino acids with a small charge, which is correlated with its highly nucleophilic nature.[140] The substrate specificity of serine proteases is closely related to the substrate-binding pocket. In case of HNE, the active pockets consist mainly of hydrophobic amino acids, with the exception of the arginine residue (Arg-217) of the side chain, which interacts with the polar or acid groups of the substrate.[139,142] Studies of the human neutrophil elastase complex using X-ray crystallography revealed 8 binding sites.[142]
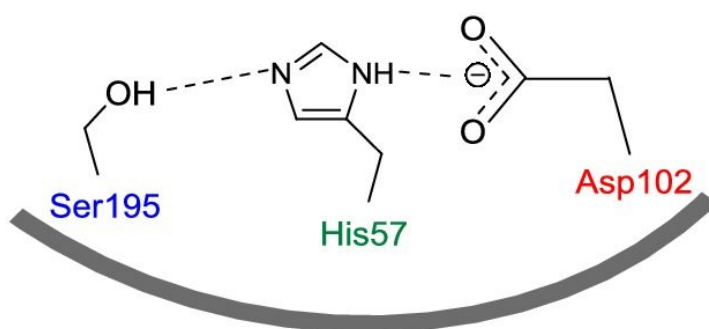
Figure 4. Catalytic triad of elastase.[143]

Catalytic activity. The classical mechanism of action of proteolytic enzymes belonging to the group of serine proteases has a two-stage character. The first step after non-covalent binding of the substrate to the active site of the enzyme is the hydrolysis of the peptide bond.[144] During the acetylation process, all three amino acid residues of the

catalytic triad play an important role. The role of aspartic acid (Asp-102) is to impart basic properties to histidine (His-57), which then leads to the deprotonation of serine (Ser-195).[145] Subsequently, a nucleophilic attack of the Ser-195 hydroxyl group on the carbon atom (from the carbonyl residue of the substrate) takes place. As a consequence, a *tetrahedral transition state* is formed, stabilized by the binding site, called *oxyanion hole*.[146] Breakdown of the transition molecule leads to the formation of a tetrahedral acyl-enzyme.[147]

The second step consists of deacylation of the formed complex with a water molecule, resulting in the formation of another intermediate compound which breaks down until the release of serine and the carboxylic acid product.[139,145] Serine proteases share the same mechanism of catalysis, but differ in their binding sites. Trypsin is specific for the basic amino acids (lysine and arginine). Elastase is specific for the small, uncharged amino acids, e.g., alanine, valine, and threonine.[148]
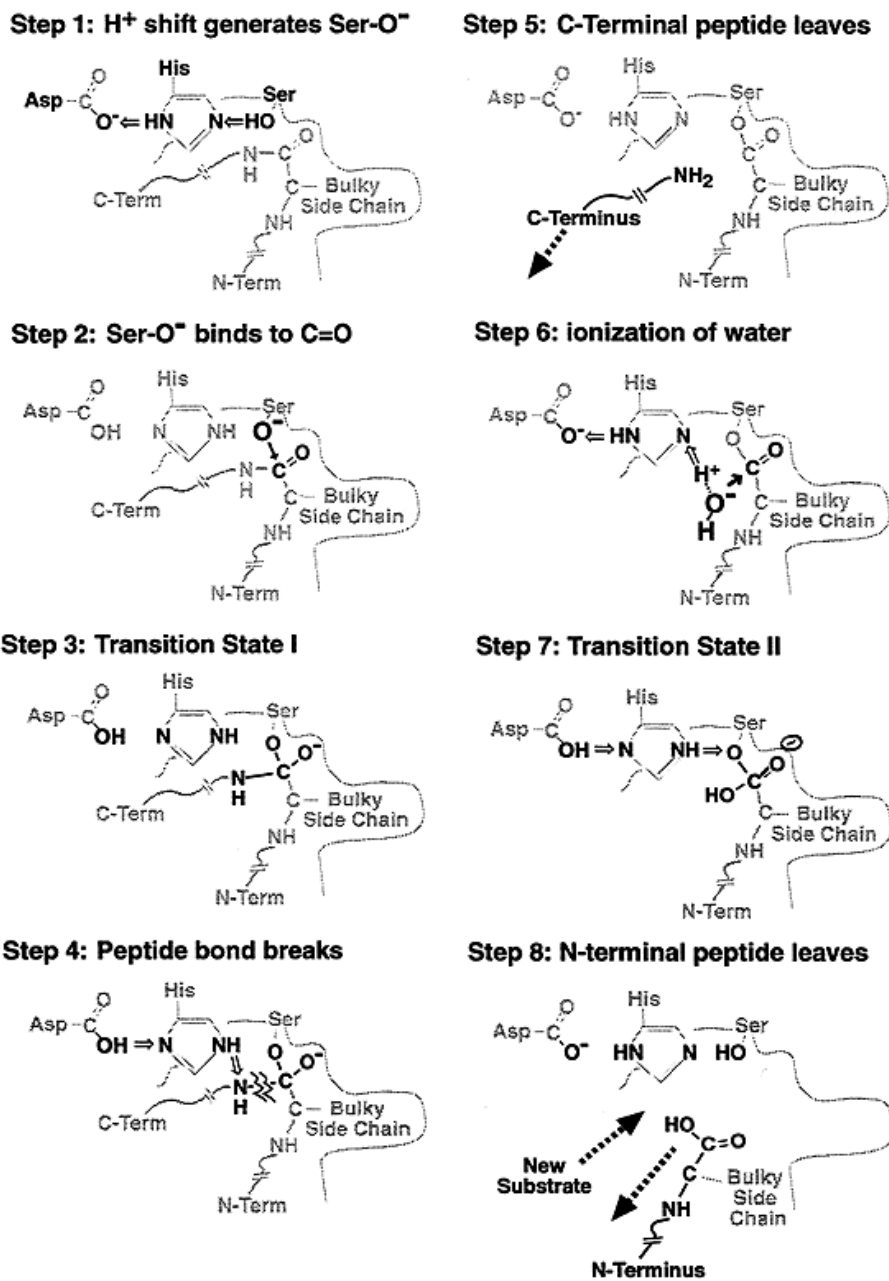
Figure 5. Catalytic mechanism of serine proteases.[148]
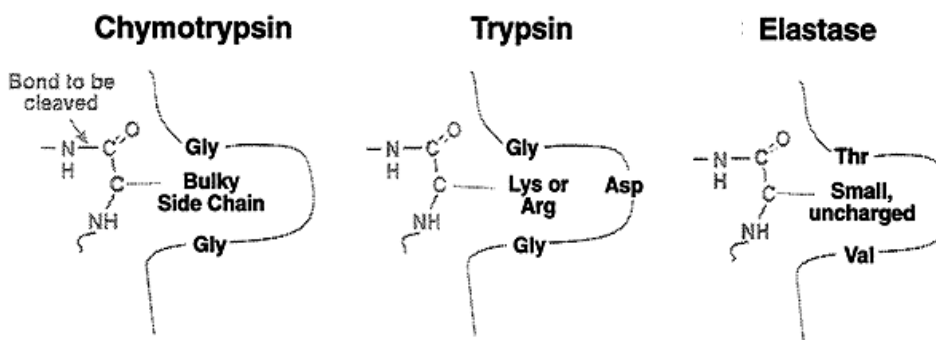
Figure 6. Binding sites of different serine proteases.[148]

Despite the availability of three-dimensional structures of proteolytic enzymes, the design of new inhibitors is now a challenge. New inhibitors, as relevant biological tools, must be highly selective and possess good specificity for target peptidases. In fact, in case of human neutrophil elastase this search is particularly complicated due to the similarity to other serine proteases in the human body.[149] Moreover, potential inhibitors should be highly resistant to proteolytic degradation and have a long life in the bloodstream, so they must not be susceptible to rapid elimination from the body.[150]

2.5 Already known elastase inhibitors

According to the current state of knowledge, neutrophil elastase inhibitors are compounds with hydrophobic nature.[135] In addition, the amino acid residues that build the peptide inhibitor should contain a branched, aliphatic side chain.[151] Conferring to the mentioned literature, there are two types of mechanisms known for HNE inhibitors:

1) *Transition state inhibitors*, forming a tetrahedral complex with the active cavity of the enzyme. Due to the substantial number of interactions, these inhibitors are highly effective and have a K_i value of the order of nanomoles,

2) *Alternate substrate inhibitors*, compounds acetylating the active site of the protease and undergoing the slow deacylation themselves. Because they are more reactive than transition state inhibitors, they may have more side effects.

2.5.1 Peptide derivatives

Chloromethyl ketones. Already in 1977 Powers *et al.* as one of the first Authors described the inhibition of porcine pancreas elastase (PPE), human leukocyte elastase (HLE), and cathepsin G (CatG).[152] By examining the cleavage pattern of various peptides catalyzed by PPE, the structural preferences of this enzyme were determined. According to these results, some new chloromethyl ketones were synthesized, with general sequence Ac-Ala-Ala-Pro-**AA**CH$_2$Cl (where AA=Ile, Val, Thr). It was demonstrated that peptides with Ile were inhibiting PPE more rapidly, while the sequence with Thr was not as efficient as the isoleucine derivative. Regarding HLE, sequences with Ile and Val were the most effective; water-soluble MeO-Suc-Ala-Ala-Pro-ValCH$_2$Cl was found to be a very good inhibitor of HLE. The research of peptide chloromenthyl ketones as HNE inhibitors was then continued, and in 1989 Navia and co-workers published further results with side effects of peptides presented by Powers *et al.* in humans. Therefore, they designed new molecules with diminished toxicity.[141] Methoxysuccinyl-Ala-Ala-Pro-Ala chloromethyl ketone (MSACK) was found

to be able to form the cross-linkage between His-57 and Ser-195 residues, responsible for the catalytic activity (**Figure 7**).
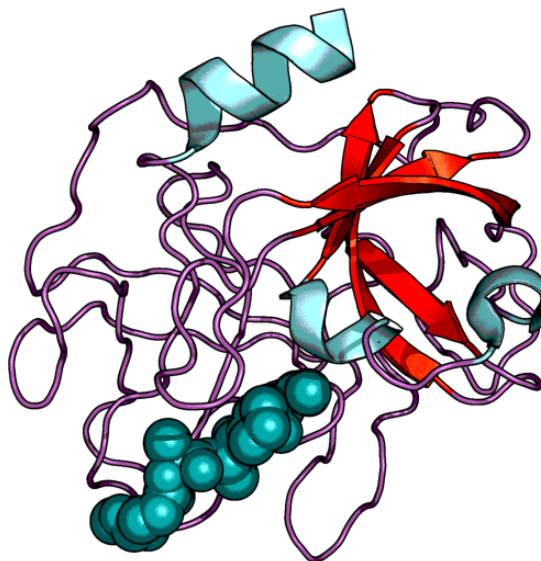
Figure 7. Structure of human neutrophil elastase in complex with MSACK (based on PDB code: 1HNE).[141] The inhibitor molecule is presented as spheres.[46]

At the beginning of 2000s, peptidyl trifluoromethylketone serine elastase inhibitors, namely ZD0892 and M249314, were published.[153] The *in vivo* treatment of animals suffering from advanced pulmonary vascular disease treated with M249314 showed noticeable elastase inhibitory activity over the first 6 hours. Then it was decreasing but remained visible until the second dose. In the control group, 900% loss of cellular matrix after 21 days was observed for untreated rats, with further increase of 800% within next week. Another important result from this research regarded the mortality of rats. Sick and untreated animals have died after 23 days. Inversely, in two groups treated with ZD0892 and M249314 for 1 week, only one rat in each group has died. Summing up, all untreated rats were dead by 30 days of the trial; the survival of M249314-treated rats was 86%.

2.5.2 Cyclic peptides

Cyclic depsipeptides. Peptides with one or more amides replaced by the ester groups are called *depsipeptdes*. The importance of conformationally constrained peptides was emphasized and investigated for various applications, mainly for drug-design purposes.[102,154–157] Two cyclic depsipeptides were isolated from cyanobacterium *Scytonema hofmanni* PCC7110, and named *scyptolin A* and *B*. This research together with the PPE inhibitory properties of scyptolin A and B was described in 2001 and 2003.[158,159] Crystal structure of scyptolin A bound to the enzyme is

presented in **Figure 8**. Both compounds were found to be good and selective inhibitors of PPE, with IC_{50} values of approximately 3 mg/mL. X-ray experiment evidenced the relevance of the rigid ring of scyptolin A in the elastase active site, which prevents the catalytic reaction and decreases the enzyme activity.
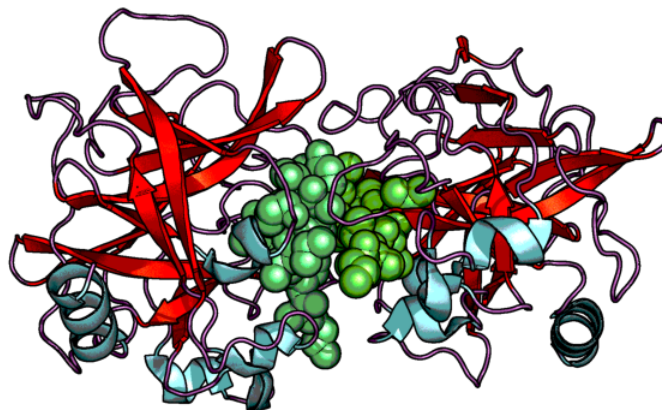
Figure 8. Scyptolin A in complex with PPE (PDB code: 1OKX).[159] The inhibitor is presented as spheres.[46]

Cyclopeptides. Elastase inhibitors from natural sources with cyclic structure were described recently.[160] Inhibitors called *tutuilamides A-C* are cyclic peptides with IC_{50} values against PPE below 5 nM (1.18, 2.05 and 4.93 for analogs A, B, and C, respectively). In addition, they resulted to be selective (IC_{50} value for trypsin >20 000). Hydrogen bond between the amino acid backbone of tutuilamide A and the enzyme binding pocket stabilized the complex and was the reason of such a good inhibitory activity.

2.5.3 Unmodified peptides

Except these structurally modified peptides, unmodified sequences were described as well in the literature. Already in 1995, *in vitro* and *in vivo* studies relating to lipophilic peptide inhibitors of human neutrophil elastase were done.[161] Four lipopeptides showed significant HNE inhibition, demonstrating the IC_{50} values of 2.9×10^{-9}, 2.8×10^{-10}, 1.8×10^{-10}, and 4.1×10^{-10} mmol/mL for the most relevant compounds **1b-e**, respectively. Sequences were based on X-AAPV-Y fragment, with proper N- and C-terminal modifications (X and Y, respectively) (**Table 4**). Interestingly, the lipophilicity increased the inhibitory potency: on the contrary, carboxylic acid esterification **1e** led to obtaining less effective compound. Lipopeptide **1d** administered intradermally during *in vivo* experiments on rabbit skin resulted with elastic fiber protection against elastolysis.

Table 4. Lipopeptides reported by Toth *et al.* as good inhibitors of elastase.[161]

NAME	STRUCTURE
1b	$(CH_3)_3COCO$-DL-$NH[CH(CH_2)_{11}CH_3]$-AAPV-OH
1c	$(CH_3)_3COCO\{DL$-$NH[CH(CH_2)_{11}CH_3]CO\}_2$-AAPV-OH
1d	$(CH_3)_3COCO\{DL$-$NH[CH(CH_2)_{11}CH_3]CO\}_3$-AAPV-OH
1e	$(CH_3)_3COCO\{DL$-$NH[CH(CH_2)_{11}CH_3]CO\}_3$-AAPV-OCH_3

Very broad investigation designed to find efficient inhibitors of PPE was performed in 2000, basing on the sequence of OMTKY3 (third domain of turkey ovomucoid inhibitor).[162] Synthesis of sequences on the cellulose membrane was followed by the binding affinity measurements on the membrane as well. The role of each amino acid among 19 coded residues was determined by their exchange in the sequence. Over 700 different chains were evaluated, and 320 of them were found to exhibit some binding potential. Afterwards, they were measured in the inhibition assay. Importantly, cyclization did not provide any benefits (such as additional interactions or elevated inhibition). Among all tested sequences, the shortest one and decreasing the PPE activity by 84% was peptide PMTLEYR. Its binding to PPE was 1,000 times stronger than to HLE or bovine pancreas α-chymotrypsin. Further experiments involving this sequence during the design of hybrid mini-protein resulted with PPE inhibition alike.[163]

Synthetic peptides as HNE inhibitors were examined by Vasconcelos *et al.* in 2011.[164] Two sequences were investigated against HNE and PPE, and the results were compared with elastatinal (commercially available inhibitor). Sequences were based on the literature data, where Bowman-Birk protein-derived peptides were found to be good HNE inhibitors.[165] Peptides MGWCTASVPPQCYG and MGWCTASVPPQCYG(GA)$_7$ were compared, and the second sequence was found to be more efficient. IC$_{50}$ values were calculated and resulted with 8.1 and 6.3 μM for the first peptide, and 7.0 and 0.4 μM for the second one (in case of PPE and HNE, respectively). This data was explained by the presence of (GA)$_7$ tail, providing probably additional interactions with the enzyme. Similar results were obtained previously by Toth *et al.*[161]

Another non-modified peptide sequence relevant for the discussed argument was presented in 2013.[166] This serine protease inhibitor, namely *AvKTI*, was found in *Araneus ventricosus* spider. cDNA GenBank data provided the sequence, which resulted to be relatively long (KDRCLLPKVTGPCKASLTRYYYDKDTKACVEFIYGGCRGNRNNFKQK-DECEKACTDH, 57 residues). IC$_{50}$ values were established as 10.07 and 446.93 nM for plasmin and elastase, respectively.

Peptide sequences with unnatural amino acids. The crystal structure of PPE in the complex with inhibitor FR901277 was published in 2000 (**Figure 9**).[167] The inhibitor was extracted from the culture filtrate of *Streptomyces resistomicificus.*
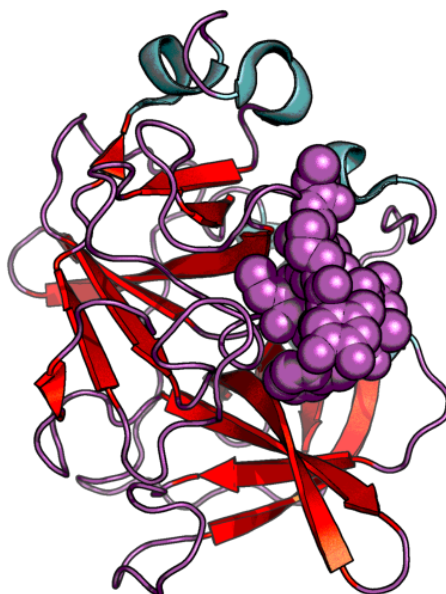
Figure 9. Crystal structure of PPE in complex with FR901277 (PDB code: 1QR3).[167] The inhibitor is presented as spheres.[46]

This compound was examined previously against HLE and PPE, and was found to inhibit these enzymes with IC_{50} values of 18 and 26 µM, respectively.[168] FR901277 is a short sequence consisting of 7 amino acid residues, among which 4 are natural [L-Orn^1, L-Thr^2, L-Phe^5, and L-Val^7] and 3 are unnatural [dehydroxyThr^3, AA^4, and AA^6]. Additionally, the bridge between residues L-Thr^2 and L-Val^7 was found. The crystal structure provided the data about the location of FR901277 in PPE active site (**Figure 10**), and the hydrophobic residues of FR901277 were responsible for the binding. The whole complex is stabilized by van der Waals interactions. This data confirms the relevance of hydrophobic amino acid residues in the sequence of the potential elastase inhibitor.
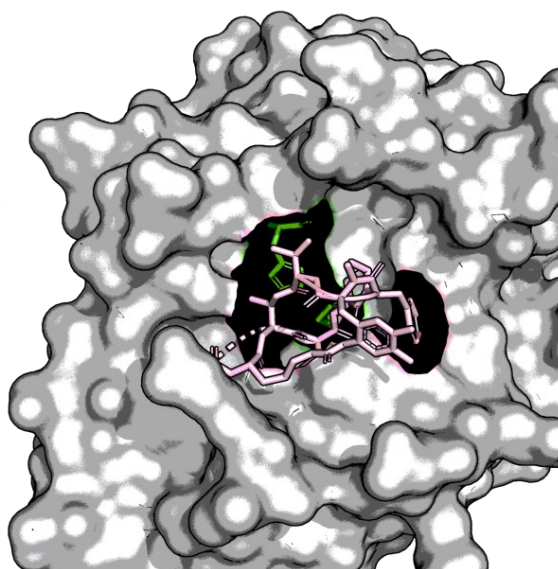
Figure 10. Crystal structure of PPE in complex with FR901277 (PDB code: 1QR3).[167]. The proximity of His-57 and Ser-195 residues (green) and the inhibitor molecule (pink) is visible.[46]

Peptides without structural modifications, including natural and unnatural amino acids, can be good inhibitors of elastase as well as cyclic or modified structures. Examples of unmodified sequences discussed in this chapter are summarized in **Table 5**.

Table 5. Summary of discussed peptide sequences, found to be relevant elastase inhibitors.

PEPTIDE SEQUENCE	REFERENCE
$(CH_3)_3COCO\{DL-NH[CH(CH_2)_{11}CH_3]CO\}_3$-AAPV-OH	161
PMTLEYR	162
MGWCTASVPPQCYG MGWCTASVPPQCYG(GA)$_7$	164
KDRCLLPKVTGPCKASLTRYYYDKDTKACVEFIYGGCRGNRNNFKQKDECEKACTDH	166
OT-dehydroxyT-AA$_1$-F-AA$_2$-V *(AA$_{1,2}$ – non-abbreviated, unnatural amino acids)*	167,168

Peptide derivatives. Well-known inhibitor of metalloproteases, phosphoramidon,[169] penetrates poorly the skin layers due to the presence of hydrophilic rhamnose moiety in its structure. In early 2000s in the study published by Tsukahara *et al.* Authors synthesized a series of phosphoramidon derivatives.[6] Among them, *N*-phenetylphosphonyl-leucyl-tryptophane (NPLT) with rhamnose residue replaced by a lipophilic phenetyl residue, was found to be able to inhibit specifically normal fibroblast-derived elastase. Authors reported a significant role of elastase in the damage of dermal elastic fibers, what leads to wrinkle formation. NPLT was applied topically on rat skin five times a week. It resulted with diminished wrinkle formation and maintained skin elasticity. The range of tested concentrations was 0.1±10.0 mM,

with the peak of efficacy at 1.0 mM concentration. Structural differences between these two compounds are visible in **Figure 11**.
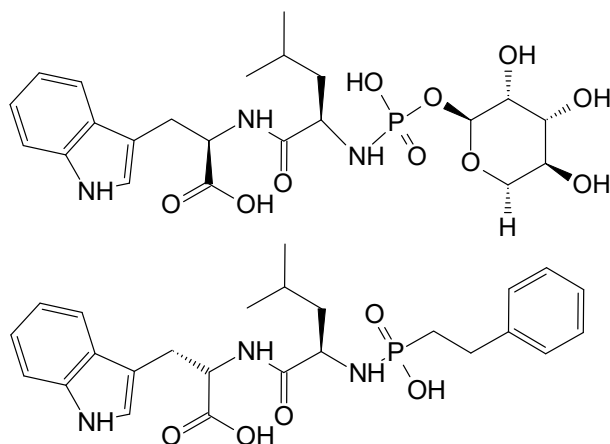
Figure 11. Phosphoramidon (*top*) and *N*-phenetylphosphonyl-leucyl-tryptophane (NPLT), its derivative (*bottom*).[6,169]

2.5.4 Heterocyclic compounds

Since the purpose of this thesis is to present end evaluate the relevance of peptide conjugation with small organic molecules, in this subchapter a particular attention will be paid to novel inhibitors, thereby providing additional information about elastase inhibitors design. In majority they are low-molecular compounds exhibiting significant inhibitory activity, due to the presence of some particular structural elements.

N-benzoylpyrazoles. Interesting approach to HNE inhibition by low-molecular compounds was described in 2007, when Schepetkin and co-authors presented the pioneering data in the area of heterocyclic elastase inhibitors.[170] All evaluated structures were based on *N*-benzoylpyrazoles (**Figure 12**), then modified and optimized. 17 new derivatives were chosen for further investigations and SAR (**S**tructure-**a**ctivity **r**elationship) analysis. Molecular docking and *in silico* studies were performed to clarify the differences in the interaction with HNE amongst the most and the least potent compounds (K_i values in the range 6-300 nM). The most important results from this investigation shown the interaction of the carbonyl group of the inhibitor within NE binding site. Inactive analogs were either sterically hindered, or showed unpreferable orientation, hence excluding the presence of relevant interactions.
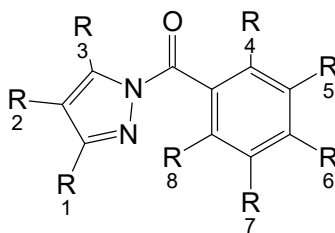
Figure 12. General chemical structure of *N*-benzoylpyrazoles.[170]

N-benzoylindazoles. After the results of Quinn's group regarding *N*-benzoylpyrazoles, Giovannoni group started working on similar derivatives based on *N*-benzoylindazole backbone (**Figure 13**).[171] This research showed the competitive and pseudo-irreversible inhibition of some of the derivatives, with IC_{50} values of ≈ 0.089 and ≈ 0.13 µM for the most effective compounds, so-called **8a** and **8b**. Another time, the efficacy of these compounds was explained by molecular modelling studies. This experiment highlighted once again the importance of the carbonyl group, capable of forming the favorable interactions with -OH group from Ser-195 in the active cleft.

The progress of this research resulted with revealing of another two good inhibitors, **5b** and **20f** (**Figure 13**).[172] IC_{50} values were calculated and were found to be at very satisfying nanomolar level – 7 and 10 nM, respectively.

8a   R = Ph; R^1 = CH_3 **5b**   R = CN; R^1 = m-CH_3 **20f**   R = $COcC_3H_5$

8b   R = 3-CH_3; Ph; R^1 = CH_3
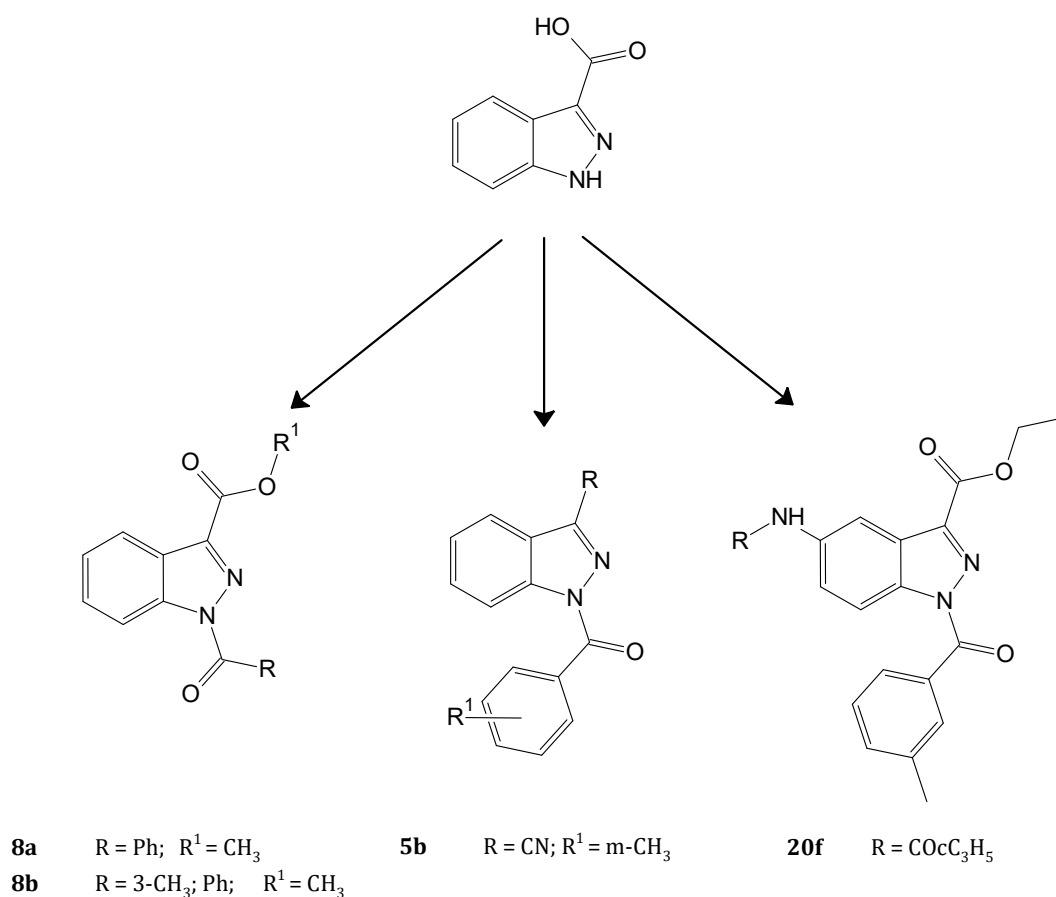
Figure 13. *N*-benzoylindazole derivatives discussed in the papers by Crocetti *et al.* [171,172]

Summing up, the paragraph describing peptides, peptide-like compounds, and small organic compounds as relevant inhibitors of elastase provided the following information, useful for the design of new inhibitors:

1) Amino acids incorporated in the peptide backbone should be hydrophobic, possess aliphatic, small, and uncharged side chains,

2) Peptide length should be rather small to enhance the permeability through skin layers, however considering only the activity and regardless of permeability, also long peptides were found to be good inhibitors of elastase,

3) Further step of the peptide sequence optimization may include the exchange of relevant residues for unnatural or D-amino acids,

4) Small, organic compounds, potentially conjugated with the peptide, can possess heterocyclic ring (e.g., pyrazole, indazole) and carboxyl group, which provides the interactions with -OH group of Ser-195 in the elastase active cleft.

2.6 Melanogenesis

Melanins (**Figure 14**) are natural pigments with polymeric structure responsible for the skin coloration and are one of the most widely distributed pigments in nature. They are known to be present in bacteria, fungi, plants, and animals and its color varies from yellow to black. In animals, melanins are products of the oxidation and polymerization of L-tyrosine during the process called *melanogenesis*. It takes place in melanocytes, functional cells of the basal layer of the dermis. Melanocytes release melanins in the deepest layer of epidermidis, called *basal* layer into the surrounding *stratum corneum* (**Figure 15**).[173] The amount and type of pigment synthesized in melanocytes and its distribution in keratocytes determines the color of human skin and hair. Synthetic pathway of melanins is a complex process, broadly discussed and investigated.[8,174]
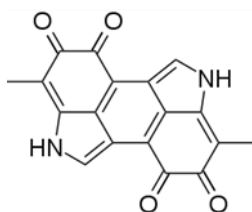
Figure 14. Structure of melanin.
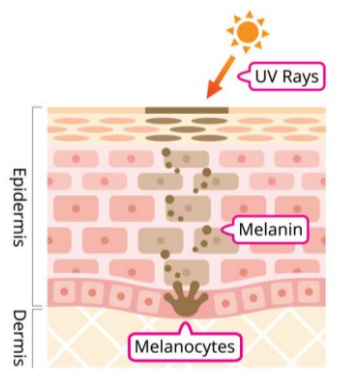
Figure 15. Melanins distribution in skin layers.[173]

Melanogenesis and types of melanins. Melanogenesis catalyzed by tyrosinase was introduced firstly by Raper in 1927.[175] It was the pioneering paper explaining the involvement of tyrosinase and L-tyrosine in the melanogenesis process. Further investigations permitted to understand it more in details,[176] leading to the scheme published by Prota in 1988.[177] It depicted two pathways where eumelanin and pheomelanin, two types of melanins present in the human skin, are obtained (**Figure 16** and **Figure 17**).
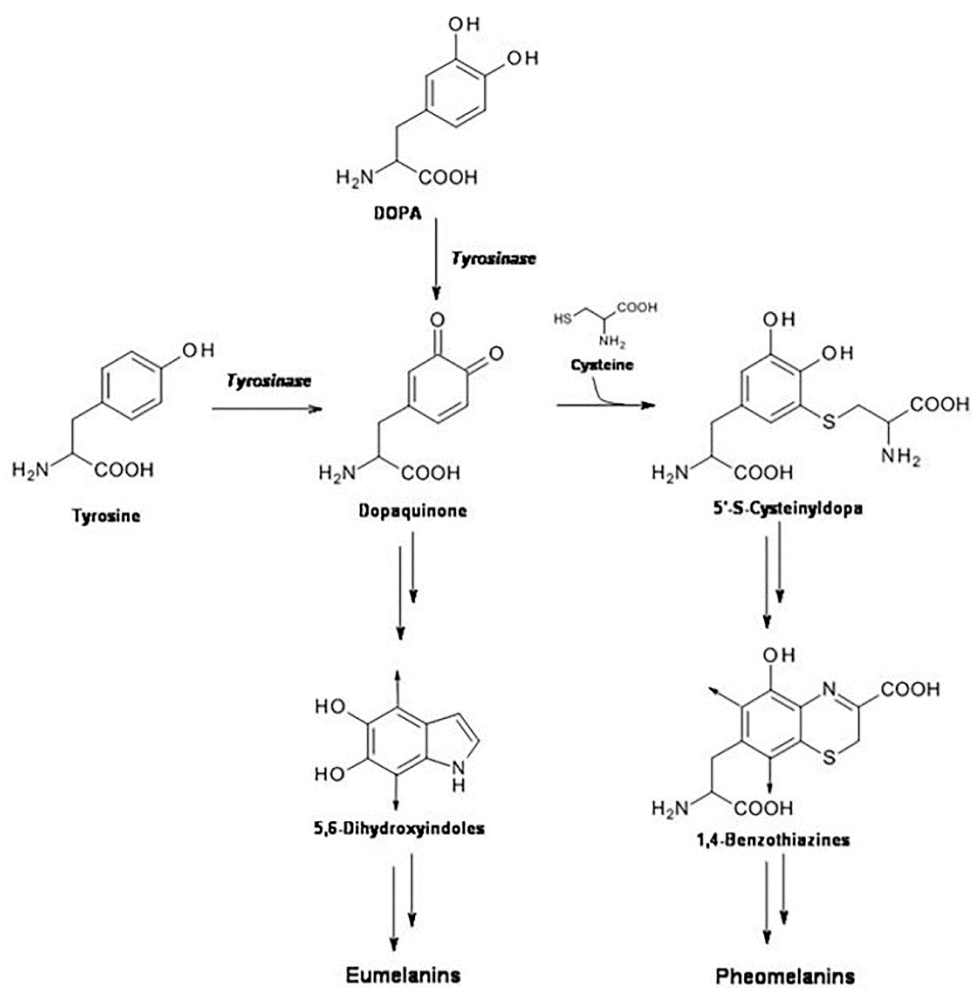
Figure 16. Simplified scheme of melanogenesis, leading to eumelanins and pheomelanins.[178]
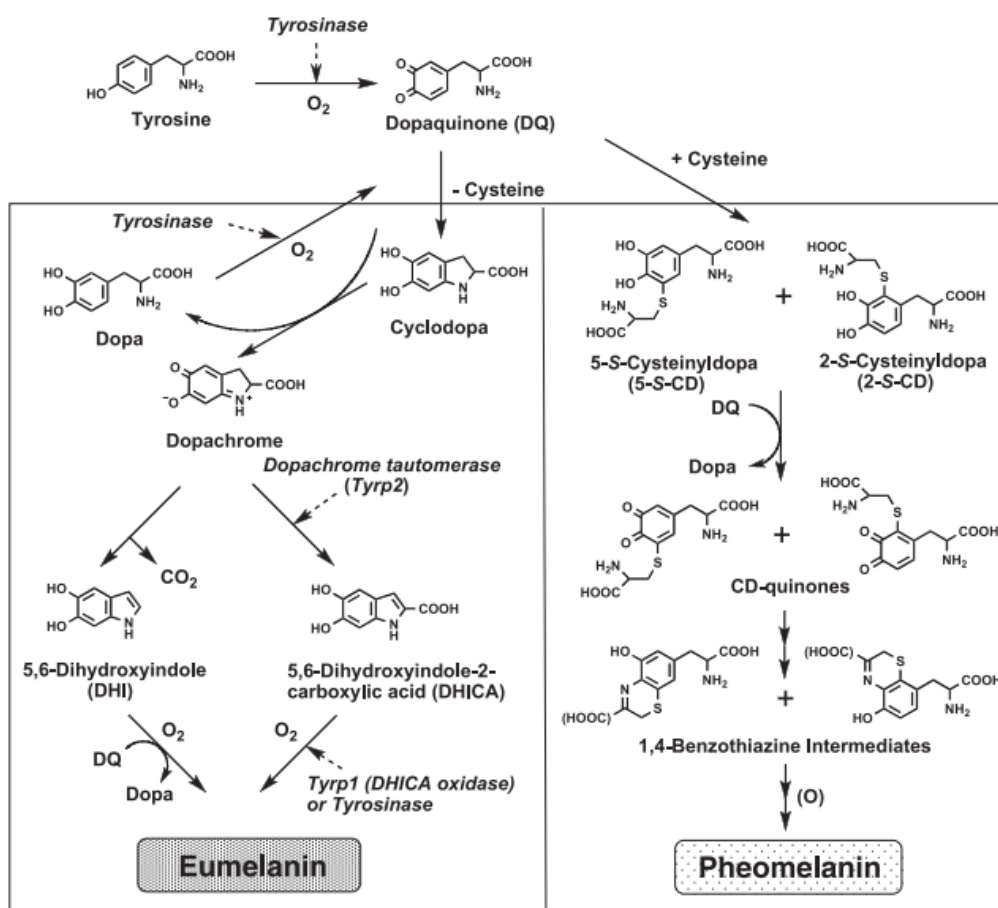
Figure 17. More detailed pathway of melanogenesis.[179]

Eumelanin is a black to brown, heterogeneous polymer composed mainly of dihydroxyindole units. It is obtained *via* the oxidation of tyrosine or 3,4-dihydroxyphenylalanine (DOPA) to dopaquinone, catalyzed by tyrosinase. On the contrary, pheomelanin is the yellowish-reddish pigment obtained during the pathway of pigment biosynthesis, involving non-enzymatic addition of cysteine to dopaquinone. Both melanins are synthesized during the melanogenesis, and they share a common composition of repeating units, but their chemical, structural, and physical properties are different. It was found that slight variations in the composition of pigment monomer, leading to the polymer backbone, are responsible for differences such as light absorption, antioxidant and redox activity, or metal-chelating properties.[178,179] Eumelanin has photoprotective activity and absorbs UV light; on the contrary, pheomelanin is photo-unstable and phototoxic.[180] Thus, pheomelanin is mostly responsible for UV-induced damage including photoaging. Importantly, both melanin types can be produced within the same cell, but in different proportions. Lack of eumelanin leads to enhanced susceptibility to UV-induced damage and hyperpigmentation disorders.

Differences in human skin and hair color are a major feature of the human phenotype and are primarily associated with the melanin pigment. The ratio of these pigments determines the color of our hair, eyes, and skin. Black hair has the highest eumelanin content in the order of deep brown, brown, light brown, light blond, and red. This is often seen in areas with red skin, such as red hair and lips. The skin of people with low levels of black pigment produced by melanocytes burns more easily when exposed to sunlight, and these people have been found to be more prone to skin cancer than people with dark skin. This suggests that higher levels of constitutive pigmentation are associated with reduced susceptibility to the adverse effects of UV radiation. Dark and Asian skin usually contains more melanin than fair skin. White hair does not contain melanin, and gray hair contains only a few melanin granules.

Tyrosinase plays a pivotal role in melanogenesis process, and undoubtedly is an essential factor for the melanin production. Therefore, tyrosinase became a target of research area focused on skin whitening. Due to the tyrosinase contribution in skin blemishing and age spots appearing, inhibitors of this enzyme are frequently investigated as cosmeceutically relevant active ingredients.

2.7 Tyrosinase

Tyrosinase can be found in melanosomes, synthesized by previously introduced melanocytes. This copper-containing enzyme belongs to class called *oxygen oxidoreductases*, with a catalytic center consisting of oxygen molecule (O_2) and two copper atoms – Cu(A) and Cu(B).[181] Phenols, such as tyrosine or dopamine, are oxidized by tyrosinase with O_2. There are two catalytic reactions involving tyrosinase: monooxygenation of monophenols to *o*-diphenols (*monophenolase activity*) and oxidation of *o*-diphenols to *o*-quinones (*diphenolase activity*) (**Figure 18**). Both activities are provoked by the dioxygen binding to Cu(A) and Cu(B).
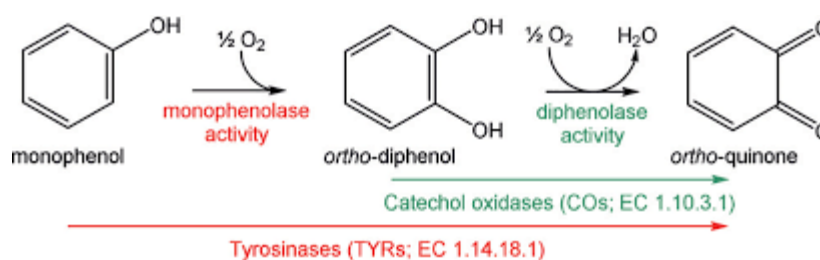
Figure 18. Double catalytic nature of tyrosinase. In red: monooxygenation of monophenols to o-diphenols (monophenolase activity). In green: oxidation of o-diphenols to o-quinones (diphenolase activity).[182]

Catalytic cleft. Tyrosinase is an enzyme widely distributed in the nature, present in both plant and animal tissues. It may differ in terms of the primary structure or size, pattern of glycosylation, activation mode, localization in cells, or tissue distribution. No general structure of tyrosinase found in all species has been determined; however, all of them possess three domains: N-terminal, C-terminal, and central.[183] The central domain is conserved in all tyrosinases, and contains two copper binding sites. Three histidine residues coordinate each of two copper atoms.[184,185] Three-dimensional structure of the active cleft is presented in **Figure 19** based on Zou *et al.*[186] An example of monophenol hydroxylation mechanism including natural substrate – tyrosine, is presented in **Scheme 3**.[187,188]
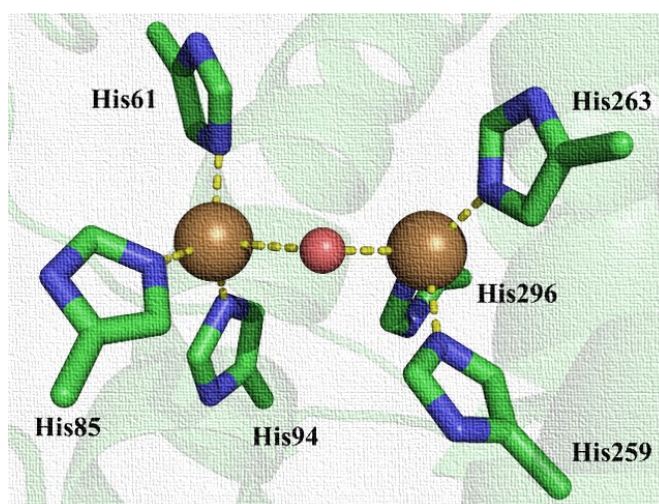
Figure 19. Tyrosinase active site. Copper atoms are presented as brown, and oxygen atom as red spheres.[186]
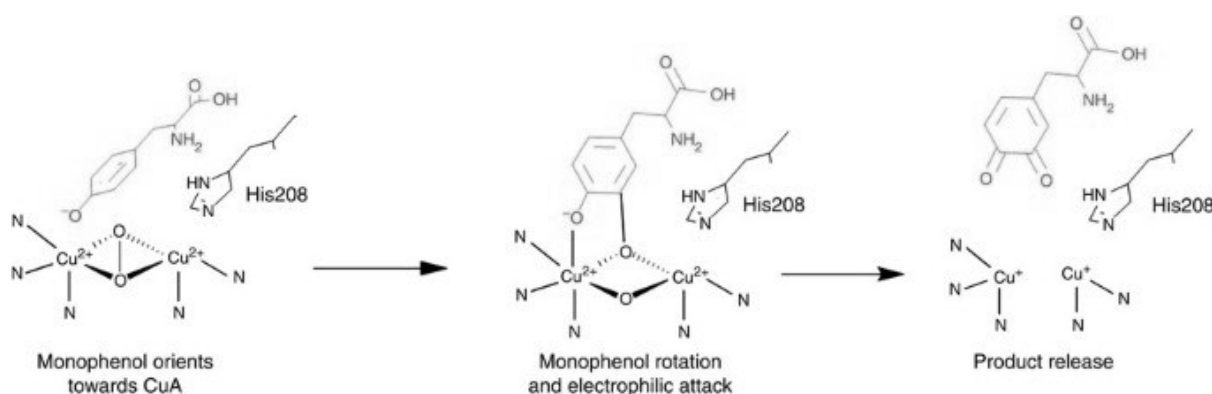
Scheme 3. Monophenol hydroxylation mechanism based on Deeth and Dietrich, adopted from Goldfeder *et al.*[187,188] Natural substrate, tyrosine, is present at the very first step of this process (gray).

With a view to this thesis, mushroom tyrosinase (mTYR) isolated from the species *Agaricus bisporus* was used. It is a common model applied during the investigations of new tyrosinase inhibitors, instead of use of human tyrosinase (hTYR). Hence, the structural properties of mTYR will be described below. Nevertheless, there are some papers indicating major differences between mTYR and hTYR. To be consistent and not to omit the significance of this aspect, recognized discrepancies between these two tyrosinase types will be briefly indicated in the next subsection.

Tyrosinase from *A. biosporus.* Mushroom tyrosinase from *A. bisporus* consists of two heavy and two light subunits, marked as H and L, respectively. Quaternary structure of tyrosinase was described in 1976 by Strothkamp *et al.*, and has been investigated by sodium dodecylsulfate-acrylamide gel electrophoresis.[189] Total molecular mass of this enzyme is 120 kDa, with two heavy subunits of ~43 kDa each, and two light subunits of ~14 kDa each. The H-subunit is responsible for the catalytic activity. The role L-subunit is unknown, but in 2017 is the first report on the biological characteristics and implication of L-subunit of tyrosinase was published.[190] Beside the catalytic cleft, there are other structural properties of tyrosinase that are important for its activity. Protein structure is stabilized primarily by sulfide linkages, but their location varies among organisms. Six disulfide bridges are conserved in the entire family of tyrosinases: Cys30-Cys41, Cys42-Cys65, Cys56-Cys99, Cys101-Cys110; Cys258-Cys261, and Cys290-Cys303.[191]

Differences between human and mushroom tyrosinase. A plentiful of tyrosinase inhibitors were synthesized and described in the literature. Despite this fact, only a few of them are applied in the industry due to the unsatisfactory clinical efficacy.[192] It is because of the fact that mTYR from *Agaricus bisporus* is the most widely

used tyrosinase during the inhibitory assays. It has been already demonstrated that the catalytic activity and substrate specificity of mTYR is different from mammalian enzyme.[193] Difficulties in obtaining enough quantity of hTYR impedes the progress in kinetic or structural exploration regarding human tyrosinase. Therefore, the data on hTYR inhibitors mechanisms is still missing.[193]

A while ago, an interesting paper concerning structural differences between mushroom and human tyrosinase was published.[194] These two enzymes share only about 23% of their amino acid sequences. Consequently, the differences in their active pockets were investigated by comparing the inhibitory activities of 6 stilbenes possessing two aromatic rings A and B, already known tyrosinase inhibitors. hTYR was obtained by cells homogenization, where supernatant was dialyzed afterwards to obtain human crude tyrosinase. It resulted that the compounds without active hydroxyl group in the ring A did not show any activity against mTYR but were effective for hTYR. On the contrary, the absence of -OH groups in the B ring provoked weak activity against hTYR, but good against mTYR. These results depicted that the A ring of stilbene can enter only in the active pocket of mTYR, and ring B – in the active pocket of hTYR.[194]

Due to the lack of information and limited availability of hTYR for its wide structural investigations, majority of research in tyrosinase inhibition is still conducted applying mushroom model. Accordingly, also the research presented in this thesis employed mTYR during the biological evaluation of new inhibitors. Summing up, it must be known that the difference of the tyrosinase active pockets among species may mislead the design of new inhibitors, and the scientists should be warned to choose the suitable resources for their biological assays, according to the current scientific development, materials availability, and the state of art.

External factors associated with hyperpigmentation. Skin darkening is most frequently caused by the melanin overproduction. Therefore, the control of tyrosinase activity is essential for the treatment of hyperpigmentation disorders. Melanogenesis can be enhanced by extended exposure to sun, skin injuries, inflammatory diseases, or abnormal skin growths, such as moles and melanomas. UV radiation, tobacco smoking, and air pollution are highly involved in so-called *environmental skin aging*, and consequently the skin in more prone for faster appearance of signs of aging, originally provoked by biological processes.[180] Also oxidative stress is one of the most important mechanisms affecting skin condition.

Interestingly, hormones such as melatonin were found to play critical role in photoaging.[180]

Auspiciously, a strong interest in photoaging and hyperpigmentation prevention is recently observed. Due to esthetical, but mostly health reasons, people consider the everyday use of UV filters, thus protecting the skin and counteracting the overactivity of tyrosinase. It must be underlined that fast and uncontrolled cellular processes, such as melanogenesis, may lead to unproper cell proliferation, generating the possibility of melasma.

For those who already have problems with skin pigmentation, various cosmetics and cosmeceuticals have been introduced to the market. These formulas are mostly based on tyrosinase inhibiting agents, which will be discussed later in the next subchapter.

2.8 Already known tyrosinase inhibitors

Various compounds were found to be good tyrosinase inhibitors, from both natural and synthetic sources. A few relevant examples of such compounds are presented in **Figure 20**, based on paper by Karimian *et al.*[195] Different tyrosinase inhibitors were the point of various reviews in the past years.[196–199] Herein the particular attention will be paid to kojic acid (KA) and its derivatives, thiosemicarbazones (TSCs), and peptide inhibitors together with examples of peptide conjugates. These classes of compounds were relevant for the design of new inhibitors, further synthesized and evaluated in this thesis.
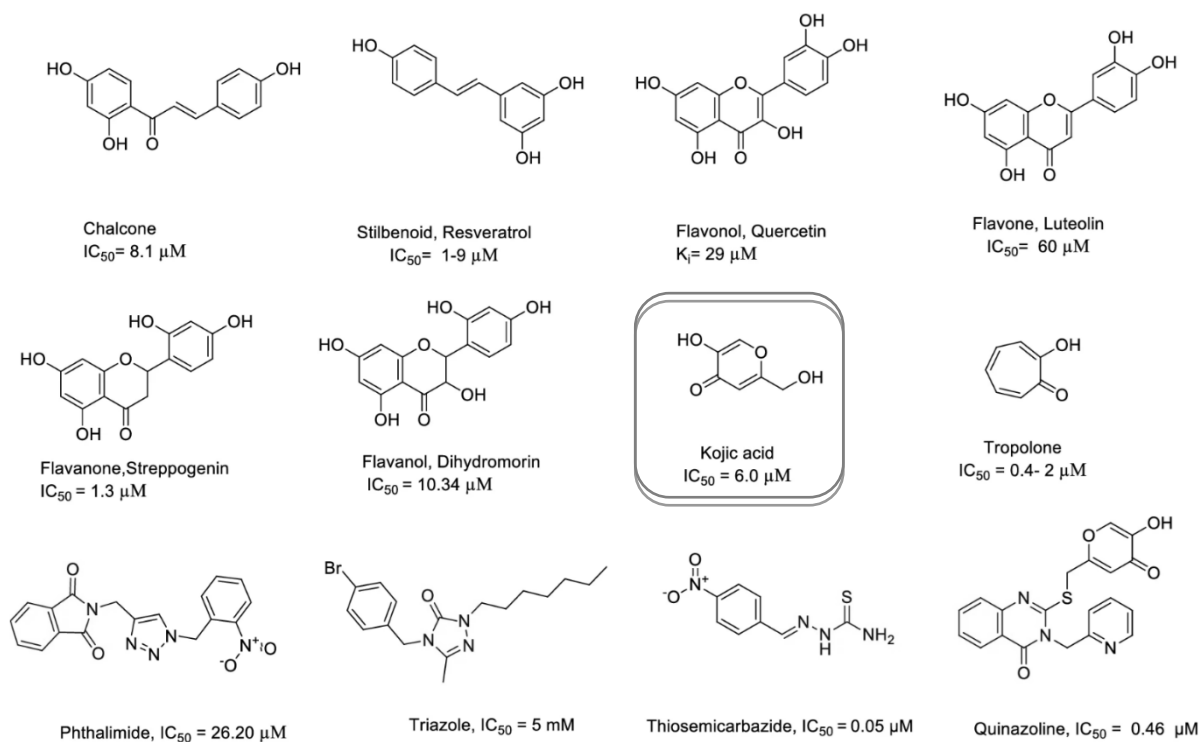
Figure 20. Structures of some examples of tyrosinase inhibitors from natural or synthetic sources, based on Karimian *et al.*[195] Kojic acid structure was framed; its IC_{50} value depends on the source.

2.8.1 Kojic acid and its derivatives

Kojic acid (5-hydroxy-2-(hydroxymethyl)-4*H*-pyran-4-one, **Figure 21**), a fungal metabolite, is the most extensively studied and well-described tyrosinase inhibitor.[200] Kojic acid was found also in bacterial strains, such as *aspergillus* and *penicillium*.[201] It has already been applied in various cosmeceutical formulas as skin-whitening agent. Kojic acid is also used in food industry, hence it prevents enzymatic browning of fruits and vegetables.
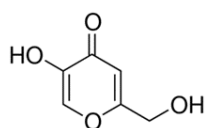
Figure 21. Kojic acid (KA).

Mechanism of action of KA is based on competitive inhibition on monophenolase activity, and a mixed inhibitory effect on the diphenolase activity against mTYR. It is able to chelate copper atoms in tyrosinase active cleft.[202] Biological activity of KA is connected to its γ-pyranone structure, containing an enolic hydroxyl group.[201] Together with tropolone and L-mimosine, kojic acid is very often used as the positive control and reference compound in the papers regarding new tyrosinase inhibitors. Very broad review article regarding the properties of kojic acid, its application in different sectors of

industry, and recent clinical trials was published in 2019, what emphasizes the large use of KA nowadays.[203]

Toxicity of kojic acid. Nevertheless the fact that kojic acid is widely used and applied in cosmetics and cosmeceuticals, it has been known that it has relatively insufficient inhibitory activity and stability (IC_{50}: 20 µM), with recognized toxicity: KA concentration safe for human topical applications is 1%, while the satisfactory depigmentation effect was observed at 4%.[204] The percentage of cell survive in the presence of 1, 10, and 100 ppm of KA was found to be 91.75, 92.36, and 86.92%, respectively.[205] Therefore, there is a strong need for new compounds, acting as effective tyrosinase inhibitors, but causing less side effects than originally used kojic acid.

Kojic acid derivatives. Various structural modifications have been applied in order to improve the inhibitory potential and stability of KA, they were mostly based on atom replacements or several conjugations:[201]

1) The replacement of O in the γ-pyranone ring with N, giving 4-pyridinone analogs,[206]
2) Conjugation with hydroxypyridinone–L-phenylalanine,[206]
3) Esterification of 2-(hydroxymethyl) group of kojic acid,[207]
4) Compounds with two KA moieties, e.g., connected by various linkers, such as ester, amide, and thioether.[208,209]

Evaluation of compounds from **1)** and **2)** showed good inhibition of one of the analogs against mTYR, cell viability assay indicated that it was non-toxic to assessed cell lines. 3,4-methylenedioxycinnamic acid ester of kojic acid from **3)** was more effective inhibitor of tyrosinase than kojic acid. Also, the method from **4)** provided *N*-kojic–amino acid–kojiate with higher inhibitory activity than *N*-kojic–amino acid by itself. Butylene dithioether derivative possessed superior inhibitory activity of melanin synthesis (1000-fold better than KA).

Kojic acid conjugated with amino acids. Noh *et al.* in 2009 evaluated the influence of the KA conjugation with amino acids on the inhibition of tyrosinase.[210] Twenty conjugates with general structure KA-aa-NH$_2$ were examined as inhibitors of mTYR. Most of them presented higher tyrosinase inhibition than KA alone. Interestingly, amino acids with aromatic side chains, such as Phe, Trp, Tyr, and His conjugated with KA provoked the increase of anti-mTYR activity to over 90% (in 20 µM concentration). The

most active compound, phenylalanine conjugate KA-Phe-NH$_2$, resulted with 99% of inhibition at 20 μM and IC$_{50}$ value 14.7 μM. Moreover, the stability of KA-Phe-NH$_2$ and KA were compared by their storage as 20 μM solutions in water in 50℃. The inhibitory activity of KA against mTYR decreased from 18% to 8% in 3 days, while the properties of Phe-derivative were maintained even after 3 months of the storage.

Kojic acid conjugated with peptides. Peptides conjugated with kojic acid were recently described in the literature, designed mostly to reduce KA cytotoxicity. In the paper by Noh *et al.*, twenty two kojic acid–tripeptide amides were prepared *via* solid-phase Fmoc/*t*Bu strategy.[211] Importantly, KA-tripeptide amides were as good inhibitors as KA-tripeptide free acids, but possessed superior activity to that of KA itself. It is a significant indication, regarding the fact that for the synthesis of such conjugates it is possible to use the resin of choice (both Wang and Rink Amide). KA-tripeptides amides remained stable under various conditions and maintained the inhibitory activity even after the storage. Among all tested compounds, FWY-derivative (either in amide or acid form) showed the best efficacy and stability.

Similar research was published in the intervening years by Kim *et al.*, where the kojic acid-FWY conjugate was found to be the most relevant tyrosinase inhibitor among all tested tripeptide-conjugates, and exhibited 100-fold better inhibitory against mTYR than KA (**Table 6**).[205] Additionally, the storage stability and cytotoxicity were evaluated. As previously, kojic acid-tripeptides maintained the stability for over 15 days; that of kojic acid decreased rapidly after just one day. Significantly, KA-tripeptides were less toxic than KA and were safe even at high concentrations, providing no changes in cell viability (up to 100 ppm).

Table 6. Conjugates of tripeptides with kojic acid, evaluated as mTYR inhibitors by Kim *et al.* [205]. Results are in accordance with Noh *et al.*[211]

CONJUGATE	IC$_{50}$ (μM)
Kojic acid, KA	22.94
KA-**Phe-Trp-Tyr**	0.24
KA-**Phe-Phe-Tyr**	0.33
KA-**Phe-Tyr-Tyr**	0.39
KA-**Trp-Trp-Tyr**	0.78
KA-Phe-Trp-Asp	2.13
KA-Phe-Trp-Ile	2.18
KA-Phe-Trp-Phe	4.48
KA-Phe-Trp-Trp	6.17

Finally, in 2016 another study regarding peptide conjugates with KA was published.[212] Peptides with different chain lengths and various amino acid residues were evaluated. One of the sequences, namely KA-PS, was found to be stable good inhibitor of tyrosinase and melanin content of B16F10 mouse melanoma cells, without exhibiting cell toxicity. However, in this research the selection of peptide sequences was not explained and justified sufficiently.

Additionally, the relevance of peptide conjugation with already known good inhibitors of tyrosinase was proven in case of mimosine.[213] Accordingly to results summarized in **Table 6**, also in this case mimosine conjugated with FFY, FYY, and FWY provided the most efficient tyrosinase inhibitors in the tested group (IC$_{50}$ in µM: 5.6, 6.1, and 7.4, respectively).

2.8.2 Thiosemicarbazones

Thiosemicarbazones as tyrosinase inhibitors were examined extensively over the past years. Examples of the most recent research in the field of thiosemicarbazones as tyrosinase inhibitors are those from Wroclaw University of Science and Technology,[214–216] and also from different groups.[217,218] TSCs usually act as chelators for transition metal ions, forming a bond *via* the sulfur or hydrazine nitrogen atoms located on the thiosemicarbazide moiety (**Figure 22**).[8,219] Due to these properties, thiosemicarbazones are great candidates for copper coordination in the active site of tyrosinase. In fact, different TSCs were evaluated for this purpose, and the most relevant examples of such inhibitors will be discussed below.
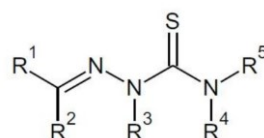
Figure 22. General structure of thiosemicarbazones. R^1-R^5: possible positions for the substituition.

Benzaldehyde thiosemicarbazone and its derivatives. TSCs based on benzaldehyde structure has been often investigated as tyrosinase inhibitors. Various substitutions at R^1 positions led to discovering active compounds, mostly by the incorporation of the aromatic ring: it provoked the affinity enhancement to the enzyme due to the similarity to natural substrates, such as L-Tyr and L-DOPA. Van deer Waals interactions were found between the aromatic ring and the active cleft of tyrosinase.[220] Various substitutions in the proximity of the phenyl ring were adopted in order to find

the derivative with high efficacy (**Table 7**). Importantly, bulky substituent Br did not provoke any decrease in the overall efficacy.

Table 7. Benzaldehyde thiosemicarbazone and its hydroxy- and methoxy-substituted derivatives, examined as tyrosinase inhibitors.[8]
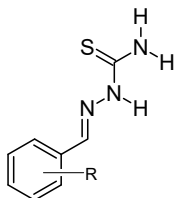
STRUCTURE NUMBERING FROM THE LITERATURE	R	IC_{50} (μM)
1	-	0.84-9.00
2	2-OH	0.38
3	3-OH	3.90
4	4-OH	0.41
5	4-OCH$_3$	1.48
6	4-Br	0.28
7	2-Br 4-OH	0.33
8	2,4-OH	0.18
9	2,5-OH	6.50
10	3,5-OH	>30
11	3,4-OH	>40
12	3-OCH$_3$ 4-OH	5.68
13	3-OH 4-OCH$_3$	4.88
14	2,5-OCH$_3$	>50

Acetophenone thiosemicarbazone and its 4-substituted derivatives. Investigations of *para* substitution in phenyl ring of acetophenone thiosemicarbazone containing methyl group in R^2 position were performed. They showed that the incorporation of different substituents in the proximity of phenyl ring gave the products with low IC_{50} values (<1 μM); significantly, even Br or huge biphenyl-aliphatic substituents did not affect the efficacy (**Table 8**).

Table 8. Acetophenone thiosemicarbazone and its derivatives, examined as tyrosinase inhibitors.[8]
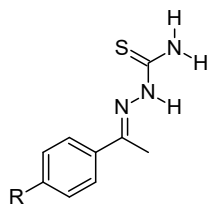
STRUCTURE NUMBERING FROM THE LITERATURE	R	IC_{50} (μM)
81	Aliphatic substituents C_4-C_6	<1
82		
83		
84		
85		
86	Cyclohexyl	0.632
87	CH_3	0.27
88	Br	0.17
89	F	0.54
90	Ph-CH_2COOH	1.661
91	Ph-CH_2COOCH_3	0.278
92	Ph-CH_2COOCH_2CH_3	0.437
93	Ph-CH_2COOCH_2CH_2CH_3	0.485
94	Ph-CH_2COOCH_2CH_2CH_3	0.562

Substitution with alkyl chain in R^2 position. Substitutions in the R^2 position has been found as highly undesirable when dealing with tyrosinase inhibitors.[214] When R^1 was occupied by (un)substituted phenyl ring, the elongation in in the R^2 position of the initial TSC led to decrease of tyrosinase inhibition, or total loss of such properties. It was demonstrated that methyl substituent does not affect the efficacy, but longer chains are unwanted.

Figure 23 demonstrates the summary of all abovementioned results published in the literature, to understand better the relevance of substitution in R^1-R^5 positions of thiosemicarbazone structure. As visible, the most convenient position for further modifications of TSCs is R^1, where the replacement with bulky substituents, such as Br, (bi)phenyl, or aromatic rings, did not decrease the anti-tyrosinase activity.

- *para*-substituted phenyl ring
- 5-membered aromatic, heterocyclic compounds
- Preferably H or Ph
- Preferably CH$_3$ or H
- Preferably H
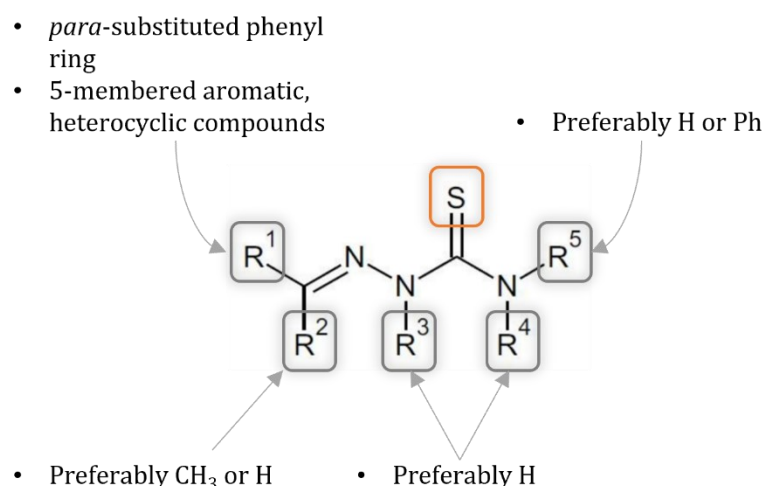
Figure 23. Structure-activity relationship of thosemicarbazones as tyrosinase inhibitors. Sulfur atom, essential for the inhibitory activity, was evidenced.[8]

Up to now, no data regarding peptides conjugated with thiosemicarbazones as tyrosinase inhibitors has been published. Very recently Haseloer *et al.* investigated the L-lysine-TSC ligands conjugated *via* standard SPPS (**S**olid-**p**hase **P**eptide **S**ynthesis) to the cell-penetrating peptide sC18.[221] The purpose of this research was to enhance the overall solubility of TSC by the lysine linkage, and highlight the application of sC18-conjugates as nontoxic and stable Pt^{II}-chelators for radioisotope labeling. Important finding is that thiosemicarbazone structure is stable both in coupling conditions and during the acidic cleavage from the resin.

2.8.3 Peptides as inhibitors of tyrosinase

Various peptides were found to inhibit tyrosinase. The inhibition was not always at the satisfactory level, however the observations from obtained data provide valuable indications for the further design of peptide-based tyrosinase inhibitors. From the results summarized in the subsection regarding kojic acid and its conjugates (**Table 6**), it can be deduced that preferable amino acids are aromatic and hydrophobic (Phe, Trp, and Tyr), and the tyrosine should be located on C-terminus of the chain. In case of the inhibition by KA-conjugates, there was no difference between free acid and amide compounds. In this chapter, more examples from the recent studies regarding tyrosinase inhibition by peptides will be discussed. Current development in this field was summarized in the review from 2021, one of a few review articles regarding aforementioned topic.[222] Food-deriving peptides with similar properties were described too.[223] Nevertheless, it must be underlined that this summary evidenced the fact that peptides by themselves are rather poor tyrosinase inhibitor (e.g., one of the most potent

Cyclo[Gly-Gly-Tyr-Leu-Pro-Pro-Leu-Ser] exhibited IC_{50} value of 50 μM), but the conjugation with already known inhibitors, e.g., kojic acid or mimosine, resulted with very good efficacy associated with lower cellular toxicity than the conjugated ligand. Another time, the C-terminal location of Tyr was found to be relevant for the inhibitory activity.

One of the first reports about peptides as tyrosinase inhibitors are from 1993 and 1994, when the properties of cyclic peptides from lactic bacterium *Lactobacillus helveticus* and *Pseudostellaria heterophylla* roots were studied.[224,225] Bacteria-deriving cyclotetrapeptide cyclo(-L-Pro-L-Tyr-L-Pro-L-Val-) caused 50% of tyrosinase inhibition in 1.5 mM concentration, with the reference to arbutin as positive control (IC_{50}: 5 mM). Compounds isolated from *Pseudostellaria heterophylla*: cyclo[Gly-Pro-Tyr-Leu-Ala], cyclo[Gly-Ile-Gly-Gly-Gly-Pro-Pro-Phe], and cyclo[Gly-Thr-Leu-Pro-Ser-Pro-Phe-Leu] inhibited mTYR with the following values of IC_{50}: 131, 187, and 63 μM, respectively. Interestingly, the research regarding plant-derived compounds published only 1 year after the paper regarding *Lactobacillus helveticus*, declares the IC_{50} value of arbutin as 1.2 mM; nowadays it is about 115 μM.[226] It shows how the accuracy of measuring methods has been improved in the past 30 years.

SPOT synthesis was applied in order to screen for new peptides interacting with tyrosinase.[227] A variety of different peptides was examined towards binding abilities with tyrosinase, but also their inhibitory properties. It was found that peptides with Glu and Asp residues usually do not bind well to mTYR; Lys was found in both binding and non-binding peptides; hydrophobic and/or aliphatic residues were noticed to be important for the inhibition. Despite the very broad study performed in this work, no precise values of IC_{50} were reported; the percentage values of binding and inhibition without declaring the concentration cannot be considered as indicative.

Due to the presence of copper atoms in tyrosinase active site, diverse studies implemented Cys residue in new inhibitors, for the chelating properties.[228] C-terminal tyrosine residue was crucial for the activity – this property was confirmed i.e. by the activity of dipeptide WY and tripeptide KFY (IC_{50} of KFY: 564.9 μM; KFY$_{activity}$≥WY$_{activity}$>arbutin$_{activity}$). The relevance of cysteine residue at N-terminus was demonstrated by RCY and CRY tripeptides with high tyrosinase inhibitory potency. CRY sequence presented the most striking inhibitory potency against mTYR (IC_{50}: 6.16 μM). The continuation of this study resulted with potent cysteine-containing dipeptide

inhibitors against tyrosinase.[229] Inversion of dipeptides sequences in major advantage resulted in worse activity of peptides with C-terminally located Cys (**Table 9**). Cys-Cys analog possessed IC_{50} value equal to 3.2 μM.

Table 9. Cys-containing dipeptides examined as mTYR inhibitors by Tseg *et al.*[229]

PEPTIDE SEQUENCE (H-aa$_1$-aa$_2$-OH)	IC_{50} (μM)	PEPTIDE SEQUENCE (H-aa$_1$-aa$_2$-OH)	IC_{50} (μM)
Cys-Glu	2.0	Glu-Cys	140.1
Cys-Phe	2.7	Phe-Cys	7.9
Cys-Tyr	3.1	Tyr-Cys	131.6
Cys-Gln	3.5	Gln-Cys	5.9
Cys-Ile	4.0	Ile-Cys	4.5
Cys-Ser	4.5	Ser-Cys	28.3
Cys-Met	4.9	Met-Cys	10.7
Cys-Trp	5.4	Trp-Cys	47.3
Cys-Gly	5.9	Gly-Cys	24.6
Cys-Lys	5.9	Lys-Cys	39.9
Cys-Leu	8.0	Leu-Cys	14.5
Cys-Arg	8.0	Arg-Cys	32.3
Cys-Val	8.2	Val-Cys	8.3
Cys-Thr	8.2	Thr-Cys	44.0
Cys-Ala	9.6	Ala-Cys	62.2
Cys-His	10.7	His-Cys	20.0
Cys-Asp	14.1	Asp-Cys	56.1
Cys-Asn	22.6	Asn-Cys	5.3
Cys-Pro	55.8	Pro-Cys	20.3

Another example of cysteine-containing peptide with tyrosinase inhibitory activity was discovered recently.[230] Pentapeptide EF-5 with a sequence ECGYF was found to possess free radical scavenging ability, and inhibit tyrosinase with moderate potential (IC_{50}: 0.46 mM). Molecular docking showed that the EF-5 binding to tyrosinase was stabilized mostly by hydrogen bonds and hydrophobic interactions. Importantly, once again the peptide resulted to be nontoxic to cells.

Eleven different tripeptides were evaluated as inhibitors of tyrosinase, amongst them the cysteine-containing sequences showed the highest efficacy (**Table 10**).[228] Additionally, comparing this data with the results in **Table 6**, it is well visible that the conjugation of simple FFY peptide with kojic acid is highly valuable (IC_{50} 241.1 vs. 0.33 μM).

Table 10. Eleven tripeptides examined as mTYR inhibitors by Hsiao *et al.*[228]

PEPTIDE SEQUENCE (H-aa_1-aa_2-aa_3-OH)	IC_{50} (μM)
Arg-Cys-Tyr	6.16
Cys-Arg-Tyr	127.5
Phe-Phe-Tyr	241.1
Arg-Trp-Tyr	397.8
Lys-Phe-Tyr	564.9
Lys-Asn-Tyr	719.3
Asn-Phe-Tyr	761.2
Lys-Asp-Tyr	800.5
Lys-Val-Tyr	841.9
Val-Phe-Tyr	1143.0
Lys-Lys-Tyr	1512.4

Cosmeceutically relevant peptides with anti-tyrosinase activity can be obtained also by combining already known sequences and D-tyrosine at the C-terminus.[231] C-terminal implementation of D-tyrosine in GEKG or GHK peptides resulted with bifunctional products, decreasing melanin synthesis in cells without losing their anti-inflammatory properties. It has been previously demonstrated that D-tyrosine, unlike L-tyrosine, is capable of reducing the melanin content in human melanoma cells and primary human melanocytes in dose-dependent manner.[232]

Summing up, the following indications should be considered during the design of new inhibitors of tyrosinase, based on peptides:

1) Peptide sequences should be rather short (up to 5 amino acids),
2) Tyrosine should be located on C-terminus of the sequence,
3) There is no difference in the activity of peptides with amide or acid C-terminal modification,
4) Cysteine and aromatic amino acids with hydrophobic properties, such as phenylalanine, tyrosine, or tryptophan, are valuable due to their binding potential to the active cavity of tyrosinase – Cys for chelating effect, and Phe, Tyr, Trp for the formation of hydrophobic interactions,
5) Peptides by themselves usually are not excellent inhibitors of tyrosinase – in most cases they show rather moderate efficacy, with IC_{50} value over 100 μM. Therefore, it is valuable to consider their conjugation with small molecules with proven activity, such as kojic acid,
6) The conjugation of peptides with thiosemicarbazones has not been reported up to date, despite their proven efficiency in tyrosinase inhibition.

Chapter 3: Aim and objectives

Due to the expanding interest in skin health and outward appearance, and the increasing role of peptides in this field, the aim of presented research was to try to meet this demand. In this interdisciplinary thesis, by involving chemical methods of synthesis, biological evaluation of activity by *in vitro* assays, *in silico* methods to understand the interactions at molecular level, and various analytical methods for the characterization of new compounds, the main objectives were as follows:

1) Establish the current state of the art in the field of peptide inhibitors as anti-wrinkle and anti-hyperchromic agents,

2) Evaluate the possibility of conjugation of peptides with small organic molecules, possessing potential (1,2,4-triazoles) or already known (thiosemicarbazones) biological activity against two enzymes: elastase and tyrosinase,

3) Design the synthetic pathway of conjugation in rational way and in non-demanding conditions, decreasing the purification steps by the incorporation of solid-phase synthesis, when possible, thus increasing the yield,

4) If applicable, evaluate the effect of different conjugation positions on the potential activity,

5) Find out how the incorporation of the lysine linker may influence the three-dimensional structure of the final product, due to the reported data regarding the relevance of linker involvement,

6) Synthesize, purify, and analyze obtained peptides and their conjugates,

7) Evaluate the biological activity of synthesized compounds by *in vitro* assays,

8) Understand and explain obtained results,

9) Investigate possible interactions and explain eventual discrepancies using molecular modeling and molecular docking methods,

10) Finally, summarize obtained data to clarify the prospective in new elastase and tyrosinase peptide inhibitors design.

In the following chapters the rationality of the design of new compounds will be discussed, regarding the literature studies described before. The methodology implied during this PhD project will be presented, together with synthetic strategies and analytical methods. Obtained results will be discussed, providing the valuable data for understanding the nature of investigated enzymes.

Chapter 4: Experimental part

4.1   Design of new compounds

Regarding the data summarized in the previous chapters, the use of peptides and their derivatives appears to be a useful strategy in the design of new elastase and tyrosinase inhibitors. As demonstrated, in most cases peptides without any structural modification are good but not excellent inhibitors. Their activity can be improved, e.g., by the conjugation with low-molecular compounds (major advantages and strategies of the conjugation were presented in the subchapter **2.2 Peptides conjugated with small organic molecules**). Therefore, the design of new compounds for the purpose of this thesis was based on the selection of relevant peptide sequence, previously or currently investigated, and valuable small organic compound with proven or potential activity against the selected enzyme.

4.1.1   Potential elastase inhibitors: conjugates of peptides and 1,2,4-triazoles

Elastase inhibitors based on peptides should include hydrophobic, aliphatic amino acids with small side chains. Low-molecular compounds for the conjugation, potentially increasing the inhibitory activity of the final molecule, can possess a heterocyclic ring, providing additional interactions with -OH group of Ser-195 in the elastase active cleft.

Peptide sequence. Peptide SA1-III introduced in the previous chapters was found to function as collagen turnover modulator. It derives from serpin A1, natural inhibitor of serin proteases. Analyzing the properties of its amino acid sequence, the first five residues are hydrophobic (underlined: Ac-<u>MGKVV</u>N<u>P</u>TQK-NH$_2$). Considering the substrate preferences of human neutrophil elastase, and the relevance of SA1-III peptide in the cosmeceutical field, MGKVV sequence was selected as the starting point for derivatization and structural modifications described herein.

Low-molecular weight compounds for the conjugation. One of the drawbacks of peptides for topical applications is the fact that their hydrophobicity, highly required due to the increased skin permeation, frequently is problematic during the biological assays and the formulation. Hence, when choosing a structural modification of new peptide inhibitors of elastase, diverse factors should be considered. Firstly, there must be a free carboxyl group present in the structure, permitting the conjugation. Moreover, no other reactive groups (e.g., another free -COOH) should be present. Secondly, if possible, the attached moiety should increase the solubility of the

final product rather than provide more hydrophobicity. Finally, this type of modification requires a small, organic molecule, which is resistant in both acidic and basic conditions, due to the conjugation *via* amide bond formation performed in solid-phase. A great example of such compounds is the group of 1,2,4-triazolocarboxylates. One of the first reports regarding the structural data of 1,2,4-triazole-including derivatives was published in late 1960s by Bagal *et al.*[233] In the past 10 years, the group of Sączewski investigated structural properties and antibacterial activity of fluorescent 4,6-dimethylisoxazolo[3,4-*b*]pyridin-3(1*H*)-one derivatives: dihydro-[1,2,4]triazolo[4,3-*a*]pyridin-2-ium carboxylates, so-called *Safirinium* dyes (**Figure 24**).[234–237] Among various experiments, Authors reported the labeling of Ac-AKF-NH$_2$ peptide with carboxylates, however this method requires the synthesis in solution (*N,N'*-Dimethylformamide – DMF, or H$_2$O) after the peptide cleavage, and is restricted to one, free, reactive amine group present in the sequence. Up to now, derivatives of compound presented in **Figure 24** were not examined as elastase inhibitors. Moreover, they possess fluorescent properties and thus can be further used for the labeling in bioimaging assays. Peptides with inhibitory activity and deploying fluorescence could be then investigated towards their metabolic pathways in cells.
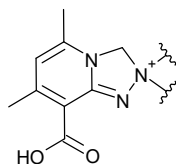
Figure 24. General structure of 5,7-dimethyl-2,3-dihydro[1,2,4]triazolo[4,3-*a*]pyridine-8-carboxylic acid derivatives.

Synthetic strategies. To provide more possibilities of the modifications in the peptide chain, and to avoid the synthesis in solution, a new strategy including building block synthesis was designed and will be discussed further in the next chapters. The purpose of such synthesis was to obtain functionalized lysine residue with heterocyclic moiety attached in the lysine side chain. It would permit to incorporate the triazolium core in any peptide of choice during the SPPS, at the selected position in a peptide chain. It would be a great advantage in respect of the method described previously. Moreover, due to the presence of free carboxyl group in such compounds, N-terminal tagging of a peptide is another synthetic strategy for the conjugation. The fact that such derivatives are obtained by the reaction of a secondary amine, provides a possibility to perform the synthesis directly with proline, which is the only proteinogenic amino acid with this kind of properties. Furthermore, the presence of quaternary nitrogen atom with

permanent positive charge provides significant increase of solubility of the final conjugate.

Therefore, in this thesis the solid-phase synthesis of lysine-based building blocks including four various heterocyclic moieties based on *Safirinium* dyes will be described. They can be incorporated easily during the peptide elongation without any limitations. Moreover, the derivatization process of two similar SA1-III-deriving sequences with four different heterocyclic compounds in two diverse positions in the chain was performed. Additionally, the possibility of on-resin reaction of N-terminal Pro (a secondary amine) and 4,6-dimethylisoxazolo[3,4-*b*]pyridin-3(1*H*)-one, providing fluorescent product achieved during one cycle of peptide synthesis, will be described.

Secondary amines were selected considering their commercial availability, price, and toxicity (i.e., piperidine was reported as a toxic compound, while selected analog 4-methylpiperidine (**A**) was not). Finally, four different amines used to obtain various analogs were chosen according to their structural properties, potentially providing differences in the bioactivity. Thus, 5- and 6-membered rings were considered, as well as linear amines; the presence of a heteroatom in the ring, such as an oxygen, was also included. Designed carboxylates with corresponding Fmoc-lysine building blocks are summarized in **Table 11**.

Table 11. Structures of desinged fluorescent building blocks and their precursors.

SECONDARY AMINE	HETEROCYCLIC MOIETY	CORRESPONDING Fmoc-Lys[Nε(...)]-OH BUILDING BLOCK
4-Methylpiperidine **A**	8-carboxy-4',5,7-trimethyl-3H-2λ⁵-spiro[[1,2,4]triazolo[4,3-a]pyridine-2,1'-piperidin]-2-ylium **4**	Fmoc-Lys[Nε**(4)**]-OH **4a**
Pyrrolidine **B**	8-carboxy-5,7-dimethyl-3*H*-2λ⁵-spiro[[1,2,4]triazolo[4,3-*a*]pyridine-2,1'-pyrrolidin]-2-ylium **5**	Fmoc-Lys[Nε**(5)**]-OH **5a**
Morpholine **C**	8-carboxy-5,7-dimethyl-3*H*-2λ⁵-spiro[[1,2,4]triazolo[4,3-a]pyridine-2,4'-morpholin]-2-ylium **6**	Fmoc-Lys[Nε**(6)**]-OH **6a**
N-Ethylisopropyla-mine **D**	8-carboxy-2-ethyl-5,7-dimethyl-2-(propan-2-yl)-2*H*,3*H*-[1,2,4]triazolo[4,3-*a*]pyridin-2-ium **7**	Fmoc-Lys[Nε**(7)**]-OH **7a**
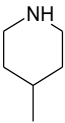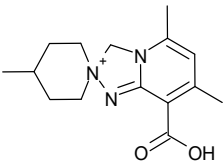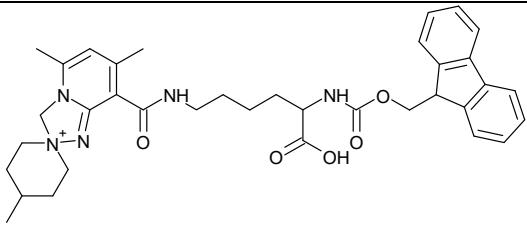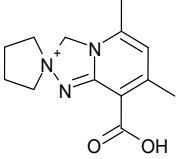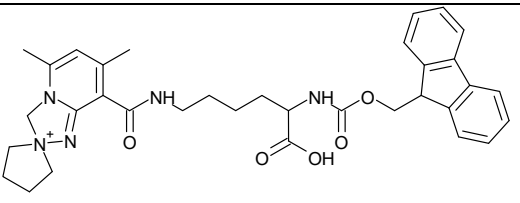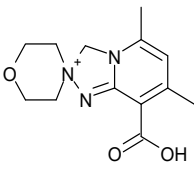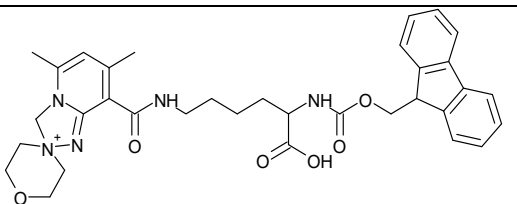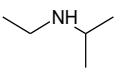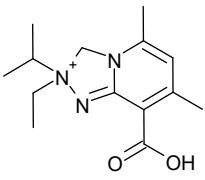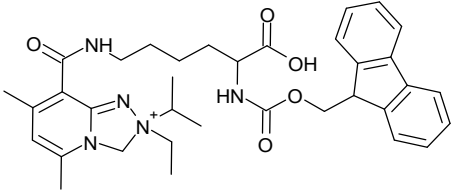
To evaluate the influence of different positions of the modification on the biological activity of the final compounds, and to estimate the influence of the lysine linker on both structural and biological properties, 17 different derivatives were designed (**Table 12**).

Table 12. Structures of all obtained peptides for the elastase inhibition assay and their derivatives. Standard amino acids are represented with a single-letter code.

	Ac-MGKVV-NH$_2$ **8**	Ac-PGKVV-NH$_2$ **9**
Method I: tagging N-terminal Pro residue	*no N-terminal Pro residue*	**10**
Method II: N-terminal tagging	**11**	**15**
	12	**16**
	13	**17**
	14	**18**
Method III: Fmoc-Lys[N$^\varepsilon$(…)]-OH building block can be introduced during the SPPS	**19**	**23**
	20	**24**
	21	**25**
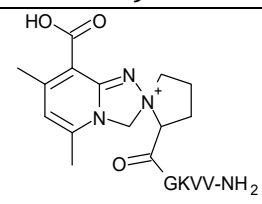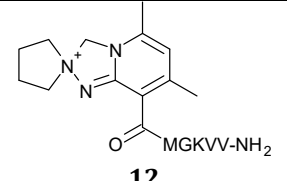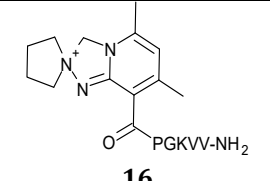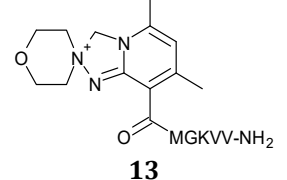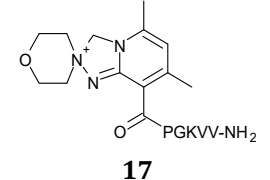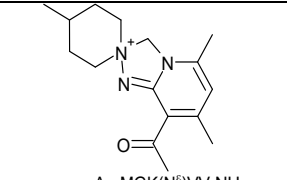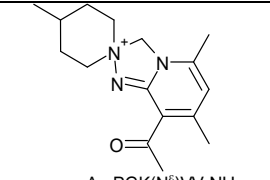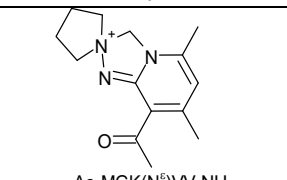
	Ac-MGK(N$^\varepsilon$)VV-NH$_2$ **22**	Ac-PGK(N$^\varepsilon$)VV-NH$_2$ **26**
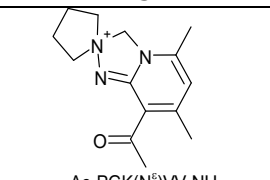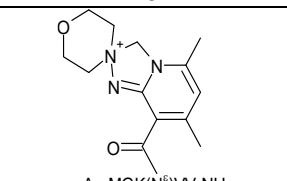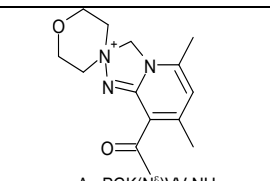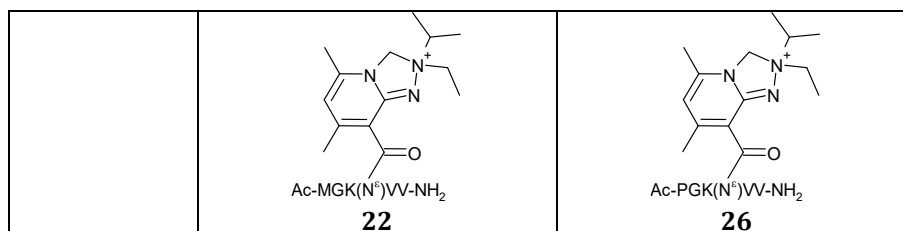
The synthesis of compounds **4-7**, **4a-7a**, and **8-26** will be reported in the subchapter **4.3**.

4.1.2 Potential tyrosinase inhibitors: conjugates of peptides and thiosemicarbazones

According to the current state of the art, peptides as potent inhibitors of tyrosinase should be rather short (di-, tri-, tetrapeptides). Preferential amino acid residues are cysteine (for Cu-chelating properties), phenylalanine, tyrosine, and tryptophan (due to their similarity to the natural substrate, and hydrophobic interactions provided by the aromatic ring). Nevertheless, peptides by themselves are not excellent tyrosinase inhibitors and various conjugations were applied to improve this attribute, e.g., with previously described kojic acid, or mimosine and kaffeic acid. More often than not, such conjugation provided also lower toxicity and prolonged shelf-life of the final compound in comparison with small moiety alone.

Peptide sequence. Up to now, peptides including Phe, Tyr, and Trp were examined as tyrosinase inhibitors only in one of the possible sequences: Phe-Phe-Tyr and resulted with IC$_{50}$=241 µM against mTYR. Considering the proven necessity of Tyr located on the C-terminus, and preferential location of Phe at the beginning of the sequence, herein other variants of such tripeptides will be evaluated: Phe-Phe-Tyr (FFY), Phe-Tyr-Tyr (FYY), and Phe-Trp-Tyr (FWY). Moreover, in case of different conjugates of active compounds with tripeptides, these examples resulted with extremely high efficacy in the inhibition assays against mushroom tyrosinase (**Table 13**).

Table 13. Examples of conjugates with peptides FWY, FFY, and FFY, reported and evaluated as tyrosinase inhibitors. Data from previously discussed literature.

Conjugated molecule	Final compound	IC$_{50}$ against mTYR (μM)
Kojic acid	KA-Phe-Trp-Tyr	0.24
	KA-Phe-Phe-Tyr	0.33
	KA-Phe-Tyr-Tyr	0.39
Mimosine	Mimosine-Phe-Trp-Tyr	7.4
	Mimosine-Phe-Phe-Tyr	5.6
	Mimosine-Phe-Tyr-Tyr	6.1
-	Phe-Phe-Tyr	241.1

Low-molecular weight compounds for the conjugation. Kojic acid, widely described and evaluated tyrosinase inhibitor, results with IC$_{50}$=20 μM against mTYR. This compound was conjugated with peptides in various combinations and the conjugation was always advantageous. Other examples of excellent tyrosinase inhibitors are thiosemicarbazones with IC$_{50}$ at micromolar level, even below the value of 1 μM. Up to now, there is no reported data on the topic of thiosemicarbazones conjugated with peptides. During the structure-activity relationship studies of TSCs, it has been shown that the most convenient position for further conjugation of thiosemicarbazones with another molecules is *para* position of the aromatic ring. This location of a bulky substituent generally did not affect their activity as inhibitors of tyrosinase. Nevertheless, there are other positions in TSC structure (R^1-R^3) which can be substituted. The influence of various substitutions in these positions (**27-41**), with simultaneous maintaining of a bulky Br in position *para* of the aromatic ring was examined (**Table 14**). Thereby, the most convenient type of substitution in the proximity of thiourea group could be determined. Previously investigated analog **42** (IC$_{50}$=1 μM) was added as a positive control.

Table 14. Thiosemicarbazones used for the optimization of the position of further conjugation.
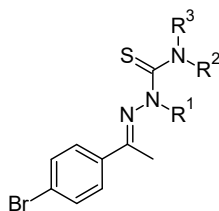
COMPOUND NUMBER	R^1	R^2	R^3	MW [g/mol]
27	H	H	1-adamantyl	406
28	H	H	CH_2CH_2Ph	376
29	H	H	*n*-hexyl	356
30	H	H	*n*-butyl	328
31	H	H	CH_2-$C(CH_3)$=CH_2	326
32	Me	H	Me	300
33	H	Me	*n*-butyl	342
34	H	H	Ph	348
35	H	H	CH_2Ph	362
36	H	H	cyclo-hexyl	354
37	H	H	CH_2CH=CH_2	312
38	H	Me	cyclo-hexyl	368
39	H	Me	CH_2Ph	376
40	H	H	Me	286
41	H	H	*n*-octyl	384
42	H	H	H	272

All new analogs **27-41** were found to be relatively poor inhibitors of tyrosinase. Some of them were insoluble in the assay buffer in tested range of concentrations or did not provoke any relevant inhibitory effect. Only two of all tested TSCs in this group provoked a moderate inhibition of tyrosinase and did not precipitate in the assay buffer. In the **Figure 25** the most pertinent results of this initial assay are presented.
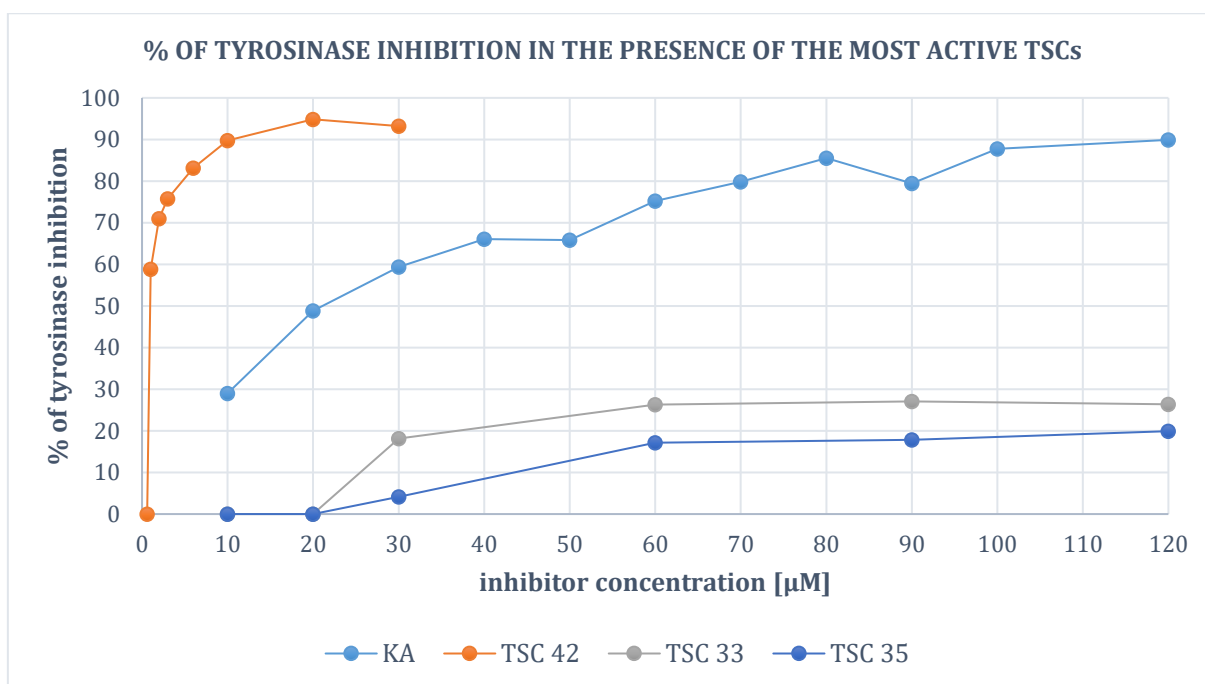
Figure 25. Percentage of tyrosinase inhibition in the presence of selected compounds among **27-42**: KA – kojic acid, commercially available positive control; TSC **42** – already known excellent inhibitor of tyrosinase; TSCs **33** and **35** – two examples of new TSCs with noticeable inhibitory effect in the tested group.

It was demonstrated that the kojic acid and TSC **42** are better inhibitors than newly tested compounds **27-41**. It indicates and confirms the importance of thiourea group in the inhibitory activity against tyrosinase, in accordance with the data summarized in the **Figure 23**. It may be assumed that the preferable position for the peptide chain attachment should not be in the proximity of the thiourea group. Therefore, different thiosemicarbazones possessing free -COOH, with small modifications in positions R^1, R^2, R^3 are required for the conjugation. Examples of such compounds, synthesized for the purpose of this thesis, are presented in **Figure 26**. Compounds **43** and **45** with carboxyl group in the position *para* of the aromatic ring differed between each other with one additional methyl group. TSC **44**, the most branched among three proposed structures, was included to evaluate the influence of the presence of two aromatic rings on the inhibitory properties of the final product. Thus, peptide sequences treated as bulky substituents, would have been in the most convenient position distanced from the thiourea group of each TSC.
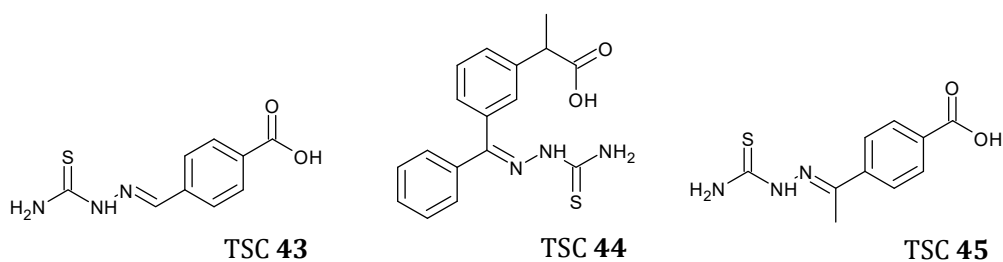
Figure 26. Thiosemicarbazones **43-45** with free and reactive carboxyl group for the conjugation with peptides.

Synthetic strategy. Free carboxyl group present in compounds **43-45** permits to perform the conjugation *via* amide bond formation in solid-phase, as N-terminal modification of selected tripeptides. Proposed structures of conjugates are summarized in **Table 15**. Control sequences **46-48** will be acetylated at N-terminus instead of the conjugation with TSC.

Table 15. Structures of all obtained peptides for the tyrosinase inhibition assay, and their conjugates with thiosemicarbazones. Standard amino acids are represented with a single-letter code.

The synthesis of compounds **46-57** will be reported in the subchapter **4.3**.

4.2 Materials

All Fmoc-protected amino acids were purchased from Iris Biotech GmbH (Marktredwitz, Germany). Peptide-synthesis grade *N,N′*-Dimethylformamide (DMF) and acetonitrile (ACN) were purchased from Carlo Erba (Milan, Italy). Dichloromethane (DCM), trifluoroacetic acid (TFA), triisopropylsilane (TIS), methanol (MeOH), piperidine,

N,N′-Diisopropylethylamine (DIPEA), *N*-Methylmorpholine (NMM), 1,2-Ethanedithiol (EDT), acetic anhydride, KOH, HCl, NH$_2$OH·HCl, ethyl cyanoacetate, 2,4-Pentanedione (acetylacetone), formaldehyde, secondary amines: 4-Methylpiperidine, pyrrolidine, morpholine were purchased from Sigma-Aldrich (Milan, Italy). *N*-Ethylisopropylamine was purchased from TCI Chemicals. Rink amide AM resin (100-200 mesh, loading: 0.74 mmol/g) was purchased from CBL. Fmoc-Tyr(*t*Bu)-Wang resin (100-200 mesh, loading: 0.70 mmol/g) and Fmoc-Lys(Mtt)-Wang resin (100-200 mesh, loading: 0.54 mmol/g) were purchased from Novabiochem. All the ingredients for elastase activity (enzyme – Porcine Pancreas Elastase, PPE, EC 3.4.21.36; substrate – N-Succinyl-Ala-Ala-Ala-*p*-nitroanilide, SucAla$_3$-*p*NA; control inhibitor – MeOSuc-Ala-Ala-Pro-Val-chloromethylketone, MeOSuc-AAPV-CMK, SPCK) and tyrosinase activity assays (enzyme – tyrosinase from mushroom, EC 1.14.18.1; substrate – L-3,4-dihydroxyphenylalanine, levodopa, L-DOPA; control inhibitor – kojic acid) were purchased from Sigma-Aldrich.

For the synthesis of TSCs: all solvents were of commercial quality and purchased from a local supplier (Avantor). Thiosemicarbazide (catalog nr T33405); racemic ketoprofen (catalog nr K1751); 4-acetylbenzoic acid (catalog nr 177458); 4-formylbenzoic acid (catalog nr 124915); and *p*-toluenesulfonic acid monohydrate (catalog nr T35920) were purchased from Merck.

For the melanogenesis and cell proliferation assay: α-melanocyte-stimulating hormone (α-MSH), sodium dodecyl sulfate (SDS), Thiazolyl Blue Tetrazolium Bromide (MTT) were purchased from Merck. Streptomycin, penicillin, and Fetal Bovine Serum (FBS) were purchased from Sigma-Aldrich. Gibco™ RPMI 1640 Medium, GlutaMAX™ Supplement (HEPES) was purchased from Thermo Fisher Scientific.

4.3 Synthesis

Peptides **8-26** and **46-57** were synthesized manually on solid-phase following the Fmoc/*t*Bu strategy.[238,239] The cleavage of synthesized compounds from the resin was performed in acidic conditions with TFA solution. When necessary, the EDT was added to the cleavage mixture to prevent the oxidation of methionine. Peptide and building block synthesis was performed in polypropylene vessels (syringes) with filter.

Thiosemicarbazones **27-42** and **43-45** used for the synthesis of conjugates **49-57** were prepared by **Dr. Waldemar Goldeman** from Wroclaw University of Science and Technology in Poland.

The derivatives of 5,7-dimethyl-2,3-dihydro[1,2,4]triazolo[4,3-*a*]pyridine-8-carboxylic acid **4-7** were obtained according to the procedure published for the first time by Khan and Rafla in 1970s.[240–242] The synthetic pathway was also described and diversified by Sączewski *et al.* in 2013.[234] Herein the synthesis based on these protocols will be reported.

4.3.1 Unmodified peptides

Before the synthesis, dry Rink amide AM resin (100-200 mesh, loading: 0.74 mmol/g) or dry Fmoc-Tyr(*t*Bu)-Wang resin (100-200 mesh, loading: 0.70 mmol/g) was swelled for 40 min in DMF. Fmoc-deprotection was performed with a solution of 20% (v/v) piperidine in DMF. Peptide chain elongation was performed by repeated cycles of deprotection, washing, and coupling with Fmoc-protected amino acids (2.5 eq.), HBTU (2.5 eq.), and DIPEA (4.5 eq.) in DMF. Unless otherwise indicated, coupling reactions were performed for 40 min, deprotection reactions for 5+15 min, and washings with DMF between each step for 4×1 min. Uncertain couplings were confirmed by the ninhydrin test described by Kaiser.[243] Unmodified sequences **8-9** and **46-48** were acetylated N-terminally before the cleavage, using the solution of Ac_2O (20 eq.) and NMM (20 eq.) in DCM for 2×45 min.

Final cleavage and sidechain deprotections were performed using a mixture of TFA/TIS/H_2O, (95/2.5/2.5, v/v/v) at room temperature. For the derivatives of **8** (compounds **11-14**), EDT was added to prevent unwanted methionine oxidation (TFA/H_2O/EDT/TIS, 94/2.5/2.5/1, v/v/v/v). The solution was filtered off, resin was washed additionally with 1 mL of cleavage cocktail, and TFA was evaporated under N_2 flux. Then, cold diethyl ether was added for the precipitation of a final product. Precipitated peptides and their derivatives were centrifuged and washed additionally two times with Et_2O, then lyophilized.

4.3.2 Organic synthesis of 5,7-dimethyl-2,3-dihydro[1,2,4]triazolo[4,3-*a*]pyridine-8-carboxylic acid precursors

Potassium cyanohydroxyamate (**1**). 17.5 g (0.25 mol) $NH_2OH \cdot HCl$ was dissolved in 150 mL of MeOH. 28.1 g (0.5 mol) KOH was dissolved in 80 mL of MeOH, then both solutions were cooled in the fridge for 2 h. Afterwards, KOH solution was added dropwise to $NH_2OH \cdot HCl$ in MeOH, stirring continuously. When finished, the mixture was still stirred for 20 min. Potassium chloride, insoluble in MeOH, was filtered off and washed three times with 3 mL of MeOH. The filtrate containing NH_2OK was cooled in ice bath for 15 mins. Then, 28 mL (0.25 mol) of ethyl cyanoacetate was added

in one portion to the filtrate, the mixture was shaken well and left for the crystallization in the ice bath. After 15 min, crystals have begun to form spontaneously. Erlenmeyer flask with crystallizing potassium cyanohydroxyamate (**1**) was cooled overnight. After 20 h, white solid was filtered under vacuum, washed three times with MeOH, and dried in desiccator. *Yield: 64% (literature: 50%).*

N-hydroxy-3-(hydroxyamino)-3-iminopropanamide (**2**). 11.07 g (0.16 mol) of $NH_2OH·HCl$ was dissolved in 55 mL of H_2O. 22.1 g (0.16 mol) of **1** was dissolved in 30 mL of H_2O. Both solutions were mixed, put in the ice bath for 15 min and then left in the fridge overnight for further crystallization. After two days, high quantity of white powder, *N*-hydroxy-3-(hydroxyamino)-3-iminopropanamide (**2**), was filtered off under the vacuum, washed with H_2O (3×5 mL), and lyophilized. *Yield: 35%.*

4,6-dimethylisoxazolo[3,4-*b*]pyridin-3(1*H*)-one (**3**). 6.0 g (0.045 mol) of **2**, 4.64 mL (0.045 mol) of acetylacetone, 4.44 mL (0.045 mol) of piperidine, and 140 mL of H_2O were mixed in round-bottom flask, then the mixture was boiled under the reflux for 15 min and cooled to room temperature. 5% $HCl_{(aq.)}$ was added to the reaction mixture to neutralize the piperidine. Yellow isoxazolone has started to precipitate at once. HCl was added until no more product was precipitating. 4,6-Dimethylisoxazolo[3,4-*b*]pyridin-3(1*H*)-one (**3**) was washed with H_2O (3×5 mL) and then lyophilized. ^{1}H-NMR spectra confirming the purity of the final product **3** can be found in SI (**Figure SI 1**). Full synthetic pathway is summarized in **Scheme 4**. *Yield: 41%.*
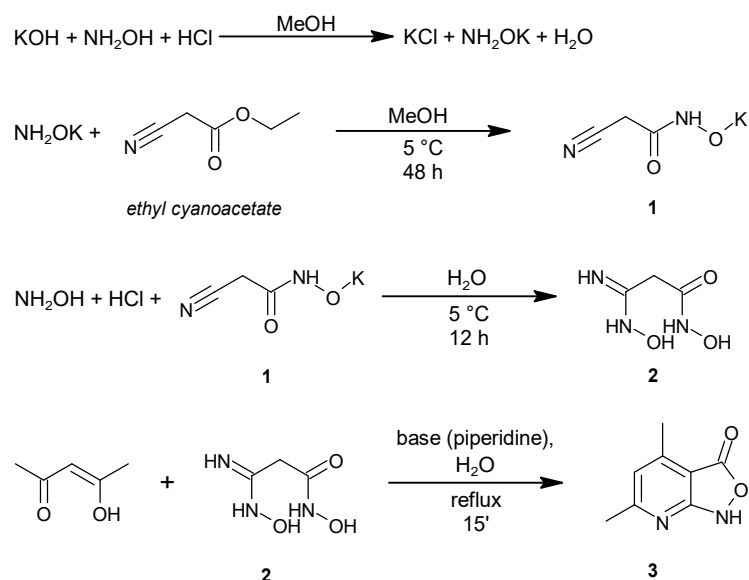
Scheme 4. Synthetic pathway for 4,6-dimethylisoxazolo[3,4-*b*]pyridin-3(1*H*)-one (**3**).[234,241,242]

4.3.3 5,7-dimethyl-2,3-dihydro[1,2,4]triazolo[4,3-*a*]pyridine-8-carboxylic acid derivatives (4-7)

700 mg (4.27 mmol) of **3** was dissolved in 13 mL of MeOH. 0.330 mL of formaldehyde 37%$_{(aq.)}$ and 4.27 mmol of corresponding secondary amine (**A**: 0.504 mL, **B**: 0.354 mL, **C**: 0.373 mL, **D**: 0.517 mL) were mixed and incubated for 15 min in the Eppendorf tube. The solution was added to **3** in MeOH. Reaction mixture was stirred overnight, resulting with yellowish-greenish solution, strongly absorbing UV light (λ=366 nm). Reaction progress was controlled with TLC (eluent: 100% MeOH). MeOH was evaporated under the N_2 flux from the reaction mixture, then each product **4-7** was lyophilized from H_2O and used without further purification.

4.3.4 Fmoc-Lys-triazolopyridylium and -triazolopirydynium building blocks

Lysine-based building blocks were synthesized according to standard SPPS Fmoc/*t*Bu strategy. 4-Methyltrityl (Mtt) protective group is labile in slightly acidic conditions, therefore Mtt-protected amines can be deprotected selectively, without entire amino acid/peptide cleavage from the resin.
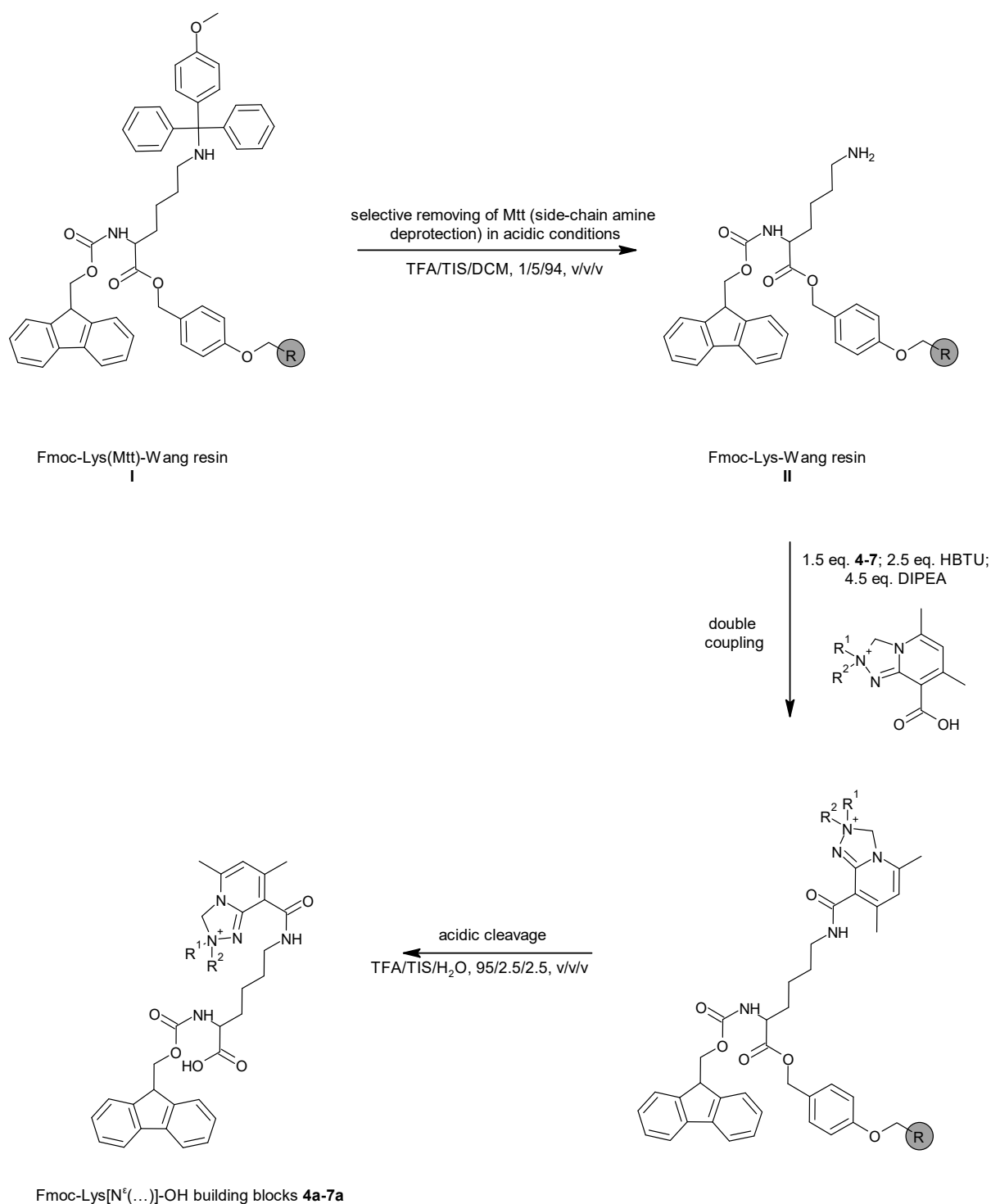
Scheme 5. Synthetic pathway of Fmoc-Lys-triazolopyridylium and -triazolopirydynium building blocks **4a-7a**.

Fmoc-Lys(Mtt)-Wang resin (*Novabiochem*, 100-200 mesh, loading: 0.54 mmol/g) was swelled for 40 min in DMF, then washed with DCM (3×1 min). Mtt deprotection was performed according to the first step in **Scheme 5** (TFA/TIS/DCM, 1/5/94, v/v/v; 1 mL/100 mg of resin), in the following cycles: 2×25 min+3×10 min and series of 5 min cycles until complete discoloration, washing with DCM after each deprotection step. Yellow coloration of the solution is indicative for free Mtt presence in the deprotection

cocktail. Thus, the last 2-3 cycles should be colorless. Thereby deprotected resin was washed repeatedly with pure DCM, until the solvent was transparent and pH value was neutral. The most effective washing occurred with continuous flow of pure DCM through the resin beads, with simultaneous water-pump filtering. Deprotected resin was dried overnight by lyophilization to evaporate all residual solvents. The day after, resin was swelled again in DMF for 20 min. Double coupling (1 h each) was performed in DMF with following equivalents of reagents: 1.5 eq. of corresponding moiety **4-7**, 2.5 eq. of HBTU and 4.5 eq. of DIPEA. Resin was washed well with DMF and then DCM, until both solvents were colorless. **Figure 27** shows the resin beads after the coupling.

Cleavage of all building blocks **4a-7a** was performed for 3 h in room temperature in standard cleavage cocktail (TFA/TIS/H_2O, 95/2.5/2.5, v/v/v). The solution was filtered off, resin was washed additionally with 1 mL of cleavage cocktail and TFA was evaporated under N_2 flux. Then, cold diethyl ether was added for further precipitation. Precipitated compound was centrifuged and washed additionally two times with cold diethyl ether, then lyophilized. As each of building blocks tends to form sticky, dense clumps, it is necessary to use vortex between diethyl ether washings and ultrasounds before lyophilization to obtain a suspension, and then to carefully lyophilize the product. All compounds **4a-7a** were then used without further purification. The purity of crude products was sufficient to characterize the final products by NMR.
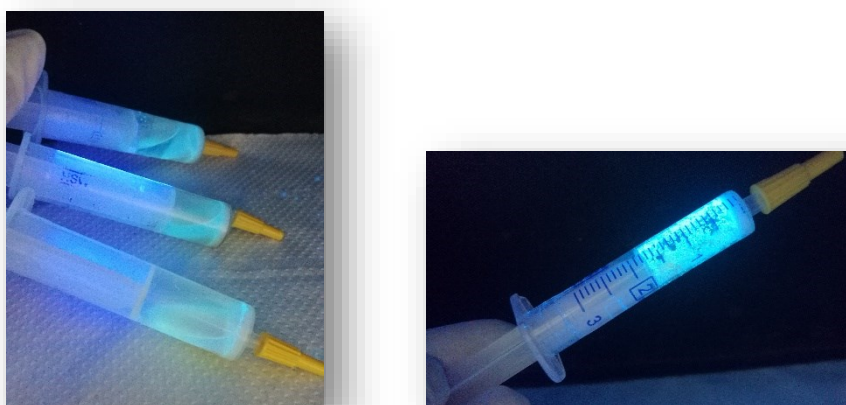
Figure 27. Wet (left) and dried (right) resin beads after the synthesis of building blocks **4a-7a**, visible under the UV lamp (λ=366 nm).

4.3.5 Peptide modifications with triazolopyridylium and triazolopirydynium moieties

Method I. The fragment PGKVV-NH_2 of **10** was synthesized manually according to the SPPS procedure described above. The resin containing Fmoc-deprotected

fragment PGKVV-NH$_2$ was washed 3×1 min with MeOH. Free secondary amine of Pro residue could therefore react with **3** on the solid phase in the presence of formaldehyde. 36.0 mg of **3** (3 eq.) and 20 µL of formaldehyde 37%$_{(aq.)}$ in MeOH (3 mL) were added to the reactor with the resin and left stirring overnight. The day after the resin was filtrated and washed with MeOH until the solution was clear. Modified peptide **10** was cleaved according to the procedure described above and purified.

Method II. Modified peptides **11-18** were synthesized manually according to the SPPS procedure described above. Moieties **4-7** were coupled using standard conditions and equivalents, exceeding the coupling time to 1 h. Products **11-18** were cleaved according to the procedure described above, and purified.

Method III. Modified peptides **19-26** were synthesized manually according to the SPPS procedure described above. Building blocks **4a-7a** were coupled using standard conditions (building blocks: 1.5 eq.), exceeding the coupling time to 1.5 h. Building blocks are not susceptible for decomposition in acidic and basic conditions and they are stable in each step of the SPPS. Peptides **19-26** were cleaved according to the procedure described above and purified.

4.3.6 Peptide conjugates with thiosemicarbazones

Conjugates of peptides and TSCs **49-57** were synthesized according to the procedure described for peptides. TSCs were dissolved in DMF and attached to the peptide chain at Fmoc-free N-terminus, following the standard coupling protocol. To enhance the coupling yield, the double coupling with 1.5 eq was performed. TSCs, well soluble in DMF, do not require any treatment and undergo the conjugation easily. Products **49-57** were cleaved from the solid support according to the procedure described above and purified.

4.4 Purification

4.4.1 Flash chromatography

Crude peptides were purified by Reversed-phase Flash Liquid Chromatography (RP-HPLC) on Isolera One Flash Chromatography (Biotage, Uppsala, Sweden) using a SNAP Ultra C18 column (40 g) at 20 mL/min flow. Eluent systems: 0.1% TFA in H$_2$O (A), 0.1% TFA in ACN (B). Despite the hydrophobic properties of amino acids in the sequences, crude products **10-26** were very well soluble in water due to the presence of N$^+$ ion in the structure. On the other hand, hydrophobic tripeptides **46-48** and their conjugates with thiosemicarbazones **49-57** were poorly soluble and required the

sample treatment with ultrasounds prior to the purification. Moreover, crude products **46-57** were dissolved in the mixture of solvents equal to the initial percentage of the mobile phase.

The purification was performed using linear gradient of solvents. For products **8-26** the gradient applied was 10-35% of B in A in 30 min. For products **46-57** the gradient was 35-65% of B in A in 30 min. Before the purification, the column was stabilized with the solvent at the initial percentage of the gradient; after the purification, the column was washed with 100% of solvent B.

4.4.2 Semi-preparative liquid chromatography

If further purification was necessary, it was performed by semipreparative RP-HPLC on a Waters instrument (Separation Module 2695, Detector Diode Array 2996) using a Sepax Bio-C18 column (Sepax Technologies, Newark, United States; 5 µM, 250 mm×10 mm), at 4 mL/min flow, using the solvent systems A (0.1% TFA in H_2O) and B (0.1% TFA in ACN).

4.5 Analysis

4.5.1 High Performance Liquid Chromatography (HPLC) and Mass Spectrometry (MS) – LC-MS

Characterization of the peptides and the conjugates was performed by analytical HPLC. Due to the instrument availability, the analyses of products **4a-7a**, **8-26** and **46-57** were performed using two different chromatographs. **4a-7a**, **8-26** were analyzed by Thermo Scientific Ultimate 3000 UHPLC coupled with Thermo Scientific MSQ plus, supplied with a CSH C18 Acquity UPLC® column (1.7 µm, 2.1×100 mm, 45°C) with the solvent systems A (0.1% TFA in H_2O) and B (0.1% TFA in ACN). Chromatograms presented in the SI were obtained using linear gradient 5-95% of B in A in 10 min, injection volume: 10 µL. Compounds **46-57** were analyzed using Alliance Chromatography model 2695 (Waters) with a Phenomenex Kinetex C18 column (2.6 µm, 3.0×100 mm) working at flow 0.6 mL/min, coupled to a single quadrupole ESI-MS (Micromass ZQ), with the solvent systems 0.1% TFA in H_2O (A), 0.1% TFA in 84% ACN/H_2O (B), λ=254 nm, gradient: 30-90% B in 5 min, injection volume: 20 µL. All chromatograms and mass spectra are reported in the SI (**Chapter 1**). The analytical data is summarized in **Table 16** and **Table 17**.

Table 16. Analytical data for compounds **4a-7a** and **8-26**. Legend: building blocks, unmodified peptides, Method I, Method II, Method III.

COMPOUND	RETENTION TIME [min]	*m/z* calc. [1+] [a]	*m/z* exp. [1+] [a]	UV Absorbance [b]
4a	6.10	626.33	626.6	yes
5a	5.90	598.30	598.6	yes
6a	5.80	614.30	614.6	yes
7a	6.00	614.33	614.7	yes
8	3.70	574.33 (M_w+1H)	574.39 (M_w+1H)	no
9	3.30	540.34 (M_w+1H)	540.38 (M_w+1H)	no
10	4.45	674.40	674.59	yes
11	4.10	789.48	789.7	yes
12	3.74	761.45	761.7	yes
13	3.65	777.44	777.8	yes
14	3.89	778.04	777.7	yes
15	3.60	755.49	755.8	yes
16	3.25	727.46	727.7	yes
17	3.14	743.46	743.8	yes
18	3.37	743.96	743.8	yes
19	4.50	831.49	831.9	yes
20	4.20	803.46	803.5	yes
21	4.13	819.45	819.8	yes
22	4.30	820.07	819.9	yes
23	4.20	797.50	797.8	yes
24	3.90	769.47	769.8	yes
25	3.85	785.47	785.8	yes
26	4.00	785.99	785.8	yes

[a] *Permanent positive charge due to the presence of quaternary nitrogen atom in compounds* **4a-7a** *and* **10-26**.
[b] *λ=366 nm.*

Table 17. Analytical data for compounds **46-57**. Legend: unmodified peptides, TSC**43**-derivatives, TSC**44**-derivatives, TSC**45**-derivatives.

COMPOUND	RETENTION TIME [min]	*m/z* calc. [M_w+1]+	*m/z* exp. [M_w+1]+
46	2.70	518.6	518.31
47	1.42	534.6	534.32
48	2.55	557.6	557.36
49	3.40	681.2	681.49
50[a]	3.80	697.2	697.8
51	3.53	720.2	720.34
52	3.62	785.3	785.60
53	2.95	801.3	801.51
54	3.52	824.3	824.60
55	3.40	695.3	695.47
56	2.68-93	711.3	711.46
57	3.45-68	734.3	734.47

[a] *Gradient applied: 20-70% B in A in 5 min.*

4.5.2 Nuclear Magnetic Resonance (NMR)

Peptides synthesized for the purpose of the elastase project possess the structural variety with the heterocyclic 1,2,4-triazolium core located in distinct positions of the peptide chain. Therefore, the NMR analysis of these compounds was applied to evidence the differences in chemical shift values among the derivatives, hence confirm their diversified structures. On the contrary, the conjugates of short tripeptides with thiosemicarbazones were synthesized maintaining only one position of the modification, thus their extensive structural investigations, such as NMR and CD, were omitted.

The samples for one-dimensional (1D) and two-dimensional (2D) NMR spectroscopy were prepared by dissolving purified products in 10% D_2O in H_2O (for compounds **10-26**) or 100% DMSO-d_6 (for water-insoluble compounds **8**, **9**, **4a-7a**). The ^1H and ^{13}C NMR spectra were recorded on a 600 MHz Bruker Avance spectrometer. Spectra were recorded at a temperature of 300K and calibrated relative to TSP (0.00 ppm) as internal standard. 1D-NMR spectra were recorded in the Fourier mode with quadrature detection. The water signal was suppressed with the watergate 3-9-19 pulse sequence.[244] 1D-NMR spectra were processed and analyzed using *SpinWorks*. 2D-NMR (including 2D-COSY[245,246] and TOCSY[247]) spectra were analyzed with *NMRFAM-Sparky* software.[248] The purity of Fmoc-building blocks **4a-7a** without any treatment after their cleavage from the resin was found to be sufficient to assign the signals observed in the recorded NMR spectra.

Symbols of proton groups assigned for the derivatives of each secondary amine **A-D** are presented in **Figure 28.** and detailed in **Table 18**. Carbon atoms in aromatic ring, unassociated with any hydrogen atom are signed with numbers (1-4). In case of unmodified peptides **8** and **9**, amino acid residues are marked with standard three-letter code (Met/Pro-Gly-Lys-Val[1]-Val[2]). Assignments with values of chemical shifts are summarized in SI (**Table SI 1-7**).

4-Methylpiperidine   Pyrrolidine   Morpholine   *N*-Ethylisopropylamine
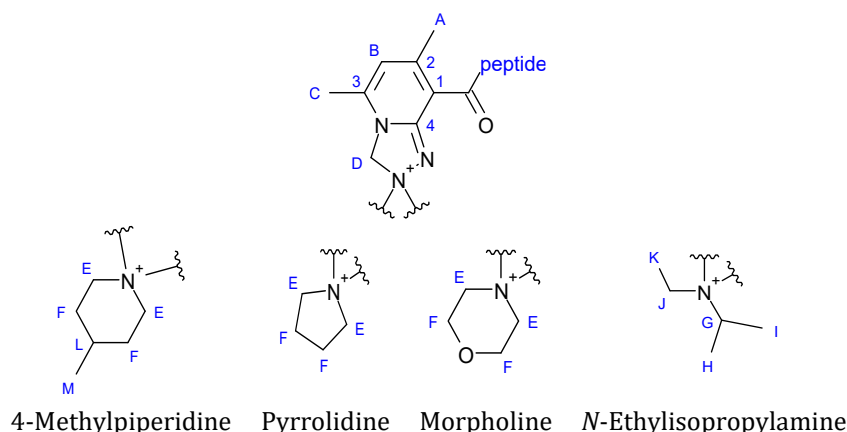
Figure 28. Signed atoms in 5,7-dimethyl-2,3-dihydro[1,2,4]triazolo[4,3-*a*]pyridine-8-carboxylic acid derivatives, for the purpose of NMR chemical shifts assignment. Proton groups are signed with letters (A-M); carbons with numbers (1-4).

Table 18. Number of protons in each assigned group in the structures from **Figure 28.**

	A	B	C	D	E	F	G	H	I	J	K	L	M
Number of protons in the group	3	1	3	2	4 (2×CH$_2$)	4 (2×CH$_2$)	1	3	3	2	3	1	3

Fmoc (protecting group)
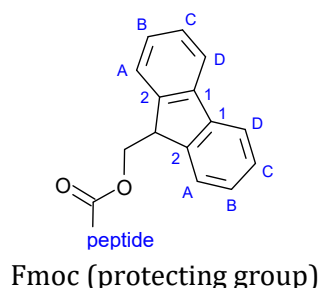
Figure 29. Signed atoms in Fmoc protecting group rings, for the purpose of NMR chemical shifts assignment. Proton groups are signed with letters (A-D); carbon atoms with numbers (1-2). Two remaining aliphatic groups were assigned as CH and CH$_2$.

4.5.3 Circular Dichroism (CD)

Peptides **8** and **9** derive from the longer sequence investigated previously, which was found to form the β-sheet conformation in the complex with trypsin (**Figure 1**, **Figure 2**). Regarding that, it was valuable to perform the CD analysis of these sequences and their conjugates to evaluate the maintenance of this conformation by shorter peptides, and the influence of the presence of 1,2,4-triazoles on the conformational properties. Consequently, peptides **8-26** were analyzed and obtained spectra are presented and talked through in the **Results and discussion** chapter.

CD spectra for peptides **8-26** were recorded on JASCO J-1500 in temperature of 25°C, between λ=270 and 185 nm with the interval of 1 nm. The CD measurements were conducted in Tris-HCl buffer (H$_2$O with 1% DMSO, pH=8) to maintain the conditions

optimized for the bioassay of elastase activity. All peptides and their derivatives were measured in 100 µM concentration. The spectra were registered with the following parameters: 0.2 nm resolution, 1.0 nm bandwidth, 20 mdeg sensitivity, 0.25 s response, 100 nm/min scanning speed, 5 scans, and 0.02 cm cuvette path length. The CD spectra of the buffer was recorded and subtracted from the raw data. The spectra were corrected by a baseline, measured with the identical solvent in the same cell. The CD intensity is given as mean residue molar ellipticity (θ) [deg×cm^2×dmol^{-1}].

4.6   Enzyme activity assays

4.6.1   Porcine Pancreas Elastase (PPE) inhibition evaluation

Elastase activity screenings were performed according to a modified procedure from the literature,[249] and compared with the protocol suggested by Sigma Aldrich.[250] The final protocol was then optimized with the measurement procedure published for tyrosinase assay, successfully applied in the group in the past years.[214] The assay was performed in 96-well transparent plate, convenient for the UV-Vis reading with the spectrophotometer UV-Vis SpectraMax® Plus 384 Microplate Reader (Molecular Devices). Instead of neutrophil elastase, the structurally similar, more stable after the reconstitution, and commonly used porcine pancreas elastase was used. During the procedure optimization it was found out that ursolic acid reported in the literature as a control inhibitor was not soluble in required concentrations in the assay buffer. Therefore, the commercially available inhibitor SPCK, with excellent solubility and inhibitory activity around 95% in 10 µM concentration was used. For this assay the control inhibitor SPCK and the substrate *N*-Suc-AAA-*p*-nitroanilide were applied.

Ingredients preparation. Peptides **8-26** were prepared as stock solutions (C$_M$=500 µM) in the Tris-HCl (pH=8.0, 0.1 M) buffer without DMSO due to their good solubility in water in this concentration. The buffer used for the assay was prepared in H$_2$O with an addition of 1% (vol.) DMSO to enhance the solubility of all ingredients in the well. The percentage of DMSO, best for elastase highest activity and viability, was adjusted experimentally. There was no significant difference in the enzyme activity between 0 and 1% DMSO in the assay buffer; 5% of DMSO slightly decreased the PPE activity, however in case of poorly soluble compounds it can be used anyway. To balance the best solubility and optimal enzyme activity, an addition of 1% of DMSO in the Tris-HCl buffer was then applied for each assay.

1 mg of PPE powder (4.8 units/mg) was dissolved in 1 mL of buffer and then divided into aliquots of 50 μL for the storage in -80℃. Shortly before the assay, 50 μL aliquot was reconstituted with 1150 μL of assay buffer to achieve 0.2 unit/mL concentration.

The substrate, *N*-Suc-AAA-*p*-Nitroanilide, was prepared as stock solution by dissolving 10 mg of powder in 764 μL of buffer (C_M=29 mM) and then divided into aliquots of 80 μL for the storage in -80℃. Shortly before an assay, 80 μL aliquot was reconstituted with 720 μL of assay buffer to achieve 2.9 mM concentration.

Protocol description. The total volume in the well was adjusted to 100 μL to decrease the consuming of enzyme. 50 μL of the enzyme stock solution (4.8 units/mL) was dissolved in 624 μL of assay buffer, achieving the concentration of 0.35 units/mL. 100 μL of the substrate stock solution (29 mM) was dissolved in 887 μL of assay buffer, achieving 1.45 mM concentration.

10 μL of enzyme solution was added into each well (0.035 units/mL in the well). Inhibitor control, SPCK, was added into Inhibitor Control well (IC) for the final concentration of 5 μM. All tested compounds – peptides, modified peptides, Fmoc-deprotected building blocks, and triazolopyridinium moieties – were added in different volumes of 100 μM solution to achieve 5 different tested concentrations in the range of 10-50 μM. The plate was agitated for 1 min and incubated for 10 min. Eventually, 20 μL of substrate solution was added into each well (0.29 mM in the well) to start the reaction. The absorbance in each well was measured with 10 s interval in a kinetic mode for 10 min (λ=410 nm). Details are summarized in **Table 19.** The well with enzyme only was used as a blank.

Table 19. Ingredients of the PPE activity assay; an example of inhibitors concentrations set. The total volume in each well=100 μL.

	Blank [μL]	IC [μL]	EC [μL]	C_{final}= 10 μM [μL]	C_{final}= 20 μM [μL]	C_{final}= 30 μM [μL]	C_{final}= 40 μM [μL]	C_{final}= 50 μM [μL]
Evaluated compound (100 μM)	-	-	-	10	20	30	40	50
SPCK, inhibitor control (50 μM)	-	10	-	-	-	-	-	-
PPE, enzyme (0.35 unit/mL)	10	10	10	10	10	10	10	10
N-Suc-AAA-*p*-NA, substrate (1.45 mM)	-	20	20	20	20	20	20	20
Assay buffer	90	60	90	60	50	40	30	20

Data elaboration. PPE activity in the presence of tested compounds was calculated by the **Equation 1**, where Sample$_{slope}$: the slope value of linear fragment of reaction progress curve for the reaction mixture with tested sample; EC$_{slope}$: the slope value of linear fragment of reaction progress curve for the reaction mixture without inhibitor (Enzyme Control, EC). The linear fragment of the curve and the slope value was automatically calculated by the spectrophotometer software after each measurement.

$$\% \text{ of } ENZ_{activity} = \frac{Sample_{slope}}{EC_{slope}} \times 100$$

(**Equation 1**)

4.6.2 Tyrosinase inhibition evaluation

The tyrosinase enzymatic assay was performed according to the protocol described previously and successfully applied in the group in the previous years.[214–216] The assay was performed in 96-well transparent plate, convenient for the UV-Vis reading with the spectrophotometer UV-Vis SpectraMax® Plus 384 Microplate Reader (Molecular Devices). Instead of human tyrosinase, the structurally similar and commonly used in thus type of assay mushroom tyrosinase was employed. L-3,4-dihydroxyphenylalanine (L-DOPA) was used as a substrate.

Ingredients preparation. Sodium phosphate buffer (0.1 M, pH 6.8; assay buffer) was prepared by mixing two solutions: 46.3 mL of 1 M Na_2HPO_4 and 53.7 mL of 1 M NaH_2PO_4, and diluting the mixture to the final volume of 1 L. The buffer was stored in 2°C. Peptides **46-57** were prepared as stock solutions (C_M=1 mM) in the mixture of 10%$_{DMSO}$/90%$_{assay\ buffer}$ and were fully soluble in these conditions. Thiosemicarbazones **43-45** were prepared as stock solutions (C_M=10 mM) in 100% DMSO, due to their general poor solubility in water. All compounds were then diluted in the assay buffer to test concentrations (DMSO concentrations in final reaction mixtures did not exceed 1% of volume). All compounds were fully soluble in the assay conditions.

Mushroom tyrosinase powder (8503 units/1 mg of solid) was dissolved in the assay buffer to obtain the concentration of 50,000 units/mL. This stock solution was divided into 50 μL aliquots, each containing 2500 units of tyrosinase, and stored in -80°C. Shortly before the assay, one of the aliquots was reconstituted in the assay buffer up to 3000 μL.

L-DOPA was dissolved in aqueous 0.15 mM phosphoric(V) acid water solution, preventing its oxidation. The final L-DOPA concentration for the assay was 5 mM.

Protocol description. Total volume in the well was adjusted to 100 µL in order to decrease the consuming of enzyme. 50 µL of the enzyme stock solution (50,000 units/mL) was dissolved in 2950 µL of assay buffer, achieving the concentration of 835 units/mL. The substrate was used in the stock concentration of 5 mM.

10 µL of enzyme solution was added into each well (83.5 units/mL in the well). Inhibitor control, kojic acid, was added into Inhibitor Control well for the final concentration of 10 µM. All tested compounds – peptides, thiosemicarbazones, and the conjugates – were added in different volumes of 100 µM solution to achieve 5 different tested concentrations in the range of 10-50 µM. If observed inhibition was too low, the initial concentration was increased up to 1000 µM; if it was too high, the initial concentration was decreased to 10 µM. The enzyme solution was preincubated with samples in various concentrations for 5 min at 25°C. Afterwards, 20 µL of L-DOPA solution was added. The reaction was immediately monitored by measuring the change in absorbance of the color product (dopachrome) for 10 min in kinetic mode with 5 s interval (λ=475 nm, 25°C). Enzyme control (EC) sample did not contain the inhibitor; blank sample did not contain neither the inhibitor nor the substrate. Kojic acid was treated the same way as the other inhibitors.

Details are summarized in **Table 20.** The well with enzyme only was used as a blank.

Table 20. Ingredients of the mTYR activity assay: an example of inhibitors concentrations set. The total volume in each well=100 µL.

	Blank [µL]	IC [µL]	EC [µL]	C_{final}= 10 µM [µL]	C_{final}= 20 µM [µL]	C_{final}= 30 µM [µL]	C_{final}= 40 µM [µL]	C_{final}= 50 µM [µL]
Tested compound (100 µM)	-	-	-	10	20	30	40	50
KA, inhibitor control (100 µM)	-	10	-	-	-	-	-	-
mTYR, enzyme (835 unit/mL)	10	10	10	10	10	10	10	10
L-DOPA, substrate (5 mM)	-	20	20	20	20	20	20	20
Assay buffer	90	60	90	60	50	40	30	20

Data elaboration. Tyrosinase activity in the presence of tested compounds was calculated by the **Equation 1**, where Sample$_{slope}$: the slope value of linear fragment of reaction progress curve for the reaction mixture with tested sample; EC$_{slope}$: the slope value of linear fragment of reaction progress curve for the reaction mixture without

inhibitor (EC). The linear fragment of the curve and the slope value was automatically calculated by the spectrophotometer software after each measurement.

IC$_{50}$ (half maximal inhibitory concentration) calculation. After collecting the slope values and calculating the percentage of tyrosinase activity in the presence of various inhibitor concentration, it was possible to see the range of activity of every compound. If the inhibitor was efficient, and there was a possibility to characterize its full inhibitory potential (e.g., when the tested concentrations provoked the inhibition from 0-100% range), the IC$_{50}$ value was calculated. The effect on the diphenolase activity of the enzyme was expressed as IC$_{50}$ using *GraphPad Prism* software.[251]

4.7   Molecular modeling and docking

Elastase inhibitors. The structures of compounds **4a-7a**, **10-26** were optimized using the software *Gaussian09* at the B3LYP/6-31g(d,p) level of theory with the PCM solvent model using water as the solvent.[252] Additionally, Merz-Singh-Kollman scheme has been used for the determination of the atomic charges.[253] Visualization of modelling results was prepared using *PyMOL* software.[46] Obtained 3D structures are presented and explained in the **Results and discussion** chapter.

Tyrosinase inhibitors. Structure optimization and molecular docking with tyrosinase for compounds **46-57** was performed by **Dr. Michał Jewgiński** from Wroclaw University of Science and Technology in Poland.

Before the simulation of the docking process, ligand structures were prepared with *Discovery Studio Client.* The structures of all the ligands were optimized in the program *Gaussian16* at the B3LYP/6-311g (d,p) level of theory.[254] During the structure optimization, solvent model PCM were applied. The crystal structure of tyrosinase from *Agaricus bisporus* was obtained from the RCSB Protein Data Bank ID: 2Y9X.[184] The ligand, besides copper ions, was removed from the crystal structure of the enzyme. Lacking protons and charges were added to the protein using the *H++* serve according to pH value 6.8.[255,256] The active site sphere was selected based on the location of tropolone with a radius 18 Å. Molecular docking in the defined active site of tyrosinase was carried out using *GOLD Algorithm* (2021.3.0 version, CCDC, Cambridge, United Kingdom) using the ChemPLP scoring function. The docking using genetic algorithm used default settings (population size: 100, selection pressure: 1.1; the number of operations: 100000; the number of islands: 5; niche size: 2; crossover frequency: 95; mutation frequency: 95; migration frequency: 10). For each inhibitor, ten alignments were

obtained. Analysis of inhibitor-enzyme interactions of docked molecules was performed with *Discovery Studio Visualizer 5* (Dassault Systemes BIOVIA, U.S.A.).

4.8   Melanogenesis inhibition and melanoma cell lines viability

Melanogenesis inhibition and the viability assay of melanoma cell lines was performed by **Dr. Joanna Rossowska** from Ludwik Hirszfeld Institute of Immunology and Experimental Therapy, Polish Academy of Science in Wroclaw, Poland. **Dr. Katarzyna Hałdys** from Wroclaw University of Science and Technology in Poland contributed to the data interpretation.

Cell proliferation assay. B16F0 murine melanoma cell line was cultured in DMEM medium supplemented with 100 U/ml streptomycin, 100 U/ml penicillin, and 10% FBS. Cells were maintained in 5% CO_2 at 37°C. Cells viability was estimated by MTT colorimetric assay as described by Bellei *et al.*[257] B16 cells were seeded into 96-well plate (4×10^3 cells/well) and incubated in the presence of the investigated compounds at various concentration (1000, 400, 100, 40, 10, 1, 0.1 μM) for 48 h. Kojic acid and DMSO were used as controls. MTT was added into wells (0.625 mg/ml) for the last 4 h. Then lysing buffer was added to dissolve insoluble formazan. The absorbance was measured (λ=570 nm) using Thermo Lab Multiscan RC microplate reader.

Measurement of melanin production. Measurement of melanin production in B16F0 murine melanoma cell line was performed as described by Bellei *et al.*[257] The cells were seeded into 96-well plate (5×10^3 cells/well) and stimulated with α-MSH. After 24 h cells were treated with the investigated compounds as well as DMSO and kojic acid at a final concentration of 100, 40, 10, 4, and 1 μM. After 48 h of incubation with inhibitors, melanin production was measured by evaluation the absorbance (λ=405 nm) using a microplate reader.

Chapter 5: Results and discussion

5.1 Synthesis

All compounds mentioned in this thesis were summarized at the beginning of the document (page 14). Compounds available commercially or provided were highlighted. All remaining products were synthesized by the Author during the thesis preparation, and the results of these syntheses will be discussed below.

5.1.1 Peptide conjugates with 1,2,4-triazoles

The synthesis of the Lys-based building blocks started with the preparation of the *Safirinium* carboxylic acid analogs. Four different secondary amines were selected for the synthesis: 4-Methylpiperidine (A), pyrrolidine (B), morpholine (C), and *N*-Ethylisopropylamine (D). The structural differences between these four amines are noticeable: 5- or 6-membered ring in cyclic amines A and B; the presence of oxygen atom in the ring (C), and the branch amine (D). Following a reported procedure, 4,6-dimethylisoxazolo[3,4-*b*]pyridin-3(1*H*)-one (**3**) was synthesized starting from KOH and $NH_2OH\times HCl$ in four steps (**Scheme 4**, page 77).[234,240–242] Reaction of **3** with the corresponding amines in the presence of formaldehyde in MeOH gave 5,7-dimethyl-2,3-dihydro[1,2,4]triazolo[4,3-*a*]pyridine-8-carboxylic acid derivatives **4-7**.[234,235] The reaction progress was followed by the TLC (elution in MeOH). In case of the presence of **3** in the reaction mixture, the next portion of formaldehyde was added, and the reaction was prolonged until the total consuming of **3** as a substrate. Therefore, compounds **4-7** were obtained in high yields (over 90%) and were used without further purification. The presence of a permanent positive charge located on the nitrogen atom provides particularly good solubility and ionization of the final product. Moreover, obtained carboxylic acid derivatives exhibit fluorescence, and strongly absorb the UV light (λ=366 nm).

Building blocks **4a-7a** were prepared starting from Fmoc-Lys(Mtt)-Wang resin, treated with 5% TFA in DCM to deprotect the amine group in Lys side chain (**Scheme 5**, page 78). These conditions permit to avoid the complete cleavage of lysine from the resin. Resin was washed from remaining TFA with pure DCM and swelled in DMF. Then, derivatives **4-7** were conjugated in standard coupling conditions according to Fmoc/tBu strategy. Final compounds were cleaved from the resin in standard cleavage cocktail (TFA/TIS/H_2O, 95/2.5/2.5, v/v/v). Following that procedure, it was possible to obtain Fmoc-protected building blocks ready to be implemented during the synthesis of any

peptide. They do not require any additional treatment and can be used for the derivatization without further purification (obtained experimental data is presented in SI, subchapter **1.1**). The purity of crude **4a-7a** resulted high enough to fully analyze and characterize these compounds by NMR techniques. It also confirmed the relevance of solid-phase synthesis application in the building block synthesis. According to the presented synthetic pathway, building blocks were obtained in high yields, slightly lower for the derivative of **7** (**4a**: 76%; **5a**: 83%; **6a**: 73%; **7a**: 66%).

Different examples of peptide derivatization with synthesized compounds **4-7** and **4a-7a** were implemented, involving the model sequences MGKVV and PGKVV. All modified peptides and building blocks maintain the fluorescent properties provided by the dyes **4-7**, as it can be observed by exposing the solutions of **4a-7a** and **10-26** to the UV light (λ=366 nm). As mentioned before, the synthesis of 5,7-dimethyl-2,3-dihydro[1,2,4]triazolo[4,3-*a*]pyridine-8-carboxylic acid derivatives requires the use of a secondary amine. Therefore, Met residue in the model SA1-III-deriving peptide MGKVV was exchanged for Pro, obtaining free secondary amine at the N-terminus. This swap permitted to perform a direct, on-resin reaction between **3** and N-terminal proline in the presence of formaldehyde. Consequently, structural modifications were implemented following three different methods: (I) on-resin reaction between **3** and N-terminal Pro; (II) N-terminal tagging of Met or Pro with compounds **4-7** *via* amide bond formation; (III) building blocks **4a-7a** incorporation during the peptide synthesis, thus replacing the Lys residue in the middle of the sequence. The most time-consuming was the method (I), while the method (II) was the fastest one and did not require any particular treatment – compounds **4-7** can be coupled with the peptide in standard conditions. The method (III) is the most complex due to the prior building block synthesis. Furthermore, comparing the yields of the syntheses, peptides synthesized *via* method (II) were obtained with the yields between 30-50%, somewhat better for MGKVV-derivatives rather than PGKVV-derivatives. On the other hand, the peptides requiring the incorporation of building blocks were obtained with yields around 20-30%. Presented on-resin reaction (I) provided peptide **10** with 27% yield.

5.1.2 Peptide conjugates with thiosemicarbazones

Synthesis of tripeptides conjugated with thiosemicarbazones was based on standard SPPS protocol without any changes. Thiosemicarbazones, well soluble in DMF, are perfect candidates for the on-resin N-terminal modification of selected peptide sequence. The progress of a coupling reaction was controlled by the Kaiser test, and no

repetitive coupling was needed during the synthesis of all conjugates. Unmodified peptides **46-48** were obtained in high (50-60%) yields. Their conjugates with thiosemicarbazones resulted with pure products obtained in yields around 20-30%. This inconsistency is provoked by the overall hydrophobicity of synthesized conjugates and side-products present in the crude powder, providing additional difficulties during the purification. The presence of other hydrophobic moiety, thiosemicarbazone, did not significantly affect the retention time of the final compound regarding the basic tripeptide (

Table 17, page 82). Nevertheless, the purification procedure was more problematic in case of TSC-conjugates due to their weaker solubility in the initial eluent, rather than peptides **46-48**. Noticeably, conjugates with tripeptide FYY and the FYY alone have lower retention time in equal conditions of column elution (in the reversed-phase conditions), thus indicating their lower hydrophobicity than this for FWY- and FYY-derivatives. This factor may be considered as an advantage due to the good balance between hydrophobicity and feasible purification of the final product based on FYY.

5.2   Structural properties

To investigate the structural properties of compounds **4a-7a** and **10-26**, *in silico* methods for structure optimization were applied. These calculations allowed to observe the structural differences between compounds possessing triazole moiety, attached to the peptide with and without lysine linker. Moreover, peptide SA1-III derives from a longer sequence, found to adopt a β-sheet conformation. Thus, it was beneficial to perform CD analyses of peptides **8-26** and evaluate the structural properties of these sequences, deriving from peptide SA1-III.

Tripeptides **46-57** were not investigated by circular dichroism methods due to their short sequences. *In silico* calculations and structural optimization of these compounds were performed for the purpose of molecular docking with tyrosinase, and the results will be further discussed in the subchapter **5.5**.

5.2.1   Optimized structures of compounds 4a-7a and 10-26

To have additional information on the structure of obtained peptides, molecular modelling was applied to calculate their most stable conformations. The structures of compounds **4a-7a** and **10-26** were optimized using the software *Gaussian09* at the B3LYP/6-31g(d,p) level of theory with the PCM solvent model, using water as the solvent.[252] Additionally, Merz-Singh-Kollman scheme has been used for the

determination of the atomic charges.[253] Visualization of modelling results was prepared using *PyMOL* software.[46]

Molecular modeling methods showed the presence of stabilizing polar interactions within most of the compounds, with particular attention to **23-26** (PGKV^{1}V^2-deriving peptides with derivatization on the lysine side chain) (**Table 21**).

Table 21. Stabilizing polar interactions found in compounds from the group **23-26** (PGKV^{1}V^2-deriving peptides with derivatization on the lysine side chain).

COMPOUND	POLAR INTERACTIONS
23	(Gly)C=**O**---(Val^1)N**H** (Lys)C=**O**---(Val^2)N**H** (Lys)N**H$^\xi$**---(ring)C=**N**-N
25	(Gly)C=**O**---(Val^1)N**H**
26	(Pro)C**O**CH3---(Val^2)N**H₂** (Gly)N**H**---(Val^2)C**O** (Gly)C=**O**---(Val^1)N**H**

It should be noted that compounds **19-26** (all peptides with incorporated building blocks) adopt consequently a bended conformation, where the heterocyclic moiety located on the lysine side chain is exposed (e.g., for potential interactions with a receptor) (**Figure 3** and **Figure 34**, **Figure 35**); lateral amino acid residues do not provide any steric hindrance in the proximity of the heterocyclic part. This exposure of functionalized moiety on the lysine linker is particularly important because it may have an influence on the inhibitory activity of the final compound. Indeed, we observed differences in the inhibition of porcine pancreas elastase, where the incorporation of the lysine linker in the conjugates provided the increase of inhibitory value from 0 to 25% (described in more detail later). In this conformation the active portion of the conjugate is fully available for the interaction with targeted molecule. In addition, the peptide fragment does not provide the unwanted steric hindrance in the region of the triazolium core but may stabilize the final complex. **Figures 30-35** shows all obtained 3D structures of synthesizes compounds **4a-7a** and **10-26**. Polar interactions are marked as yellow lines.
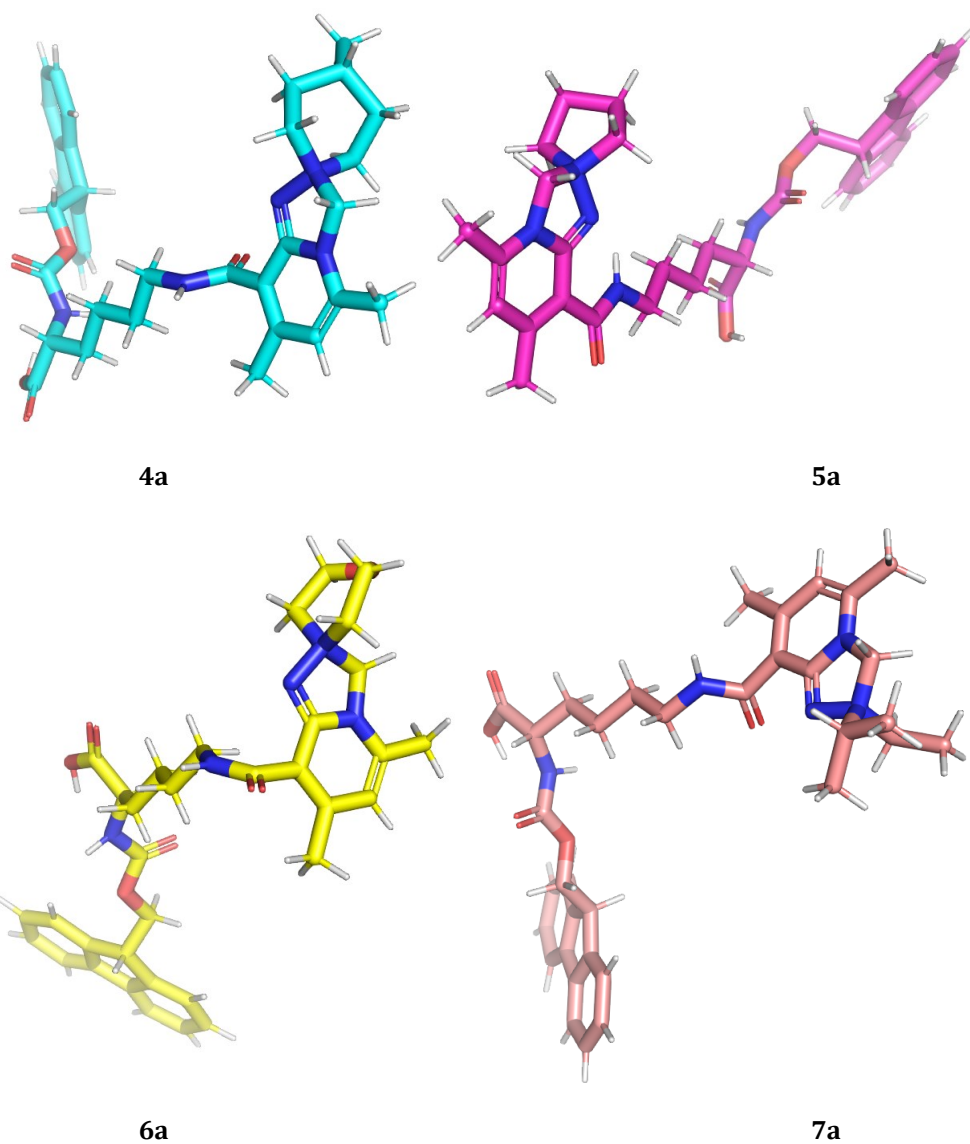
4a   **5a**
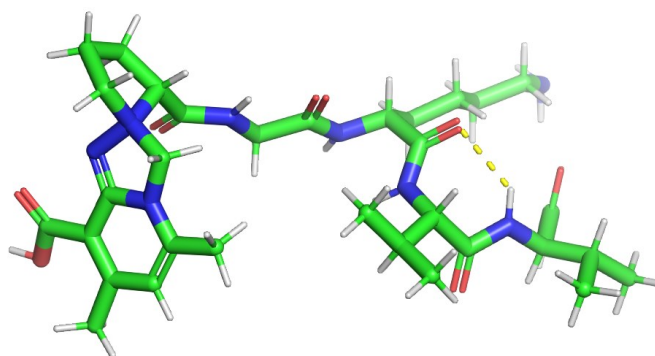

6a   **7a**

Figure 30. Optimized three-dimensional structures of **4a-7a**.

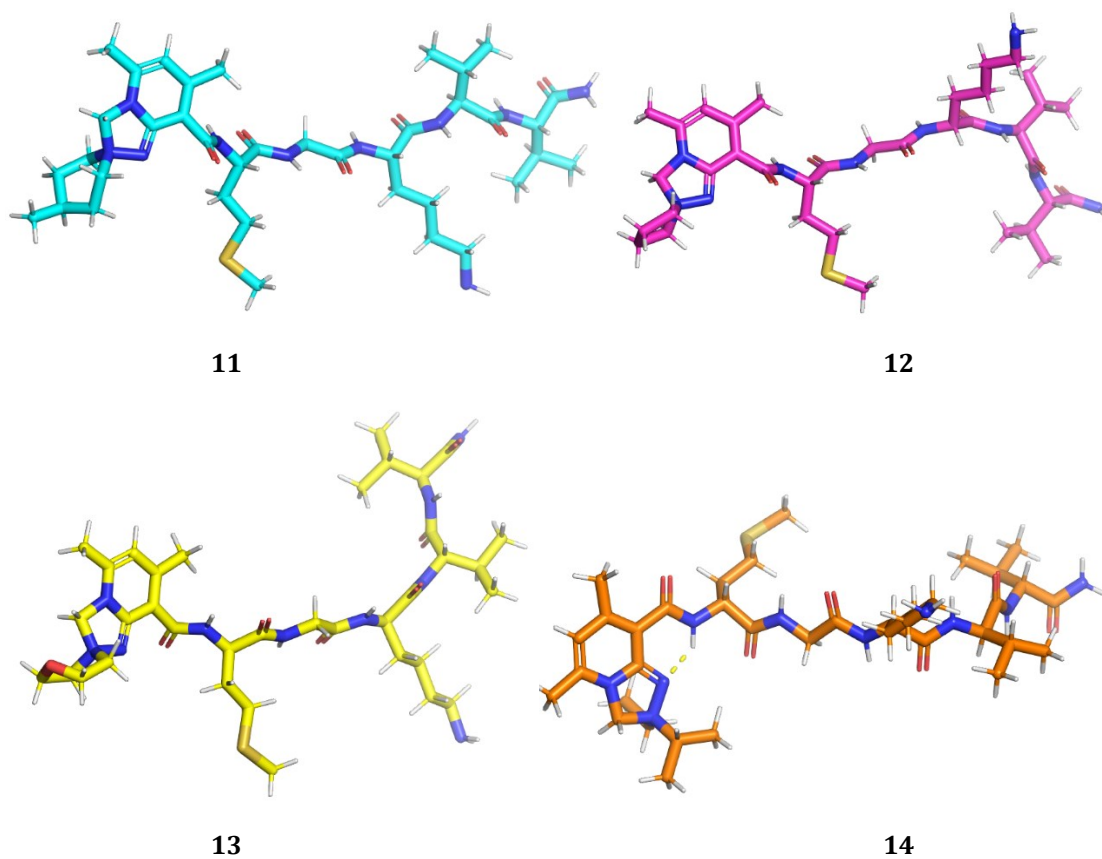**Figure 31.** Optimized three-dimensional structure of **10**.

11

12

13

14

Figure 32. Optimized three-dimensional structures of **11-14**.

15

16

17

18
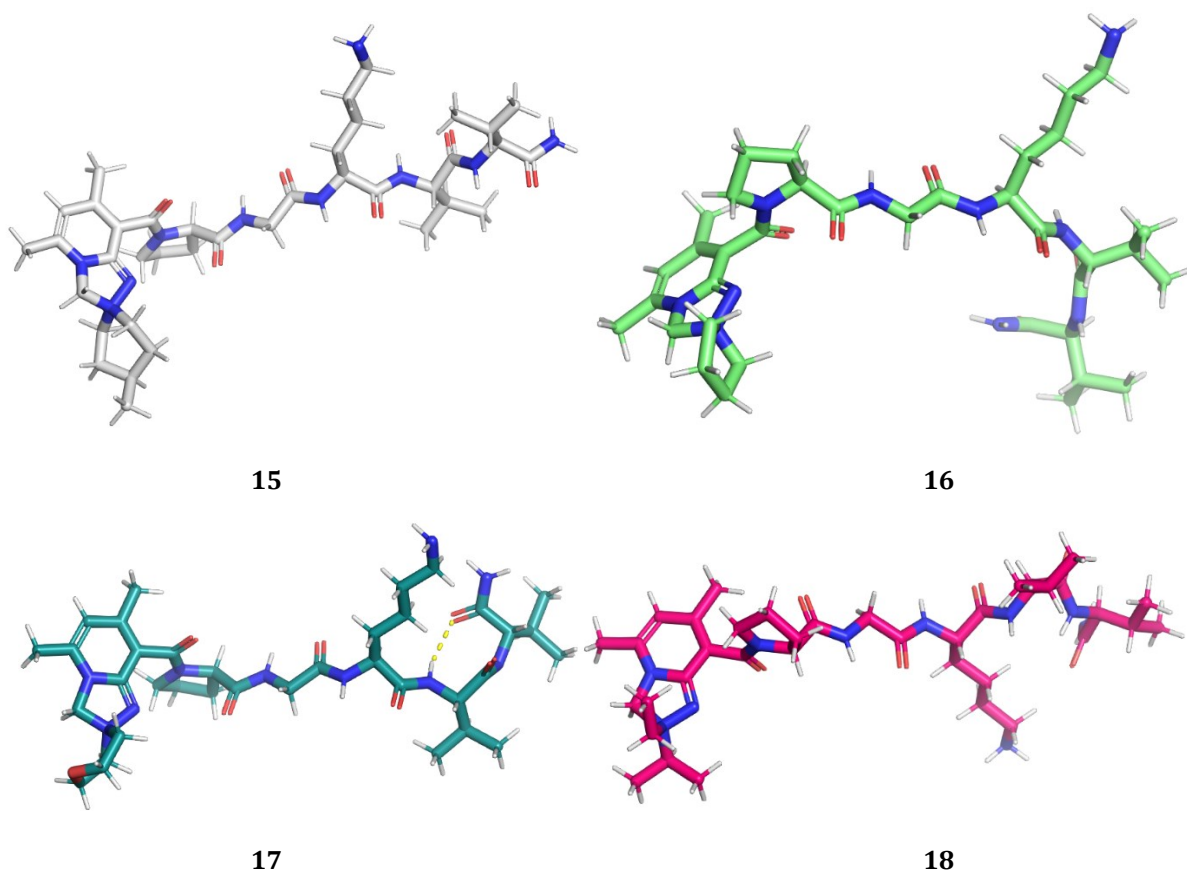
Figure 33. Optimized three-dimensional structures of **15-18**.

19

20

21

22

Figure 34. Optimized three-dimensional structures of **19-22**.

Figure 35. Optimized three-dimensional structures of **23-26**.

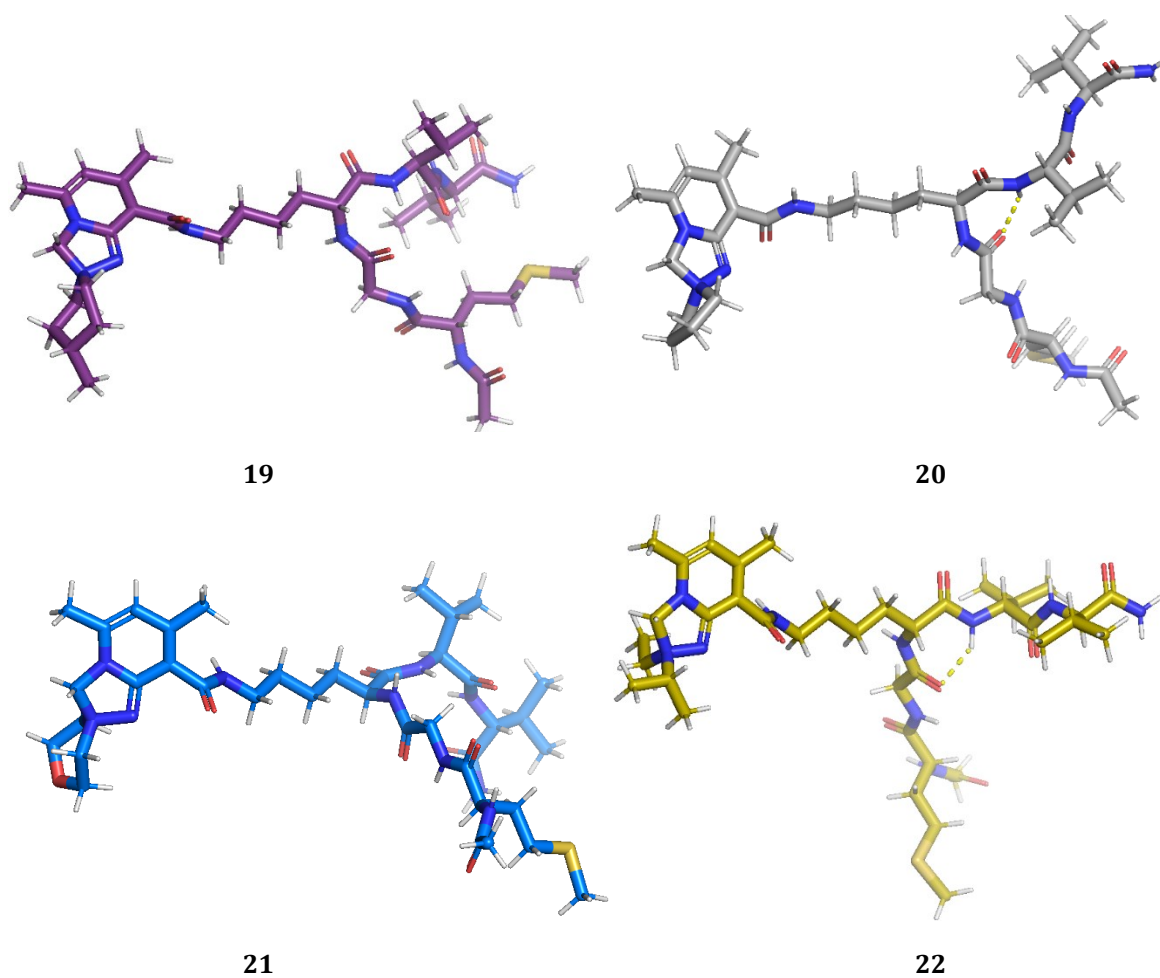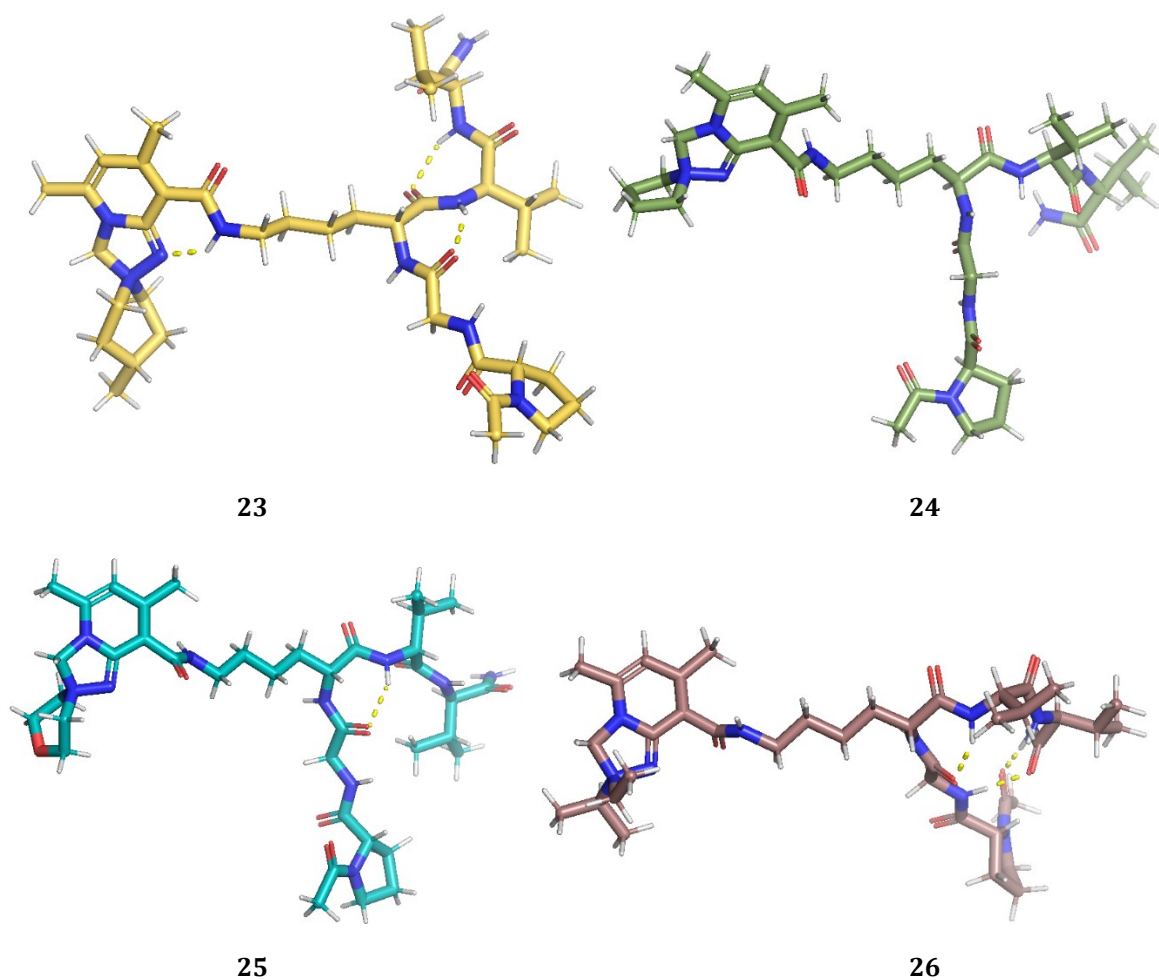### 5.2.2 Circular Dichroism (CD) measurements of compounds 8-26

To investigate the structural properties of the prepared peptide conjugates, circular dichroism spectra of each compound were measured between 240 and 190 nm. To interpret the results and understand the structural properties of obtained peptides, CD spectra of peptides **8-26** were compared with standard spectra representing α-helix, β-sheet, and random coil (disordered) conformations.[258] β-sheet conformation is characterized mostly by a positive signal around 190-200 nm and a negative peak at 210 nm. On the contrary, the random coil conformation is represented by a negative signal at 190-200 nm and no peak at 210 nm.
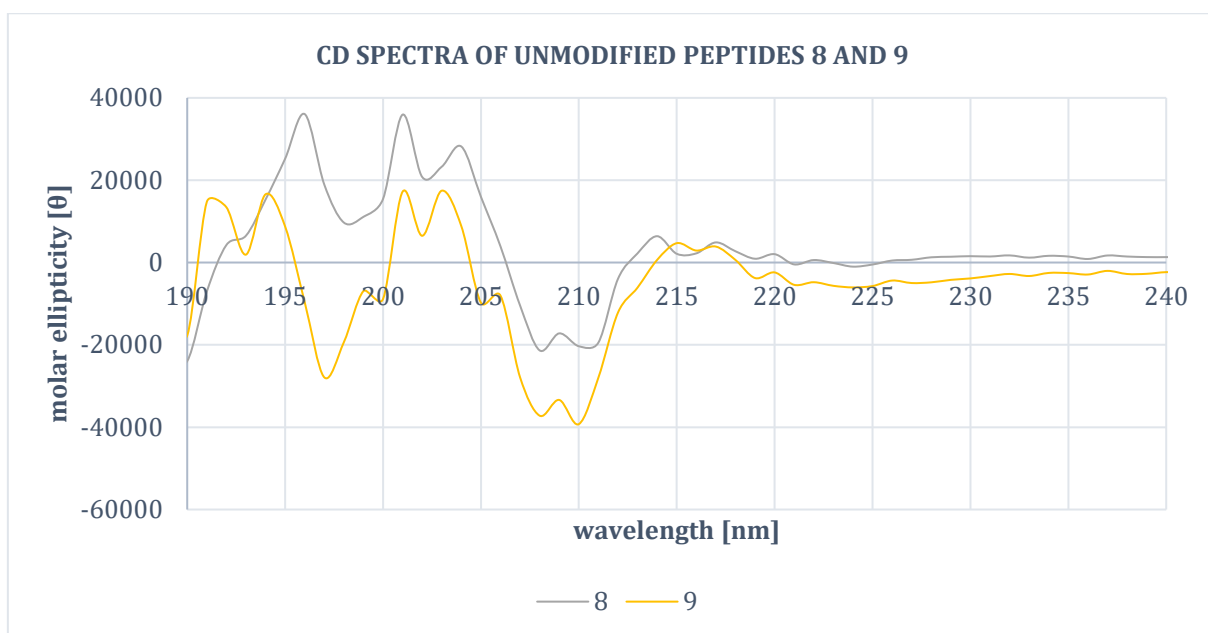
Figure 36. Overlapped CD spectra of unmodified peptides **8** (Ac-MGKVV-NH$_2$) and **9** (Ac-PGKVV-NH$_2$).

Comparing the sequences without modifications, peptides **8** and **9** both adopt a β-sheet conformation in equal concentration and assay conditions (**Figure 36**). The shape of their CD spectra is similar, but the graph obtained for peptide **8** possess a positive signal at 195-200 nm. Pro-containing sequence in this range results with a negative peak. It can be assumed that the exchange of the first amino acid in the original sequence (Met to Pro) leads to a slight disturbance of the initially adopted, ordered β-sheet shape.

Furthermore, the spectra of modified sequences **10-26** were registered to observe if there is any influence of the heterocyclic moiety on the structural properties of the conjugates (**Figure 37**-**Figure 41**).
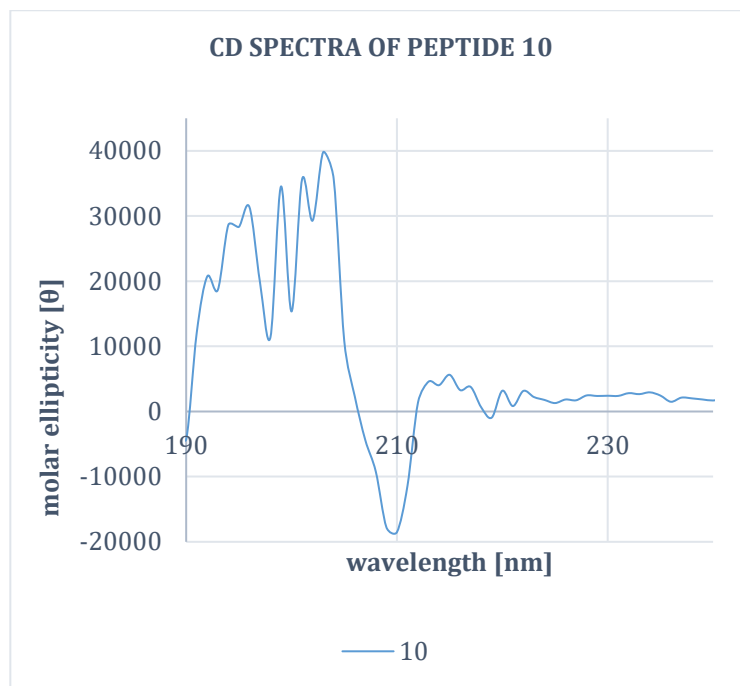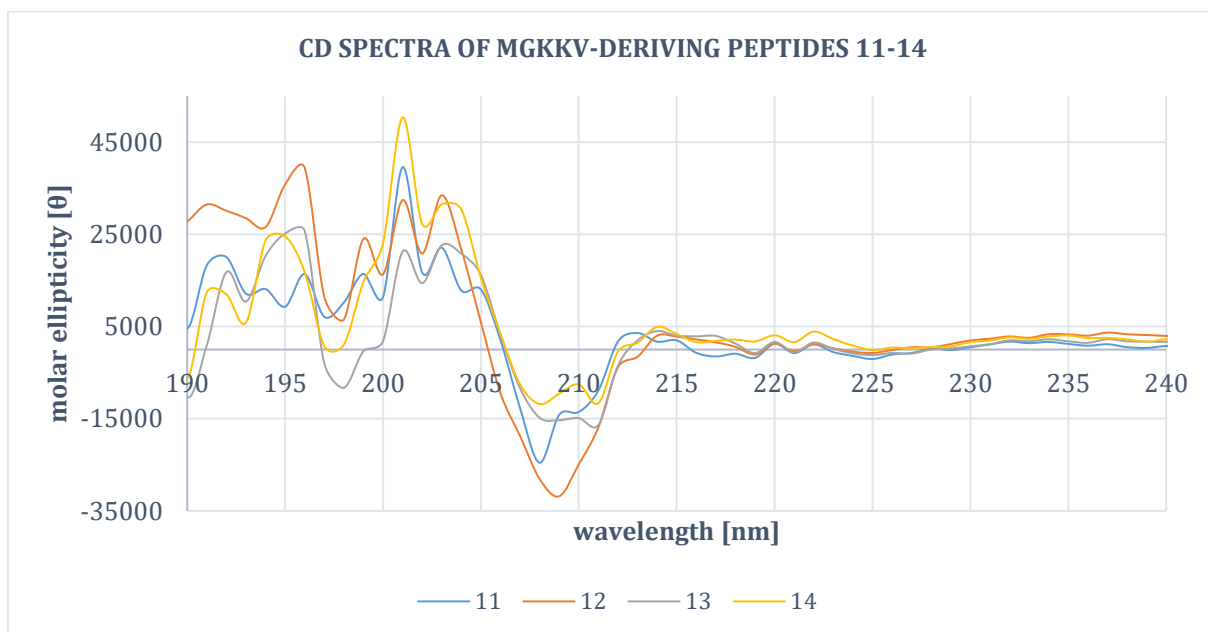
Figure 37. CD spectra of peptide **10**.

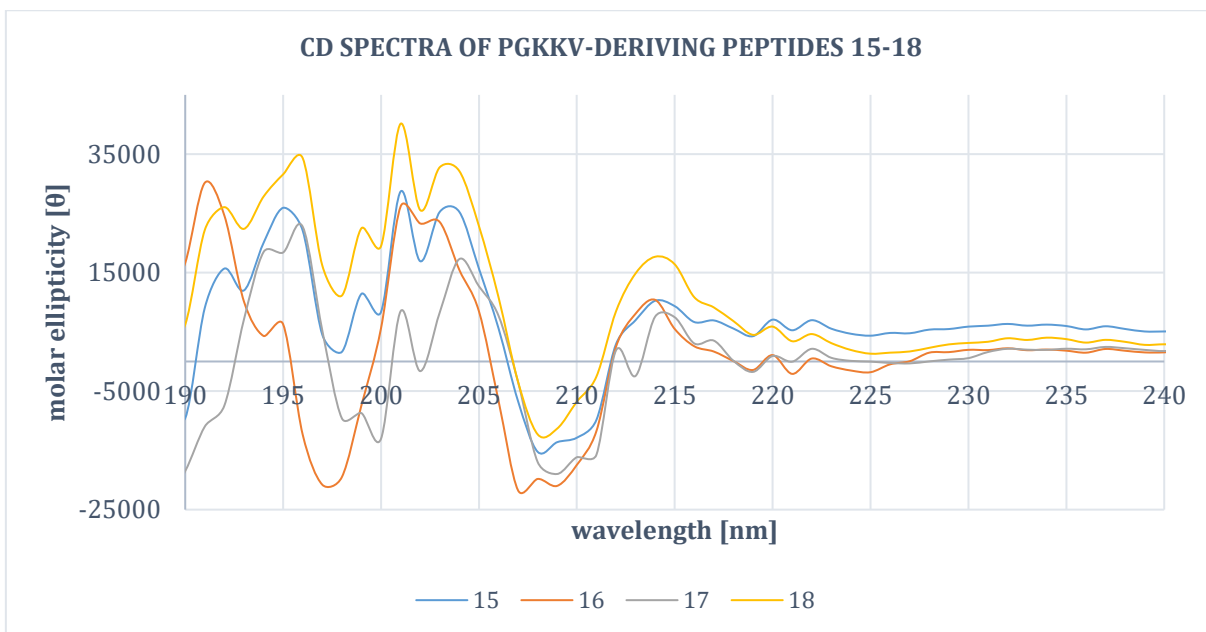**Figure 38.** Overlapped CD spectra of compounds **11-14**.

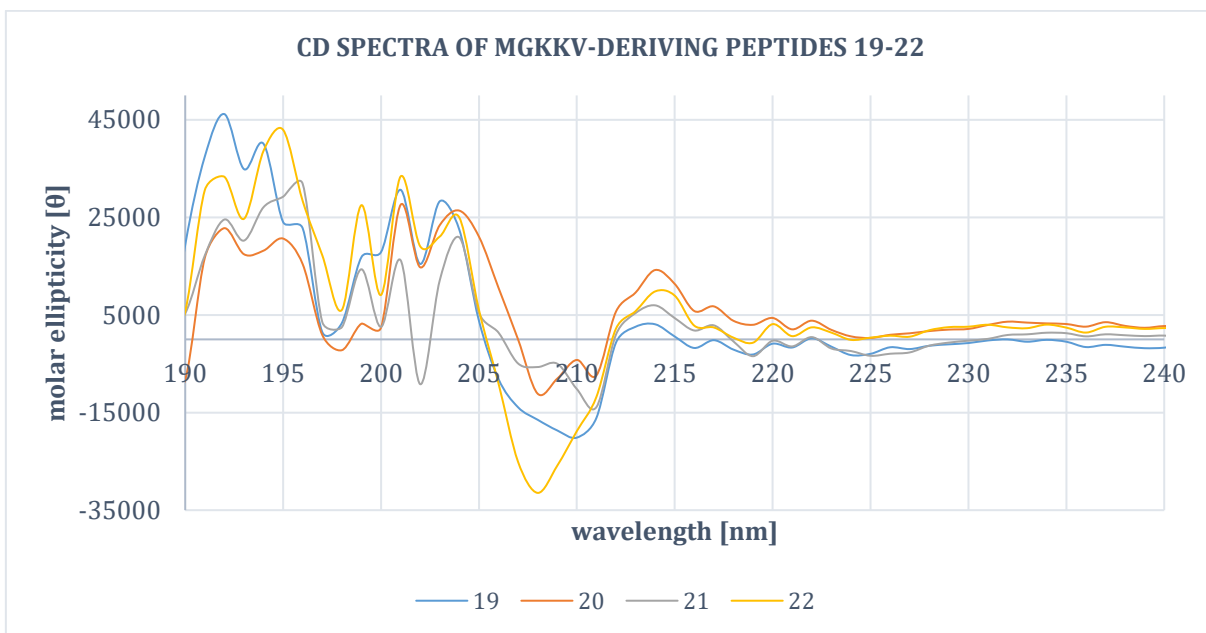**Figure 39.** Overlapped CD spectra of compounds **15-18**.

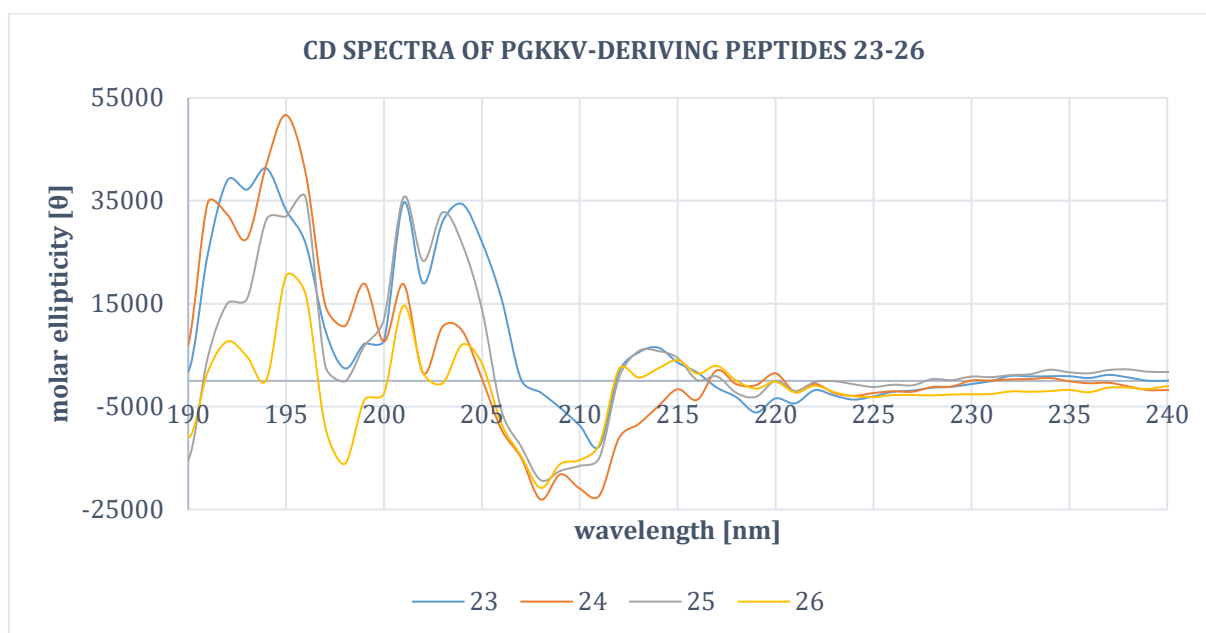**Figure 40.** Overlapped CD spectra of compounds **19-22**.

Figure 41. Overlapped CD spectra of compounds **23-26**.

None of the analyzed peptides fully adopts the random coil conformation (defined negative peak around 200 nm without other signals). The Met-containing peptides adopt β-sheet conformation at pH=8 and at room temperature, with high positive peaks around 195 nm, and negative signals around 205-210 nm. These observations are in accordance with the results published by Huntington *et al.*, subsequently mentioned by other authors, where the role of β-sheet domain identified in the complex of serpin-A1 with antitrypsin was underlined.[45,36,43] The results of CD analyses showed that the shorter, pentapeptide fragment of A1-C26 sequence (and then SA1-III peptide) maintains the β-sheet conformation. Exchange of Met residue for Pro at the first position of the chain visibly destabilizes the structure, as demonstrated by a more defined negative signal around 200 nm in PGKVV-derivatives spectra. Nevertheless, the β-sheet conformation remained unimpaired.

5.2.3 NMR analysis of compounds 4a-7a and 8-26

NMR studies were performed to confirm the structures of novel building blocks **4a-7a**, and evidence the structural differences among peptides **8-9** and their derivatives **10-26**. Obtained data – one-dimensional NMR spectra and the assignments with chemical shifts values, found for each of mentioned compounds, are summarized in SI attached to this thesis. Some of the representative examples of spectra, and chemical shifts values comparison will be mentioned below.
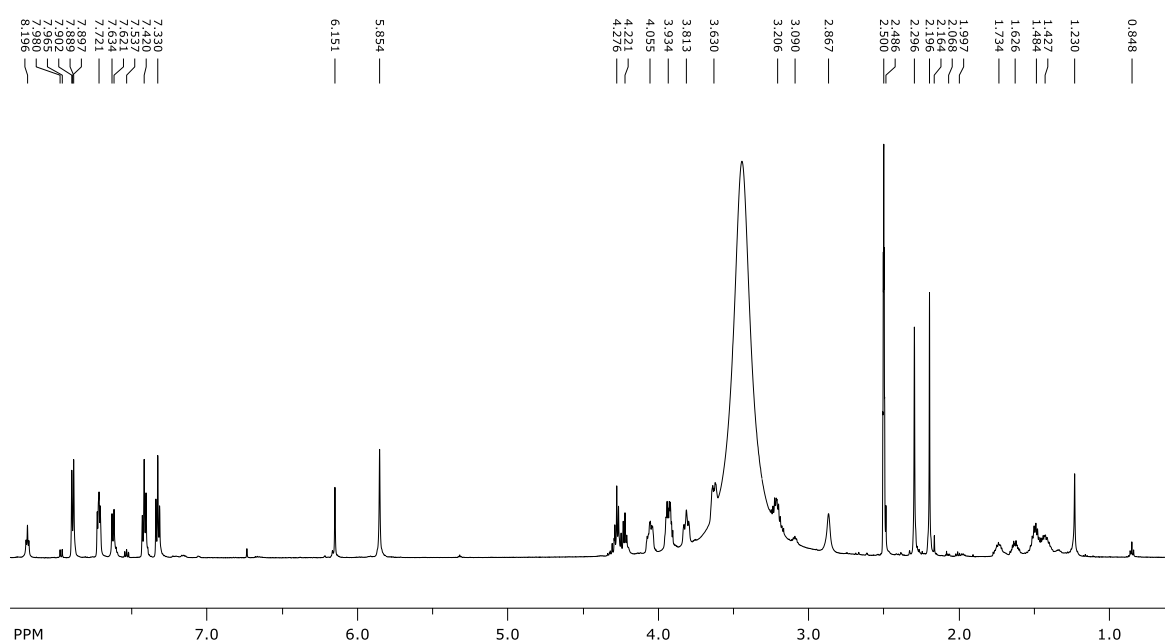
Building blocks **4a-7a** were analyzed without previous purification, confirming the applicability of solid-phase synthesis leading to decreased number of impurities in the final product. One of the examples of obtained data is presented below in **Figure 42** and **Figure 43**. Chemical shifts with their assignments for compound **6a** are summarized in **Table 22**. Due to the large number of peaks in all obtained spectra, most of them found as multiplets or overlapping signals, all assignments were collected in tables instead of the standard way of NMR results representation.

Table 22. Summary of peak assignments with chemical shift values [ppm] found in ^{1}H- and ^{13}C-NMR spectra of **6a**. Reference signal: DMSO (C; 39.50 ppm; H: 2.500 ppm).

1,2,4-triazole moiety		CH	CH$_2$	CH$_3$
	A	-	-	C: 17.77; H: 2.296
	B	C: 110.4; H: 6.152	-	-
	C	-	-	C: 19.44; H: 2.195
	D	-	C: 75.98; H: 5.854	-
	E	-	C: 61.13; H: 3.934	-
	F	-	C: 63.55; H: 3.629	-

Fmoc	CH	CH$_2$	A	B	C	D
	C: 46.43	C: 65.38	C: 125.1	C: 126.9	C: 127.4	C: 120.0
	H: 4.219	H: 4.273	H: 7.723	H: 7.329	H: 7.418	H: 7.922

Lys	COO(H)	α	β	γ	δ	ε	NH
	H: 8.199	C: 38.16	C: 28.25	C: ~22	C: 30.15	C: 53.52	H: 7.628
		H: 3.215	H: 1.632	H: 1.494	H: 1.734	H: 3.925	
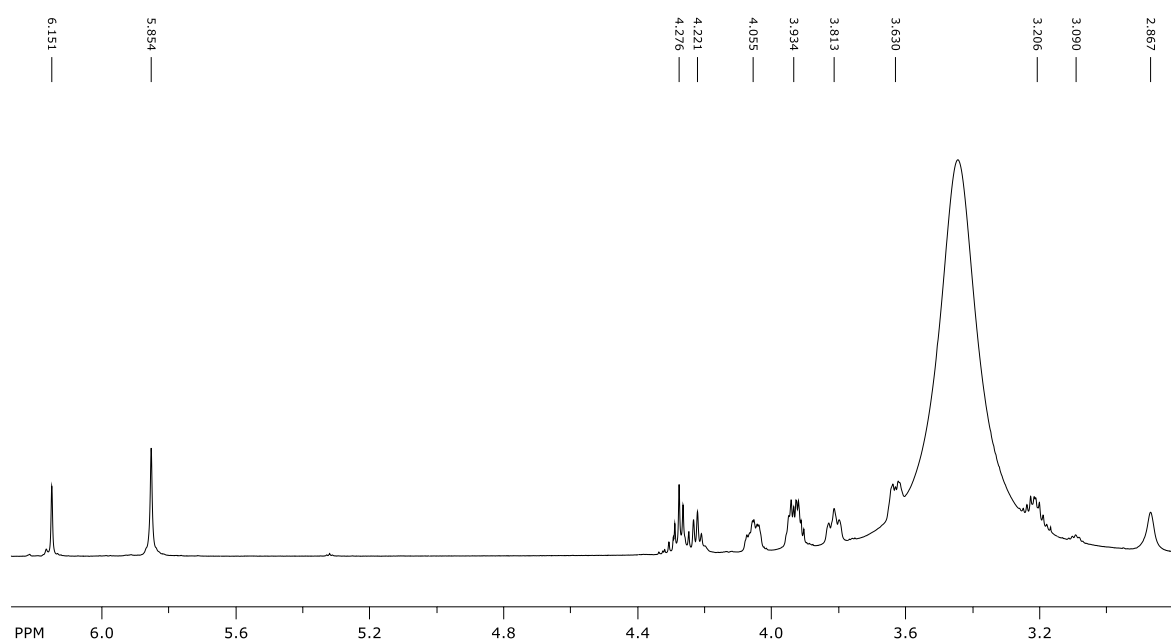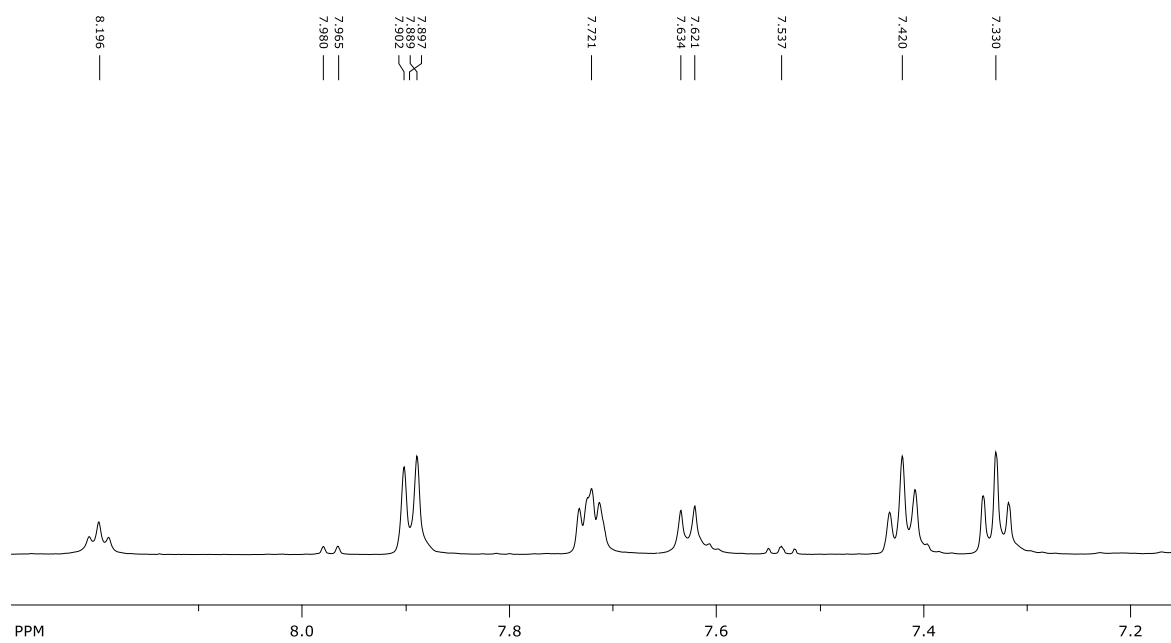
Figure 42. ^{1}H-NMR spectra obtained for building block **6a** without purification.

Figure 43. ^{13}C-NMR spectra obtained for building block **6a** without purification.

Chemical shifts values were rather equal amongst all tested compounds and were in accordance with standard chemical shift values of amino acids 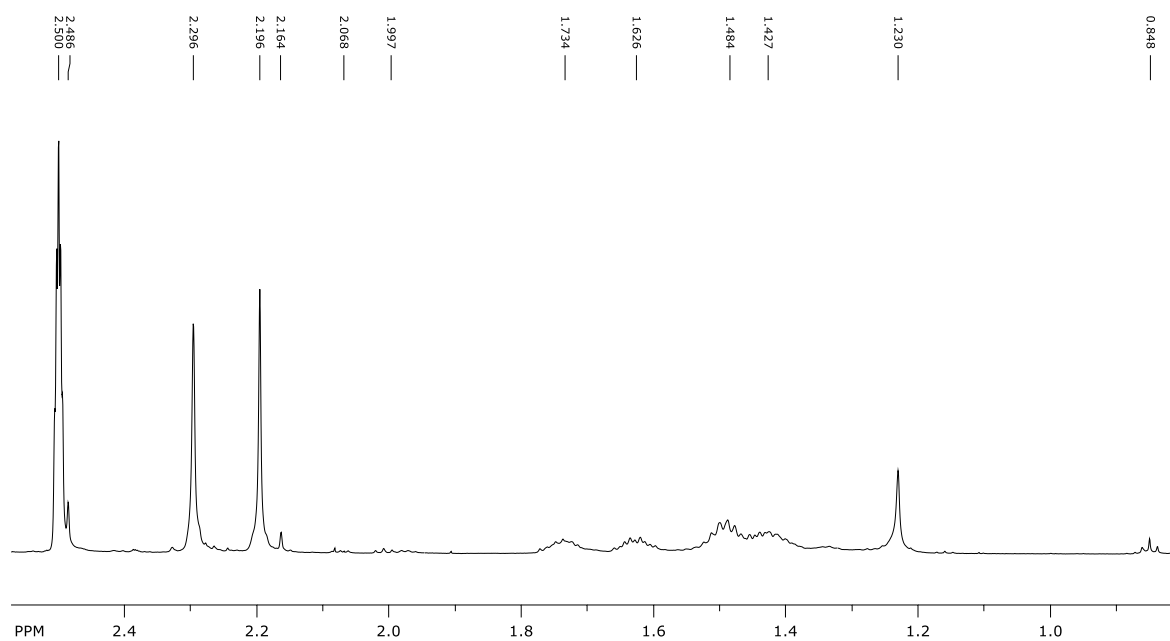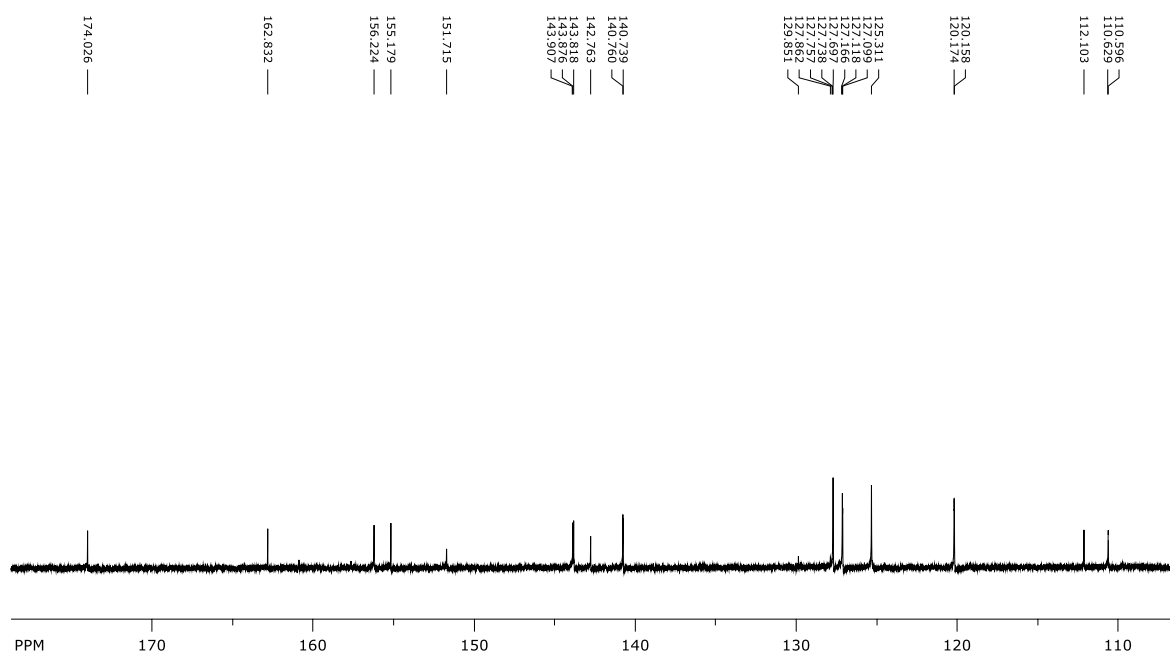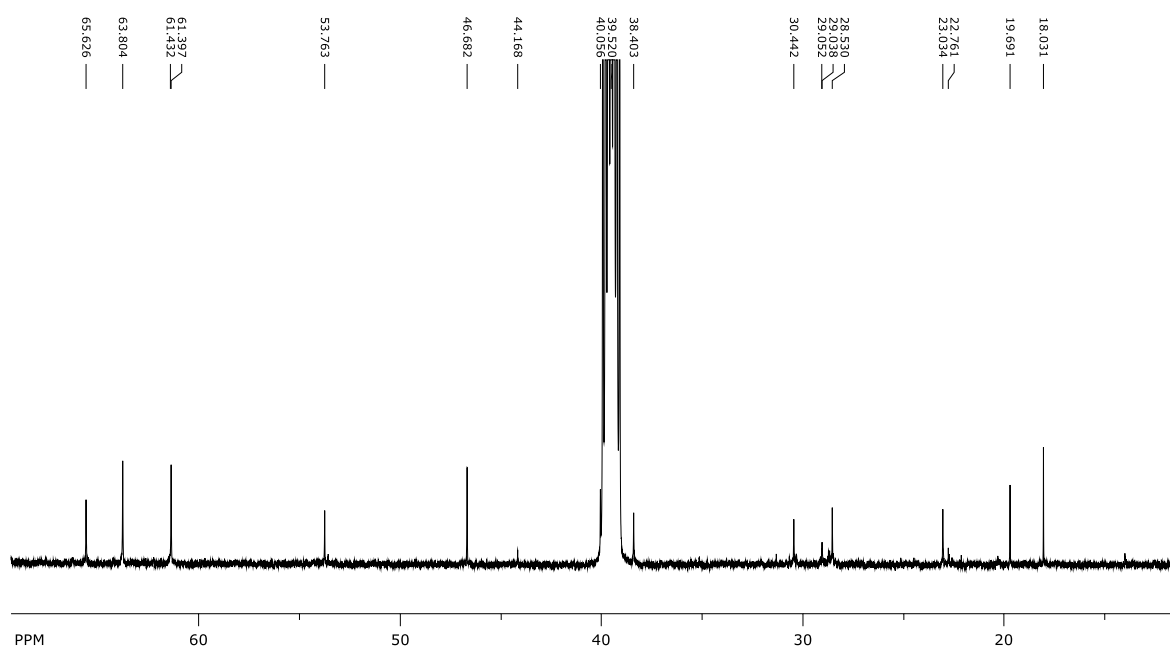described elsewhere. Due to the structural differences between conjugates obtained *via* three different synthetic pathways, some changes in the value of chemical shifts were noticeable. *Safirinium* moiety in the synthesized conjugates is located or N-terminally, or in the lysine side chain. Thus, chemical shift values were slightly variable for proton groups and carbon atoms in this area. Examples of such differences are summarized in **Table 23**. However, these values are not indicative and cannot be treated as an unambiguous structural indication. The most significant differences were observed in two-dimensional spectra, where the correlation of heterocyclic moiety proton groups with proton groups of Met and Gly (conjugates **10-18**), or Lys (conjugates **19-26**) was observed.

Table 23. Comparison of chemical shifts values among carbons and proton groups of **13** and **21**, **14** and **22** in the proximity of the structural modification. The nearness of heterocyclic moiety usually provoked slightly higher chemical shift value.

	HETEROCYCLIC MOIETY LOCATED AT N-TERMINUS		HETEROCYCLIC MOIETY ATTACHED TO LYSINE SIDECHAIN	
	Chemical shifts in **13** [ppm]	Chemical shifts in **14** [ppm]	Chemical shifts in **21** [ppm]	Chemical shifts in **22** [ppm]
Lys C$^{\varepsilon}$	53.01	53.42	53.27	53.25
Lys H$^{\varepsilon}$	4.366	4.310	4.338	4.383
Met C$^{\gamma}$	29.24	29.17	29.13	29.09
Met H$^{\gamma}$	2.676	2.655	2.520	2.578

5.3 Enzymatic assays

Enzymatic *in vitro* assays were performed to evaluate the inhibitory potency of all synthesized compounds. If the results of these assays were satisfactory, and evaluated peptides or conjugates provided significant inhibition, they were further characterized by IC_{50} calculation. Potential "good inhibitors" for the purpose of this thesis would possess IC_{50} value lower than 100 µM, ideally below 50 µM. Thus, if in the initial screening during the colorimetric tests no significant activity was observed around the concentration of 50 µM, the compound has not been qualified for further investigation and the IC_{50} was not calculated. In this case, the percentage of inhibition in different concentrations will be reported. It is another common way of comparing new compounds as potential inhibitory agents.[249]

5.3.1 Elastase inhibition

As previously mentioned, to test the versatility of synthesized building blocks in peptide modification, two analogs of SA1-III peptide were selected. SA1-III has been demonstrated to act as an inhibitor of collagen degradation processes. It was then possible that the obtained derivatives could have elastase inhibitory activity. To verify this hypothesis, elastase activity screenings were performed according to a modified procedure from the literature,[249] and compared with the protocol suggested by Sigma Aldrich, as described in the section **4.6.1**.[250] Then, the final protocol was optimized with the measurement procedure published for tyrosinase assays.[214] The assay was performed in 96-well transparent plate.

In addition to the peptides, it was important to evaluate the inhibitory properties of compounds **4-7** and **4a-7a** alone. To avoid confusing results descendent from the presence of Fmoc group in **4a-7a**, building blocks were treated with piperidine before the cleavage from the solid support and thereby the amine groups were deprotected for the purpose of the assay.

Compounds **10-26** showed a weak inhibitory activity toward PPE, while no activity was observed for **8** and **9**, even in increased concentrations (10-50 µM). No correlation between the concentration and inhibition was found, therefore peptides **8-26** were classified as inactive and were not further investigated (**Figure 44**).
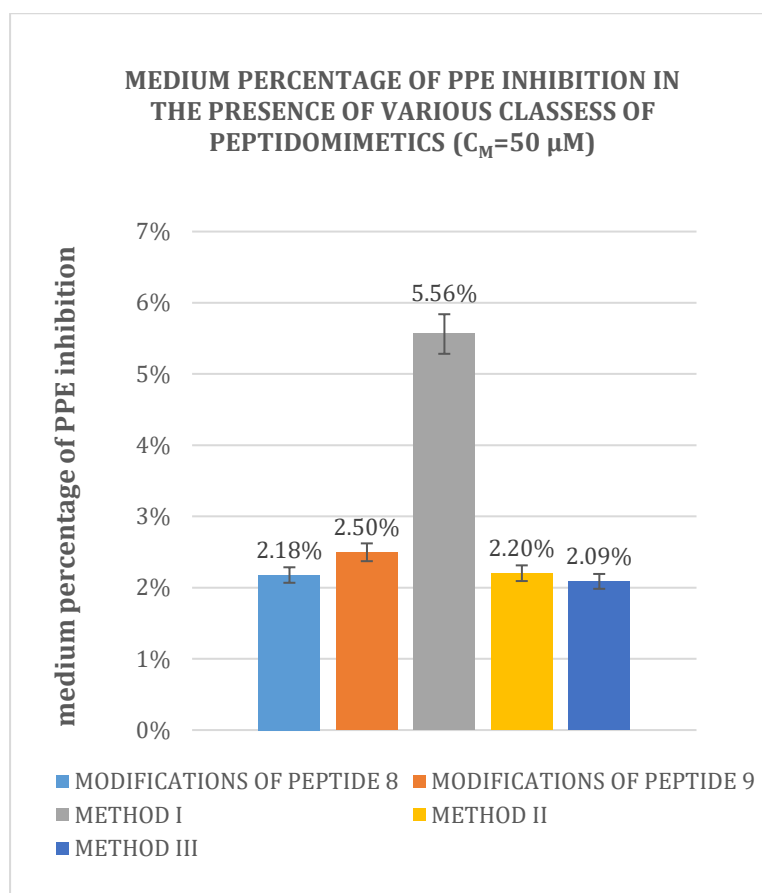
Figure 44. Results of PPE inhibition assay in the presence of synthesized compounds **10-26**, divided into classes according to their structural properties.

Due to the poor inhibition observed for peptides and their analogs, additional screening for compounds **4-7** and their derivatives **4a-7a** without protecting Fmoc group (H-Lys[N$^\varepsilon$**(4-7)**]-OH) was performed. The results are presented in **Table 24** and in the graph (with standard deviations) in **Figure 45**.

Table 24. Average values (*n*=2) of the percentage of PPE inhibition [%] in the presence of compounds **4a-7a** (without Fmoc) in various concentrations [μM].

CONCENTRATION ^{a}	COMPOUND			
	H-Lys[N$^\varepsilon$**(4)**]-OH ^{b}	H-Lys[N$^\varepsilon$**(5)**]-OH	H-Lys[N$^\varepsilon$**(6)**]-OH	H-Lys[N$^\varepsilon$**(7)**]-OH
10 μM	2%	8%	3%	0%
20 μM	5%	11%	10%	2%
30 μM	11%	18%	9%	10%
40 μM	12%	15%	20%	9%
50 μM	9%	25%	19%	12%

^{a} Final concentration in the assay well.
^{b} All tested compounds were Fmoc-free.

PERCENTAGE OF PPE INHIBITION IN THE PRESENCE OF Fmoc-DEPROTECTED COMPOUNDS 4a-7a

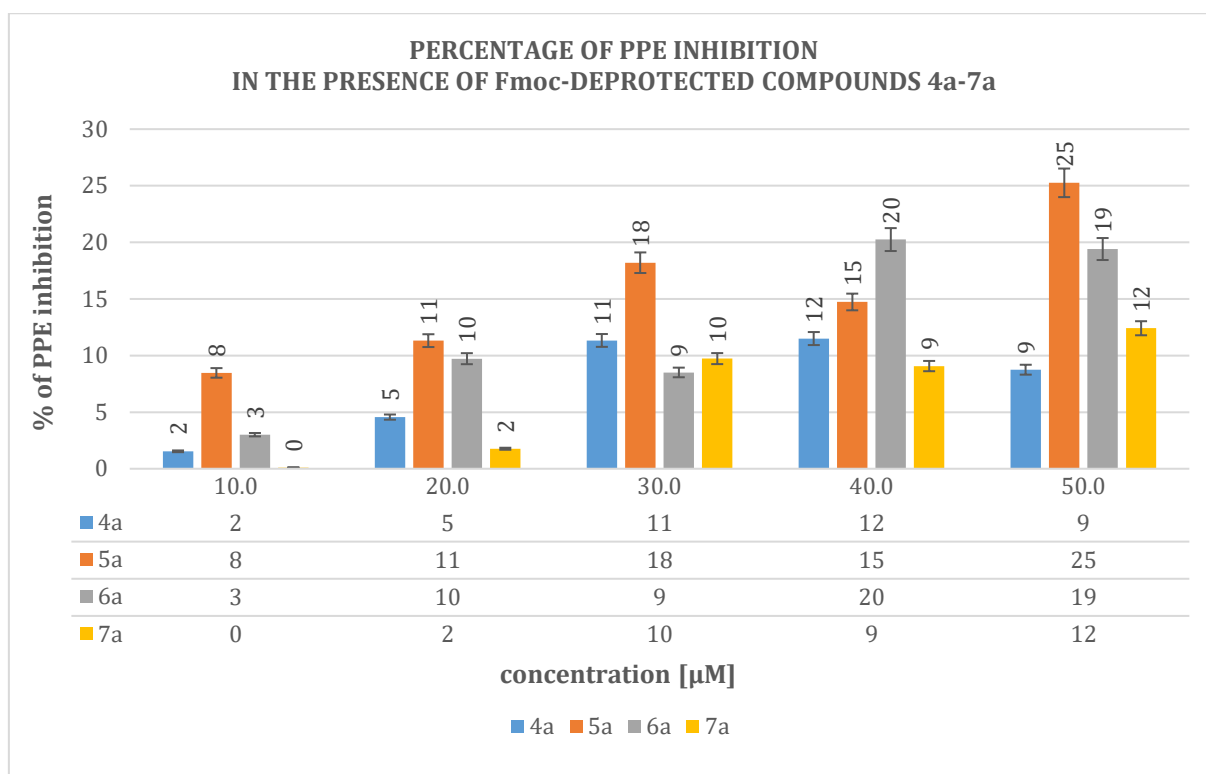| concentration [µM]	10.0	20.0	30.0	40.0	50.0
4a	2	5	11	12	9
5a	8	11	18	15	25
6a	3	10	9	20	19
7a	0	2	10	9	12

Figure 45. Average values (*n*=2) of the percentage of PPE inhibition [%] in the presence of compounds **4a-7a** (without Fmoc) in various concentrations [µM].

Surprisingly, compounds **4-7** do not show any significant inhibition, but when conjugated with lysine they are able to moderately inhibit the activity of PPE in a dose-dependent manner. All compounds were evaluated in five different concentrations, from 10 to 50 µM. H-Lys[N$^{\varepsilon}$**(4)**]-OH shows no changes in PPE inhibition over 30 µM concentration (constant inhibition around 10% in the range of 30-50 µM). H-Lys[N$^{\varepsilon}$**(5)**]-OH results as the best PPE inhibitor amongst all tested compounds. It shows increasing percentage of PPE inhibition in the tested concentration range (8-25%). Slightly weaker but still visible inhibitory activity was observed for H-Lys[N$^{\varepsilon}$**(6)**]-OH, with maximum inhibition value of 20% for two of the highest tested concentrations. On the other hand, H-Lys[N$^{\varepsilon}$**(7)**]-OH with aliphatic and bulky substituent (*N*-Ethylisopropylamine) reveals similar activity to H-Lys[N$^{\varepsilon}$**(4)**]-OH, with comparable tendency and no changes in the percentage of PPE activity over 30 µM concentration.

The differences between **4-7** and no-Fmoc **4a-7a** in PPE inhibition confirm the results obtained with molecular modeling, where the lysine linker induced a bended conformation, thereby facilitating and stabilizing the interaction with the targeted molecule. While for the compounds **4-7** no inhibition was observed, their lysine analogs synthesized by the conjugation and followed by Fmoc deprotection, resulted with

compounds of moderate and dose-depending inhibitory activity against PPE. Therefore, it can be assumed that the lysine linker is responsible for the stabilizing interactions within the PPE active site. The structures obtained during the optimization of described molecules clearly show the role of lysine linker as a separating fragment, which is in great accordance with the design strategy of peptide-drug conjugates: small drug molecule, a linker, and a peptide (or amino acid).
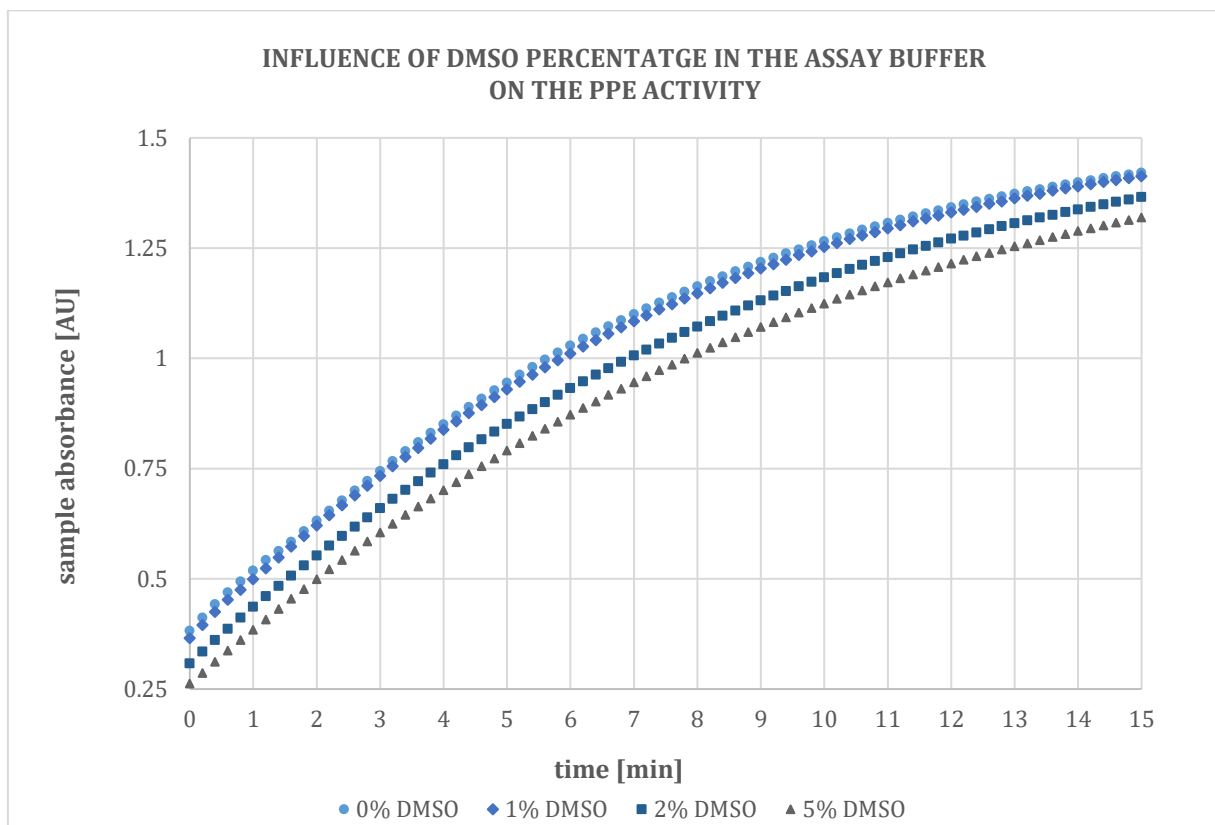

Figure 46. Evaluation of the influence of DMSO percentage in the assay buffer on the PPE activity.

Moreover, the described protocol was initially adapted from diverse procedures in the literature, and then modified for the purpose of our measurements, providing new and quick method of elastase activity screening. The new protocol describes the fast and simultaneous measurement of wide range of inhibitor concentrations, provides clear and easy to elaborate results, and was optimized to decrease the consume of all assay ingredients. Besides, the influence of DMSO percentage in the assay buffer on the PPE activity was evaluated, proving that 1% of DMSO does not influence the activity of the enzyme, but may significantly increase the solubility of the assay components (**Figure 46**). While peptides probably were too bulky and did not fit well in the enzyme active cleft, synthesized lysine conjugates (Fmoc-free) exhibited moderate inhibitory activity with the most efficient inhibitor H-Lys[N$^\varepsilon$**(5)**]-OH amongst all tested compounds.

5.3.2 Tyrosinase inhibition

Compounds **43-45** (thiosemicarbazones), **46-48** (unmodified peptides) and **49-57** (conjugates) were investigated towards their diphenolase activity, leading to the tyrosinase inhibition. All compounds and assay ingredients were prepared as mentioned in the subchapter **4.6.2.**

The percentage of tyrosinase activity was calculated after the measurements performed according to the protocol described before. In the plots summarized in **Figure 47**-**Figure 50**, all obtained data is presented. The results obtained for kojic acid, a positive control, has been shown previously in the **Figure 25**.

Unmodified peptides **46-48** did not exhibit any significant activity in the assay conditions, and their inhibitory effect on mTYR was lower than 5%. Moreover, the tyrosinase activity in the presence of **46-48** was mostly around 100% despite the increase of inhibitor concentration. Therefore, the graphs regarding the activity of mTYR in the presence of unmodified peptides **46-48** are not displayed. Other compounds considered in this investigation showed dose-dependent inhibition of mTYR. Thiosemicarbazones were the most active inhibitors among all tested compounds, with particular attention to TSC **43** and **45** resulting with very similar inhibitory profile (**Figure 47**). The range of tested concentrations for TSC was 0-150 µM, hence this range permitted to obtain the inhibition values from 0 to 100% and calculate the IC_{50}. Due to the fact that the aim of this research was to find new inhibitors with activity superior to kojic acid (IC_{50}=20 µM), the assay was not performed for the concentrations of new inhibitors exceeding 500 µM. The results for TSC-conjugates showed in **Figure 48**, **Figure 49**, and **Figure 50** consider the range of concentrations 0-250 µM, due to no changes in the inhibition observed for higher values.
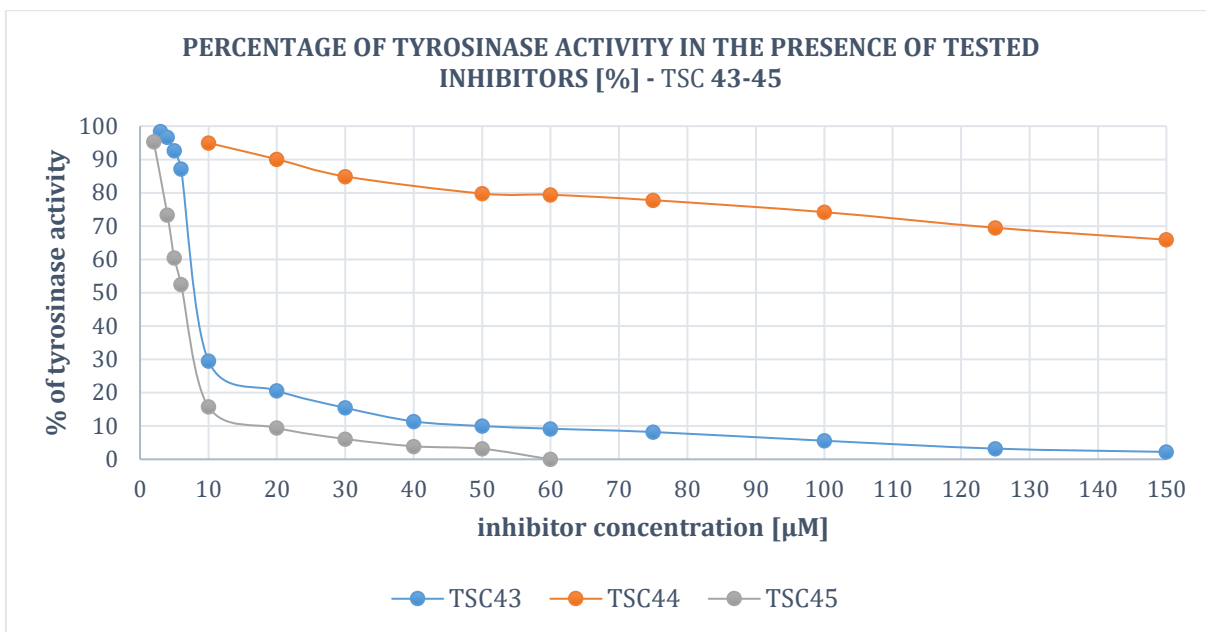
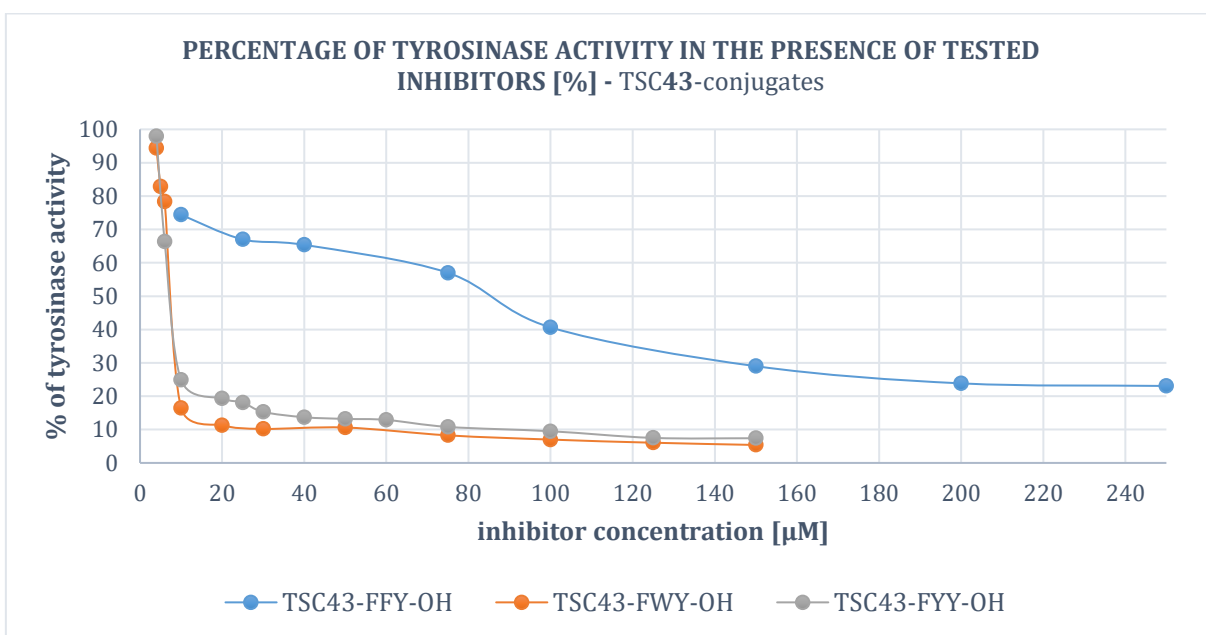**Figure 47.** The percentage of tyrosinase activity [%] in the presence of TSC **43-45** in various concentrations [μM].

Figure 48. The percentage of tyrosinase activity [%] in the presence of the conjugates of TSC **43** (**49-51**) in various concentrations [μM].
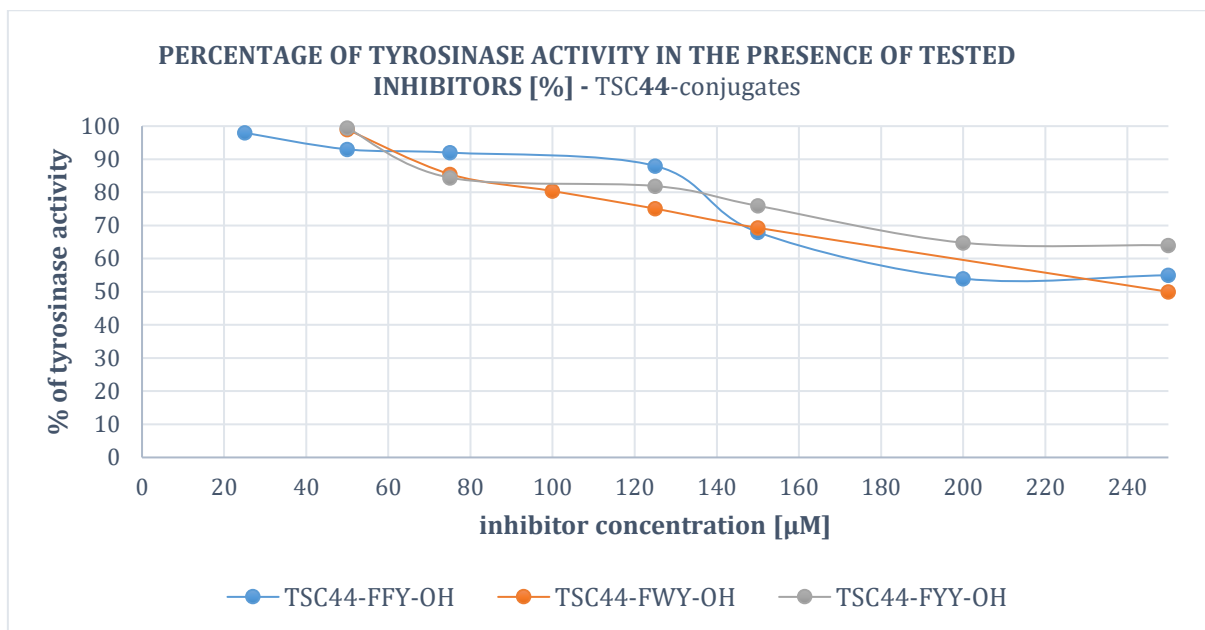
Figure 49. The percentage of tyrosinase activity [%] in the presence of the conjugates of TSC **44** (**52-54**) in various concentrations [μM].
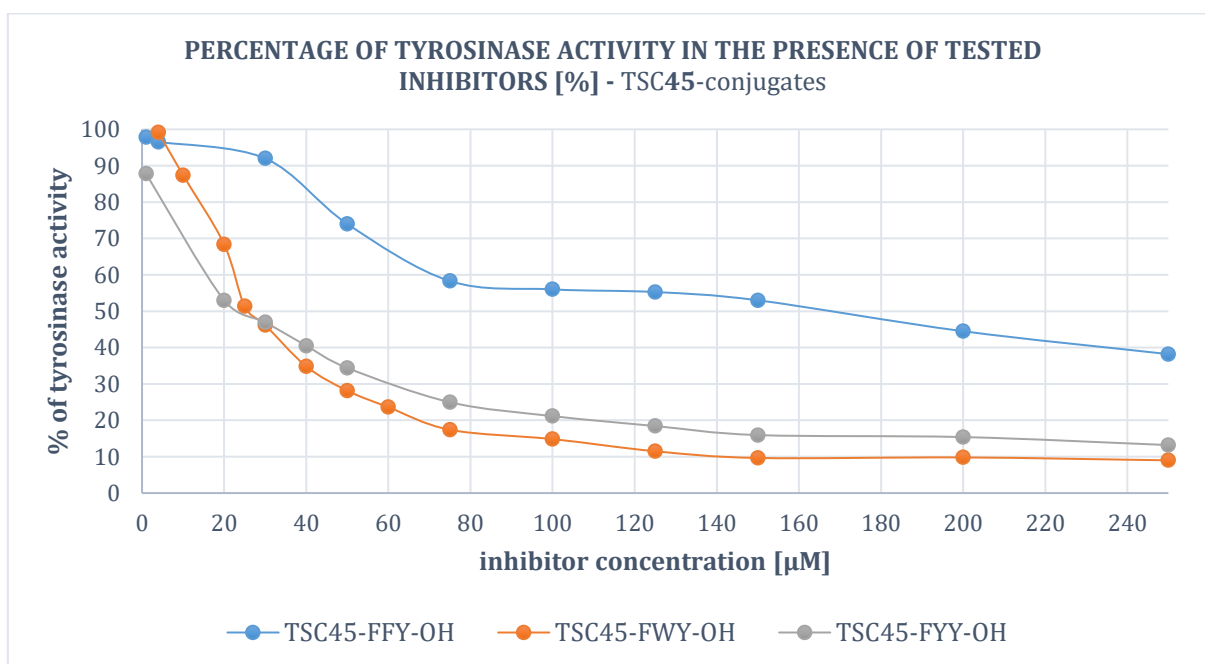

Figure 50. The percentage of tyrosinase activity [%] in the presence of the conjugates of TSC **45** (**55-57**) in various concentrations [μM].

The results obtained during the assay permitted to calculate the IC_{50} value for the inhibitors with the highest efficacy. The effect on the diphenolase activity of the enzyme was expressed as IC_{50} using *GraphPad Prism* software (**Figure 51**-**Figure 53**, and **Table 25** summarizing obtained data with standard deviation values).[251] Significant differences in the activity among TSCs **43**, **44**, and **45** were observed. The bulkiest

TSC **44** acted as the worst tyrosinase inhibitor among the three tested thiosemicarbazones. It provided the maximum of 34% of enzyme inhibition at 150 µM concentration. At higher concentrations of TSC **44** no further decrease of the tyrosinase activity was observed. On the other hand, the two structurally similar TSC **43** and **45**, demonstrated comparable inhibition potential at micromolar level (IC$_{50}$ 5.3 and 5.8 µM, respectively). In accordance with the results obtained for thiosemicarbazones, their tripeptide conjugates **52**-**54** with TSC **44** were poor inhibitors of tyrosinase (max. 50% of inhibition for C$_M$=250 µM). In contrast, the conjugates with TSC **43** generally maintained the inhibitory activity of the thiosemicarbazone (IC$_{50}$=6.57 and 6.66 µM), except for FFY sequence (IC$_{50}$=95.56±25 µM). The tripeptide conjugates with TSC **45**, i.e., **55-57** displayed a slight decrease of inhibitory activity compared to the TSC molecule alone. Once more, FYY- and FWY-tripeptide derivatives (**56** and **57**) displayed similar tyrosinase inhibition (IC$_{50}$=26 and 25 µM, respectively), but that was remarkably worse in the case of the FFY-conjugate **55** (62% of inhibition for 250 µM).
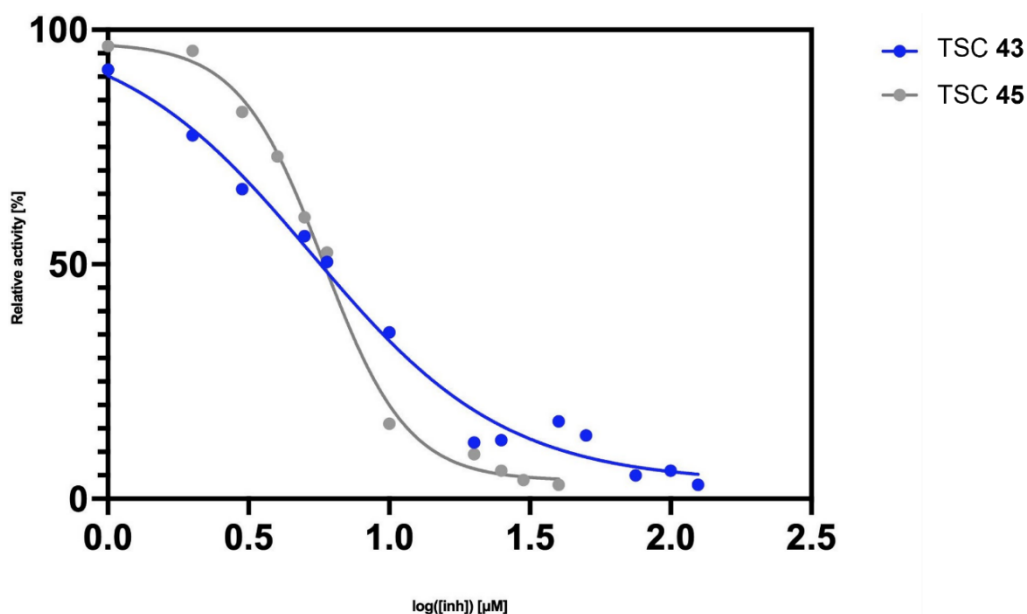

Figure 51. Inhibitory activity against mTYR of TSC **43** (blue) and **45** (gray). IC$_{50}$ representation – relative activity in % *versus* log[inh] in µM.
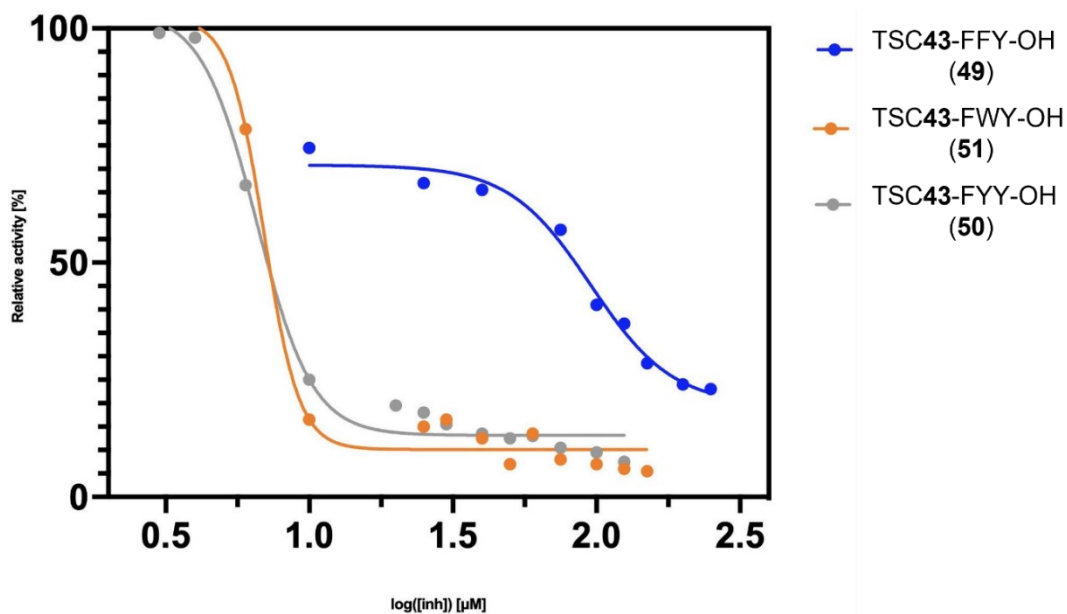
Figure 52. Inhibitory activity against mTYR of **49** (TSC**43**-FFY-OH, blue), **50** (TSC**43**-FYY-OH, gray) and **51** (TSC**43**-FWY-OH, orange). IC_{50} representation – relative activity in % *versus* log[inh] in µM.
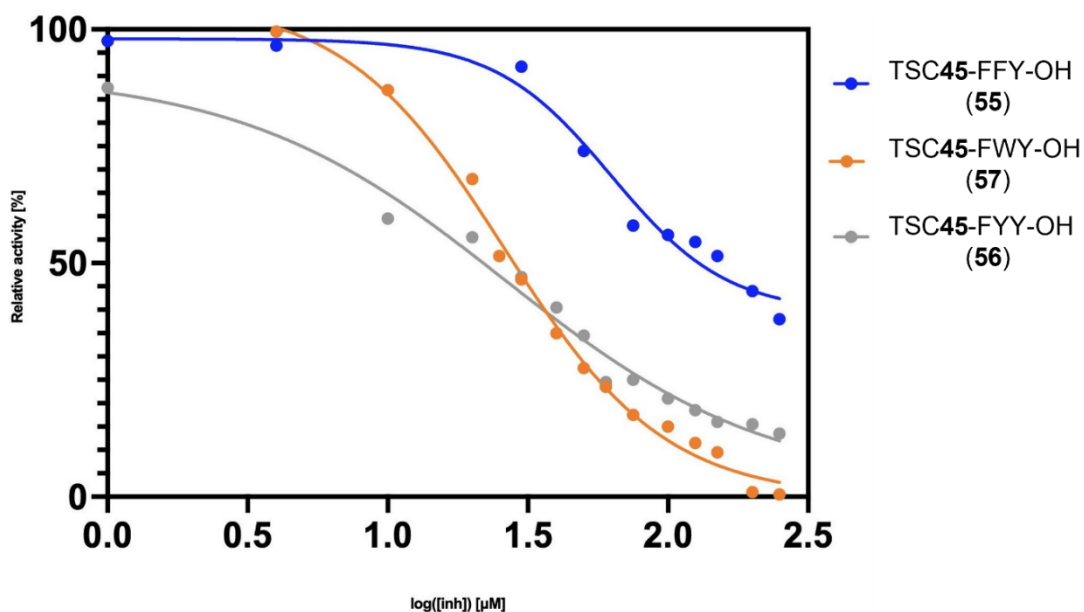
Figure 53. Inhibitory activity against mTYR of **55** (TSC**45**-FFY-OH, blue), **56** (TSC**45**-FYY-OH, gray) and **57** (TSC**45**-FWY-OH, orange). IC_{50} representation – relative activity in % *versus* log[inh] in µM.

Table 25. Results of tyrosinase inhibition assay. Compounds were compared with the well-known tyrosinase inhibitor, kojic acid.

COMPOUND		IC_{50} [µM]	Maximum percentage of inhibition reached for poor inhibitors
		OBTAINED VALUES (*n*=3)	
Kojic acid		20	-
43	TSC43	5.3 ± 2.2	-
44	TSC44	-	34% (150 µM)
45	TSC45	5.8 ± 0.5	-
46	Ac-FFY-OH	*no significant inhibition was observed in the tested range of concentrations*	
47	Ac-FYY-OH		
48	Ac-FWY-OH		
49	TSC43-FFY-OH	-	77% (250 µM)
50	TSC43-FYY-OH	6.57 ± 0.5	-
51	TSC43-FWY-OH	6.66 ± 0.5	-
52	TSC44-FFY-OH	-	45% (250 µM)
53	TSC44-FYY-OH	-	36% (250 µM)
54	TSC44-FWY-OH	-	50% (250 µM)
55	TSC45-FFY-OH	-	62% (250 µM)
56	TSC45-FYY-OH	26.12 ± 9	-
57	TSC45-FWY-OH	25.14 ± 2.5	-

The most surprising result of the tyrosinase activity assay regards the serendipitous inhibitory properties of all FFY-derivatives against the background of other sequences (FYY, FWY). It is transparently visible that the presence of Phe in the middle of the sequence impedes the interaction of inhibitor with the enzyme. This particularity will be then investigated and discussed in the subchapter regarding *in silico* experiments for synthesized compounds (**5.5**).

The efficacy of new compounds against the inhibitory potential of already known mTYR inhibitors discussed previously can be evaluated. Most of the new inhibitors show very good or moderate inhibition of mTYR. Compounds **43**, **45** (TSCs) and their derivatives are better (**50-51**) or equal (**56-57**) tyrosinase inhibitors than kojic acid. The data obtained for already described unmodified peptide Ac-FFY-OH is in accordance with the results in the literature, where this compound was reported as relatively poor inhibitor with IC_{50}=240 µM. Moreover, the efficiency of compounds **52-54** and TSC **44** alone cannot be omitted. It is not excellent, but in comparison with other compounds reported in the literature as "tyrosinase inhibitors", TSC **44** and its derivatives still should be considered as potential candidates of melanogenesis inhibitors.

Indeed, all compounds evaluated towards their tyrosinase inhibitory potential were then examined as inhibitors of melanogenesis, in parallel with their cytotoxic effect on melanoma cell lines.

5.4 Melanogenesis and cell proliferation inhibition

Effect of the synthetic compounds on melanogenesis inhibition was performed in B16F0 murine melanoma cell line. Mouse model of human skin is often employed in skin biology and cancer research due to numerous similarities.[185] B16F0 murine melanoma cell line shares most of the melanogenesis with human melanocytes. Therefore, it is the proper model for screening of the effect of potential inhibitors on melanogenesis.[259]

The results of percentage inhibition of melanogenesis by synthetic compounds **43-57** as well as dose-response measurements (IC_{50}) along with confidence intervals for melanin production and cell proliferation in B16F0 mouse melanoma cells are shown in **Table 26**. Kojic acid was used as a standard control, DMSO was used as a solvent control, TSC **43-45** were used as thiosemicarbazone controls for TSC-tripeptide conjugates **49-57**, and the corresponding tripeptide sequences **46-48** were also used as controls.

Table 26. Results of inhibition of melanin production and cell proliferation in B16F0 cell line.

COMPOUND		% Of melanogenesis inhibition		IC_{50}[a] of melanin production [μM]	95% CI[b] IC_{50} [μM]	IC_{50} of cell proliferation [μM]	95% CI[b] IC_{50} [μM]
		40 [μM]	10 [μM]				
Kojic acid		12	1	121.0	105.5-138.8	162.2	116.6-225.6
DMSO		4	2	n/a[c]	n/a	144.6	114.9-181.9
43	TSC43	30	14	101.5	88.38-116.6	113.6	90.50 - 142.6
44	TSC44	77	28	19.8	17.3-22.6	71.5	48.4 - 105-6
45	TSC45	13	1	126.4	109.3-146.2	113.1	101.4 - 126.3
46	Ac-FFY-OH	3	1	245.7	58.5-1033	106.2	76.94-146.6
47	Ac-FYY-OH	2	0	174.7	79.5-383.8	96.6	80.07 - 116.5
48	Ac-FWY-OH	4	0	140.9	104.5-189.9	81.0	62.74 - 104.6
49	TSC43-FFY-OH	10	1	138.4	114.1-167.9	72.8	62.95 - 84.23
50	TSC43-FYY-OH	12	3	158.5	131.8-190.6	99.0	82.07 - 119.5
51	TSC43-FWY-OH	11	0	150.6	123.5-183.7	77.1	59.49 - 99.96
52	TSC44-FFY-OH	4	0	146.1	99.0-215-5	77.4	55.52-107.9
53	TSC44-FYY-OH	0	0	n/a	n/a	77.2	68.76 - 86.38
54	TSC44-FWY-OH	3	0	89.9	74.87-107.9	63.2	49.67-80.38
55	TSC45-FFY-OH	3	0	162.4	113.0-233.5	49.8	35.55 - 69.89
56	TSC45-FYY-OH	4	0	144.9	110.1-190.8	83.7	68.94 - 101.6
57	TSC45-FWY-OH	20	5	67.1	63.8-70.7	67.5	59.58 - 76.52

[a] *Inhibitor concentration required for 50% inhibition.*
[b] *Confidence interval.*
[c] *Not applicable.*

The results show that melanogenesis in B16F0 cells was inhibited by all the synthetic compounds **43-57** (except for compound **53**), kojic acid, and DMSO in

dose-dependent manner. Almost all compounds (**45-56**) inhibited 0-3% of melanogenesis at the concentration of 10 μM, and 4-13 % at 40 μM. These values do not place them among the most potent melanogenesis inhibitors. Nevertheless, TSC **43-45** and the tripeptide conjugate **57** inhibited melanogenesis more than kojic acid at these two concentrations.

Interestingly, TSC **44** possessing the bulkiest structure and being the poorest inhibitor of tyrosinase, turned out to be the most potent melanogenesis inhibitor. It inhibited 77% of melanogenesis activity at 40 μM. This result is in agreement with the results of one of the previous papers where thiosemicarbazone of benzophenone and of (*E*)-2-phenylacetophenone (possessing an additional aromatic bulky substituent) revealed IC$_{50}$ value for melanogenesis below 2 μM.[214] Interestingly, this phenomenon seemed to be independent on the tyrosinase inhibition, as thiosemicarbazone of benzophenone was an efficient tyrosinase inhibitor, while thiosemicarbazone of (*E*)-2-phenylacetophenone did not inhibit tyrosinase at all.

All the investigated compounds (except for compound **53**) revealed IC$_{50}$ at the micromolar level. TSC **43** and **44** as well as the tripeptide conjugates **54** and **57** showed stronger potency of melanogenesis inhibition than the positive control kojic acid (lower IC$_{50}$ values in comparison with kojic acid, which gave IC$_{50}$ of 121 μM). These results were verified with the effect of tested inhibitors on proliferation of B16F0 cells (**Table 26**). Low melanin production might have been caused by high toxicity (low IC$_{50}$ of inhibition of cell proliferation) of the inhibitors which, in turn, can lead to inhibition of melanin production. IC$_{50}$ of cell proliferation is in the range of 49.8-113.6 μM, and all are lower than kojic acid (162.2 μM).

The investigated compounds are not highly toxic to B16F0 cells but at the same time they inhibit melanogenesis with relatively low efficacy. The potency of TSCs to inhibit melanin production regarding their toxicity, is visualized in **Figure 54**.
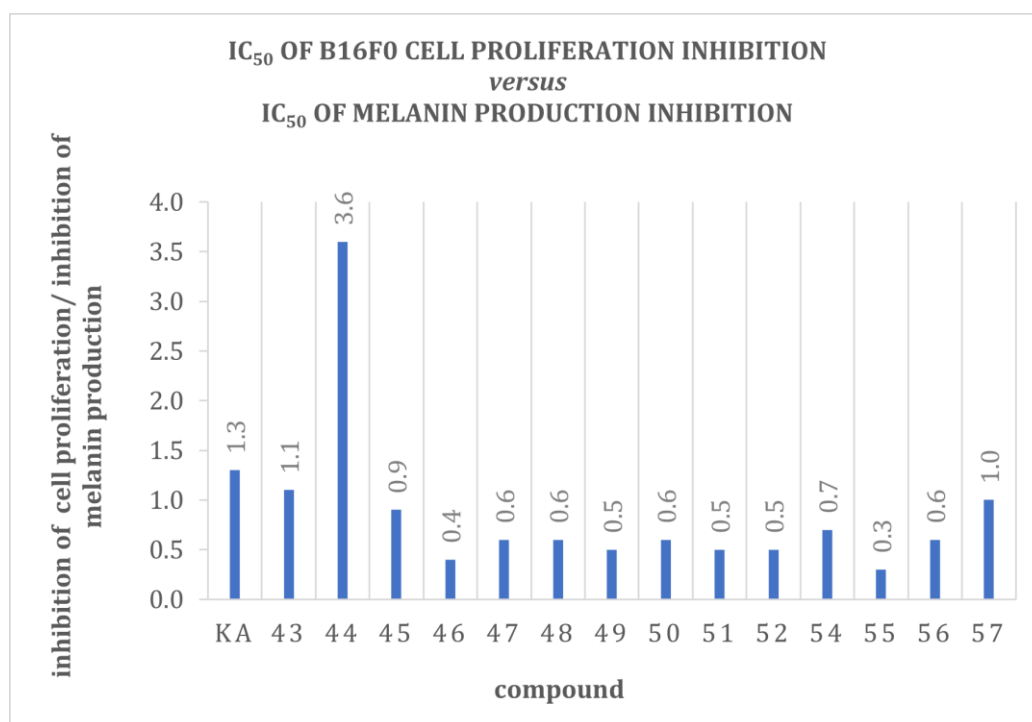
Figure 54. Inhibition of B16F0 cell proliferation *versus* inhibition of melanin production. The bar graph represents the ratio of IC_{50} for B16F0 cell proliferation to IC_{50} referred to melanin production, counted for all investigated compounds (except compound **53**) and kojic acid.

The higher bars in **Figure 54** indicate the higher ratio of melanogenesis inhibition to the toxicity against melanoma cell lines. Low ratio values, especially <1.0, does not let to conclude if melanin production inhibition depends on the inhibitor or inhibition of cell proliferation. Therefore, IC_{50} of melanin production should be higher than IC_{50} of cell proliferation. The highest ratio refers to TSC **44** (ratio: 3.6) and this is the only thiosemicarbazone displaying better ratio value than kojic acid (ratio: 1.3). TSC **44** inhibits melanogenesis in B16F0 cell line but shows no significant inhibition toward tyrosinase. It appears that TSC **44** inhibits the pathway at different stages than the step catalyzed by tyrosinase, for example affecting activity of other key enzymes in melanin biosynthesis, e.g., dopachrome tautomerase, microphthalmia associated transcription factor, or tyrosinase c protein 1.[260]

In summary, the results obtained for melanogenesis, and melanoma cell lines proliferation inhibition are not fully in line with mTYR inhibition assay. It should be underlined that one of the goals in this project was to find good inhibitors of tyrosinase with decreased cytotoxicity. Therefore, the further step of this project will include the cytotoxicity assay in healthy cell culture. Thus, for these new compounds, it will be possible to evaluate the ratio between inhibition and healthy cells viability. This data

surely will provide additional information on conjugates relevance as tyrosinase and melanogenesis inhibitors.

Moreover, the differences between the inhibitory properties for tyrosinase and melanogenesis probably are caused by the different source of tyrosinase in these two assays. As mentioned before, tyrosinase structure is slightly different among species. It could be possible to solve this problem by using the murine cell lysate for the inhibition assay instead of mTYR.

5.5 *In silico* investigations of tyrosinase inhibitors

Understanding the nature of guest–host interactions is mandatory for rational design of inhibitors. Molecular modeling, especially simulation of the docking process, can contribute to understanding the physical nature of those interactions. Performing docking simulations allows to better understand the results of biological tests. During the preliminary steps, structures of the investigated thiosemicarbazones and their conjugates with tripeptide sequences have been optimized by using *Gaussian16* code at the B3LYP/6-311g(d,p) level with a solvent model and water as solvents. In the case of TSC **43**, containing an asymmetric carbon atom, both R and S isomers have been considered. Isomer *E* were docked as default configuration, however during the docking process there was a possibility to freely change between *E* and *Z*. No meaningful results were found for *Z* isomer; therefore, all the presented data refer to the preferential *E* configuration. In the second preliminary step, the structure of tyrosinase was protonated at pH 6.8 using *H++* web server.[255,256] Calculated structures of inhibitors were docked to the active site of tyrosinase by using *Gold ver. 2021.3* algorithm.[261] Ten orientations of each investigated inhibitor were obtained, among which the ones with the best value of the ChemPLP scoring function were selected for further investigations.

During the previous results of docking studies, it was demonstrated that the thiourea moiety of thiosemicarbazone inhibitors usually interacts with copper ions of tyrosinase molecule.[214–216] Because of that, according to the previously published procedure, a docking protocol without any additional inhibitor-enzyme constraints was adopted.

Structural analysis of inhibitor-enzyme complexes for TSC **43-45** shows that alignment of each thiosemicarbazone inhibitor is stabilized by π-π stacking interaction between the inhibitor phenyl moiety and the imidazole ring of His263 (**Figure 55**, top). Additionally, strong interaction between the negatively charged carboxylate moiety of inhibitors and copper ions (**Figure 56**) firmly anchors them into the active site.
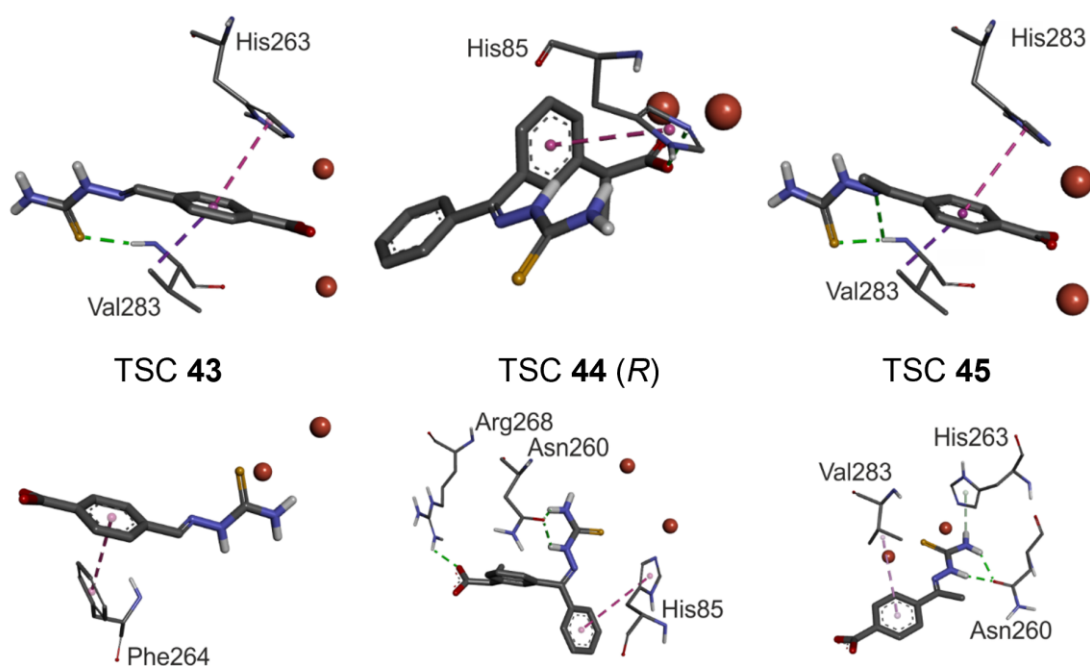
Figure 55. Orientation of TSC **43-45** in the tyrosinase active site. Top: free docking; bottom: constrained docking. Intermolecular interactions are represented as dash lines – green: H-bond; purple: π-π interaction. Copper ions are shown as red spheres.
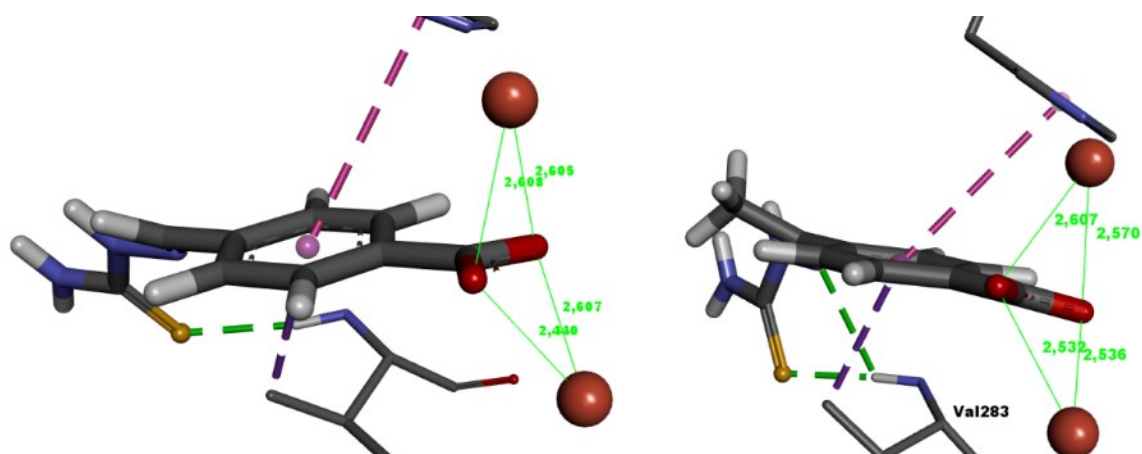

Figure 56. Distance values between the carboxylic group of inhibitor and mTYR copper ions. (TSC**43** - left, TSC**45** - right). Copper ions are shown as red spheres.

These unexpected results deriving from calculations show that inhibitors TSC **43-45** interact with the enzyme not through the thiourea moiety, but through the carboxylate group. To confirm this surprising preference, docking studies using additional structural constraints were performed, forcing the distance between the sulfur atom of the thiourea group and copper ions in the range of 1.5-5.0 Å. The use of these structural constraints allowed to obtain distances in which the thiourea group interacted with copper ions (**Figure 55**, bottom). However, comparing the scoring function values it can be observed that these positions are less preferred regardless of

the considered inhibitor. Similar conclusions can be drawn from comparing free and constrained docking results for peptide conjugates, summarized in **Table 27**. Nevertheless, in the case of these inhibitors, differences are not significant.

Table 27. Comparison of ChemPLP scoring values for free and constrained docking protocols.

COMPOUND	ChemPLP VALUE	
	Free docking	*Constrained docking*
TSC43	80.6	23.0
TSC44-*R*	65.7	47.1
TSC44-*S*	50.9	47.1
TSC45	82.9	33.6
TSC43-FYY	97.1	93.7
TSC43- FWY	102.0	81.0
TSC43-FFY	69.5	51.9
TSC44-*R*-FYY	66.7	46.9
TSC44-*S*-FYY	61.1	47.3
TSC44-*R*- FWY	60.3	41.3
TSC44-*S*- FWY	61.5	41.5
TSC44-*R*-FFY	62.1	51.1
TSC44-*S*-FFY	64.8	47.1
TSC45-FYY	95.8	83.0
TSC45- FWY	97.9	58.6
TSC45-FFY	78. 1	56.1
Kojic acid	53.5	-

The relationship between inhibitory activity and the sequence of the tripeptide linked in the conjugates can be analyzed using the example of thiosemicarbazone TSC **43**. As mentioned above, the scores of the scoring function obtained in free and constrained docking are similar, suggesting that the interaction *via* the thiourea group is also possible. Therefore, we analyzed the impact of the tripeptide sequence on the ability to interact with the protein surface for both docking variants.

In the case of free docking, the small cavity binding of both copper ions is occupied by the phenyl moiety of Phe1 sidechain of the tripeptide conjugate. Similar behavior is also found for the other thiosemicarbazone conjugates. Only a few distances, less than 5% of all obtained orientations, present diverse ways of impact. Apart from minimal frequency of their occurrence, they are also characterized by lower values of the scoring function. This observation is a bit surprising in the face of the published results, where interactions through tyrosine sidechain, a natural substrate, is suggested.[223]

Comparing the arrangement of the tripeptide conjugates TSC**43**-FFY (**49**), TSC**43**-FYY (**50**), and TSC**43**-FWY (**51**), the main differences can be found in how the

peptide sidechains interact with the tyrosinase surface. For the TSC**43**-FYY (**50**) and TSC**43**-FWY (**51**) the highest number of intermolecular hydrogen bonds has been found. The position of TSC**43**-FYY (**50**) in the enzymatic active site is stabilized by four intermolecular hydrogen bonds, involving hydroxyl groups of Tyr2 and Tyr3 sidechains. The alignment of TSC**43**-FWY (**51**) is stabilized by three intermolecular hydrogen bonds, involving indole amide proton of Trp2 and hydroxyl group of Tyr3 of the inhibitor. The orientation of the TSC**43**-FFY (**49**) in the tyrosinase active site is stabilized only by two intermolecular hydrogen bonds, involving carbonyl oxygen from Phe2 and Tyr3. Detailed information on the formed hydrogen bonds is presented in **Table 28**. Moreover, the alignments of all inhibitors are stabilized by π-π interactions (TSC**43**-FYY (**50**): π-π stacking Phe1-His263; π-π edge-to-face Ph(TSC**43**)-Phe264; Tyr2-His244; TSC**43**-FFY (**49**): π-π edge-to-face Ph(TSC**43**)-Phe264). Additionally, in case of TSC**43**-FYY (**50**) and TSC**43**-FWY (**51**) the stabilizing interactions of the sulfur atom of the thiourea group with the π-electrons of the Trp227 indole ring can also be observed. Obtained orientations of the investigated inhibitors in the active site are shown in **Figure 57** (top).

Table 28. List of amino acid residues of inhibitors **49-51** and tyrosinase, involved in the intermolecular hydrogen bonds formation during the free docking.

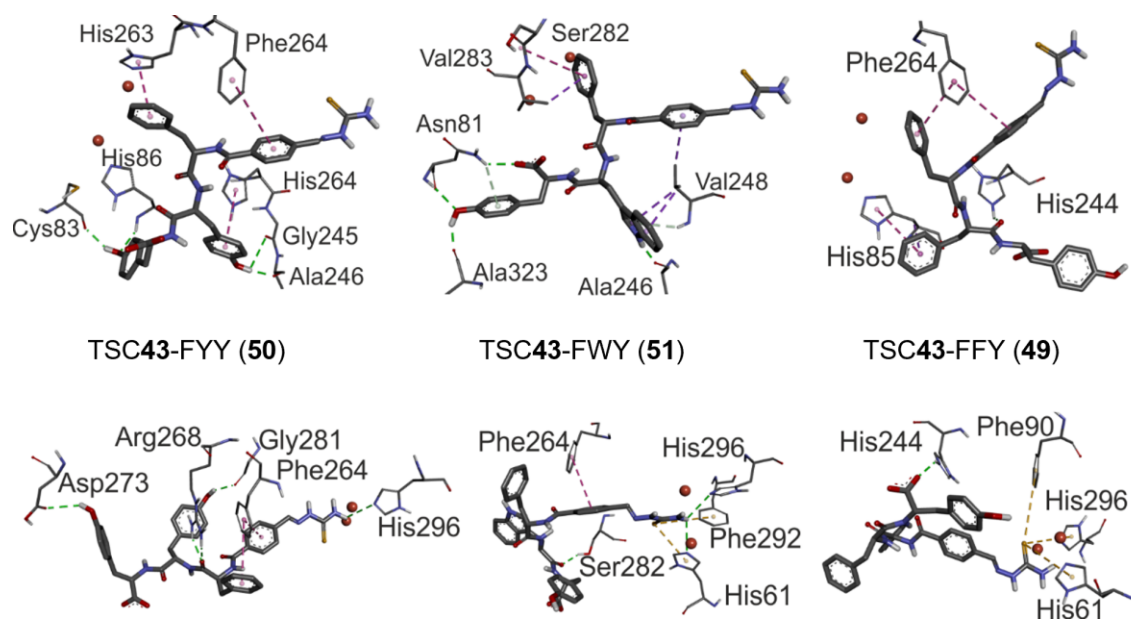| INHIBITOR			TYROSINASE	
Compound	**Residue**	**Functional group**	**Residue**	**Functional group**
TSC**43**-FFY (**49**)	Phe2	CO	His244	$HN^{imidazole}$
	Tyr3	CO_2	Val248	HN^{amide}
TSC**43**-FYY (**50**)	Tyr2	OH	Gly245	CO
	Tyr2	OH	Ala246	CO
	Tyr3	OH	Cys83	CO
	Tyr3	OH	His85	HN^{amide}
TSC**43**-FWY (**51**)	Trp2	HN^{indol}	Ala246	CO
	Tyr3	OH	Ala323	CO
	Tyr3	OH	Asn81	HN

Figure 57. Orientation of TSC**43**-tripeptide conjugates in the tyrosinase active site. Top: free docking; bottom: constrained docking. Intermolecular interactions are shown as dash lines – green: H-bond; purple: π-π interaction. Copper ions are shown as red spheres.

In contrast, in the case of constrained docking, the alignment of each inhibitor is stabilized by the π-electron-sulfur atom interaction. This result is expected since such an orientation of the inhibitors towards the active cavity is forced. The sulfur atom of thiourea moiety interacts with the aromatic ring of His61, Phe90, and His296, regardless of the peptide sequence of the conjugates. As in the case of free docking and constraint docking, differences in the strength of the interaction of inhibitors with the enzyme can be explained based on the number of intermolecular hydrogen bonds. Similarly, the arrangement of TSC**43**-FYY (**50**) is stabilized by the highest number of hydrogen bonds, TSC**43**-FWY (**51**) by 3 hydrogen bonds, and in TSC**43**-FFY (**49**) by only one hydrogen bond (**Table 29**). The orientations obtained for the investigated inhibitors in the active site are shown in **Figure 57** (bottom).

Table 29. List of amino acid residues of inhibitors **49-51** and tyrosinase, involved in the intermolecular hydrogen bonds formation during the costrained docking.

INHIBITOR			TYROSINASE	
Compound	Residue	Functional group	Residue	Functional group
TSC**43**-FFY (**49**)	Tyr3	CO_2	His244	$HN^{imidazole}$
TSC**43**-FYY (**50**)	TSC**43**	H_2N	His296	$N^{imidazole}$
	Phe1	CO	Arg268	$H_2N^{guanidine}$
	Tyr2	HO	Gly281	CO
	Tyr3	HO	Asp273	$CO_2^{sidechain}$
TSC**43**-FWY (**51**)	TSC**43**	H_2N	His61	$N^{imidazole}$
	TSC**43**	H_2N	His296	$N^{imidazole}$
	Trp2	CO	Ser282	$HO^{sidechain}$

The presented results allow to conclude that introducing an amino acid in the second position without the donor hydrogen bond in the side chain causes a drastic decrease in the ability to form intermolecular hydrogen bonds. This, in turn, significantly limits the inhibitory properties, which is reflected in the values of the scoring function. The inhibitory properties of the tripeptide conjugates containing tyrosine or tryptophan in the second position are comparable. On the other hand, inhibitors containing a phenylalanine residue at this position have a much weaker affinity for the tyrosinase active cavity. What is worth to be noticed, compound **50** during the interaction with tyrosinase active cleft forms numerous hydrogen bonds involving both thiosemicarbazone moiety, and each of amino acid residues in the sequence.

Chapter 6: Conclusions

Recently, peptides become interesting candidates for active ingredients in drugs. They can be found in cosmeceuticals (cosmetic products with proven bioactivity) or nutraceuticals (products employed for human nutrition and as medicine as well). Since peptides are highly susceptible to enzymatic degradation when applied orally or topically, but on the other hand they can decrease the toxicity and increase the biocompatibility of organic drug molecules, peptide conjugation with small compounds became more common in the past years.

In this PhD thesis, two projects aiming to synthesize, characterize, and evaluate the bioactivity of diverse peptide conjugates were investigated. All compounds were designed in accordance with the current state of science, following the previous findings in the field of elastase and tyrosinase inhibitors. Thus, 42 compounds were synthesized, purified, characterized, and evaluated towards their bioactivity as enzymes inhibitors.

6.1 Peptide conjugates with 1,2,4-triazoles as elastase inhibitors

Regarding the project discussing 1,2,4-triazole moieties conjugated with peptides, new Fmoc-Lys-triazolopyridylium and triazolopirydynium building blocks were prepared. The facile solid-phase synthesis of lysine-linked triazolium building blocks, providing products with good yields and purity, was described in detail. Pentapeptides and their conjugates based on sequences **8** (MGKVV) and **9** (PGKVV) were designed and synthesized. Sequence **8** was selected based on previous findings, where the decapeptide SA1-III (Ac-MGKVVNPTQK-NH$_2$) has been found to act as collagen turnover modulator, able to decrease the collagen degradation in cultured human dermal fibroblasts. Concerning substrate preferences of elastase, the peptide sequence should be hydrophobic and aliphatic, thus the first 5 amino acids of SA1-III were selected and further modified. Structural investigations of synthesized molecules **4a-7a** (Fmoc-lysine-building blocks based on *Safirinium* fluorescent dyes) and **8-26** (peptides **8** and **9** and their derivatives conjugated with 1,2,4-triazoles) involved Circular Dichroism measurements, one-dimensional and two-dimensional Nuclear Magnetic Resonance, and molecular modeling methods, showing the polar interactions stabilizing these molecules internally. CD measurements performed for **8-26** confirmed the maintenance of β-sheet conformation of MGKVV-deriving peptides at pH=8 (pH value of PPE bioassay), while structural perturbations were observed for proline-including sequences (PGKVV and its derivatives). According to the literature

published up to now, there was a likelihood that the obtained compounds may act as inhibitors of elastase, hence a series of compounds was evaluated as Porcine Pancreas Elastase inhibitors, the enzyme mimicking Human Neutrophil Elastase. It was demonstrated that peptides and their fluorescent derivatives do not exhibit significant inhibitory activity, confirming this observation by optimized and well-adjusted enzymatic protocol. Nevertheless, the fact that peptides turned out to be rather weak candidates for efficient elastase inhibitors, building blocks without Fmoc group and 1,2,4-triazolium derivatives were evaluated too. 25% of inhibition at 50 μM concentration was observed in case of H-Lys[N$^{\varepsilon}$**(5)**]-OH, one of synthesized lysine derivatives. Therefore, moderate inhibitory potential of this compound has been demonstrated. This observation also confirmed the relevance of lysine linker in such conjugates since compound **5** alone was inactive. Importantly, the analog **5** including secondary amine **B**, pyrrolidine, was the smallest and less hindered among all synthesized and evaluated compounds.

In cosmeceutical formulas, except the biological properties of active ingredients, there are a few other factors promoting the bioavailability of the new product. One of them is water solubility, followed by skin permeability. The synthesized compounds possess interesting structural and physiochemical properties: improved overall solubility due to the hydrophilicity of the peptide chain combined with the presence of a quaternary nitrogen atom, the presence of heterocyclic moiety, and fluorescence. All these properties are favorable when designing novel compounds with potential bioactivity and prospective applicability, e.g., in bioimaging methods. The presented novel building blocks are resistant to both acidic and basic conditions, are obtained *via* solid-phase synthesis, may be used without further purification, and can be easily incorporated in every peptide sequence during the chain elongation. Thus, they become excellent candidates as peptide derivatizing agents. The relevance of triazolium core and its application in drug discovery and development is widely described and well-known. Moreover, the use of 1,2,4-triazoles as analgesic, antiseptic, antimicrobial, antioxidant, anti-urease, anti-inflammatory, diuretics, anticancer, anticonvulsant, antidiabetic, and antimigraine agents was broadly depicted. Other examples of nitrogen-containing heterocyclic cores were indicated as good elastase inhibitors and published recently – for example the inhibitory potency of caffeine against various enzymes has already been demonstrated.[249] Heterocyclic *N*-benzoylindazole derivatives were found to be excellent inhibitors of human neutrophil elastase.[171,172] Implementation of such triazolium

moieties do not affect the secondary structure of the initial peptide. Therefore, the described Lys-based *Safirinium* analogs can be further used as new seedbed for the design of bioactive conjugates, also for the further use as e.g., cosmeceuticals, and as building blocks for the synthesis of bioactive peptides.

6.2   Peptide conjugates with thiosemicarbazones as tyrosinase inhibitors

Thiosemicarbazones were found to be great inhibitors of tyrosinase, significantly decreasing the melanogenesis leading to freckles, skin blemishing, or melasma. Up to now, there are no findings aiming to evaluate bioactivity and other properties of thiosemicarbazones conjugated with peptides, revealing potential anti-tyrosinase activity. In this thesis, the synthesis of nine conjugates of three thiosemicarbazones with designed tripeptides, including Phe-Xaa-Tyr sequences (where Xaa = Phe, Trp, or Tyr) was described. The aim was to evaluate the inhibitory potential of such conjugates, following the encouraging results published in the past years when the strong inhibitory properties of various thiosemicarbazones have been described. Furthermore, several examples of peptide conjugates, e.g., with commercially available inhibitor of tyrosinase, such as kojic acid, resulted with increased inhibitory activity and/or enhanced stability, or decreased cytotoxicity of the final product.

New thiosemicarbazone structures (TSCs) were selected considering the previous outcomes, demonstrating that the thiourea group is responsible for copper coordination in the tyrosinase active cleft. Reflecting these data, three new thiosemicarbazones with a free carboxyl group, located distantly from the active thiourea moiety, were designed. Therefore, three new TSCs possessing free carboxyl moieties necessary for the conjugation were synthesized. Tripeptide sequences were selected on the base of previously published data, suggesting the relevance of N-terminally located Phe residue and the fundamental role of aromatic and hydrophobic residues for tyrosinase inhibition. TSCs were conjugated to the tripeptide chains in solid phase *via* standard coupling strategy, by N-terminal modification through the amide bond formation. Final conjugates were cleaved from the resin, purified, and characterized.

Pure products were then evaluated as inhibitors of tyrosinase. A good inhibitory activity was found for two structurally similar thiosemicarbazones TSC **43** and **45**, and poor activity was observed in the case of bulky TSC **44** (IC$_{50}$ 5.3 and 5.8 μM *versus* >150 μM, respectively). Accordingly, all the tripeptide conjugates containing TSC **44**

showed weak inhibitory activity. As controls, the unmodified peptides **46-48** did not display significant inhibition, in accordance with the results from the literature (e.g., IC_{50} of Ac-FFY-OH found in the literature: 240 μM).[228] Among all the tested tripeptide conjugates, the set of TSC **43**-derivatives **49-51** contains the most active compounds **50** and **51** (IC_{50} value: 6.5 μM for both conjugates). Also, in the case of the conjugates of TSC **45**, the activity of **56** and **57** is similar (IC_{50} around 25 μM). Surprisingly, the derivatives including FFY sequence (compounds **49** and **55**) are significantly weaker inhibitors of tyrosinase regarding FWY and FYY conjugates (IC_{50} >150 μM). Molecular modeling supports the explanation of the influence of the amino acid sequence on the activity of conjugates. *In silico* results showed that the reason of significant differences in the activity of Phe-containing derivatives should be sought in the lack of a hydrogen bond donor group, caused by introducing a phenylalanine residue in the central position of the peptide.

Tests performed on B16F0 cell line shows that all investigated compounds inhibited melanogenesis at micromolar level. However, only TSC **43** and **44** as well as the tripeptide conjugates **54** and **57** showed stronger potency of melanogenesis inhibition than kojic acid, so they can be considered as medium melanogenesis inhibitors. For most compounds, IC_{50} of cell proliferation inhibition turned out to be lower than IC_{50} of melanin production. This observation let raise the question if the inhibited melanin production is the result of inhibitor activity towards melanogenesis process, or of toxic effect on the cells. Nevertheless, melanogenesis is a complex biosynthetic process, which might be affected by several factors. Surely, further research should be performed on normal melanocyte cell line instead of the cancer one. The differences in cell proliferation might provide more reliable results. Further investigations to explain the mechanism of inhibition of tyrosinase, and the role of peptide sequence in this mechanism should be performed in further studies.

It is worth to mention that bulky thiosemicarbazone TSC **44**, unexpectedly, revealed the highest inhibitory potency toward melanogenesis showing relatively low toxicity toward the cells. TSC **44** showed no significant inhibition toward tyrosinase, so it probably inhibits melanogenesis on the other stage of the process.

According to the results of molecular modeling, in the case of inhibitors **43-45**, their interaction with the active cavity of the enzyme through free carboxyl groups should be considered. This interaction seems so significant that it may force an

orientation opposite to that postulated for this class of compounds.[214] The previous studies indicated that introducing an additional methyl group at the R position significantly improved inhibitory activity. This could be explained by a better fit for the active site and thus, an increase in van der Waals interactions, which would only occur thanks to the interaction *via* the thiourea moiety. On the other hand, similar tyrosinase inhibiting abilities of thiosemicarbazones **43** and **45** presented in this thesis indicate that the presence of this additional methyl group does not have such a significant effect on the activity, which would suggest their different interaction with the enzyme.

The above-mentioned results might be helpful in designing and developing novel products for cosmeceutical use.

Chapter 7: References

(1) Cohen, G. N. Regulation of Enzyme Activity in Microorganisms. *Annu. Rev. Microbiol.* **1965**, *19* (1), 105–126. https://doi.org/10.1146/annurev.mi.19.100165.000541.

(2) Aragón, J. J.; Sols, A. Regulation of Enzyme Activity in the Cell: Effect of Enzyme Concentration. *FASEB j.* **1991**, *5* (14), 2945–2950. https://doi.org/10.1096/fasebj.5.14.1752361.

(3) Tsuji, N.; Moriwaki, S.; Suzuki, Y.; Takema, Y.; Imokawa, G. The Role of Elastases Secreted by Fibroblasts in Wrinkle Formation: Implication through Selective Inhibition of Elastase Activity. *Photochem Photobiol* **2001**, *74* (2), 283–290. https://doi.org/10.1562/0031-8655(2001)074<0283:troesb>2.0.co;2.

(4) Morisaki, N.; Moriwaki, S.; Sugiyama-Nakagiri, Y.; Haketa, K.; Takema, Y.; Imokawa, G. Neprilysin Is Identical to Skin Fibroblast Elastase. *Journal of Biological Chemistry* **2010**, *285* (51), 39819–39827. https://doi.org/10.1074/jbc.M110.161547.

(5) Ledwoń, P.; Papini, A. M.; Rovero, P.; Latajka, R. Peptides and Peptidomimetics as Inhibitors of Enzymes Involved in Fibrillar Collagen Degradation. *Materials* **2021**, *14* (12), 3217. https://doi.org/10.3390/ma14123217.

(6) Tsukahara, K.; Takema, Y.; Moriwaki, S.; Tsuji, N.; Suzuki, Y.; Fujimura, T.; Imokawa, G. Selective Inhibition of Skin Fibroblast Elastase Elicits a Concentration-Dependent Prevention of Ultraviolet B-Induced Wrinkle Formation. *Journal of Investigative Dermatology* **2001**, *117* (3), 671–677. https://doi.org/10.1046/j.0022-202x.2001.01450.x.

(7) Solomon, E. I.; Baldwin, M. J.; Lowery, M. D. Electronic Structures of Active Sites in Copper Proteins: Contributions to Reactivity. *Chem. Rev.* **1992**, *92* (4), 521–542. https://doi.org/10.1021/cr00012a003.

(8) Hałdys, K.; Latajka, R. Thiosemicarbazones with Tyrosinase Inhibitory Activity. *Med. Chem. Commun.* **2019**, *10* (3), 378–389. https://doi.org/10.1039/C9MD00005D.

(9) Draelos, Z. D. Cosmeceuticals: What's Real, What's Not. *Dermatologic Clinics* **2019**, *37* (1), 107–115. https://doi.org/10.1016/j.det.2018.07.001.

(10) Errante, F.; Ledwoń, P.; Latajka, R.; Rovero, P.; Papini, A. M. Cosmeceutical Peptides in the Framework of Sustainable Wellness Economy. *Front. Chem.* **2020**, *8*, 572923. https://doi.org/10.3389/fchem.2020.572923.

(11) Ledwoń, P.; Errante, F.; Papini, A. M.; Rovero, P.; Latajka, R. Peptides as Active Ingredients: A Challenge for Cosmeceutical Industry. *Chem. Biodiversity* **2021**, *18* (2), e2000833. https://doi.org/10.1002/cbdv.202000833.

(12) Papini, A. M. Cosmetics toward Peptide-Based Cosmeceutics. *chimica oggi/Chemistry Today* **2010**, *28* (6), 3–5. https://doi.org/Not available.

(13) Ledwoń, P.; Staśkiewicz, A.; Jewgiński, M.; Latajka, R. Peptydomimetyki i Foldamery Aromatyczne w Chemii Biologicznej. *Wiad. Chem.* **2022**, *76* (5–6), 9–32. https://doi.org/10.53584/wiadchem.2022.5.6.

(14) Draelos, Z. D. The Cosmeceutical Realm. *Clinics in Dermatology* **2008**, *26* (6), 627–632. https://doi.org/10.1016/j.clindermatol.2007.09.005.

(15) Pickart, L.; Thaler, M. M. Tripeptide in Human Serum Which Prolongs Survival of Normal Liver Cells and Stimulates Growth in Neoplastic Liver. *Nature New Biol.* **1973**, *243* (124), 85–87.

(16) Campbell, J. D.; McDonough, J. E.; Zeskind, J. E.; Hackett, T. L.; Pechkovsky, D. V.; Brandsma, C.-A.; Suzuki, M.; Gosselink, J. V.; Liu, G.; Alekseyev, Y. O.; Xiao, J.; Zhang, X.; Hayashi, S.; Cooper, J. D.; Timens, W.; Postma, D. S.; Knight, D. A.; Marc, L. E.; James, H. C.; Avrum, S. A Gene Expression Signature of

Emphysema-Related Lung Destruction and Its Reversal by the Tripeptide GHK. *Genome Med* **2012**, *4* (8), 67. https://doi.org/10.1186/gm367.

(17) Pickart, L.; Vasquez-Soltero, J. M.; Margolina, A. GHK Peptide as a Natural Modulator of Multiple Cellular Pathways in Skin Regeneration. *BioMed Research International* **2015**, *2015*, 1–7. https://doi.org/10.1155/2015/648108.

(18) Pai, V.; Bhandari, P.; Shukla, P. Topical Peptides as Cosmeceuticals. *Indian J Dermatol Venereol Leprol* **2017**, *83* (1), 9. https://doi.org/10.4103/0378-6323.186500.

(19) Blanes-Mira, C.; Clemente, J.; Jodas, G.; Gil, A.; Fernandez-Ballester, G.; Ponsati, B.; Gutierrez, L.; Perez-Paya, E.; Ferrer-Montiel, A. A Synthetic Hexapeptide (Argireline) with Antiwrinkle Activity. *Int J Cosmet Sci* **2002**, *24* (5), 303–310. https://doi.org/10.1046/j.1467-2494.2002.00153.x.

(20) Schagen, S. Topical Peptide Treatments with Effective Anti-Aging Results. *Cosmetics* **2017**, *4* (2), 16. https://doi.org/10.3390/cosmetics4020016.

(21) Dragomirescu, A.; Andoni, M.; Ionescu, D.; Andrei, F. The Efficiency and Safety of Leuphasyl—A Botox-Like Peptide. *Cosmetics* **2014**, *1* (2), 75–81. https://doi.org/10.3390/cosmetics1020075.

(22) Reddy, B. Y.; Jow, T.; Hantash, B. M. Bioactive Oligopeptides in Dermatology: Part II. *Exp Dermatol* **2012**, *21* (8), 569–575. https://doi.org/10.1111/j.1600-0625.2012.01527.x.

(23) *Lipotec s.a. (2020). SNAP-8*. https://www.lipotec.com/en/products/snap-8-trade-peptide (accessed 2020-06-15).

(24) *Prospector website about Lipotec s.a. (now: Lubrizol). SNAP-8*. https://www.ulprospector.com/en/na/PersonalCare/Detail/2670/81055/SNAP-8-peptide-solution-C (accessed 2022-12-20).

(25) Hussain, M.; Goldberg, D. J. Topical Manganese Peptide in the Treatment of Photodamaged Skin. *Journal of Cosmetic and Laser Therapy* **2007**, *9* (4), 232–236. https://doi.org/10.1080/14764170701704668.

(26) Floquet, N.; Héry-Huynh, S.; Dauchez, M.; Derreumaux, P.; Tamburro, A. M.; Alix, A. J. P. Structural Characterization of VGVAPG, an Elastin-Derived Peptide: Structural Characterization of VGVAPG. *Biopolymers* **2004**, *76* (3), 266–280. https://doi.org/10.1002/bip.20029.

(27) Choi, Y. L.; Park, E. J.; Kim, E.; Na, D. H.; Shin, Y.-H. Dermal Stability and In Vitro Skin Permeation of Collagen Pentapeptides (KTTKS and Palmitoyl-KTTKS). *Biomolecules & Therapeutics* **2014**, *22* (4), 321–327. https://doi.org/10.4062/biomolther.2014.053.

(28) Johnson, W.; Bergfeld, W. F.; Belsito, D. V.; Hill, R. A.; Klaassen, C. D.; Liebler, D. C.; Marks, J. G.; Shank, R. C.; Slaga, T. J.; Snyder, P. W.; Gill, L. J.; Heldreth, B. Safety Assessment of Tripeptide-1, Hexapeptide-12, Their Metal Salts and Fatty Acyl Derivatives, and Palmitoyl Tetrapeptide-7 as Used in Cosmetics. *Int J Toxicol* **2018**, *37* (3_suppl), 90S-102S. https://doi.org/10.1177/1091581818807863.

(29) Kim, H. M.; An, H. S.; Bae, J.-S.; Kim, J. Y.; Choi, C. H.; Kim, J. Y.; Lim, J. H.; Choi, J.; Song, H.; Moon, S. H.; Park, Y. J.; Chang, S.-J.; Choi, S. Y. Effects of Palmitoyl-KVK-L-Ascorbic Acid on Skin Wrinkles and Pigmentation. *Arch Dermatol Res* **2017**, *309* (5), 397–402. https://doi.org/10.1007/s00403-017-1731-6.

(30) Cauchard, J.-H.; Berton, A.; Godeau, G.; Hornebeck, W.; Bellon, G. Activation of Latent Transforming Growth Factor Beta 1 and Inhibition of Matrix Metalloprotease Activity by a Thrombospondin-like Tripeptide Linked to Elaidic Acid. *Biochemical Pharmacology* **2004**, *67* (11), 2013–2022. https://doi.org/10.1016/j.bcp.2004.01.028.

(31) Sklirou, A. D.; Ralli, M.; Dominguez, M.; Papassideri, I.; Skaltsounis, A.-L.; Trougakos, I. P. Hexapeptide-11 Is a Novel Modulator of the Proteostasis Network in Human Diploid Fibroblasts. *Redox Biology* **2015**, *5*, 205–215. https://doi.org/10.1016/j.redox.2015.04.010.

(32) Puig, A.; Antón, J. M. G.; Mangues, M. A New Decorin-like Tetrapeptide for Optimal Organization of Collagen Fibres. *Int J Cosmet Sci* **2008**, *30* (2), 97–104. https://doi.org/10.1111/j.1468-2494.2008.00429.x.

(33) Marini, A.; Farwick, M.; Grether-Beck, S.; Brenden, H.; Felsner, I.; Jaenicke, T.; Weber, M.; Schild, J.; Maczkiewitz, U.; Köhler, T.; Bonfigli, A.; Pagani, V.; Krutmann, J. Modulation of Skin Pigmentation by the Tetrapeptide PKEK: In Vitro and in Vivo Evidence for Skin Whitening Effects: PKEK Acts as a Skin Whitener and Improves Pigment Spots. *Experimental Dermatology* **2012**, *21* (2), 140–146. https://doi.org/10.1111/j.1600-0625.2011.01415.x.

(34) Farwick, M.; Grether-Beck, S.; Marini, A.; Maczkiewitz, U.; Lange, J.; Köhler, T.; Lersch, P.; Falla, T.; Felsner, I.; Brenden, H.; Jaenicke, T.; Franke, S.; Krutmann, J. Bioactive Tetrapeptide GEKG Boosts Extracellular Matrix Formation: In Vitro and in Vivo Molecular and Clinical Proof. *Exp. Dermatol.* **2011**, *20* (7), 602–604. https://doi.org/10.1111/j.1600-0625.2011.01307.x.

(35) Sommer, E.; Neubert, R. H. H.; Mentel, M.; Tuchscherer, B.; Mrestani, Y.; Wohlrab, J. Dermal Peptide Delivery Using Enhancer Molecules and Colloidal Carrier Systems. Part III: Tetrapeptide GEKG. *European Journal of Pharmaceutical Sciences* **2018**, *124*, 137–144. https://doi.org/10.1016/j.ejps.2018.08.034.

(36) Pascarella, S.; Tiberi, C.; Sabatino, G.; Nuti, F.; Papini, A. M.; Giovannelli, L.; Rovero, P. Serpin A1 C-Terminal Peptides as Collagen Turnover Modulators. *ChemMedChem* **2016**, *11* (16), 1850–1855. https://doi.org/10.1002/cmdc.201500472.

(37) Cipriani, C.; Pascarella, S.; Errante, F.; Menicacci, B.; Magnelli, L.; Mocali, A.; Rovero, P.; Giovannelli, L. Serpin A1 and the Modulation of Type I Collagen Turnover: Effect of the C-Terminal Peptide 409-418 (SA1-III) in Human Dermal Fibroblasts: Serpin-A1 C-Terminal Modulates Collagen Levels. *Cell Biol Int* **2018**, *42* (10), 1340–1348. https://doi.org/10.1002/cbin.11018.

(38) Lima, T.; Carla Pedriali Moraes. Bioactive Peptides: Applications and Relevance for Cosmeceuticals. *Cosmetics* **2018**, *5* (1), 21. https://doi.org/10.3390/cosmetics5010021.

(39) Lupo, M. P.; Cole, A. L. Cosmeceutical Peptides: Cosmeceutical Peptides. *Dermatologic Therapy* **2007**, *20* (5), 343–349. https://doi.org/10.1111/j.1529-8019.2007.00148.x.

(40) Husein el Hadmed, H.; Castillo, R. F. Cosmeceuticals: Peptides, Proteins, and Growth Factors. *J Cosmet Dermatol* **2016**, *15* (4), 514–519. https://doi.org/10.1111/jocd.12229.

(41) Yamaguchi, Y.; Hosokawa, K.; Nakatani, Y.; Sano, S.; Yoshikawa, K.; Itami, S. Gastrin-Releasing Peptide, a Bombesin-like Neuropeptide, Promotes Cutaneous Wound Healing: *Dermatologic Surgery* **2002**, *28* (4), 314–319. https://doi.org/10.1097/00042728-200204000-00003.

(42) Khan, M. S.; Singh, P.; Azhar, A.; Naseem, A.; Rashid, Q.; Kabir, M. A.; Jairajpuri, M. A. Serpin Inhibition Mechanism: A Delicate Balance between Native Metastable State and Polymerization. *Journal of Amino Acids* **2011**, *2011*, 1–10. https://doi.org/10.4061/2011/606797.

(43) Congote, L. F.; Temmel, N. The C-Terminal 26-Residue Peptide of Serpin A1 Stimulates Proliferation of Breast and Liver Cancer Cells: Role of Protein Kinase C and CD47. *FEBS Letters* **2004**, *576* (3), 343–347. https://doi.org/10.1016/j.febslet.2004.09.035.

(44) Congote, L. F.; Temmel, N.; Sadvakassova, G.; Dobocan, M. C. Comparison of the Effects of Serpin A1, a Recombinant Serpin A1-IGF Chimera and Serpin A1 C-Terminal Peptide on Wound Healing. *Peptides* **2008**, *29* (1), 39–46. https://doi.org/10.1016/j.peptides.2007.10.011.

(45) Huntington, J. A.; Read, R. J.; Carrell, R. W. Structure of a Serpin–Protease Complex Shows Inhibition by Deformation. *Nature* **2000**, *407* (6806), 923–926. https://doi.org/10.1038/35038119.

(46) (Image Prepared by the Author of the Document Using the Following Software) The PyMOL Molecular Graphics System, 2018. https://pymol.org/.

(47) *Nextprot S-A1 full sequence*. https://www.nextprot.org/entry/NX_P01009/sequence (accessed 2021-10-07).

(48) Errante, F.; Giovannelli, L.; Papini, A. M.; Rovero, P. Bioactive Peptides and Compositions Comprising Them / Peptidi Bioattivi e Composizioni Che Li Contengono. WO 2020/245772 A1, December 10, 2020.

(49) Ledoux-Corbusier, M.; Achten, G. Alpha1-Antitrypsin Deficiency and Skin Abnormalities. *J Cutan Pathol* **1975**, *2* (1), 25–29. https://doi.org/10.1111/j.1600-0560.1975.tb00827.x.

(50) Draelos, Z. D. Cosmeceuticals. Efficacy and Influence on Skin Tone. *Dermatologic Clinics* **2014**, *32* (2), 137–143. https://doi.org/10.1016/j.det.2013.12.002.

(51) Errante, F.; Menicatti, M.; Pallecchi, M.; Giovannelli, L.; Papini, A. M.; Rovero, P.; Bartolucci, G. Susceptibility of Cosmeceutical Peptides to Proteases Activity: Development of Dermal Stability Test by LC-MS/MS Analysis. *Journal of Pharmaceutical and Biomedical Analysis* **2021**, *194*, 113775. https://doi.org/10.1016/j.jpba.2020.113775.

(52) Renukuntla, J.; Vadlapudi, A. D.; Patel, A.; Boddu, S. H. S.; Mitra, A. K. Approaches for Enhancing Oral Bioavailability of Peptides and Proteins. *International Journal of Pharmaceutics* **2013**, *447* (1–2), 75–93. https://doi.org/10.1016/j.ijpharm.2013.02.030.

(53) Wang, B.; Xie, N.; Li, B. Influence of Peptide Characteristics on Their Stability, Intestinal Transport, and in Vitro Bioavailability: A Review. *J Food Biochem* **2019**, *43* (1), e12571. https://doi.org/10.1111/jfbc.12571.

(54) Escobar-Chávez, J. J.; Rodríguez-Cruz, I. M.; Domínguez-Delgado, C. L. Chemical and Physical Enhancers for Transdermal Drug Delivery. In *Pharmacology*; Gallelli, L., Ed.; InTech, 2012. https://doi.org/10.5772/33194.

(55) Rodríguez-Cruz, I. M.; Domínguez-Delgado, C. L.; Escobar-Chávez, J. J.; López-Cervantes, M.; Díaz-Torres, R. Physical Penetration Enhancers: An Overview. In *Current Technologies To Increase The Transdermal Delivery Of Drugs*; BENTHAM SCIENCE PUBLISHERS, 2016; pp 3–34. https://doi.org/10.2174/9781681083636116020005.

(56) Bos, J. D.; Meinardi, M. M. H. M. The 500 Dalton Rule for the Skin Penetration of Chemical Compounds and Drugs. *Experimental Dermatology* **2000**, *9* (3), 165–169. https://doi.org/10.1034/j.1600-0625.2000.009003165.x.

(57) Nasrollahi, S. A.; Taghibiglou, C.; Azizi, E.; Farboud, E. S. Cell-Penetrating Peptides as a Novel Transdermal Drug Delivery System: **Transdermal Drug Targeting**. *Chemical Biology & Drug Design* **2012**, *80* (5), 639–646. https://doi.org/10.1111/cbdd.12008.

(58) Mathur, V.; Satrawala, Y.; Rajput, M. Physical and Chemical Penetration Enhancers in Transdermal Drug Delivery System. *Asian J Pharm* **2010**, *4* (3), 173. https://doi.org/10.4103/0973-8398.72115.

(59) Kim, Y.-C.; Park, J.-H.; Prausnitz, M. R. Microneedles for Drug and Vaccine Delivery. *Advanced Drug Delivery Reviews* **2012**, *64* (14), 1547–1568. https://doi.org/10.1016/j.addr.2012.04.005.

(60) Cho Lee, A.-R. Microneedle-Mediated Delivery of Cosmeceutically Relevant Nucleoside and Peptides in Human Skin: Challenges and Strategies for Dermal Delivery. *J. Pharm. Investig.* **2019**, *49* (6), 587–601. https://doi.org/10.1007/s40005-019-00438-y.

(61) Mathur, D.; Prakash, S.; Anand, P.; Kaur, H.; Agrawal, P.; Mehta, A.; Kumar, R.; Singh, S.; Raghava, G. P. S. PEPlife: A Repository of the Half-Life of Peptides. *Sci Rep* **2016**, *6* (1), 36617. https://doi.org/10.1038/srep36617.

(62) Gentilucci, L.; De Marco, R.; Cerisoli, L. Chemical Modifications Designed to Improve Peptide Stability: Incorporation of Non-Natural Amino Acids, Pseudo-Peptide Bonds, and Cyclization. *CPD* **2010**, *16* (28), 3185–3203. https://doi.org/10.2174/138161210793292555.

(63) Conato, C.; Gavioli, R.; Guerrini, R.; Kozlowski, H.; Mlynarz, P.; Pasti, C.; Pulidori, F.; Remelli, M. Copper Complexes of Glycyl-Histidyl-Lysine and Two of Its Synthetic Analogues: Chemical Behaviour and Biological Activity. *Biochim. Biophys. Acta* **2001**, *1526* (2), 199–210. https://doi.org/10.1016/s0304-4165(01)00127-1.

(64) Qvit, N.; Rubin, S. J. S.; Urban, T. J.; Mochly-Rosen, D.; Gross, E. R. Peptidomimetic Therapeutics: Scientific Approaches and Opportunities. *Drug Discovery Today* **2017**, *22* (2), 454–462. https://doi.org/10.1016/j.drudis.2016.11.003.

(65) Dalpozzo, A.; Kanai, K.; Kereszturi, G.; Calabrese, G. H-Gly-Hisψ(NHCO)Lys-OH, Partially Modified Retro-Inverso Analogue of the Growth Factor Glycyl-L-Histidyl-L-Lysine with Enhanced Enzymatic Stability. *International Journal of Peptide and Protein Research* **2009**, *41* (6), 561–566. https://doi.org/10.1111/j.1399-3011.1993.tb00478.x.

(66) Chorev, M. The Partial Retro-Inverso Modification: A Road Traveled Together. *Biopolymers* **2005**, *80* (2–3), 67–84. https://doi.org/10.1002/bip.20219.

(67) Adessi, C.; Soto, C. Converting a Peptide into a Drug: Strategies to Improve Stability and Bioavailability. *CMC* **2002**, *9* (9), 963–978. https://doi.org/10.2174/0929867024606731.

(68) Anzali Soheila; Jonczyk Alfred. Compositions Containing Cyclic Peptides And Methods Of Use. WO 2009/124754 A1, 2009. https://www.lens.org/lens/patent/019-797-613-967-945.

(69) Endo, K.; Endo, Y. Cyclic Peptide, and Medicine, External Preparation and Cosmetic Each Containing Said Cyclic Peptide. EP3305804A4, November 21, 2018.

(70) Endo, K.; Endo, Y. Cnp Cyclic Peptide, and Medicine, External Preparation and Cosmetic Each Containing Said Cyclic Peptide. EP3330280A4, June 12, 2019.

(71) Lombès, A.; Wolf, J.-P.; Bomsel, M. Cyclic Peptide, Cosmetic or Dermatological Composition, and Eye Lotion. BR112018005457A2, October 9, 2018.

(72) 陳建添. Cyclopeptide, Composition Comprising the Same and Method for Preparing the Same. TWI659044B, May 11, 2019.

(73) Arul, V.; Gopinath, D.; Gomathi, K.; Jayakumar, R. Biotinylated GHK Peptide Incorporated Collagenous Matrix: A Novel Biomaterial for Dermal Wound Healing in Rats. *J. Biomed. Mater. Res.* **2005**, *73B* (2), 383–391. https://doi.org/10.1002/jbm.b.30246.

(74) Lintner; Peschard. Biologically Active Peptides: From a Laboratory Bench Curiosity to a Functional Skin Care Product. *International Journal of Cosmetic Science* **2000**, *22* (3), 207–218. https://doi.org/10.1046/j.1467-2494.2000.00010.x.

(75) Jeong, S.; Yoon, S.; Kim, S.; Jung, J.; Kor, M.; Shin, K.; Lim, C.; Han, H. S.; Lee, H.; Park, K.-Y.; Kim, J.; Chung, H. J.; Kim, H. J. Anti-Wrinkle Benefits of Peptides Complex Stimulating Skin Basement Membrane Proteins Expression. *IJMS* **2019**, *21* (1), 73. https://doi.org/10.3390/ijms21010073.

(76) Kim, M. S.; Park, E. J.; Na, D. H. Synthesis and Characterization of Monodisperse Poly(Ethylene Glycol)-Conjugated Collagen Pentapeptides with Collagen Biosynthesis-Stimulating Activity. *Bioorg. Med. Chem. Lett.* **2015**, *25* (1), 38–42. https://doi.org/10.1016/j.bmcl.2014.11.021.

(77) Choi, H.-I.; Kim, H.-J.; Park, J.-I.; Shin, E.-H.; Kim, D.-W.; Kim, S.-S. Design and Efficient Synthesis of Novel Ascorbyl Conjugated Peptide with High Collagen Biosynthesis Stimulating Effects. *Bioorganic & Medicinal Chemistry Letters* **2009**, *19* (7), 2079–2082. https://doi.org/10.1016/j.bmcl.2008.10.112.

(78) Park, K.-Y.; Kim, J. Synthesis and Biological Evaluation of Ascorbyl-Conjugated Peptide Derivatives as Collagen Synthesis Stimulating Agents in Human Skin Fibroblasts. *Int J Pept Res Ther* **2020**. https://doi.org/10.1007/s10989-020-10041-7.

(79) Pérez-Silva, J. G.; Español, Y.; Velasco, G.; Quesada, V. The Degradome Database: Expanding Roles of Mammalian Proteases in Life and Disease. *Nucleic Acids Res* **2016**, *44* (D1), D351–D355. https://doi.org/10.1093/nar/gkv1201.

(80) Mohan, T.; Kleinschek, K. S.; Kargl, R. Polysaccharide Peptide Conjugates: Chemistry, Properties and Applications. *Carbohydrate Polymers* **2022**, *280*, 118875. https://doi.org/10.1016/j.carbpol.2021.118875.

(81) Xu, L.; Xu, S.; Xiang, T.; Liu, H.; Chen, L.; Jiang, B.; Yao, J.; Zhu, H.; Hu, R.; Chen, Z. Multifunctional Building Elements for the Construction of Peptide Drug Conjugates. *Engineered Regeneration* **2022**, *3* (1), 92–109. https://doi.org/10.1016/j.engreg.2022.02.004.

(82) Balogh, B.; Ivánczi, M.; Nizami, B.; Beke-Somfai, T.; Mándity, I. M. ConjuPepDB: A Database of Peptide–Drug Conjugates. *Nucleic Acids Research* **2021**, *49* (D1), D1102–D1112. https://doi.org/10.1093/nar/gkaa950.

(83) *ConjuPepDB. A database of drug-peptide conjugates.* https://conjupepdb.ttk.hu/ (accessed 2022-10-02).

(84) He, R.; Finan, B.; Mayer, J. P.; DiMarchi, R. D. Peptide Conjugates with Small Molecules Designed to Enhance Efficacy and Safety. *Molecules* **2019**, *24* (10), 1855. https://doi.org/10.3390/molecules24101855.

(85) Fu, C.; Yu, L.; Miao, Y.; Liu, X.; Yu, Z.; Wei, M. Peptide–Drug Conjugates (PDCs): A Novel Trend of Research and Development on Targeted Therapy, Hype or Hope? *Acta Pharmaceutica Sinica B* **2022**, S221138352200332X. https://doi.org/10.1016/j.apsb.2022.07.020.

(86) Zhang, S.; Yan, C.; Millar, D. G.; Yang, Q.; Heather, J. M.; Langenbucher, A.; Morton, L. T.; Sepulveda, S.; Alpert, E.; Whelton, L. R.; Zarrella, D. T.; Guo, M.; Minogue, E.; Lawrence, M. S.; Rueda, B. R.; Spriggs, D. R.; Lu, W.; Langenau, D. M.; Cobbold, M. Antibody-Peptide Epitope Conjugates for Personalized Cancer Therapy. *Cancer Research* **2022**, *82* (5), 773–784. https://doi.org/10.1158/0008-5472.CAN-21-2200.

(87) Camacho, R. C.; You, S.; D'Aquino, K. E.; Li, W.; Wang, Y.; Gunnet, J.; Littrell, J.; Qi, J. S.; Kang, L.; Jian, W.; MacDonald, M.; Tat, T.; Steiner, D.; Zhang, Y.-M.; Lanter, J.; Patch, R.; Zhang, R.; Li, J.; Edavettal, S.; Edwards, W.; Dinh, T.; Wang, L. Y.; Connor, J.; Hunter, M.; Chi, E.; Swanson, R. V.; Leonard, J. N.; Case, M. A. Conjugation of a Peptide to an Antibody Engineered with Free Cysteines Dramatically Improves Half-Life and Activity. *mAbs* **2020**, *12* (1), 1794687. https://doi.org/10.1080/19420862.2020.1794687.

(88) Kim, H.; Hwang, D.; Choi, M.; Lee, S.; Kang, S.; Lee, Y.; Kim, S.; Chung, J.; Jon, S. Antibody-Assisted Delivery of a Peptide–Drug Conjugate for Targeted Cancer Therapy. *Mol. Pharmaceutics* **2019**, *16* (1), 165–172. https://doi.org/10.1021/acs.molpharmaceut.8b00924.

(89) Marverti, G.; Marraccini, C.; Martello, A.; D'Arca, D.; Pacifico, S.; Guerrini, R.; Spyrakis, F.; Gozzi, G.; Lauriola, A.; Santucci, M.; Cannazza, G.; Tagliazucchi, L.; Cazzato, A. S.; Losi, L.; Ferrari, S.; Ponterini, G.; Costi, M. P. Folic Acid–Peptide Conjugates Combine Selective Cancer Cell Internalization with Thymidylate Synthase Dimer Interface Targeting. *J. Med. Chem.* **2021**, *64* (6), 3204–3221. https://doi.org/10.1021/acs.jmedchem.0c02107.

(90) Xie, S.-X.; Song, L.; Yuca, E.; Boone, K.; Sarikaya, R.; VanOosten, S. K.; Misra, A.; Ye, Q.; Spencer, P.; Tamerler, C. Antimicrobial Peptide–Polymer Conjugates for Dentistry. *ACS Appl. Polym. Mater.* **2020**, *2* (3), 1134–1144. https://doi.org/10.1021/acsapm.9b00921.

(91) Reinhardt, A.; Neundorf, I. Design and Application of Antimicrobial Peptide Conjugates. *IJMS* **2016**, *17* (5), 701. https://doi.org/10.3390/ijms17050701.

(92) Patil, N. A.; Thombare, V. J.; Li, R.; He, X.; Lu, J.; Yu, H. H.; Wickremasinghe, H.; Pamulapati, K.; Azad, M. A. K.; Velkov, T.; Roberts, K. D.; Li, J. An Efficient Approach for the Design and Synthesis of Antimicrobial Peptide-Peptide Nucleic Acid Conjugates. *Front. Chem.* **2022**, *10*, 843163. https://doi.org/10.3389/fchem.2022.843163.

(93) Jeong, W.; Bu, J.; Kubiatowicz, L. J.; Chen, S. S.; Kim, Y.; Hong, S. Peptide–Nanoparticle Conjugates: A next Generation of Diagnostic and Therapeutic Platforms? *Nano Convergence* **2018**, *5* (1), 38. https://doi.org/10.1186/s40580-018-0170-1.

(94) Demeter, O.; Kormos, A.; Koehler, C.; Mező, G.; Németh, K.; Kozma, E.; Takács, L. B.; Lemke, E. A.; Kele, P. Bisazide Cyanine Dyes as Fluorogenic Probes for Bis-Cyclooctynylated Peptide Tags and as Fluorogenic Cross-Linkers of Cyclooctynylated Proteins. *Bioconjugate Chem.* **2017**, *28* (5), 1552–1559. https://doi.org/10.1021/acs.bioconjchem.7b00178.

(95) Marinelli, E.; Ramalingam, K.; Swenson, R.; Song, B.; Lattuada, L.; Uggeri, F.; Lorusso, V.; Aime, S.; Morosini, P.; Chaabane, L. Fibrin Binding Peptide Conjugates for Diagnostic and Therapeutic Applications. WO2008071679A1, June 19, 2008.

(96) Erak, M.; Bellmann-Sickert, K.; Els-Heindl, S.; Beck-Sickinger, A. G. Peptide Chemistry Toolbox – Transforming Natural Peptides into Peptide Therapeutics. *Bioorganic & Medicinal Chemistry* **2018**, *26* (10), 2759–2765. https://doi.org/10.1016/j.bmc.2018.01.012.

(97) Wijesinghe, A.; Kumari, S.; Booth, V. Conjugates for Use in Peptide Therapeutics: A Systematic Review and Meta-Analysis. *PLoS ONE* **2022**, *17* (3), e0255753. https://doi.org/10.1371/journal.pone.0255753.

(98) Meldal, M.; Diness, F. Recent Fascinating Aspects of the CuAAC Click Reaction. *Trends in Chemistry* **2020**, *2* (6), 569–584. https://doi.org/10.1016/j.trechm.2020.03.007.

(99) Kolb, H. C.; Finn, M. G.; Sharpless, K. B. Click Chemistry: Diverse Chemical Function from a Few Good Reactions. *Angew. Chem. Int. Ed.* **2001**, *40* (11), 2004–2021. https://doi.org/10.1002/1521-3773(20010601)40:11<2004::AID-ANIE2004>3.0.CO;2-5.

(100) Rostovtsev, V. V.; Green, L. G.; Fokin, V. V.; Sharpless, K. B. A Stepwise Huisgen Cycloaddition Process: Copper(I)-Catalyzed Regioselective "Ligation" of Azides and Terminal Alkynes. *Angew. Chem. Int. Ed.* **2002**, *41* (14), 2596–2599. https://doi.org/10.1002/1521-3773(20020715)41:14<2596::AID-ANIE2596>3.0.CO;2-4.

(101) Tornøe, C. W.; Christensen, C.; Meldal, M. Peptidotriazoles on Solid Phase: [1,2,3]-Triazoles by Regiospecific Copper(I)-Catalyzed 1,3-Dipolar Cycloadditions of Terminal Alkynes to Azides. *J. Org. Chem.* **2002**, *67* (9), 3057–3064. https://doi.org/10.1021/jo011148j.

(102) Staśkiewicz, A.; Ledwoń, P.; Rovero, P.; Papini, A. M.; Latajka, R. Triazole-Modified Peptidomimetics: An Opportunity for Drug Discovery and Development. *Front. Chem.* **2021**, *9*, 674705. https://doi.org/10.3389/fchem.2021.674705.

(103) Tang, W.; Becker, M. L. "Click" Reactions: A Versatile Toolbox for the Synthesis of Peptide-Conjugates. *Chem. Soc. Rev.* **2014**, *43* (20), 7013–7039. https://doi.org/10.1039/C4CS00139G.

(104) Loh, Y.; Shi, H.; Hu, M.; Yao, S. Q. "Click" Synthesis of Small Molecule-Peptide Conjugates for Organelle-Specific Delivery and Inhibition of Lysosomal Cysteine Proteases. *Chem Commun (Camb)* **2010**, *46* (44), 8407–8409. https://doi.org/10.1039/c0cc03738a.

(105) Testa, C.; Scrima, M.; Grimaldi, M.; D'Ursi, A. M.; Dirain, M. L.; Lubin-Germain, N.; Singh, A.; Haskell-Luevano, C.; Chorev, M.; Rovero, P.; Papini, A. M. 1,4-Disubstituted-[1,2,3]Triazolyl-Containing Analogues of MT-II: Design, Synthesis, Conformational Analysis, and Biological Activity. *J. Med. Chem.* **2014**, *57* (22), 9424–9434. https://doi.org/10.1021/jm501027w.

(106) Testa, C.; Papini, A. M.; Chorev, M.; Rovero, P. Copper-Catalyzed Azide-Alkyne Cycloaddition (CuAAC)-Mediated Macrocyclization of Peptides: Impact on Conformation and Biological Activity. *CTMC* **2018**, *18* (7), 591–610. https://doi.org/10.2174/1568026618666180518095755.

(107) Yue, B. Biology of the Extracellular Matrix: An Overview. *Journal of Glaucoma* **2014**, *23*, S20–S23. https://doi.org/10.1097/IJG.0000000000000108.

(108)   Żelaszczyk, D.; Waszkielewicz, A.; Marona, H. Kolagen – Struktura Oraz Zastosowanie w Kosmetologii i Medycynie Estetycznej. *Estetol Med Kosmetol* **2012**, 14–20. https://doi.org/10.14320/EMK.2012.003.

(109)   Veit, G.; Kobbe, B.; Keene, D. R.; Paulsson, M.; Koch, M.; Wagener, R. Collagen XXVIII, a Novel von Willebrand Factor A Domain-Containing Protein with Many Imperfections in the Collagenous Domain. *Journal of Biological Chemistry* **2006**, *281* (6), 3494–3504. https://doi.org/10.1074/jbc.M509333200.

(110)   Smith, K.; Rennie, M. J. New Approaches and Recent Results Concerning Human-Tissue Collagen Synthesis: *Current Opinion in Clinical Nutrition and Metabolic Care* **2007**, *10* (5), 582–590. https://doi.org/10.1097/MCO.0b013e328285d858.

(111)   Burgeson, R. E.; Nimni, M. E. Collagen Types. Molecular Structure and Tissue Distribution. *Clin Orthop Relat Res* **1992**, No. 282, 250–272.

(112)   Bhattacharjee, A.; Bansal, M. Collagen Structure: The Madras Triple Helix and the Current Scenario. *IUBMB Life (International Union of Biochemistry and Molecular Biology: Life)* **2005**, *57* (3), 161–172. https://doi.org/10.1080/15216540500090710.

(113)   Brodsky, B.; Thiagarajan, G.; Madhan, B.; Kar, K. Triple-Helical Peptides: An Approach to Collagen Conformation, Stability, and Self-Association. *Biopolymers* **2008**, *89* (5), 345–353. https://doi.org/10.1002/bip.20958.

(114)   Fields, G. B. Interstitial Collagen Catabolism. *Journal of Biological Chemistry* **2013**, *288* (13), 8785–8793. https://doi.org/10.1074/jbc.R113.451211.

(115)   Bishop, J. E.; Laurent, G. J. Collagen Turnover and Its Regulation in the Normal and Hypertrophying Heart. *European Heart Journal* **1995**, *16* (suppl C), 38–44. https://doi.org/10.1093/eurheartj/16.suppl_C.38.

(116)   Karsdal, M. A.; Genovese, F.; Madsen, E. A.; Manon-Jensen, T.; Schuppan, D. Collagen and Tissue Turnover as a Function of Age: Implications for Fibrosis. *Journal of Hepatology* **2016**, *64* (1), 103–109. https://doi.org/10.1016/j.jhep.2015.08.014.

(117)   Sprangers, S.; Everts, V. Molecular Pathways of Cell-Mediated Degradation of Fibrillar Collagen. *Matrix Biology* **2019**, *75–76*, 190–200. https://doi.org/10.1016/j.matbio.2017.11.008.

(118)   Kim, M.; Park, H. J. Molecular Mechanisms of Skin Aging and Rejuvenation; InTech, 2016; pp 57–76.

(119)   Vannella, K. M.; Wynn, T. A. Mechanisms of Organ Injury and Repair by Macrophages. *Annu. Rev. Physiol.* **2017**, *79* (1), 593–617. https://doi.org/10.1146/annurev-physiol-022516-034356.

(120)   Rodriguez-Feo, J.; Sluijter, J.; Kleijn, D.; Pasterkamp, G. Modulation of Collagen Turnover in Cardiovascular Disease. *CPD* **2005**, *11* (19), 2501–2514. https://doi.org/10.2174/1381612054367544.

(121)   Gelse, K. Collagens—Structure, Function, and Biosynthesis. *Advanced Drug Delivery Reviews* **2003**, *55* (12), 1531–1546. https://doi.org/10.1016/j.addr.2003.08.002.

(122)   Rennard, S. I.; Stier, L. E.; Crystal, R. G. Intracellular Degradation of Newly Synthesized Collagen. *Journal of Investigative Dermatology* **1982**, *79* (1), 77–82. https://doi.org/10.1038/jid.1982.15.

(123)   McAnulty, R. J.; Laurent, G. J. Collagen Synthesis and Degradation In Vivo. Evidence for Rapid Rates of Collagen Turnover with Extensive Degradation of Newly Synthesized Collagen in Tissues of the Adult Rat. *Collagen and Related Research* **1987**, *7* (2), 93–104. https://doi.org/10.1016/S0174-173X(87)80001-8.

(124)   Laurent, G. J. Dynamic State of Collagen: Pathways of Collagen Degradation in Vivo and Their Possible Role in Regulation of Collagen Mass. *American Journal of Physiology-Cell Physiology* **1987**, *252* (1), C1–C9. https://doi.org/10.1152/ajpcell.1987.252.1.C1.

(125)   Lu, P.; Takai, K.; Weaver, V. M.; Werb, Z. Extracellular Matrix Degradation and Remodeling in Development and Disease. *Cold Spring Harb Perspect Biol* **2011**, *3* (12). https://doi.org/10.1101/cshperspect.a005058.

(126)   Zhong, S.; Khalil, R. A. A Disintegrin and Metalloproteinase (ADAM) and ADAM with Thrombospondin Motifs (ADAMTS) Family in Vascular Biology and Disease. *Biochemical Pharmacology* **2019**, *164*, 188–204. https://doi.org/10.1016/j.bcp.2019.03.033.

(127)   McClung, J. M.; Davis, J. M.; Wilson, M. A.; Goldsmith, E. C.; Carson, J. A. Estrogen Status and Skeletal Muscle Recovery from Disuse Atrophy. *Journal of Applied Physiology* **2006**, *100* (6), 2012–2023. https://doi.org/10.1152/japplphysiol.01583.2005.

(128)   Miller, B. F.; Hansen, M.; Olesen, J. L.; Flyvbjerg, A.; Schwarz, P.; Babraj, J. A.; Smith, K.; Rennie, M. J.; Kjaer, M. No Effect of Menstrual Cycle on Myofibrillar and Connective Tissue Protein Synthesis in Contracting Skeletal Muscle. *American Journal of Physiology-Endocrinology and Metabolism* **2006**, *290* (1), E163–E168. https://doi.org/10.1152/ajpendo.00300.2005.

(129)   Miller, B. F.; Hansen, M.; Olesen, J. L.; Schwarz, P.; Babraj, J. A.; Smith, K.; Rennie, M. J.; Kjaer, M. Tendon Collagen Synthesis at Rest and after Exercise in Women. *Journal of Applied Physiology* **2007**, *102* (2), 541–546. https://doi.org/10.1152/japplphysiol.00797.2006.

(130)   Kehlet, S. N.; Willumsen, N.; Armbrecht, G.; Dietzel, R.; Brix, S.; Henriksen, K.; Karsdal, M. A. Age-Related Collagen Turnover of the Interstitial Matrix and Basement Membrane: Implications of Age- and Sex-Dependent Remodeling of the Extracellular Matrix. *PLoS ONE* **2018**, *13* (3), e0194458. https://doi.org/10.1371/journal.pone.0194458.

(131)   Baló, J.; Banga, I. Elastase and Elastase-Inhibitor. *Nature* **1949**, *164* (4168), 491–491. https://doi.org/10.1038/164491a0.

(132)   Godeau, G.; Hornebeck, W. Morphometric Analysis of the Degradation of Human Skin Elastic Fibres by Human Leukocyte Elastase (EC 3-4-21-37) and Human Skin Fibroblast Elastase (EC 3-4-24). *Pathol Biol (Paris)* **1988**, *36* (9), 1133–1138.

(133)   Ohbayashi, H. Current Synthetic Inhibitors of Human Neutrophil Elastase in 2005. *Expert Opinion on Therapeutic Patents* **2005**, *15* (7), 759–771. https://doi.org/10.1517/13543776.15.7.759.

(134)   Kelly, E.; Greene, C. M.; McElvaney, N. G. Targeting Neutrophil Elastase in Cystic Fibrosis. *Expert Opinion on Therapeutic Targets* **2008**, *12* (2), 145–157. https://doi.org/10.1517/14728222.12.2.145.

(135)   Groutas, W. C.; Dou, D.; Alliston, K. R. Neutrophil Elastase Inhibitors. *Expert Opinion on Therapeutic Patents* **2011**, *21* (3), 339–354. https://doi.org/10.1517/13543776.2011.551115.

(136)   Ahmad, S.; Saleem, M.; Riaz, N.; Lee, Y. S.; Diri, R.; Noor, A.; Almasri, D.; Bagalagel, A.; Elsebai, M. F. The Natural Polypeptides as Significant Elastase Inhibitors. *Front. Pharmacol.* **2020**, *11*, 688. https://doi.org/10.3389/fphar.2020.00688.

(137)   Bijak, M.; Ponczek, M. B.; Nowak, P. Proteazy serynowe i ich klasyfikacja według systemu merops*. *Kosmos* **2015**, *64* (1), 31–45.

(138)   Crocetti, L.; Quinn, M.; Schepetkin, I.; Giovannoni, M. A Patenting Perspective on Human Neutrophil Elastase (HNE) Inhibitors (2014-2018) and Their Therapeutic Applications. *Expert Opinion on Therapeutic Patents* **2019**, *29*, 1–24. https://doi.org/10.1080/13543776.2019.1630379.

(139)   Hajjar, E.; Broemstrup, T.; Kantari, C.; Witko-Sarsat, V.; Reuter, N. Structures of Human Proteinase 3 and Neutrophil Elastase – so Similar yet so Different. *The FEBS Journal* **2010**, *277* (10), 2238–2254. https://doi.org/10.1111/j.1742-4658.2010.07659.x.

(140)   Lee, W. L.; Downey, G. P. Leukocyte Elastase: Physiological Functions and Role in Acute Lung Injury. *Am J Respir Crit Care Med* **2001**, *164* (5), 896–904. https://doi.org/10.1164/ajrccm.164.5.2103040.

(141)   Navia, M. A.; McKeever, B. M.; Springer, J. P.; Lin, T. Y.; Williams, H. R.; Fluder, E. M.; Dorn, C. P.; Hoogsteen, K. Structure of Human Neutrophil Elastase in Complex with a Peptide Chloromethyl Ketone Inhibitor at 1.84-A Resolution. *Proceedings of the National Academy of Sciences* **1989**, *86* (1), 7–11. https://doi.org/10.1073/pnas.86.1.7.

(142)   Korkmaz, B.; Moreau, T.; Gauthier, F. Neutrophil Elastase, Proteinase 3 and Cathepsin G: Physicochemical Properties, Activity and Physiopathological Functions. *Biochimie* **2008**, *90* (2), 227–242. https://doi.org/10.1016/j.biochi.2007.10.009.

(143)   Ameta, S. *RNA as serine protease: Activity-based selection of RNA catalysts*. https://www.researchgate.net/publication/325645574_RNA_as_serine_protease_Activity-based_selection_of_RNA_catalysts (accessed 2023-02-07).

(144)   Walker, B.; Lynas, J. F. Strategies for the Inhibition of Serine Proteases. *Cell Mol Life Sci* **2001**, *58* (4), 596–624. https://doi.org/10.1007/PL00000884.

(145)   Hedstrom, L. Serine Protease Mechanism and Specificity. *Chem. Rev.* **2002**, *102* (12), 4501–4524. https://doi.org/10.1021/cr000033x.

(146)   Robertus, J. D.; Kraut, J.; Alden, R. A.; Birktoft, J. J. Subtilisin; a Stereochemical Mechanism Involving Transition-State Stabilization. *Biochemistry* **1972**, *11* (23), 4293–4303. https://doi.org/10.1021/bi00773a016.

(147)   Polgár, L. The Catalytic Triad of Serine Peptidases. *Cell Mol Life Sci* **2005**, *62* (19–20), 2161–2172. https://doi.org/10.1007/s00018-005-5160-x.

(148)   Sturm, N. *Enzyme Mechanisms: Serine Proteases*. https://www2.csudh.edu/nsturm/CHE450/11_Enz.%20Mech.-Ser%20Protea.htm (accessed 2022-12-26).

(149)   Saleem, M.; Nazir, M.; Hussain, H.; Tousif, M. I.; Elsebai, M. F.; Riaz, N.; Akhtar, N. Natural Phenolics as Inhibitors of the Human Neutrophil Elastase (HNE) Release: An Overview of Natural Anti-Inflammatory Discoveries during Recent Years. *Antiinflamm Antiallergy Agents Med Chem* **2018**, *17* (2), 70–94. https://doi.org/10.2174/1871523017666180910104946.

(150)   Leung, D.; Abbenante, G.; Fairlie, D. P. Protease Inhibitors: Current Status and Future Prospects. *J Med Chem* **2000**, *43* (3), 305–341. https://doi.org/10.1021/jm990412m.

(151)   Maryanoff, B. E.; Costanzo, M. J. Inhibitors of Proteases and Amide Hydrolases That Employ an α-Ketoheterocycle as a Key Enabling Functionality. *Bioorganic & Medicinal Chemistry* **2008**, *16* (4), 1562–1595. https://doi.org/10.1016/j.bmc.2007.11.015.

(152)   Powers, J. C.; Gupton, B. F.; Harley, A. D.; Nishino, N.; Whitley, R. J. Specificity of Porcine Pancreatic Elastase, Human Leukocyte Elastase and Cathepsin G Inhibition with Peptide Chloromethyl Ketones. *Biochimica et Biophysica Acta (BBA) - Enzymology* **1977**, *485* (1), 156–166. https://doi.org/10.1016/0005-2744(77)90203-0.

(153)   Cowan, K. N.; Heilbut, A.; Humpl, T.; Lam, C.; Ito, S.; Rabinovitch, M. Complete Reversal of Fatal Pulmonary Hypertension in Rats by a Serine Elastase Inhibitor. *Nat Med* **2000**, *6* (6), 698–702. https://doi.org/10.1038/76282.

(154)   Cantel, S.; Le Chevalier Isaad, A.; Scrima, M.; Levy, J. J.; DiMarchi, R. D.; Rovero, P.; Halperin, J. A.; D'Ursi, A. M.; Papini, A. M.; Chorev, M. Synthesis and Conformational Analysis of a Cyclic Peptide Obtained via *i* to *i* +4 Intramolecular Side-Chain to Side-Chain Azide–Alkyne 1,3-Dipolar Cycloaddition. *J. Org. Chem.* **2008**, *73* (15), 5663–5674. https://doi.org/10.1021/jo800142s.

(155)   Kracker, O.; Góra, J.; Krzciuk-Gula, J.; Marion, A.; Neumann, B.; Stammler, H.-G.; Nieß, A.; Antes, I.; Latajka, R.; Sewald, N. 1,5-Disubstituted 1,2,3-Triazole-Containing Peptidotriazolamers: Design Principles for a Class of Versatile Peptidomimetics. *Chemistry* **2018**, *24* (4), 953–961. https://doi.org/10.1002/chem.201704583.

(156)   Schröder, D. C.; Kracker, O.; Fröhr, T.; Góra, J.; Jewginski, M.; Nieß, A.; Antes, I.; Latajka, R.; Marion, A.; Sewald, N. 1,4-Disubstituted 1H-1,2,3-Triazole Containing Peptidotriazolamers: A New Class of Peptidomimetics With Interesting Foldamer Properties. *Front Chem* **2019**, *7*, 155. https://doi.org/10.3389/fchem.2019.00155.

(157)   D'Ercole, A.; Sabatino, G.; Pacini, L.; Impresari, E.; Capecchi, I.; Papini, A. M.; Rovero, P. On-resin Microwave-assisted Copper-catalyzed Azide-alkyne Cycloaddition of H1-relaxin B Single Chain 'Stapled' Analogues. *Peptide Science* **2020**, *112* (4). https://doi.org/10.1002/pep2.24159.

(158)   Matern, U.; Oberer, L.; Falchetto, R. A.; Erhard, M.; König, W. A.; Herdman, M.; Weckesser, J. Scyptolin A and B, Cyclic Depsipeptides from Axenic Cultures of Scytonema Hofmanni PCC 7110. *Phytochemistry* **2001**, *58* (7), 1087–1095. https://doi.org/10.1016/s0031-9422(01)00400-9.

(159)   Matern, U.; Schleberger, C.; Jelakovic, S.; Weckesser, J.; Schulz, G. E. Binding Structure of Elastase Inhibitor Scyptolin A. *Chemistry & Biology* **2003**, *10* (10), 997–1001. https://doi.org/10.1016/j.chembiol.2003.10.001.

(160)   Keller, L.; Canuto, K. M.; Liu, C.; Suzuki, B. M.; Almaliti, J.; Sikandar, A.; Naman, C. B.; Glukhov, E.; Luo, D.; Duggan, B. M.; Luesch, H.; Koehnke, J.; O'Donoghue, A. J.; Gerwick, W. H. Tutuilamides A-C: Vinyl-Chloride-Containing Cyclodepsipeptides from Marine Cyanobacteria with Potent Elastase Inhibitory Properties. *ACS Chem Biol* **2020**, *15* (3), 751–757. https://doi.org/10.1021/acschembio.9b00992.

(161)   Toth, I.; Christodoulou, M.; Bankowsky, K.; Flinn, N.; Gibbons, W. A.; Godeau, G.; Moczar, E.; Hornebeck, W. Design of Potent Lipophilic-Peptide Inhibitors of Human Neutrophil Elastase: In Vitro and in Vivo Studies. *International Journal of Pharmaceutics* **1995**, *125* (1), 117–122. https://doi.org/10.1016/0378-5173(95)00127-5.

(162)   Hilpert, K.; Hansen, G.; Wessner, H.; Schneider-Mergener, J.; Hohne, W. Characterizing and Optimizing Protease/Peptide Inhibitor Interactions, a New Application for Spot Synthesis. *Journal of Biochemistry* **2000**, *128* (6), 1051–1057. https://doi.org/10.1093/oxfordjournals.jbchem.a022833.

(163)   Hilpert, K.; Wessner, H.; Schneider-Mergener, J.; Welfle, K.; Misselwitz, R.; Welfle, H.; Hocke, A. C.; Hippenstiel, S.; Höhne, W. Design and Characterization of a Hybrid Miniprotein That Specifically Inhibits Porcine Pancreatic Elastase. *Journal of Biological Chemistry* **2003**, *278* (27), 24986–24993. https://doi.org/10.1074/jbc.M212152200.

(164)   Vasconcelos, A.; Azoia, N. G.; Carvalho, A. C.; Gomes, A. C.; Güebitz, G.; Cavaco-Paulo, A. Tailoring Elastase Inhibition with Synthetic Peptides. *Eur J Pharmacol* **2011**, *666* (1–3), 53–60. https://doi.org/10.1016/j.ejphar.2011.05.056.

(165)   McBride, J. D.; Watson, E. M.; Brauer, A. B. E.; Jaulent, A. M.; Leatherbarrow, R. J. Peptide Mimics of the Bowman-Birk Inhibitor Reactive Site Loop. *Biopolymers* **2002**, *66* (2), 79–92. https://doi.org/10.1002/bip.10228.

(166)   Wan, H.; Lee, K. S.; Kim, B. Y.; Zou, F. M.; Yoon, H. J.; Je, Y. H.; Li, J.; Jin, B. R. A Spider-Derived Kunitz-Type Serine Protease Inhibitor That Acts as a Plasmin Inhibitor and an Elastase Inhibitor. *PLoS ONE* **2013**, *8* (1), e53343. https://doi.org/10.1371/journal.pone.0053343.

(167)   Nakanishi, I.; Kinoshita, T.; Sato, A.; Tada, T. Structure of Porcine Pancreatic Elastase Complexed with FR901277, a Novel Macrocyclic Inhibitor of Elastases, at 1.6 A Resolution. *Biopolymers* **2000**, *53* (5), 434–445. https://doi.org/10.1002/(SICI)1097-0282(20000415)53:5<434::AID-BIP7>3.0.CO;2-5.

(168)   Fujita, T.; Hatanaka, H.; Hayashi, K.; Shigematsu, N.; Takase, S.; Okamoto, M.; Okuhara, M.; Shimatani, K.; Satoh, A. FR901451, a Novel Inhibitor of Human Leukocyte Elastase from Flexibacter Sp. I. Producing Organism, Fermentation, Isolation, Physico-Chemical and Biological Properties. *J Antibiot (Tokyo)* **1994**, *47* (12), 1359–1364. https://doi.org/10.7164/antibiotics.47.1359.

(169)   Kitagishi, K.; Hiromi, K. Binding between Thermolysin and Its Specific Inhibitor, Phosphoramidon. *The Journal of Biochemistry* **1984**, *95* (2), 529–534. https://doi.org/10.1093/oxfordjournals.jbchem.a134635.

(170)   Schepetkin, I. A.; Khlebnikov, A. I.; Quinn, M. T. N-Benzoylpyrazoles Are Novel Small-Molecule Inhibitors of Human Neutrophil Elastase. *J Med Chem* **2007**, *50* (20), 4928–4938. https://doi.org/10.1021/jm070600+.

(171)   Crocetti, L.; Giovannoni, M. P.; Schepetkin, I. A.; Quinn, M. T.; Khlebnikov, A. I.; Cilibrizzi, A.; Piaz, V. D.; Graziano, A.; Vergelli, C. Design, Synthesis and Evaluation of N-Benzoylindazole Derivatives and Analogues as Inhibitors of Human Neutrophil Elastase. *Bioorganic & Medicinal Chemistry* **2011**, *19* (15), 4460–4472. https://doi.org/10.1016/j.bmc.2011.06.036.

(172)   Crocetti, L.; Schepetkin, I. A.; Cilibrizzi, A.; Graziano, A.; Vergelli, C.; Giomi, D.; Khlebnikov, A. I.; Quinn, M. T.; Giovannoni, M. P. Optimization of N-Benzoylindazole Derivatives as Inhibitors of Human Neutrophil Elastase. *J. Med. Chem.* **2013**, *56* (15), 6259–6272. https://doi.org/10.1021/jm400742j.

(173)   *Melanogenesis in the skin*. https://www.istockphoto.com/nl/vector/huid-mechanisme-van-melanine-en-gezicht-donkere-vlekken-infographic-menselijke-huid-gm1140567815-305265895 (accessed 2022-12-29).

(174)   d'Ischia, M.; Wakamatsu, K.; Cicoira, F.; Di Mauro, E.; Garcia-Borron, J. C.; Commo, S.; Galván, I.; Ghanem, G.; Kenzo, K.; Meredith, P.; Pezzella, A.; Santato, C.; Sarna, T.; Simon, J. D.; Zecca, L.; Zucca, F. A.; Napolitano, A.; Ito, S. Melanins and Melanogenesis: From Pigment Cells to Human Health and Technological Applications. *Pigment Cell Melanoma Res* **2015**, *28* (5), 520–544. https://doi.org/10.1111/pcmr.12393.

(175)   Raper, H. S. The Tyrosinase-Tyrosine Reaction. *Biochemical Journal* **1927**, *21* (1), 89–96. https://doi.org/10.1042/bj0210089.

(176)   Mason, H. S. The Chemistry of Melanin; Mechanism of the Oxidation of Dihydroxyphenylalanine by Tyrosinase. *J Biol Chem* **1948**, *172* (1), 83–99.

(177)   Prota, G. Progress in the Chemistry of Melanins and Related Metabolites. *Med Res Rev* **1988**, *8* (4), 525–556. https://doi.org/10.1002/med.2610080405.

(178)   Mariano, A.; Bigioni, I.; Scotto d'Abusco, A.; Baseggio Conrado, A.; Maina, S.; Francioso, A.; Mosca, L.; Fontana, M. Pheomelanin Effect on UVB Radiation-Induced Oxidation/Nitration of l-Tyrosine. *IJMS* **2021**, *23* (1), 267. https://doi.org/10.3390/ijms23010267.

(179)   Ito, S.; Wakamatsu, K. Chemistry of Mixed Melanogenesis—Pivotal Roles of Dopaquinone. *Photochem Photobiol* **2008**, *84* (3), 582–592. https://doi.org/10.1111/j.1751-1097.2007.00238.x.

(180)   Lee, A.-Y. Skin Pigmentation Abnormalities and Their Possible Relationship with Skin Aging. *Int J Mol Sci* **2021**, *22* (7), 3727. https://doi.org/10.3390/ijms22073727.

(181)   Ismaya, W. T.; Rozeboom, H. J.; Schurink, M.; Boeriu, C. G.; Wichers, H.; Dijkstra, B. W. Crystallization and Preliminary X-Ray Crystallographic Analysis of Tyrosinase from the Mushroom *Agaricus Bisporus*. *Acta Crystallogr F Struct Biol Cryst Commun* **2011**, *67* (5), 575–578. https://doi.org/10.1107/S174430911100738X.

(182)   Prexler, S. M.; Frassek, M.; Moerschbacher, B. M.; Dirks-Hofmeister, M. E. Catechol Oxidase versus Tyrosinase Classification Revisited by Site-Directed Mutagenesis Studies. *Angew. Chem.* **2019**, *131* (26), 8849–8853. https://doi.org/10.1002/ange.201902846.

(183)   Kanteev, M.; Goldfeder, M.; Fishman, A. Structure-Function Correlations in Tyrosinases. *Protein Science* **2015**, *24* (9), 1360–1369. https://doi.org/10.1002/pro.2734.

(184)   Ismaya, W. T.; Rozeboom, H. J.; Weijn, A.; Mes, J. J.; Fusetti, F.; Wichers, H. J.; Dijkstra, B. W. Crystal Structure of *Agaricus Bisporus* Mushroom Tyrosinase: Identity of the Tetramer Subunits and Interaction with Tropolone. *Biochemistry* **2011**, *50* (24), 5477–5486. https://doi.org/10.1021/bi200395t.

(185)   Jackman, M. P.; Hajnal, A.; Lerch, K. Albino Mutants of *Streptomyces Glaucescens* Tyrosinase. *Biochemical Journal* **1991**, *274* (3), 707–713. https://doi.org/10.1042/bj2740707.

(186)   Zou, C.; Huang, W.; Zhao, G.; Wan, X.; Hu, X.; Jin, Y.; Li, J.; Liu, J. Determination of the Bridging Ligand in the Active Site of Tyrosinase. *Molecules* **2017**, *22* (11), 1836. https://doi.org/10.3390/molecules22111836.

(187)   Deeth, R. J.; Diedrich, C. Structural and Mechanistic Insights into the Oxy Form of Tyrosinase from Molecular Dynamics Simulations. *J Biol Inorg Chem* **2010**, *15* (2), 117–129. https://doi.org/10.1007/s00775-009-0577-6.

(188)   Goldfeder, M.; Kanteev, M.; Isaschar-Ovdat, S.; Adir, N.; Fishman, A. Determination of Tyrosinase Substrate-Binding Modes Reveals Mechanistic Differences between Type-3 Copper Proteins. *Nat Commun* **2014**, *5* (1), 4505. https://doi.org/10.1038/ncomms5505.

(189)   Strothkamp, K. G.; Jolley, R. L.; Mason, H. S. Quaternary Structure of Mushroom Tyrosinase. *Biochemical and Biophysical Research Communications* **1976**, *70* (2), 519–524. https://doi.org/10.1016/0006-291X(76)91077-9.

(190)   Ismaya, W. T.; Tandrasasmita, O. M.; Sundari, S.; Diana; Lai, X.; Retnoningrum, D. S.; Dijkstra, B. W.; Tjandrawinata, R. R.; Rachmawati, H. The Light Subunit of Mushroom Agaricus Bisporus Tyrosinase: Its Biological Characteristics and Implications. *International Journal of Biological Macromolecules* **2017**, *102*, 308–314. https://doi.org/10.1016/j.ijbiomac.2017.04.014.

(191)   Solano, F. On the Metal Cofactor in the Tyrosinase Family. *IJMS* **2018**, *19* (2), 633. https://doi.org/10.3390/ijms19020633.

(192)   Mann, T.; Gerwat, W.; Batzer, J.; Eggers, K.; Scherner, C.; Wenck, H.; Stäb, F.; Hearing, V. J.; Röhm, K.-H.; Kolbe, L. Inhibition of Human Tyrosinase Requires Molecular Motifs Distinctively Different from Mushroom Tyrosinase. *Journal of Investigative Dermatology* **2018**, *138* (7), 1601–1608. https://doi.org/10.1016/j.jid.2018.01.019.

(193)   Hearing, V. J.; Ekel, T. M.; Montague, P. M.; Nicholson, J. M. Mammalin Tyrosinase. Stoichiometry and Measurement of Reaction Products. *Biochimica et Biophysica Acta (BBA) - Enzymology* **1980**, *611* (2), 251–268. https://doi.org/10.1016/0005-2744(80)90061-3.

(194)   Oyama, T.; Yoshimori, A.; Ogawa, H.; Shirai, Y.; Abe, H.; Kamiya, T.; Tanuma, S. The Structural Differences between Mushroom and Human Tyrosinase Cleared by Investigating the Inhibitory Activities of Stilbenes. *Journal of Molecular Structure* **2023**, *1272*, 134180. https://doi.org/10.1016/j.molstruc.2022.134180.

(195)   Karimian, S.; Kazemi, F.; Attarroshan, M.; Gholampour, M.; Hemmati, S.; Sakhteman, A.; Behzadipour, Y.; Kabiri, M.; Iraji, A.; Khoshneviszadeh, M. Design, Synthesis, and Biological Evaluation of Symmetrical Azine Derivatives as Novel Tyrosinase Inhibitors. *BMC Chemistry* **2021**, *15* (1), 54. https://doi.org/10.1186/s13065-021-00780-z.

(196)   Rescigno, A.; Sollai, F.; Pisu, B.; Rinaldi, A.; Sanjust, E. Tyrosinase Inhibition: General and Applied Aspects. *Journal of Enzyme Inhibition and Medicinal Chemistry* **2002**, *17* (4), 207–218. https://doi.org/10.1080/14756360210000010923.

(197)   Kim, Y.-J.; Uyama, H. Tyrosinase Inhibitors from Natural and Synthetic Sources: Structure, Inhibition Mechanism and Perspective for the Future. *CMLS, Cell. Mol. Life Sci.* **2005**, *62* (15), 1707–1723. https://doi.org/10.1007/s00018-005-5054-y.

(198)   Parvez, S.; Kang, M.; Chung, H.-S.; Bae, H. Naturally Occurring Tyrosinase Inhibitors: Mechanism and Applications in Skin Health, Cosmetics and Agriculture Industries. *Phytother. Res.* **2007**, *21* (9), 805–816. https://doi.org/10.1002/ptr.2184.

(199)   Chang, T.-S. An Updated Review of Tyrosinase Inhibitors. *IJMS* **2009**, *10* (6), 2440–2475. https://doi.org/10.3390/ijms10062440.

(200)   Chen, J. S.; Wei, C. I.; Marshall, M. R. Inhibition Mechanism of Kojic Acid on Polyphenol Oxidase. *J. Agric. Food Chem.* **1991**, *39* (11), 1897–1901. https://doi.org/10.1021/jf00011a001.

(201) Hashemi, S. M.; Department of Medicinal Chemistry and Pharmaceutical Sciences Research Center, Faculty of Pharmacy, Mazandaran University of Medical Sciences, Sari, Iran; Emami, S.; Department of Medicinal Chemistry, Faculty of Pharmacy, Mazandaran University of Medical Sciences, Sari, Iran. Kojic Acid-Derived Tyrosinase Inhibitors: Synthesis and Bioactivity. *mazums-pbr* **2015**, *1* (1), 1–17. https://doi.org/10.18869/acadpub.pbr.1.1.1.

(202) Cabanes, J.; Chazarra, S.; Garcia-Carmona, F. Kojic Acid, a Cosmetic Skin Whitening Agent, Is a Slow-Binding Inhibitor of Catecholase Activity of Tyrosinase. *Journal of Pharmacy and Pharmacology* **2011**, *46* (12), 982–985. https://doi.org/10.1111/j.2042-7158.1994.tb03253.x.

(203) Saeedi, M.; Eslamifar, M.; Khezri, K. Kojic Acid Applications in Cosmetic and Pharmaceutical Preparations. *Biomedicine & Pharmacotherapy* **2019**, *110*, 582–593. https://doi.org/10.1016/j.biopha.2018.12.006.

(204) Fujimoto, N. Changes in Thyroid Function during Development of Thyroid Hyperplasia Induced by Kojic Acid in F344 Rats. *Carcinogenesis* **1999**, *20* (8), 1567–1572. https://doi.org/10.1093/carcin/20.8.1567.

(205) Kim, H.; Choi, J.; Cho, J. K.; Kim, S. Y.; Lee, Y.-S. Solid-Phase Synthesis of Kojic Acid-Tripeptides and Their Tyrosinase Inhibitory Activity, Storage Stability, and Toxicity. *Bioorganic & Medicinal Chemistry Letters* **2004**, *14* (11), 2843–2846. https://doi.org/10.1016/j.bmcl.2004.03.046.

(206) Li, D.-F.; Hu, P.-P.; Liu, M.-S.; Kong, X.-L.; Zhang, J.-C.; Hider, R. C.; Zhou, T. Design and Synthesis of Hydroxypyridinone- L -Phenylalanine Conjugates as Potential Tyrosinase Inhibitors. *J. Agric. Food Chem.* **2013**, *61* (27), 6597–6603. https://doi.org/10.1021/jf401585f.

(207) 노호식; 이재경; 안수미; Yeon, Jae-Ho; Yoo, Dae-Sung; 김덕희; 김한곤; 조재열. Ester Derivatives of Kojic Acid and Polyphenols Containing Adamantane Moiety with Tyrosinase Inhibitory and Anti-Inflammatory Properties. *Bulletin of the Korean Chemical Society* **2011**, *32* (4), 1411–1414. https://doi.org/10.5012/BKCS.2011.32.4.1411.

(208) Kobayashi, Y.; Kayahara, H.; Tadasa, K.; Tanaka, H. Synthesis of N-Kojic-Amino Acid and N-Kojic-Amino Acid-Kojiate and Their Tyrosinase Inhibitory Activity. *Bioorganic & Medicinal Chemistry Letters* **1996**, *6* (12), 1303–1308. https://doi.org/10.1016/0960-894X(96)00221-1.

(209) 노호식; 백흥수; 안수미; 김덕희; 장이섭. Synthesis of New Anti-Melanogenic Compounds Containing Two Molecules of Kojic Acid. *Bulletin of the Korean Chemical Society* **2008**, *29* (8), 1569–1571. https://doi.org/10.5012/BKCS.2008.29.8.1569.

(210) Noh, J.-M.; Kwak, S.-Y.; Seo, H.-S.; Seo, J.-H.; Kim, B.-G.; Lee, Y.-S. Kojic Acid–Amino Acid Conjugates as Tyrosinase Inhibitors. *Bioorganic & Medicinal Chemistry Letters* **2009**, *19* (19), 5586–5589. https://doi.org/10.1016/j.bmcl.2009.08.041.

(211) Noh, J.-M.; Kwak, S.-Y.; Kim, D.-H.; Lee, Y.-S. Kojic Acid–Tripeptide Amide as a New Tyrosinase Inhibitor. *Biopolymers* **2007**, *88* (2), 300–307. https://doi.org/10.1002/bip.20670.

(212) Singh, B. K.; Park, S. H.; Lee, H.-B.; Goo, Y.-A.; Kim, H. S.; Cho, S. H.; Lee, J. H.; Ahn, G. W.; Kim, J. P.; Kang, S. M.; Kim, E.-K. Kojic Acid Peptide: A New Compound with Anti-Tyrosinase Potential. *Ann Dermatol* **2016**, *28* (5), 555. https://doi.org/10.5021/ad.2016.28.5.555.

(213) Upadhyay, A.; Chompoo, J.; Taira, N.; Fukuta, M.; Gima, S.; Tawata, S. Solid-Phase Synthesis of Mimosine Tetrapeptides and Their Inhibitory Activities on Neuraminidase and Tyrosinase. *J. Agric. Food Chem.* **2011**, *59* (24), 12858–12863. https://doi.org/10.1021/jf203494t.

(214) Hałdys, K.; Goldeman, W.; Jewgiński, M.; Wolińska, E.; Anger, N.; Rossowska, J.; Latajka, R. Inhibitory Properties of Aromatic Thiosemicarbazones on Mushroom Tyrosinase: Synthesis, Kinetic Studies, Molecular Docking and Effectiveness in Melanogenesis Inhibition. *Bioorganic Chemistry* **2018**, *81*, 577–586. https://doi.org/10.1016/j.bioorg.2018.09.003.

(215)   Hałdys, K.; Goldeman, W.; Jewgiński, M.; Wolińska, E.; Anger-Góra, N.; Rossowska, J.; Latajka, R. Halogenated Aromatic Thiosemicarbazones as Potent Inhibitors of Tyrosinase and Melanogenesis. *Bioorganic Chemistry* **2020**, *94*, 103419. https://doi.org/10.1016/j.bioorg.2019.103419.

(216)   Hałdys, K.; Goldeman, W.; Anger-Góra, N.; Rossowska, J.; Latajka, R. Monosubstituted Acetophenone Thiosemicarbazones as Potent Inhibitors of Tyrosinase: Synthesis, Inhibitory Studies, and Molecular Docking. *Pharmaceuticals* **2021**, *14* (1), 74. https://doi.org/10.3390/ph14010074.

(217)   Soares, M. A.; Almeida, M. A.; Marins-Goulart, C.; Chaves, O. A.; Echevarria, A.; de Oliveira, M. C. C. Thiosemicarbazones as Inhibitors of Tyrosinase Enzyme. *Bioorganic & Medicinal Chemistry Letters* **2017**, *27* (15), 3546–3550. https://doi.org/10.1016/j.bmcl.2017.05.057.

(218)   Carcelli, M.; Rogolino, D.; Bartoli, J.; Pala, N.; Compari, C.; Ronda, N.; Bacciottini, F.; Incerti, M.; Fisicaro, E. Hydroxyphenyl Thiosemicarbazones as Inhibitors of Mushroom Tyrosinase and Antibrowning Agents. *Food Chemistry* **2020**, *303*, 125310. https://doi.org/10.1016/j.foodchem.2019.125310.

(219)   Arslan, H.; Duran, N.; Borekci, G.; Koray Ozer, C.; Akbay, C. Antimicrobial Activity of Some Thiourea Derivatives and Their Nickel and Copper Complexes. *Molecules* **2009**, *14* (1), 519–527. https://doi.org/10.3390/molecules14010519.

(220)   Zhu, T.-H.; Cao, S.-W.; Yu, Y.-Y. Synthesis, Characterization and Biological Evaluation of Paeonol Thiosemicarbazone Analogues as Mushroom Tyrosinase Inhibitors. *International Journal of Biological Macromolecules* **2013**, *62*, 589–595. https://doi.org/10.1016/j.ijbiomac.2013.09.056.

(221)   Haseloer, A.; Lützenburg, T.; Strache, J. P.; Neudörfl, J.; Neundorf, I.; Klein, A. Building up Pt II –Thiosemicarbazone–Lysine–sC18 Conjugates. *ChemBioChem* **2021**, *22* (4), 694–704. https://doi.org/10.1002/cbic.202000564.

(222)   Hariri, R.; Saeedi, M.; Akbarzadeh, T. Naturally Occurring and Synthetic Peptides: Efficient Tyrosinase Inhibitors. *J Pep Sci* **2021**, *27* (7). https://doi.org/10.1002/psc.3329.

(223)   Song, Y.; Chen, S.; Li, L.; Zeng, Y.; Hu, X. The Hypopigmentation Mechanism of Tyrosinase Inhibitory Peptides Derived from Food Proteins: An Overview. *Molecules* **2022**, *27* (9), 2710. https://doi.org/10.3390/molecules27092710.

(224)   Kawagishi, H.; Somoto, A.; Kuranari, J.; Kimura, A.; Chiba, S. A Novel Cyclotetrapeptide Produced by Lactobacillus Helveticus as a Tyrosinase Inhibitor. *Tetrahedron Letters* **1993**, *34* (21), 3439–3440. https://doi.org/10.1016/S0040-4039(00)79177-5.

(225)   Morita, H.; Kayashita, T.; Kobata, H.; Gonda, A.; Takeya, K.; Itokawa, H. Pseudostellarins A - C, New Tyrosinase Inhibitory Cyclic Peptides from Pseudostellaria Heterophylla. *Tetrahedron* **1994**, *50* (23), 6797–6804. https://doi.org/10.1016/S0040-4020(01)81333-8.

(226)   Chen, Y.-C.; Su, S.-H.; Huang, J.-C.; Chao, C.-Y.; Sung, P.-J.; Chen, Y.-F.; Ko, H.-H.; Kuo, Y.-H. Tyrosinase Inhibitors Derived from Chemical Constituents of Dianella Ensifolia. *Plants* **2022**, *11* (16), 2142. https://doi.org/10.3390/plants11162142.

(227)   Schurink, M.; van Berkel, W. J. H.; Wichers, H. J.; Boeriu, C. G. Novel Peptides with Tyrosinase Inhibitory Activity. *Peptides* **2007**, *28* (3), 485–495. https://doi.org/10.1016/j.peptides.2006.11.023.

(228)   Hsiao, N.-W.; Tseng, T.-S.; Lee, Y.-C.; Chen, W.-C.; Lin, H.-H.; Chen, Y.-R.; Wang, Y.-T.; Hsu, H.-J.; Tsai, K.-C. Serendipitous Discovery of Short Peptides from Natural Products as Tyrosinase Inhibitors. *J. Chem. Inf. Model.* **2014**, *54* (11), 3099–3111. https://doi.org/10.1021/ci500370x.

(229)   Tseng, T.-S.; Tsai, K.-C.; Chen, W.-C.; Wang, Y.-T.; Lee, Y.-C.; Lu, C.-K.; Don, M.-J.; Chang, C.-Y.; Lee, C.-H.; Lin, H.-H.; Hsu, H.-J.; Hsiao, N.-W. Discovery of Potent Cysteine-Containing Dipeptide Inhibitors against Tyrosinase: A Comprehensive Investigation of 20 × 20 Dipeptides in Inhibiting Dopachrome Formation. *J. Agric. Food Chem.* **2015**, *63* (27), 6181–6188. https://doi.org/10.1021/acs.jafc.5b01026.

(230) Shen, Z.; Wang, Y.; Guo, Z.; Tan, T.; Zhang, Y. Novel Tyrosinase Inhibitory Peptide with Free Radical Scavenging Ability. *Journal of Enzyme Inhibition and Medicinal Chemistry* **2019**, *34* (1), 1633–1640. https://doi.org/10.1080/14756366.2019.1661401.

(231) Park, J.; Jung, H.; Jang, B.; Song, H.-K.; Han, I.-O.; Oh, E.-S. D-Tyrosine Adds an Anti-Melanogenic Effect to Cosmetic Peptides. *Sci Rep* **2020**, *10* (1), 262. https://doi.org/10.1038/s41598-019-57159-3.

(232) Park, J.; Jung, H.; Kim, K.; Lim, K.-M.; Kim, J.; Jho, E.; Oh, E.-S. D-Tyrosine Negatively Regulates Melanin Synthesis by Competitively Inhibiting Tyrosinase Activity. *Pigment Cell Melanoma Res.* **2018**, *31* (3), 374–383. https://doi.org/10.1111/pcmr.12668.

(233) Bagal, L. I.; Pevzner, M. S.; Lopyrev, V. A. Basicity and Structure of 1, 2, 4-Triazole Derivatives. *Chem Heterocycl Compd* **1967**, *2* (3), 323–325. https://doi.org/10.1007/BF00742379.

(234) Sączewski, J.; Hinc, K.; Obuchowski, M.; Gdaniec, M. The Tandem Mannich-Electrophilic Amination Reaction: A Versatile Platform for Fluorescent Probing and Labeling. *Chem. Eur. J.* **2013**, *19* (35), 11531–11535. https://doi.org/10.1002/chem.201302085.

(235) Sączewski, J.; Kędzia, A.; Jalińska, A. New Derivatives of 4,6-Dimethylisoxazolo[3,4- *b*] Pyridin-3(1 *H*)-One: Synthesis, Tautomerism, Electronic Structure and Antibacterial Activity. *Heterocyclic Communications* **2014**, *20* (4), 215–223. https://doi.org/10.1515/hc-2014-0107.

(236) Fedorowicz, J.; Sączewski, J.; Konopacka, A.; Waleron, K.; Lejnowski, D.; Ciura, K.; Tomašič, T.; Skok, Ž.; Savijoki, K.; Morawska, M.; Gilbert-Girard, S.; Fallarero, A. Synthesis and Biological Evaluation of Hybrid Quinolone-Based Quaternary Ammonium Antibacterial Agents. *European Journal of Medicinal Chemistry* **2019**, *179*, 576–590. https://doi.org/10.1016/j.ejmech.2019.06.071.

(237) Sączewski, J.; Fedorowicz, J.; Wiśniewska, P.; Gdaniec, M. Theoretical and Experimental Insights into the Tandem Mannich—Electrophilic Amination Reaction: Synthesis of Safirinium Dyes. *Applied Sciences* **2021**, *11* (12), 5498. https://doi.org/10.3390/app11125498.

(238) Merrifield, R. B. Solid Phase Peptide Synthesis. I. The Synthesis of a Tetrapeptide. *J. Am. Chem. Soc.* **1963**, *85* (14), 2149–2154. https://doi.org/10.1021/ja00897a025.

(239) Carpino, L. A.; Han, G. Y. 9-Fluorenylmethoxycarbonyl Amino-Protecting Group. *J. Org. Chem.* **1972**, *37* (22), 3404–3409. https://doi.org/10.1021/jo00795a005.

(240) Rafla, F. K.; Khan, M. A. Cyclic Hydroxamic Acids. Part I. Synthesis and Reactions of 1,2-Di-Hydro-1-Hydroxy-4,6-Dimethyl-2-Oxopyridine-3-Carbonitrile. *J. Chem. Soc., C* **1971**, 2044. https://doi.org/10.1039/j39710002044.

(241) Khan, M. A.; Rafla, F. K. Synthesis and Reactions of Potassium Cyanoacetohydroxamate. *J. Chem. Soc., Perkin Trans. 1* **1974**, 327. https://doi.org/10.1039/p19740000327.

(242) Khan, M. A.; Rafla, F. K. Synthesis of Isoxazolo[3,4-b]Pyridin-3(1H)-One and Isoxazolo[5,4-b]-Pyridin-3(2H)-One. *J. Chem. Soc., Perkin Trans. 1* **1975**, No. 8, 693. https://doi.org/10.1039/p19750000693.

(243) Kaiser, E.; Colescott, R. L.; Bossinger, C. D.; Cook, P. I. Color Test for Detection of Free Terminal Amino Groups in the Solid-Phase Synthesis of Peptides. *Analytical Biochemistry* **1970**, *34* (2), 595–598. https://doi.org/10.1016/0003-2697(70)90146-6.

(244) Hwang, T. L.; Shaka, A. J. Water Suppression That Works. Excitation Sculpting Using Arbitrary Wave-Forms and Pulsed-Field Gradients. *Journal of Magnetic Resonance, Series A* **1995**, *112* (2), 275–279. https://doi.org/10.1006/jmra.1995.1047.

(245) Piantini, U.; Sorensen, O. W.; Ernst, R. R. Multiple Quantum Filters for Elucidating NMR Coupling Networks. *J. Am. Chem. Soc.* **1982**, *104* (24), 6800–6801. https://doi.org/10.1021/ja00388a062.

(246)   Marion, D.; Wüthrich, K. Application of Phase Sensitive Two-Dimensional Correlated Spectroscopy (COSY) for Measurements of 1H-1H Spin-Spin Coupling Constants in Proteins. *Biochemical and Biophysical Research Communications* **1983**, *113* (3), 967–974. https://doi.org/10.1016/0006-291X(83)91093-8.

(247)   Braunschweiler, L.; Ernst, R. R. Coherence Transfer by Isotropic Mixing: Application to Proton Correlation Spectroscopy. *Journal of Magnetic Resonance (1969)* **1983**, *53* (3), 521–528. https://doi.org/10.1016/0022-2364(83)90226-3.

(248)   Lee, W.; Tonelli, M.; Markley, J. L. NMRFAM-SPARKY: Enhanced Software for Biomolecular NMR Spectroscopy. *Bioinformatics* **2015**, *31* (8), 1325–1327. https://doi.org/10.1093/bioinformatics/btu830.

(249)   Eun Lee, K.; Bharadwaj, S.; Yadava, U.; Gu Kang, S. Evaluation of Caffeine as Inhibitor against Collagenase, Elastase and Tyrosinase Using *in Silico* and *in Vitro* Approach. *Journal of Enzyme Inhibition and Medicinal Chemistry* **2019**, *34* (1), 927–936. https://doi.org/10.1080/14756366.2019.1596904.

(250)   *Sigma Aldrich (Merck) protocol for elastase activity assay*. https://www.sigmaaldrich.com/technical-documents/protocols/biology/enzymatic-assay-of-elastase.html (accessed 2022-09-16).

(251)   GraphPad Prism Version 8.0.0 for Windows, GraphPad Software. www.graphpad.com.

(252)   Gaussian 09, Revision D.01, 2013.

(253)   Besler, B. H.; Merz, K. M.; Kollman, P. A. Atomic Charges Derived from Semiempirical Methods. *J. Comput. Chem.* **1990**, *11* (4), 431–439. https://doi.org/10.1002/jcc.540110404.

(254)   Gaussian 16, Revision C.01, 2016.

(255)   Anandakrishnan, R.; Aguilar, B.; Onufriev, A. V. H++ 3.0: Automating PK Prediction and the Preparation of Biomolecular Structures for Atomistic Molecular Modeling and Simulations. *Nucleic Acids Research* **2012**, *40* (W1), W537–W541. https://doi.org/10.1093/nar/gks375.

(256)   Onufriev, A.; Anandakrishnan, R.; Aguilar, B. *H++, VirginiaTech*. http://newbiophysics.cs.vt.edu/H++/ (accessed 2023-01-03).

(257)   Bellei, B.; Pitisci, A.; Izzo, E.; Picardo, M. Inhibition of Melanogenesis by the Pyridinyl Imidazole Class of Compounds: Possible Involvement of the Wnt/β-Catenin Signaling Pathway. *PLoS ONE* **2012**, *7* (3), e33021. https://doi.org/10.1371/journal.pone.0033021.

(258)   Greenfield, N. J. Using Circular Dichroism Collected as a Function of Temperature to Determine the Thermodynamics of Protein Unfolding and Binding Interactions. *Nat Protoc* **2006**, *1* (6), 2527–2535. https://doi.org/10.1038/nprot.2006.204.

(259)   Chang, T.-S. Natural Melanogenesis Inhibitors Acting Through the Down-Regulation of Tyrosinase Activity. *Materials* **2012**, *5* (9), 1661–1685. https://doi.org/10.3390/ma5091661.

(260)   Lehraiki, A.; Abbe, P.; Cerezo, M.; Rouaud, F.; Regazzetti, C.; Chignon-Sicard, B.; Passeron, T.; Bertolotto, C.; Ballotti, R.; Rocchi, S. Inhibition of Melanogenesis by the Antidiabetic Metformin. *Journal of Investigative Dermatology* **2014**, *134* (10), 2589–2597. https://doi.org/10.1038/jid.2014.202.

(261)   Jones, G.; Willett, P.; Glen, R. C.; Leach, A. R.; Taylor, R. Development and Validation of a Genetic Algorithm for Flexible Docking 1 1Edited by F. E. Cohen. *Journal of Molecular Biology* **1997**, *267* (3), 727–748. https://doi.org/10.1006/jmbi.1996.0897.

Publications

REGARDING THIS DOCTORAL DISSERTATION

1. F. Errante, **P. Ledwoń**, R. Latajka, P. Rovero, A.M. Papini *Cosmeceutical Peptides in the Framework of Sustainable Wellness Economy*, Frontiers in Chemistry **2020**, *8*(572923); DOI: 10.3389/fchem.2020.572923. IF: 5.221.

2. **P. Ledwoń**, F. Errante, A.M. Papini, P. Rovero, R. Latajka *Peptides as Active Ingredients: a Challenge for Cosmeceutical Industry*, Chemistry&Biodiversity **2021**, *18*(e2000833); DOI: 10.1002/cbdv.202000833. IF: 2.745. *(Among Wiley TOP 10 most downloaded papers published between 1.01.2019 – 31.12.2020)*

3. A. Staśkiewicz, **P. Ledwoń**, P. Rovero, A.M. Papini, R. Latajka *Triazole-Modified Peptidomimetics: An Opportunity for Drug Discovery and Development*, Frontiers in Chemistry **2021**, *9*(674705); DOI: 10.3389/fchem.2021.674705. IF: 5.545.

4. **P. Ledwoń**, A.M. Papini, P. Rovero, R. Latajka *Peptides and Peptidomimetics as Inhibitors of Enzymes Involved in Fibrillar Collagen Degradation*, Materials **2021**, *14*(12), 3217-46. DOI: 10.3390/ma14123217. IF: 3.748.

5. **P. Ledwoń**, A. Staśkiewicz, M. Jewgiński, R. Latajka *Peptydomimetyki i foldamery aromatyczne w chemii biologicznej*, Wiadomości Chemiczne **2022**, *76*(5-6), 9-32. DOI: 10.53584/wiadchem.2022.5.6

6. **P. Ledwoń**, W. Goldeman, K. Hałdys, M. Jewgiński, G. Calamai, J. Rossowska, A.M. Papini, P. Rovero, R. Latajka *Tripeptides conjugated with thiosemicarbazones: new inhibitors of tyrosinase for cosmeceutical use*, Bioorganic Chemistry **2023**, in revision. *IF: 5.307.

7. **P. Ledwoń**, C. Bello, A.M. Papini, P. Rovero, R. Latajka *Synthesis and Structural Properties of Fmoc-Lys-triazolopyridylium and -triazolopirydynium Building Blocks for Solid-phase Peptide Derivatization*, European Journal of Organic Chemistry **2023**, in preparation – to be submitted until March 2023. *IF: 3.261.

OTHER PROJECTS

8. M. Kijewska, F. Nuti, M. Wierzbicka, M. Waliczek, **P. Ledwoń**, A. Staśkiewicz, F. Real-Fernández, G. Sabatino, P. Rovero, P. Stefanowicz, Z. Szewczuk, A.M. Papini *An Optimised Di-Boronate-ChemMatrix Affinity Chromatography to Trap Deoxyfructosylated Peptides as Biomarkers of Glycation*, Molecules **2020**, *25*(3), 755; DOI: 10.3390/molecules25030755. IF: 4.412.

9. P. Ledwoń, A. Staśkiewicz, M. Jewgiński, R. Latajka *Wpływ reszt ΔPhe na konformację łańcucha peptydowego*, Wiadomości Chemiczne **2020**, *74*(1-2), 9-32.

10. J. Krzciuk-Gula, **P. Ledwoń**, A. Staśkiewicz, R. Latajka *Wpływ różnych reszt β-aminokwasowych na zdolności koordynacyjne peptydów wobec jonów metali przejściowych*, Wiadomości Chemiczne **2020**, *74*(3-4), 285-310.

11. P. Ledwoń, F. Errante, F. Real-Fernández, P. Rovero, R. Latajka *New Thrombospondin-1-deriving Peptides as TGF-β Activators of Cosmeceutical Interest,* Proceedings of the 36th European Peptide Symposium, Michal Lebl (Editor), European Peptide Society. DOI: 10.17952/36EPS.2022.089

* Papers submitted (in revision) or in preparation. Not included in the summary IF.

Numerical data (until 14.02.2023):

- **Summary Impact Factor:** 21.671 *(includes the IF of published papers only)*
- **_h_-index:** 4
- **Citations of listed papers**: 60

Scientific achievements

Internships

1. March-July 2022: Laboratory of Peptide and Protein Chemistry and Biology, Interdepartmental Research Unit "PeptLab", University of Florence. Supervisor: Prof. Paolo Rovero. Project: *New Thrombospondin-1-deriving Peptides as TGF-β Activators of Cosmeceutical Interest* (funded by NCN Poland, PRELUDIUM grant 2021/41/N/ST4/04020).

2. April-August 2021: Laboratory of Peptide and Protein Chemistry and Biology, Interdepartmental Research Unit "PeptLab", University of Florence. Supervisor: prof. Paolo Rovero (funded by *European Peptide Society* Mobility Fellowship).

3. August-September 2020: Faculty of Chemistry, University of Florence. PhD thesis development. Supervisors: prof. Anna Maria Papini, prof. Paolo Rovero (funded by *BioTechNan* scholarship).

4. March-June 2020: *Erasmus+* internship program, Faculty of Chemistry, University of Florence. Project title: *Professional development in the field of bioorganic chemistry*. Supervisor: prof. Anna Maria Papini.

5. June-September 2019: *BioTechNan* internship program, Faculty of Chemistry, University of Florence. PhD thesis development. Supervisors: prof. Anna Maria Papini, prof. Paolo Rovero.

6. July-September 2018: *Erasmus+* internship program, Faculty of Chemistry, University of Florence. Project title: *Development of a diagnostic technology based on mass spectrometry to fish out biologically relevant glycopeptides by phenylboronic-modified resin*. Supervisors: prof. Anna Maria Papini, prof. Paolo Rovero. Results published in 2020.

Scientific grants

1. January 2022-January 2023: National Science Center (Poland), PRELUDIUM grant no. 2021/41/N/ST4/04020. Project Title: *New Thrombospondin-1-deriving Peptides as TGF-β Activators of Cosmeceutical Interest*. Role: Principal Investigator.

Awards and scholarships

1. October 2022: The Wroclaw University of Science and Technology (Faculty of Chemistry) pro-quality scholarship for preeminent PhD Students of the Department (one-year scholarship)

2. June 2022: XVIII Polish Seminary for Students "Na Pograniczu Chemii i Biologii", Smardzewice (Poland). The Lodz University of Technology Rector's Award for the outstanding conference oral presentation for *Peptides and Peptidomimetics with Anti-aging Properties as Cosmeceutical Agents*

3. May 2022: The Wroclaw University of Science and Technology, Faculty of Chemistry Dean's Conference Participation Grant (XVIII Polish Seminary for Students "Na Pograniczu Chemii i Biologii")

4. April 2022: 36th European Peptide Symposium and 12th International Peptide Symposium Organizing Committee, Registration Fee Waivers – Conference Participation Grant

5. November 2021: The Wroclaw University of Science and Technology (Faculty of Chemistry) pro-quality scholarship for preeminent PhD Students of the Department (one-year scholarship)

6. November 2021: The Wroclaw University of Science and Technology Rector's Scholarship for preeminent PhD Students (one-year scholarship)

7. November 2021: The Wroclaw University of Science and Technology Rector's Award for scientific activity in 2020/21

8. April 2021: The Wroclaw University of Science and Technology Own Fund Scholarship (*Własny Fundusz PWr*)

9. May 2019: XVII Polish Seminary for Students "Na Pograniczu Chemii i Biologii", Jastrzębia Góra (Poland). The Award for one of the best conference oral presentations for *Serpins' role in skin treatment: structure, active fragments and mechanism of inhibition*

Conference communications

Oral presentations

1. 12-15.06.2022: XVIII Polish Seminary for Students "Na Pograniczu Chemii i Biologii", Smardzewice (Poland). **P. Ledwoń**, K. Hałdys, W. Goldeman, A.M. Papini, P. Rovero, R. Latajka *Peptides and Peptidomimetics with Anti-aging Properties as Cosmeceutical* Agents (awarded, presenting author, ENG)

2. 16.02.2022: Seminarium *Od teorii do eksperymentu: rola oddziaływań molekularnych w samoorganizacji cząsteczek*, Wrocław (Poland). **P. Ledwoń**, K. Hałdys, W. Goldeman, A.M. Papini, P. Rovero, R. Latajka *Peptydomimetyki jako inhibitory enzymów o potencjalnym zastosowaniu w kosmeceutyce* (presenting author, PL)

3. 23-17.09.2021: 63. Zjazd Naukowy Polskiego Towarzystwa Chemicznego, Łódź (Poland). **P. Ledwoń**, C. Bello, A.M. Papini, P. Rovero, R. Latajka *Synthesis and Structural Investigations of Novel Peptidomimetics with Elastase Inhibitory Properties* (presenting author, ENG)

4. 24-25.06.2021: ChemBiotIC (Chemistry & Biotechnology International Conference), Wrocław (Poland). **P. Ledwoń**, C. Bello, A.M. Papini, P. Rovero, R. Latajka *Design, Synthesis and Structural Investigations of Novel Peptide-Based Elastase Inhibitors with Fluorescent Properties* (presenting author, ENG)

5. 17-19.11.2020: IV Doctoral Forum, Jan Kochanowski University, Kielce (Poland). **P. Ledwoń**, C. Bello, A.M. Papini, P. Rovero, R. Latajka *Design, synthesis and biological investigation of new peptides and peptidomimetics preventing skin damage* (presenting author, ENG)

6. 8-12.09.2019: 25th Polish Peptide Symposium, Wojanów (Poland). M. Kijewska, F. Nuti, M. Wierzbicka, M. Waliczek, **P. Ledwoń**, A. Staśkiewicz, T. Koch, F. Real-Fernandez, G. Sabatino, P. Rovero, P. Stefanowicz, Z. Szewczuk, A.M. Papini *The novel Boronic-ChemMatrix Resin to selectively fish out deoxyfructosylated peptides* (co-author, ENG)

7. 12-15.05.2019: XVII Polish Seminary for Students "Na Pograniczu Chemii i Biologii", Jastrzębia Góra (Poland). **P. Ledwoń**, F. Errante, M. Jewgiński, P. Rovero, R. Latajka *Serpins' role in skin treatment: structure, active fragments and mechanism of inhibition* (awarded, presenting author, ENG)

Poster communications

1. 28.08-2.09.2022: 36th European Peptide Symposium and 12th International Peptide Symposium, Sitges (Spain). **P. Ledwoń**, P. Rovero, R. Latajka *New Thrombospondin-1-deriving Peptides as TGF-β Activators of Cosmeceutical Interest* (presenting author, ENG) (concerning *Preludium* grant)

2. 16-18.06.2022: 17th Naples Workshop on Bioactive Peptides, Naples (Italy). **P. Ledwoń**, P. Rovero, R. Latajka *Design, Synthesis, and Biological Investigations of New TSP-1 deriving Peptides as TGF-β Activators* (presenting author, ENG) (concerning *Preludium* grant)

3. 11-14.05.2022: X Congress of Chemical Technology, Wrocław (Poland). **P. Ledwoń**, K. Hałdys, W. Goldeman, A.M. Papini, P. Rovero, R. Latajka *Peptydowe inhibitory enzymów do zastosowań w przemyśle kosmeceutycznym* (co-author, PL)

4. 8-12.09.2019: 25th Polish Peptide Symposium, Wojanów (Poland). **P. Ledwoń**, F. Errante, M. Jewgiński, P. Rovero, R. Latajka *Serpins' role in skin treatment: structure, active fragments and mechanism of inhibition* (presenting author, ENG)

Supplementary information

Supplementary information for this thesis, including additional tables, spectra, and the analytical data of obtained products, was prepared as a PDF file and saved on CD, which is an integral part of the dissertation. The CD can be found inside the cover of the printed version of the thesis.

Acknowledgements

DESIGN, SYNTHESIS, AND BIOLOGICAL INVESTIGATION
OF NEW PEPTIDES AND PEPTIDOMIMETICS
OF COSMECEUTICAL INTEREST

Supplementary Information

DOCTORAL DISSERTATION
Patrycja Ledwoń

Supervisors:

Prof. Rafał Latajka
Wroclaw University of Science and Technology
Faculty of Chemistry
Department of Bioorganic Chemistry

Prof. Paolo Rovero
University of Florence
Department of NEUROFARBA
Interdepartmental Research Unit of Peptide and Protein Chemistry and Biology

Thesis in cotutelle prepared in the framework of the collaboration between
Wroclaw University of Science and Technology
and University of Florence (XXXV Ciclo)

February 2023

TABLE OF CONTENTS

LIST OF FIGURES

LIST OF TABLES

LIST OF DISCUSSED COMPOUNDS*

A	–	4-Methylpiperidine
B	–	Pyrrolidine
C	–	Morpholine
D	–	*N*-Ethylisopropylamine
1	–	Potassium cyanohydroxyamate
2	–	*N*-hydroxy-3-(hydroxyamino)-3-iminopropanamide
3	–	4,6-dimethylisoxazolo[3,4-*b*]pyridin-3(1*H*)-one
4	–	8-carboxy-4',5,7-trimethyl-3H-2λ^5-spiro[[1,2,4]triazolo[4,3-a]pyridine-2,1'-piperidin]-2-ylium (derivative with **A**)
4a	–	Fmoc-Lys[N$^\varepsilon$**(4)**]-OH
5	–	8-carboxy-5,7-dimethyl-3*H*-2λ^5-spiro[[1,2,4]triazolo[4,3-*a*]pyridine-2,1'-pyrrolidin]-2-ylium (derivative with **B**)
5a	–	Fmoc-Lys[N$^\varepsilon$**(5)**]-OH
6	–	8-carboxy-5,7-dimethyl-3*H*-2λ^5-spiro[[1,2,4]triazolo[4,3-a]pyridine-2,4'-morpholin]-2-ylium (derivative with **C**)
6a	–	Fmoc-Lys[N$^\varepsilon$**(6)**]-OH
7	–	8-carboxy-2-ethyl-5,7-dimethyl-2-(propan-2-yl)-2*H*,3*H*-[1,2,4]triazolo[4,3-*a*]pyridin-2-ium (derivative with **D**)
7a	–	Fmoc-Lys[N$^\varepsilon$**(7)**]-OH
8	–	Ac-MGKVV-NH$_2$
9	–	Ac-PGKVV-NH$_2$
10	–	**3**-PGKVV-NH$_2$
11	–	**4**-MGKVV-NH$_2$
12	–	**5**-MGKVV-NH$_2$
13	–	**6**-MGKVV-NH$_2$
14	–	**7**-MGKVV-NH$_2$
15	–	**4**-PGKVV-NH$_2$
16	–	**5**-PGKVV-NH$_2$
17	–	**6**-PGKVV-NH$_2$
18	–	**7**-PGKVV-NH$_2$
19	–	Ac-MGK[N$^\varepsilon$**(4)**]VV-NH$_2$
20	–	Ac-MGK[N$^\varepsilon$**(5)**]VV-NH$_2$
21	–	Ac-MGK[N$^\varepsilon$**(6)**]VV-NH$_2$
22	–	Ac-MGK[N$^\varepsilon$**(7)**]VV-NH$_2$
23	–	Ac-PGK[N$^\varepsilon$**(4)**]VV-NH$_2$
24	–	Ac-PGK[N$^\varepsilon$**(5)**]VV-NH$_2$
25	–	Ac-PGK[N$^\varepsilon$**(6)**]VV-NH$_2$
26	–	Ac-PGK[N$^\varepsilon$**(7)**]VV-NH$_2$
27-42	–	16 derivatives of (2*E*)-2-[1-(4-bromophenyl)ethylidene]hydrazine-1-carbothioamide
43	–	4-[(*E*)-(2-carbamothioylhydrazinylidene)methyl]benzoic acid
44	–	2-{3-[(*E*)-(2-carbamothioylhydrazinylidene)(phenyl)methyl]phenyl}propanoic acid
45	–	4-[(1*E*)-1-(2-carbamothioylhydrazinylidene)ethyl]benzoic acid
46	–	Ac-FFY-OH
47	–	Ac-FYY-OH
48	–	Ac-FWY-OH
49	–	TSC**43**-FFY-OH
50	–	TSC**43**-FYY-OH
51	–	TSC**43**-FWY-OH
52	–	TSC**44**-FFY-OH
53	–	TSC**44**-FYY-OH
54	–	TSC**44**-FWY-OH
55	–	TSC**45**-FFY-OH
56	–	TSC**45**-FYY-OH
57	–	TSC**45**-FWY-OH

Compounds marked with gray background were purchased (A-D**) or provided (**27-45**).*
Other compounds were synthesized and purified by the Author for the purpose of this thesis.

Chapter 1: High Performance Liquid Chromatography (HPLC) and Mass Spectrometry (MS) – LC-MS
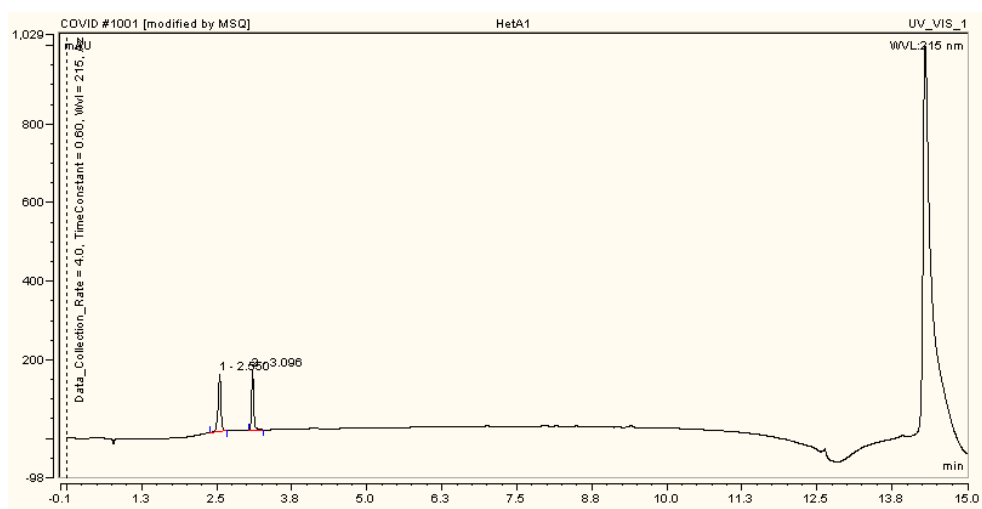
1.1 Analyses of compounds 4a-7a, 8-26
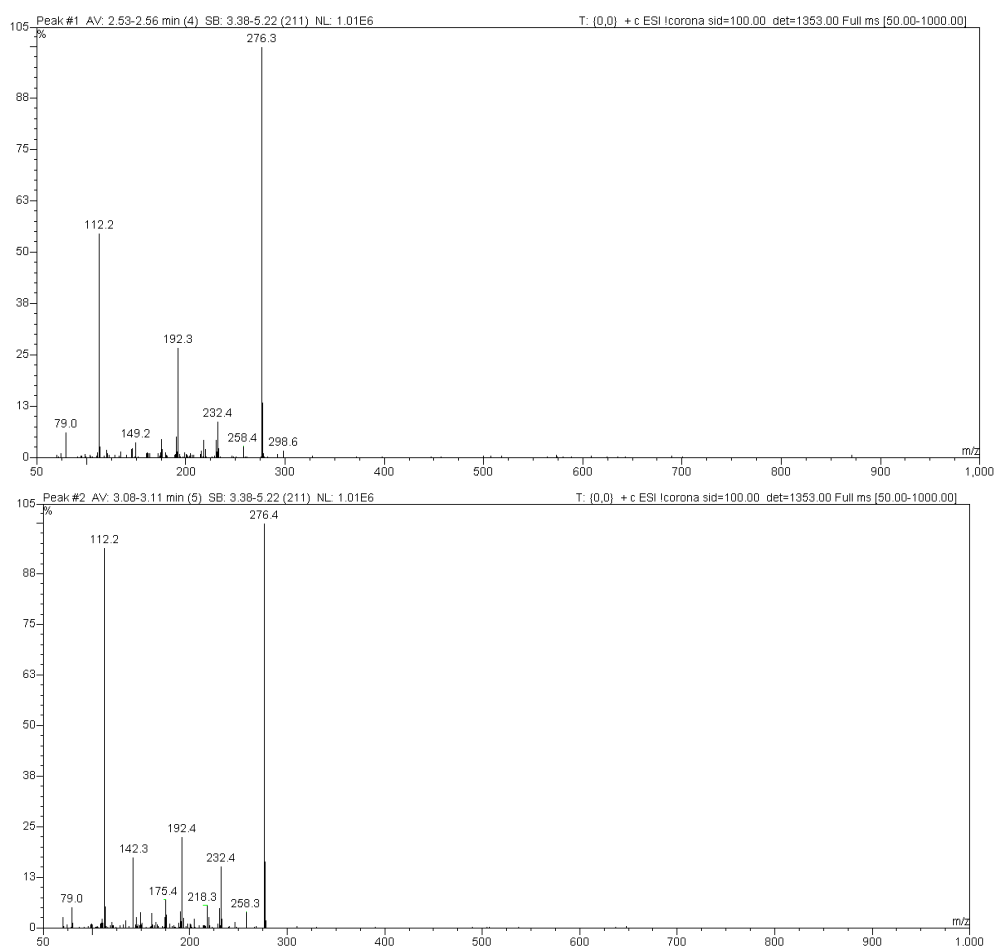

Figure SI 1. Chromatogram of **4** (crude product).

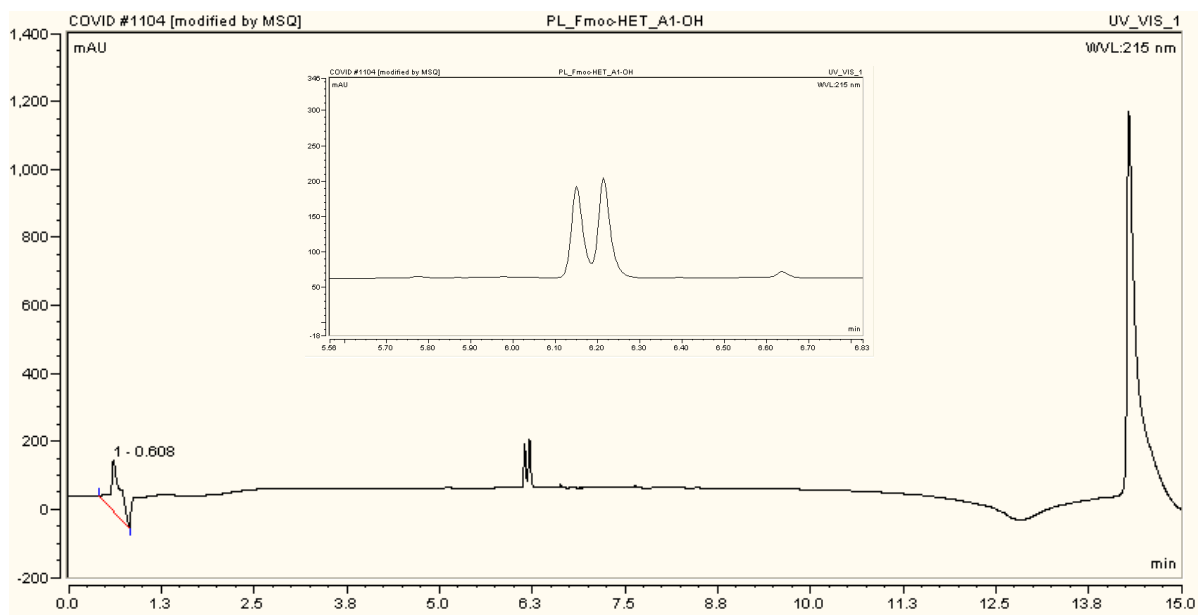**Figure SI 2.** MS spectra of **4** of two visible peaks: 2.53-2.56 and 3.08-3.11 min (crude product).

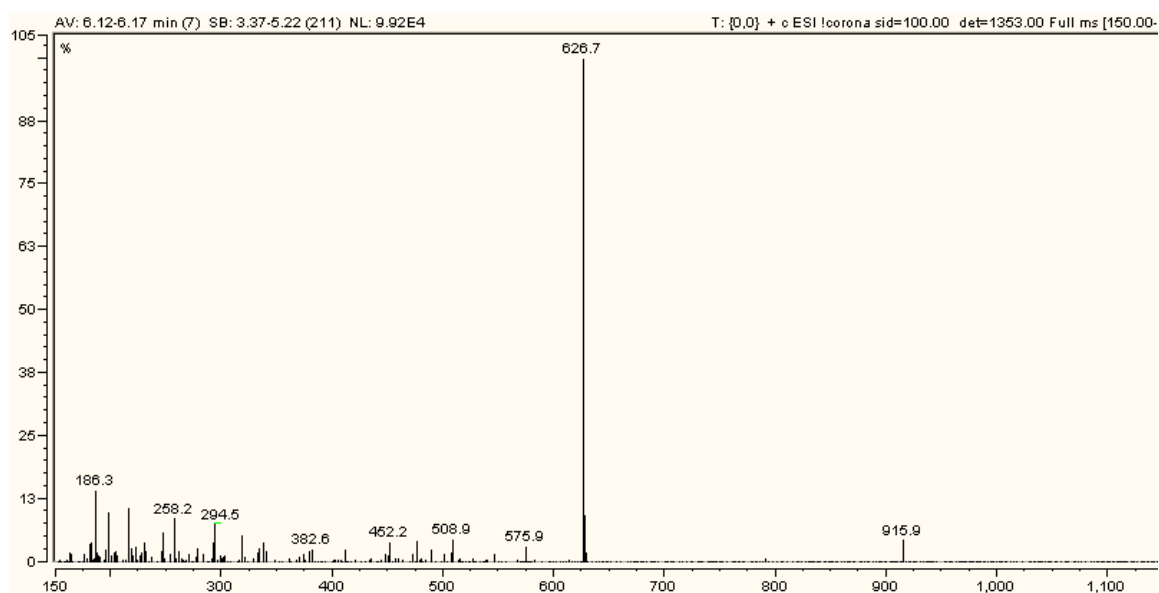**Figure SI 3.** Chromatogram of **4a** with zoomed 6.10-6.30 retention time (crude product).

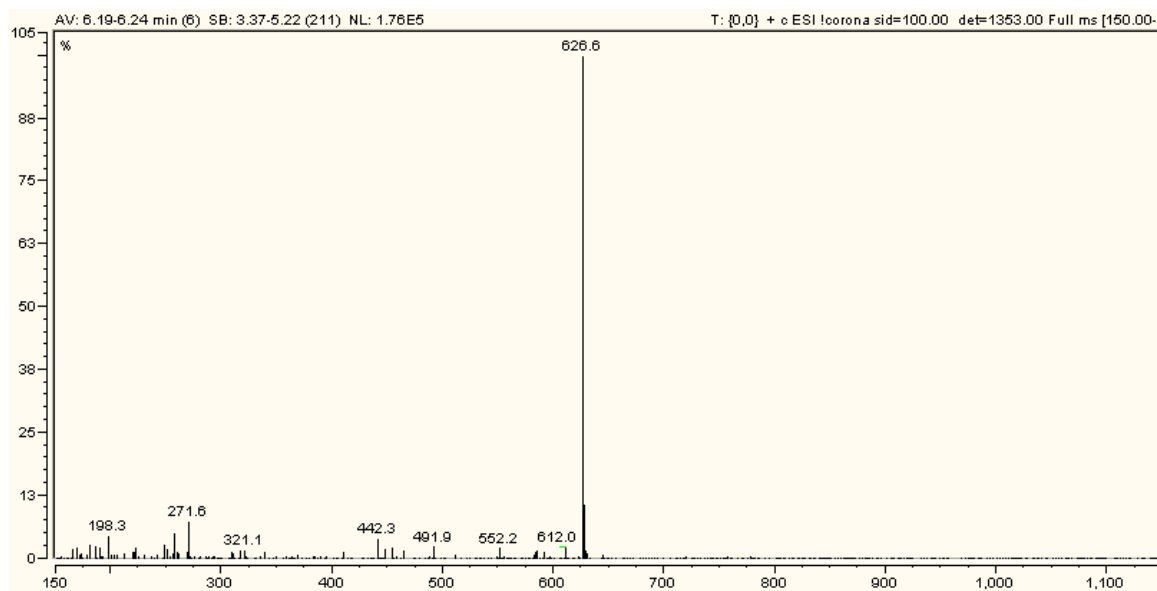**Figure SI 4.** MS spectra of **4a** of the peak 6.12-6.17 min (crude product).

Figure SI 5. MS spectra of **4a** of the peak 6.19-6.24 min (crude product).
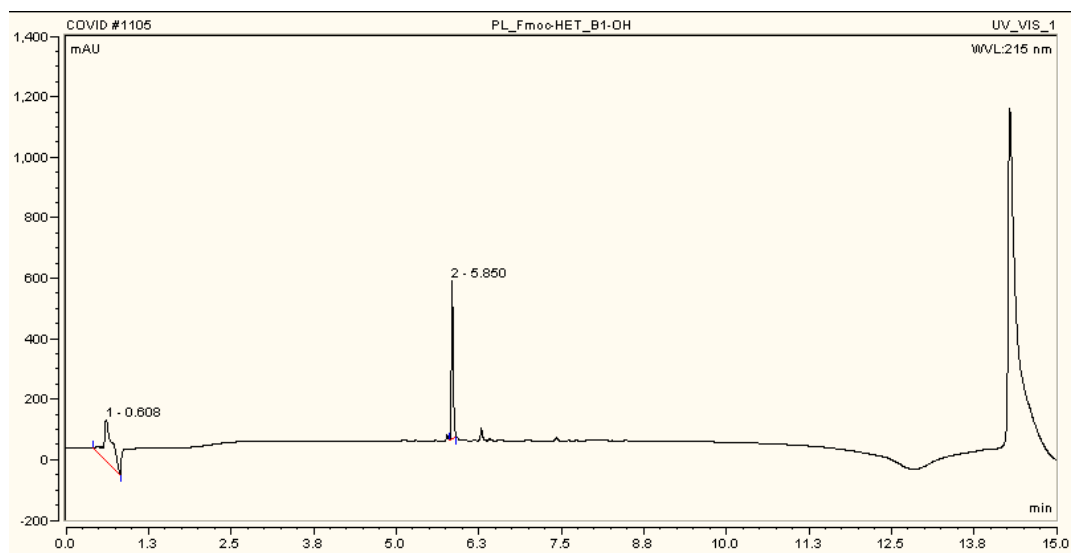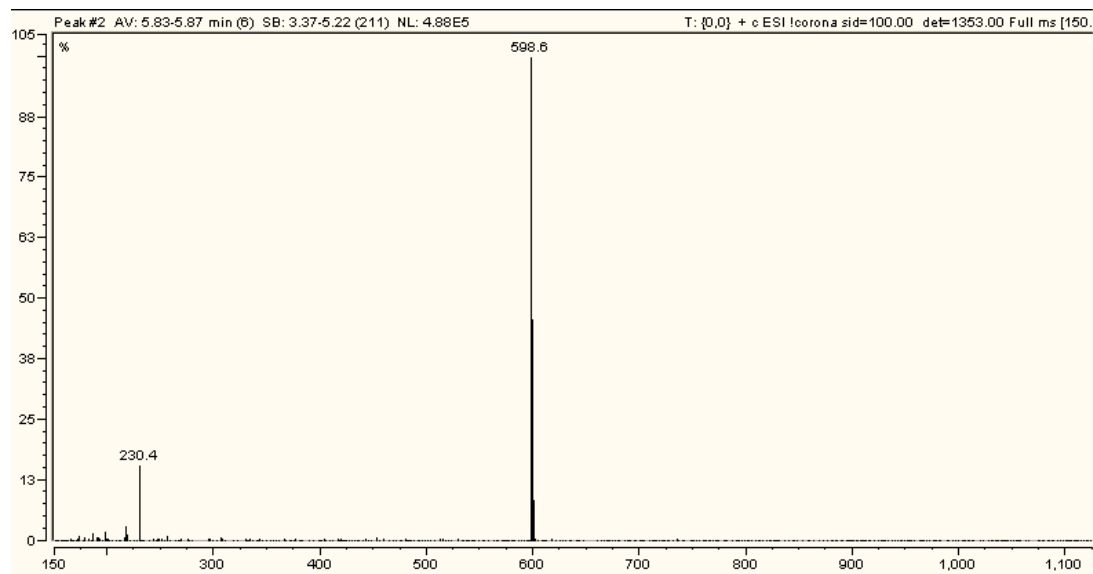

Figure SI 6. Chromatogram of **5a** (crude product).

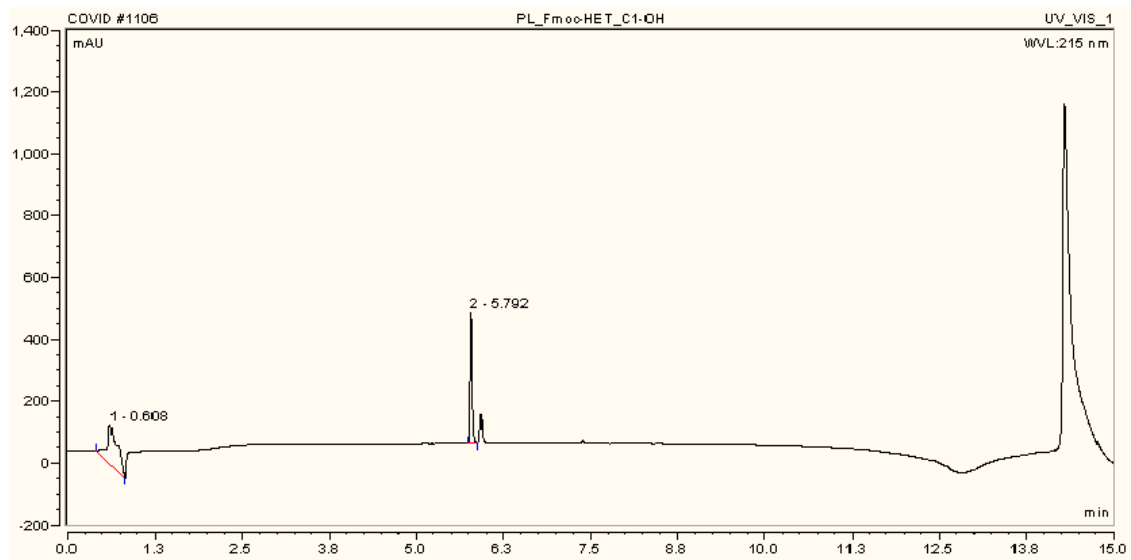**Figure SI 7.** MS spectra of **5a** of the peak 5.83-5.87 min (crude product).

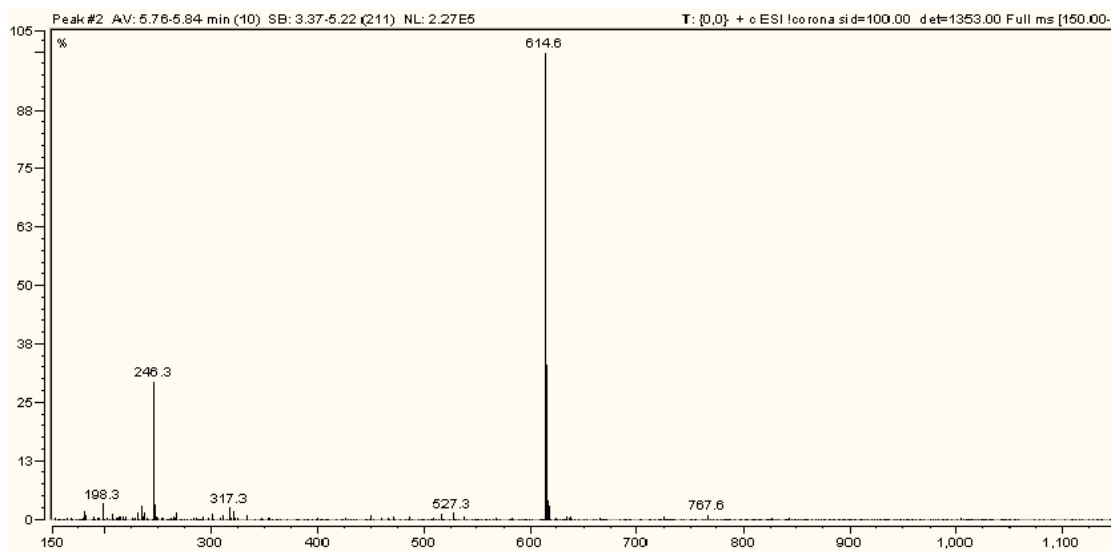**Figure SI 8.** Chromatogram of **6a** (crude product).

Figure SI 9. MS spectra of **6a** the peak 5.76-5.84 min (crude product).
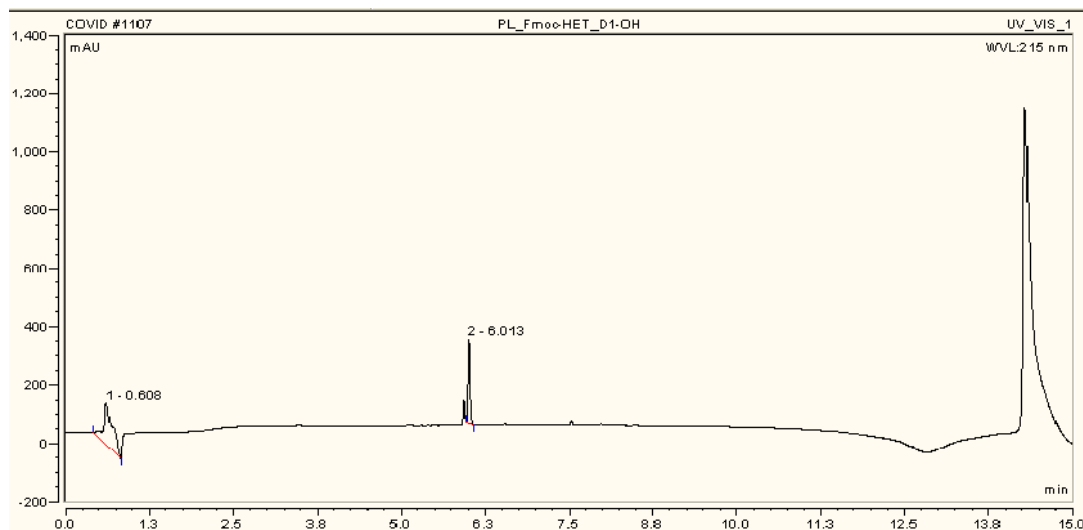

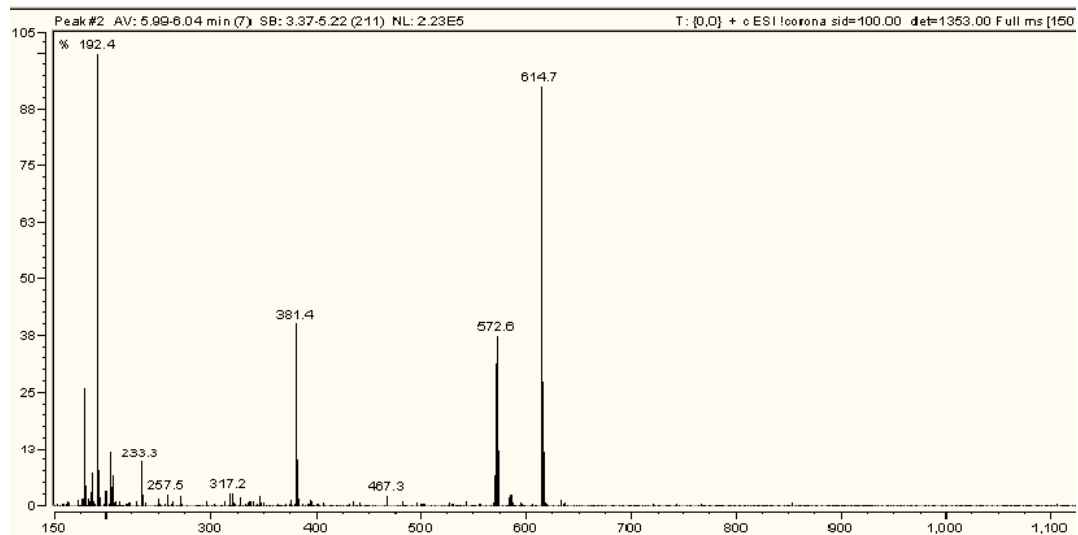**Figure SI 10.** Chromatogram of **7a** (crude product).

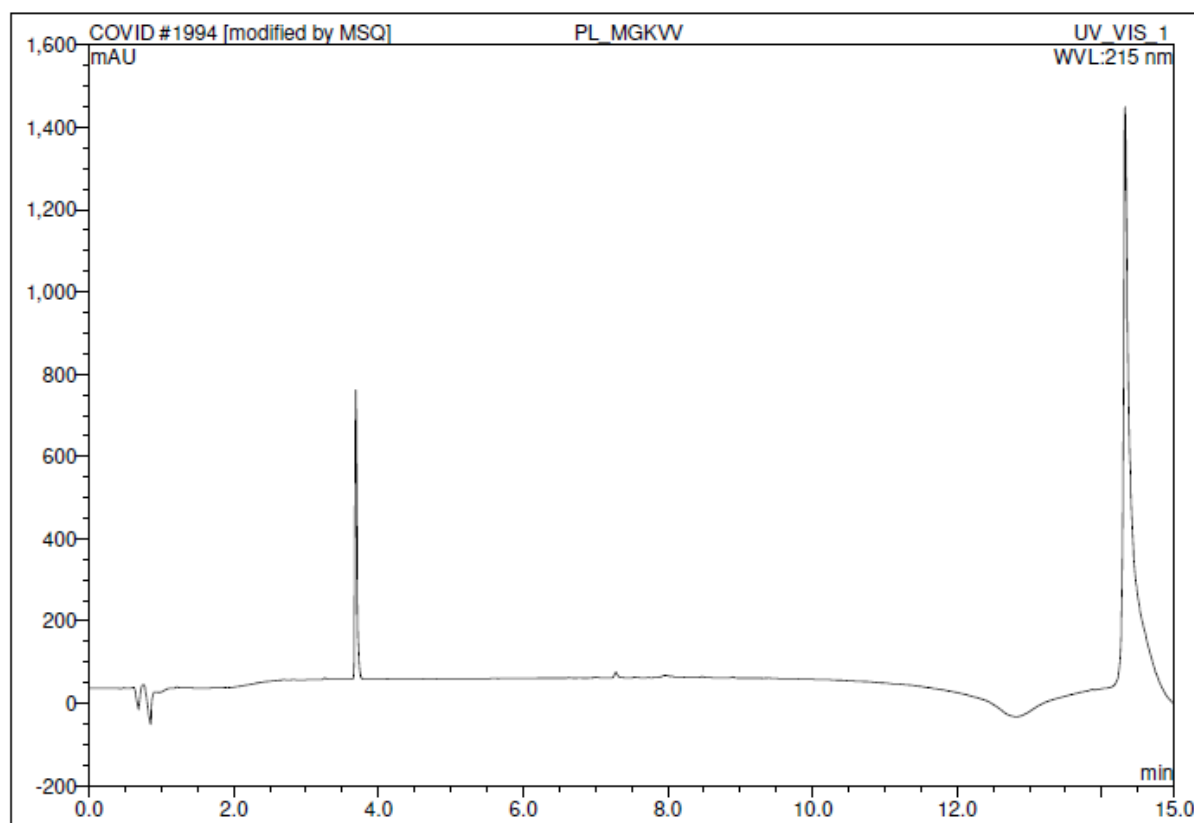**Figure SI 11.** MS spectra of **7a** of the peak 5.99-6.04 min (crude product).

Figure SI 12. Chromatogram of **8** (pure product).

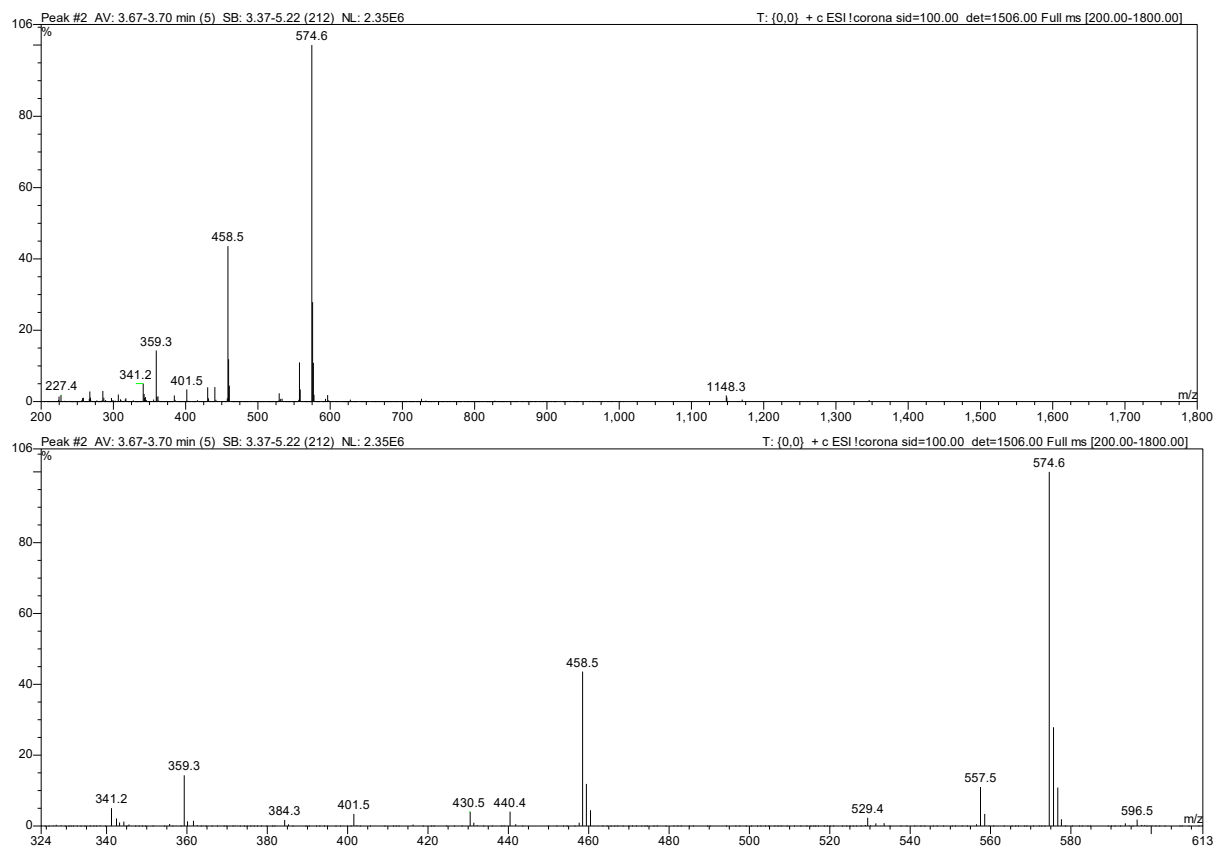**Figure SI 13.** MS spectra of **8** of the peak 3.67-3.70 min (pure product). Zoom on the range 324-613 *m/z* was shown additionally.

Figure SI 14. Chromatogram of **9** (pure product).

Figure SI 15. MS spectra of **9** of the peak 3.28-3.37 min (pure product). Zoom on the range 260-577 *m/z* was shown additionally.

Figure SI 16. Chromatogram of **10** (pure product).

Figure SI 17. MS spectra of **10** of the peak 4.45 min (pure product). Zoom on the range 671-709 *m/z* was shown additionally.

Figure SI 18. Chromatogram of **11** (pure product).

Figure SI 19. MS spectra of **11** of the peak 4.03 min (pure product).

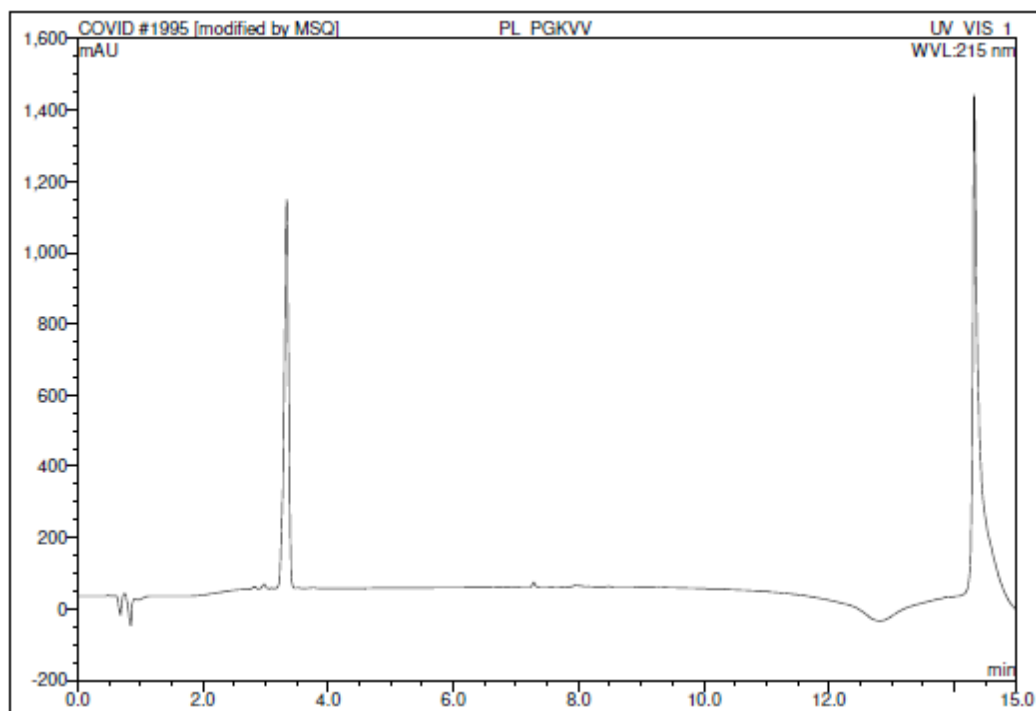**Figure SI 20.** MS spectra of **11** of the peak 4.17 min (pure product).
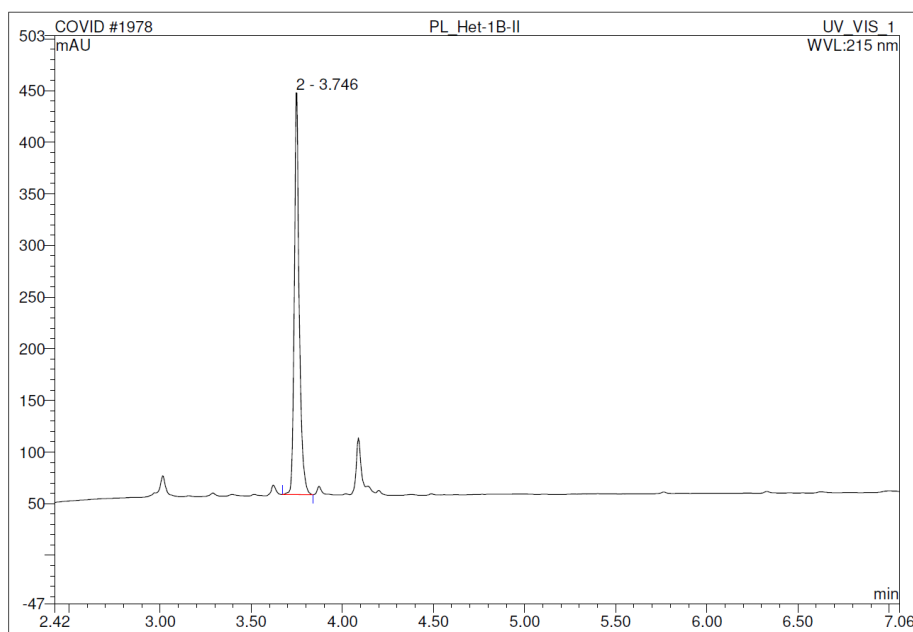
Figure SI 21. Chromatogram of **12** (pure product).
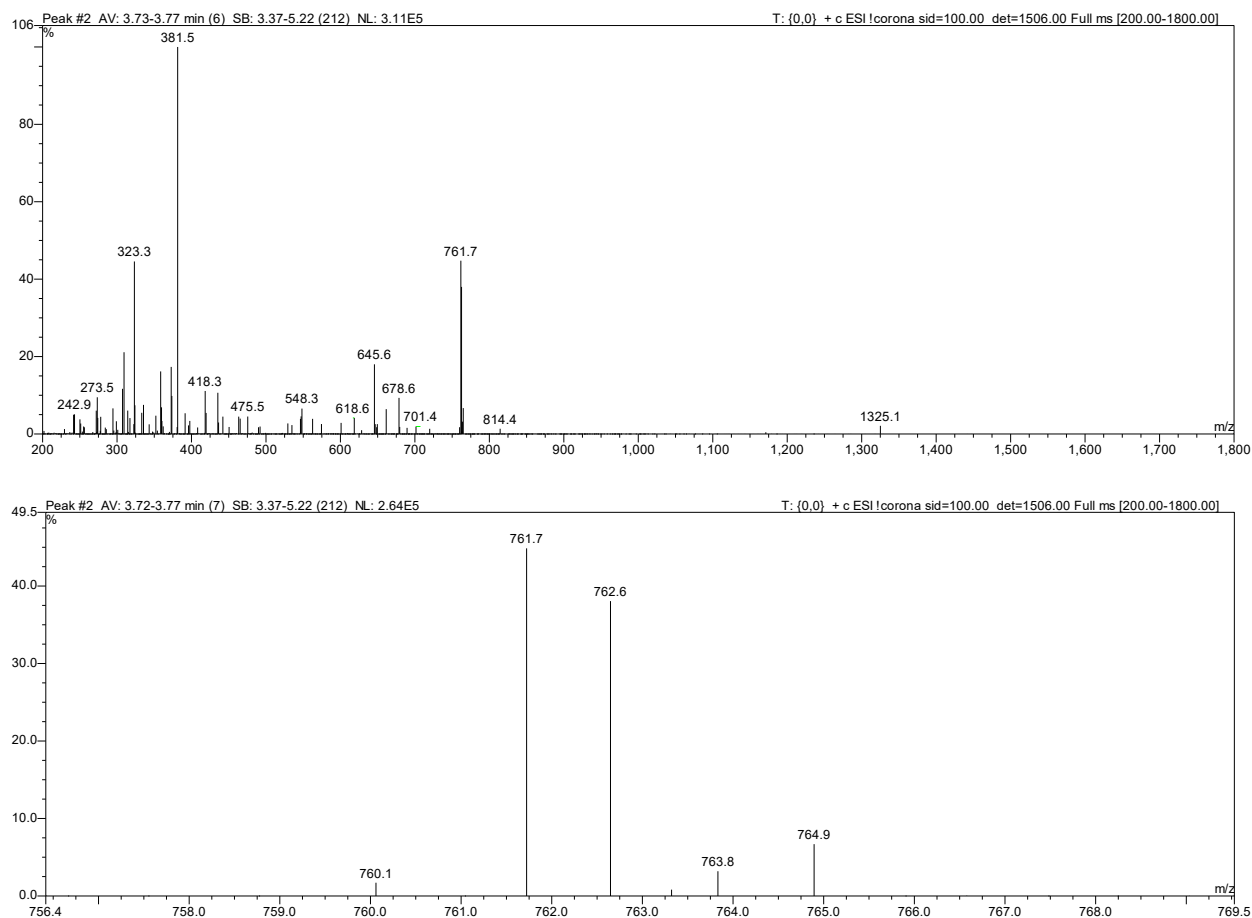
Figure SI 22. MS spectra of **12** of the peak 3.74 min (pure product). Zoom on the range 756-770 *m/z* was shown additionally.
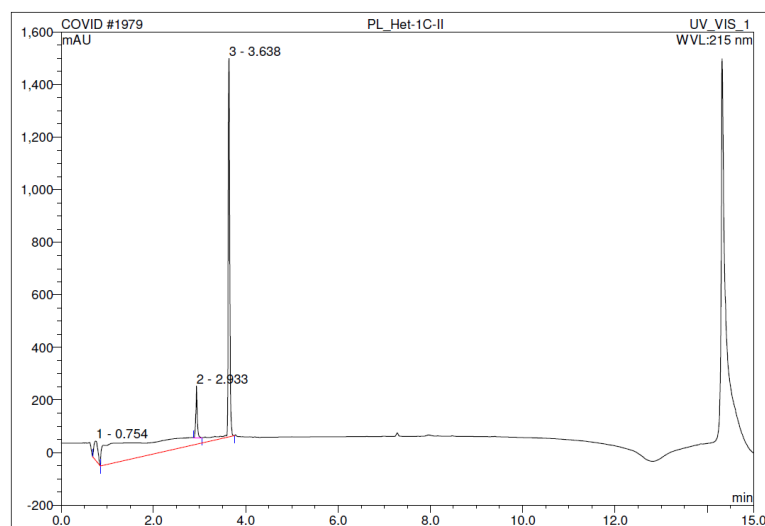
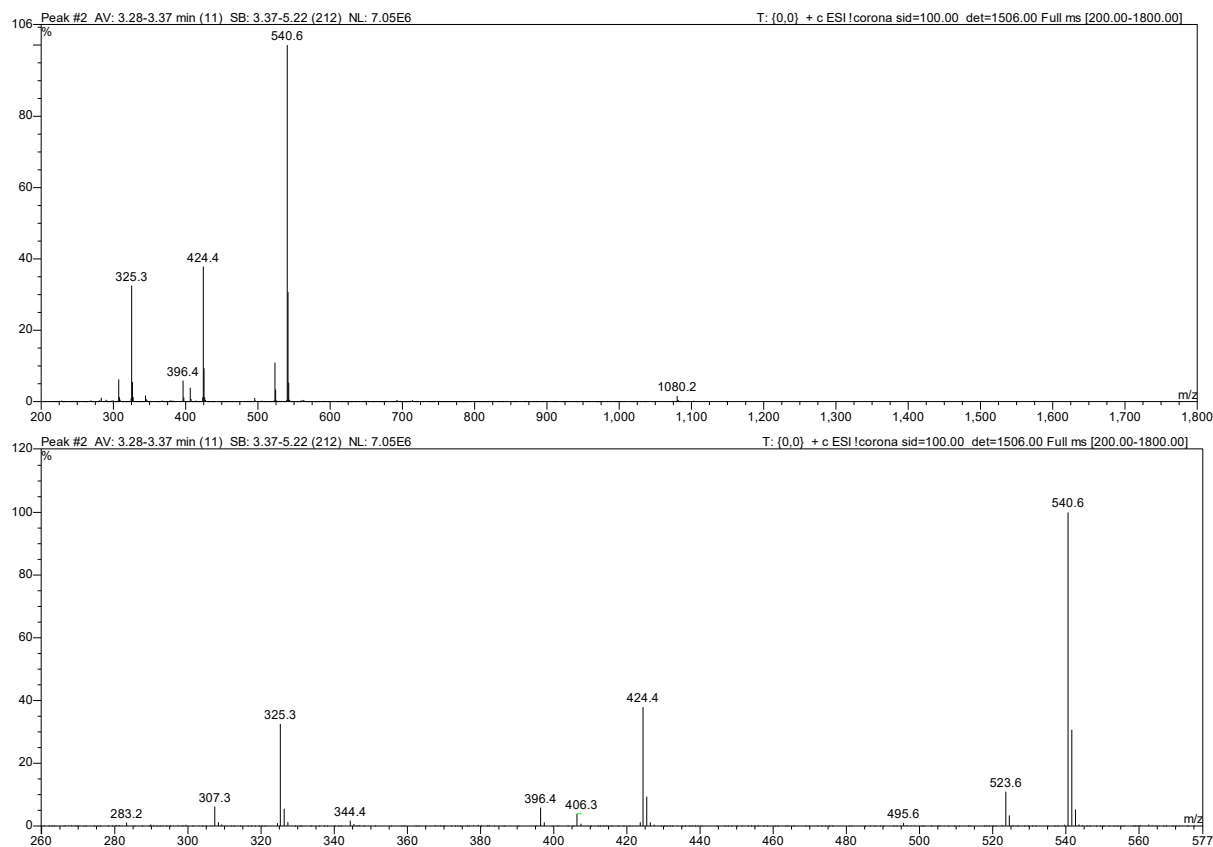**Figure SI 23.** Chromatogram of **13** (pure product).
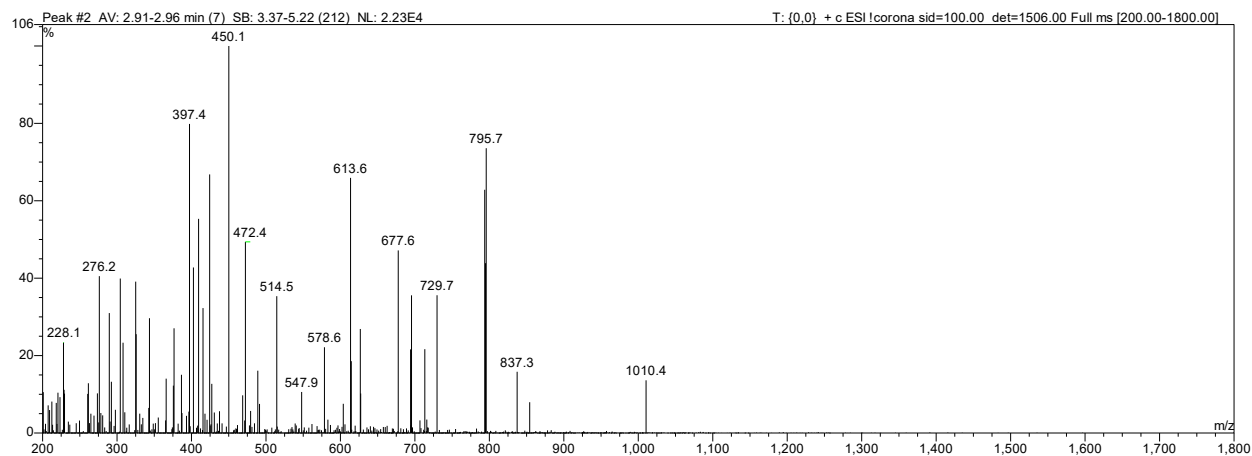
Figure SI 24. MS spectra of **13** of the peak 2.95 min (pure product).
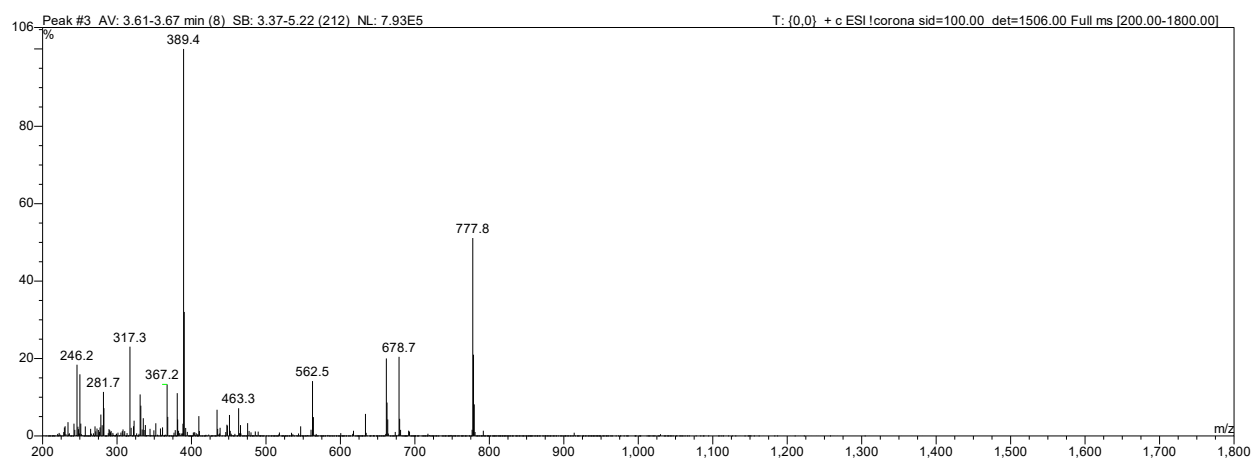
Figure SI 25. MS spectra of **13** of the peak 3.65 min (pure product). Zoom on the range 544-785 *m/z* was shown additionally.
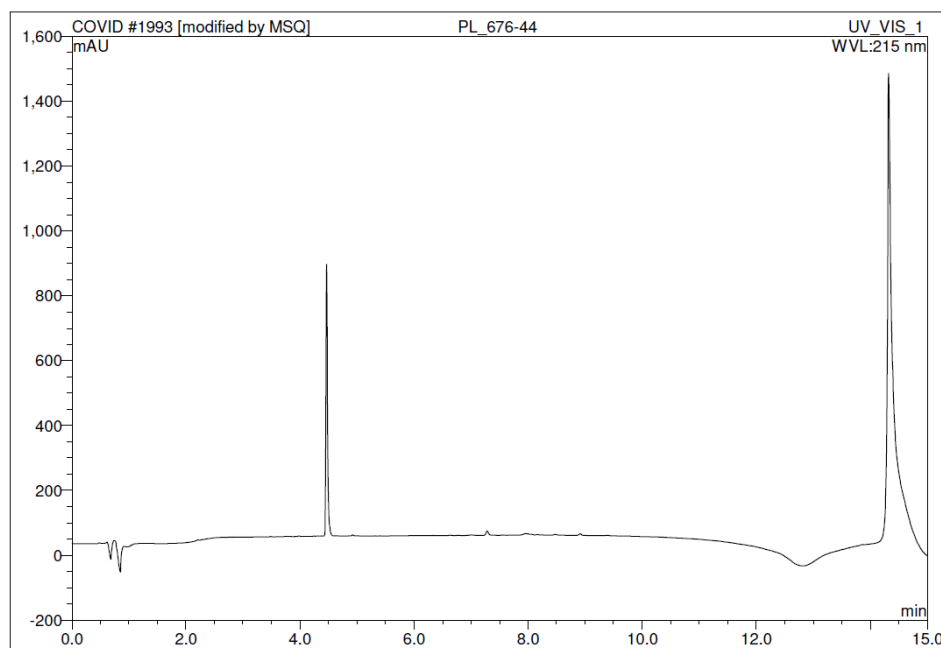

Figure SI 26. Chromatogram of **14** (pure product).

Figure SI 27. MS spectra of **14** of the peak 3.89 min (pure product). Zoom on the range 771-789 *m/z* was shown additionally.
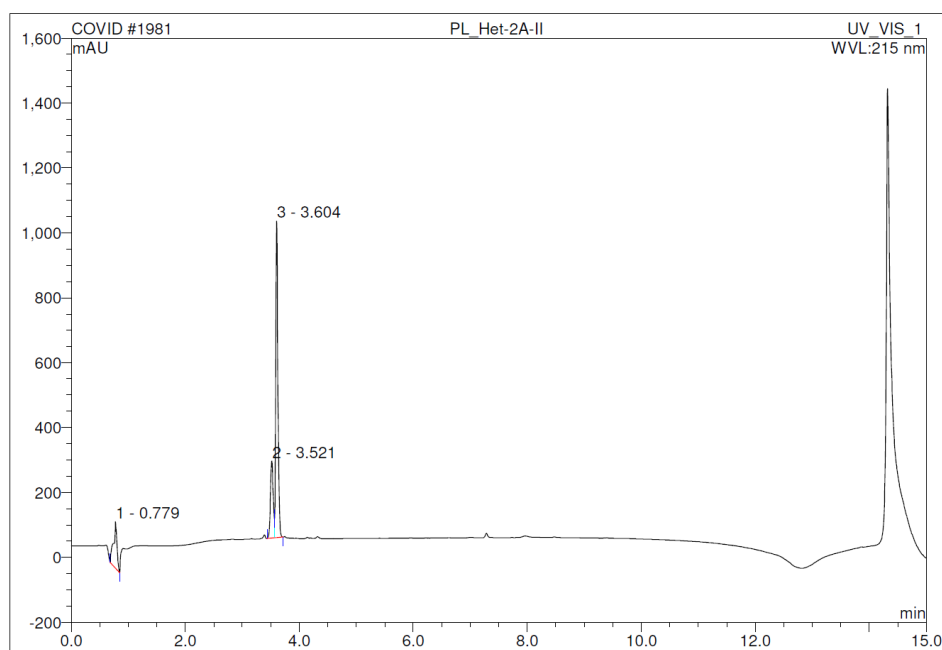
Figure SI 28. Chromatogram of **15** (pure product).
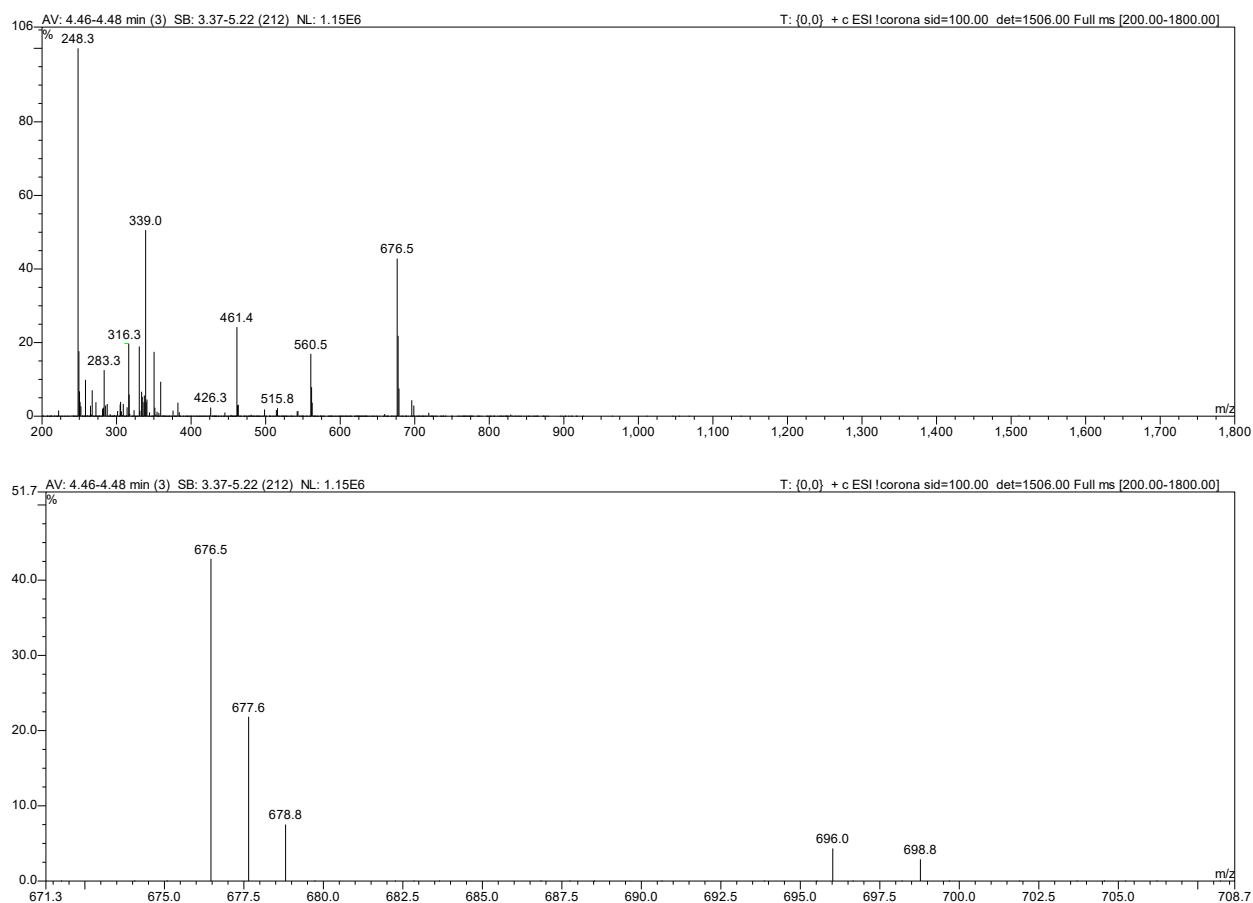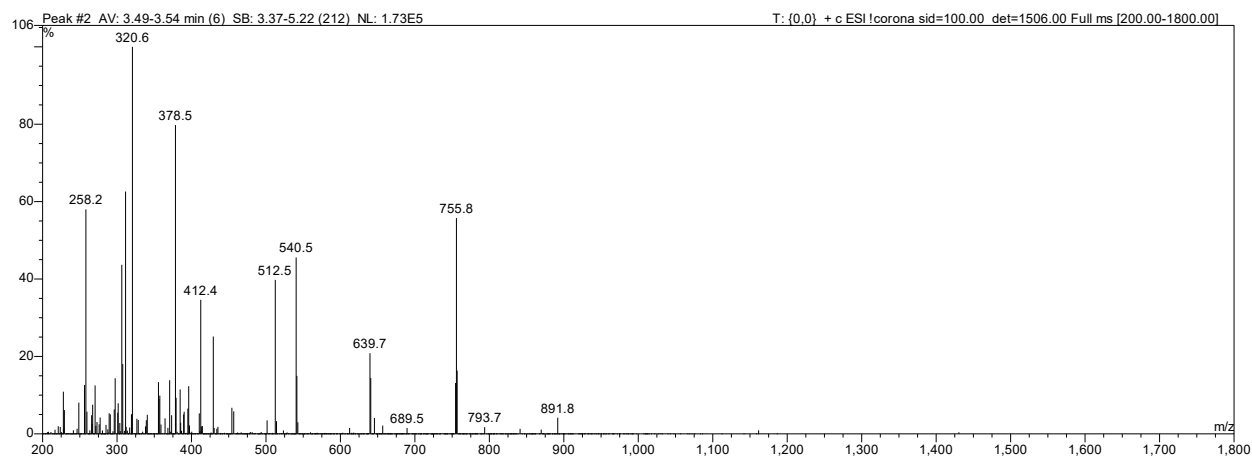
Figure SI 29. MS spectra of **15** of the peak 3.5 min (pure product).
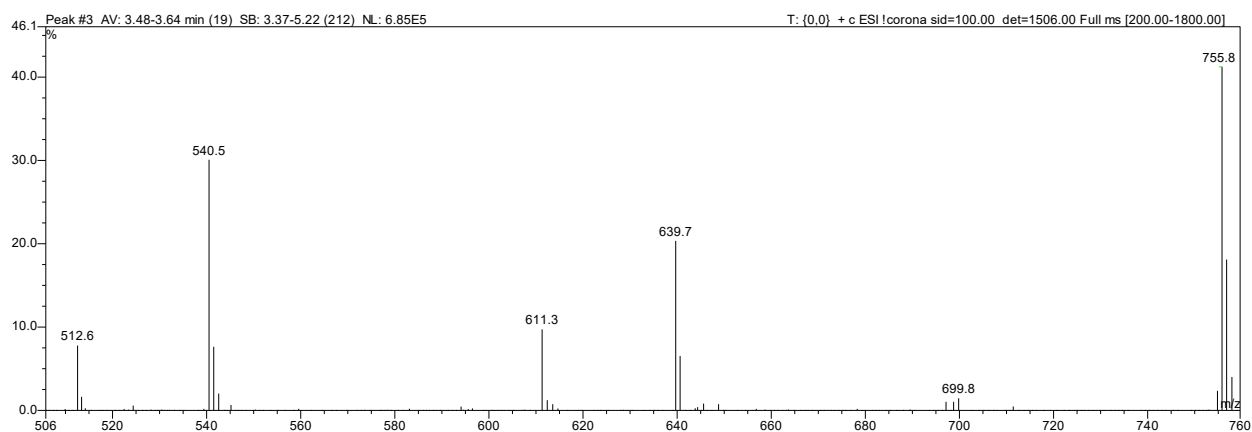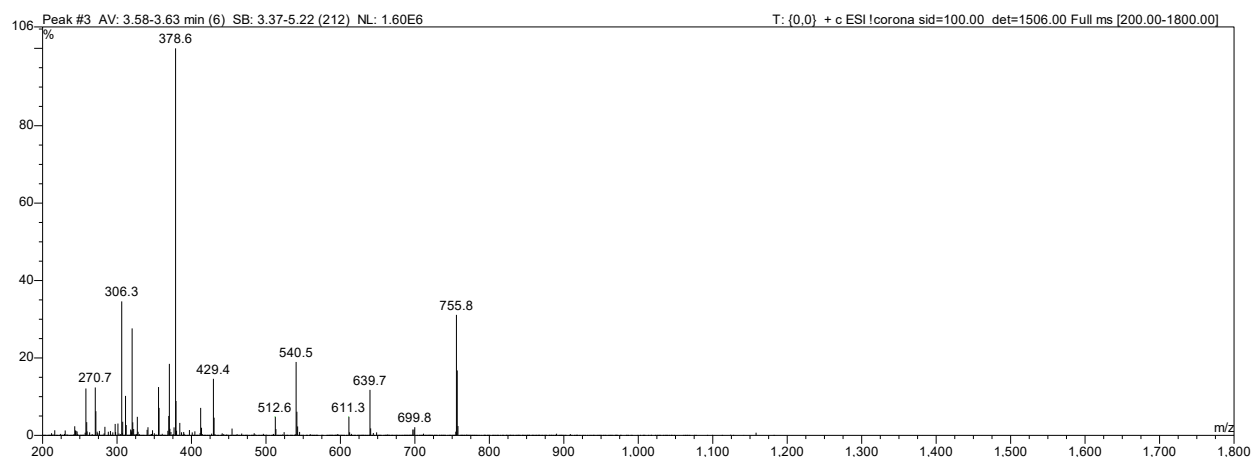
Figure SI 30. MS spectra of **15** of the peak 3.6 min (pure product). Zoom on the range 506-760 *m/z* was shown additionally.
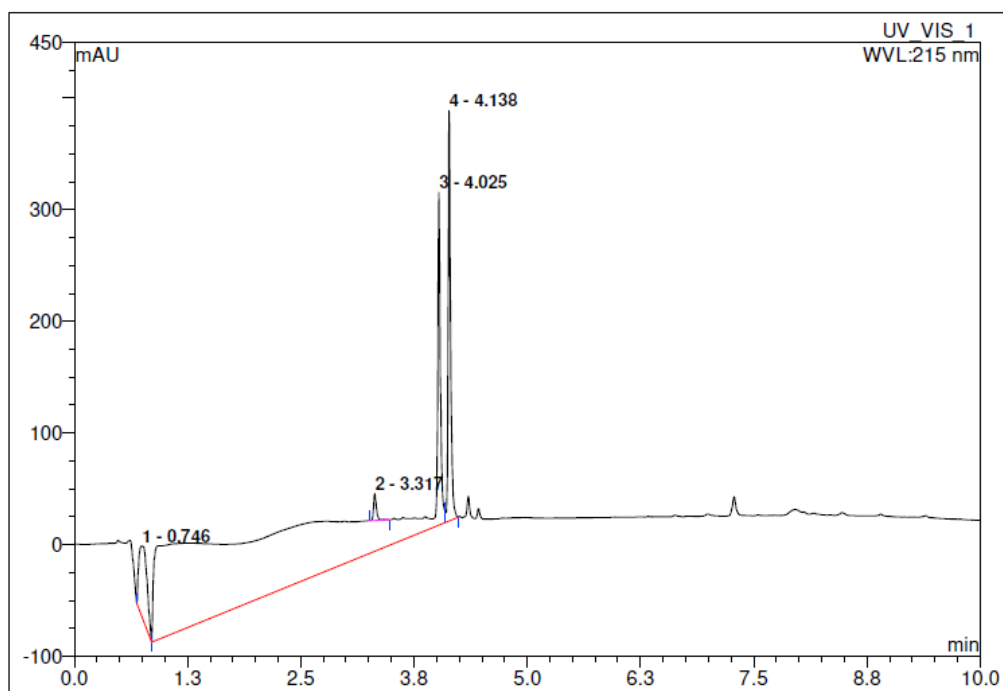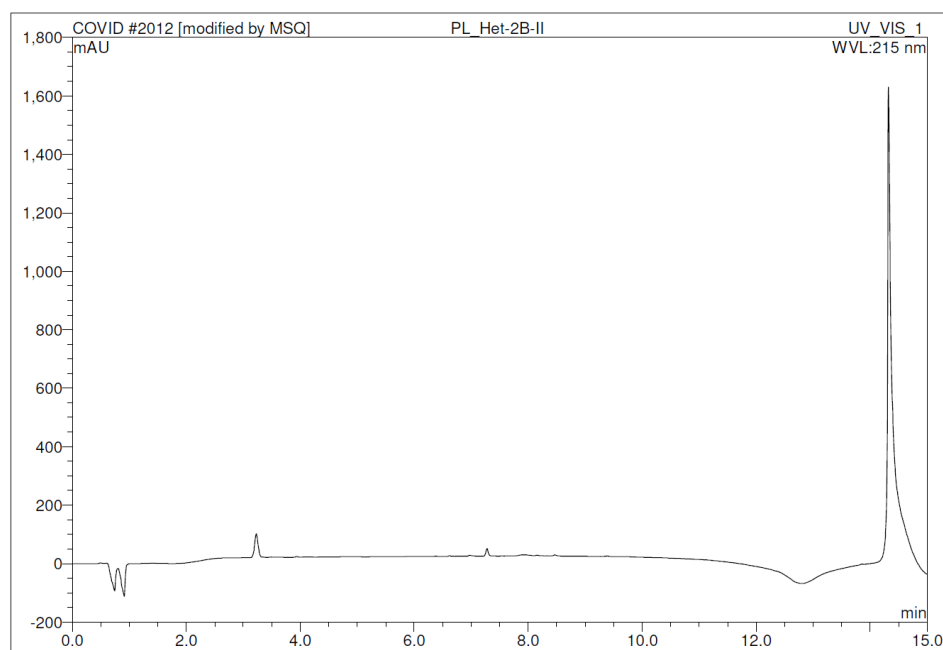
Figure SI 31. Chromatogram of **16** (pure product).
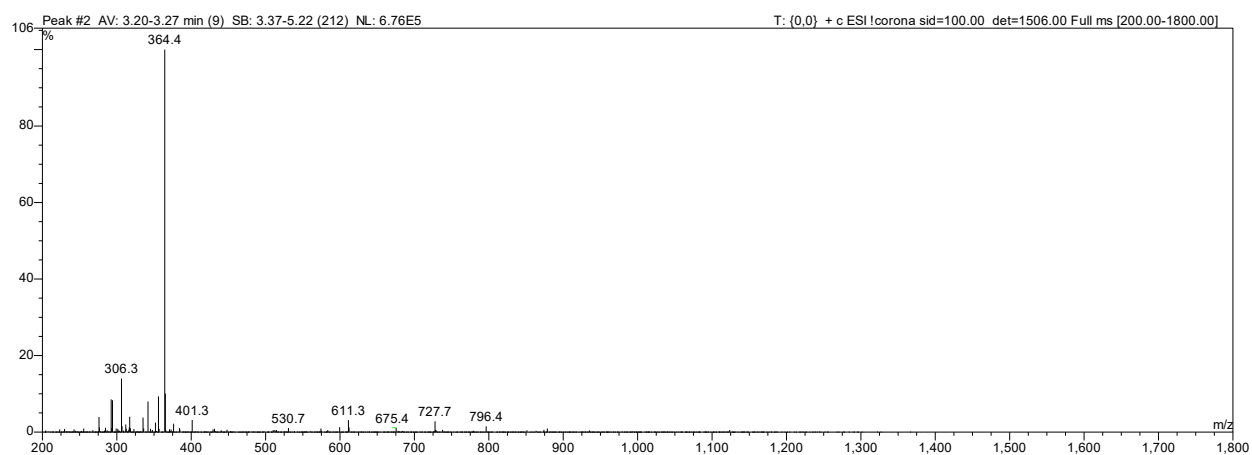
Figure SI 32. MS spectra of **16** of the peak 3.25 min (pure product).
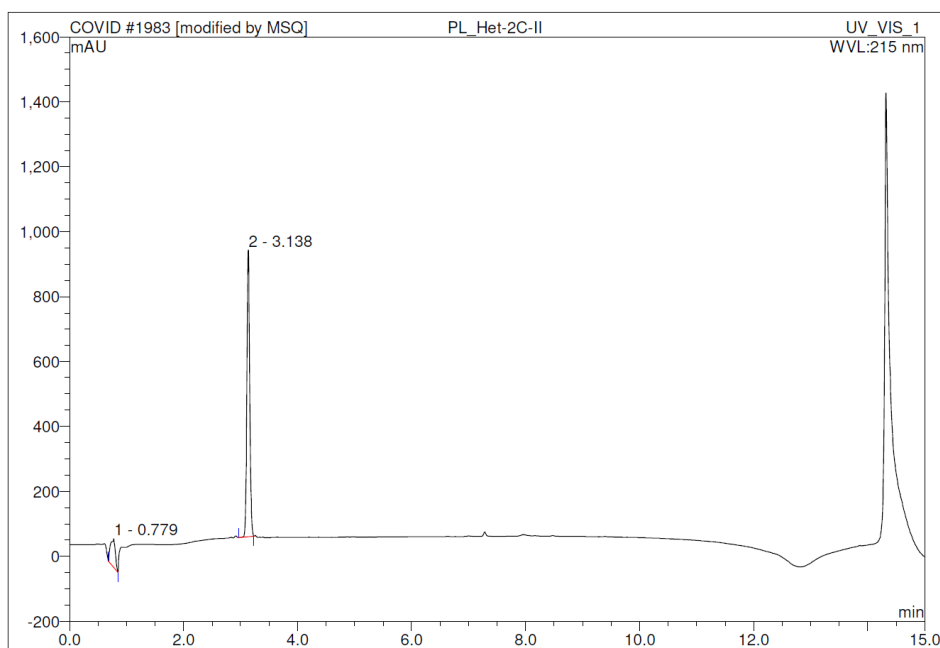
Figure SI 33. Chromatogram of **17** (pure product).
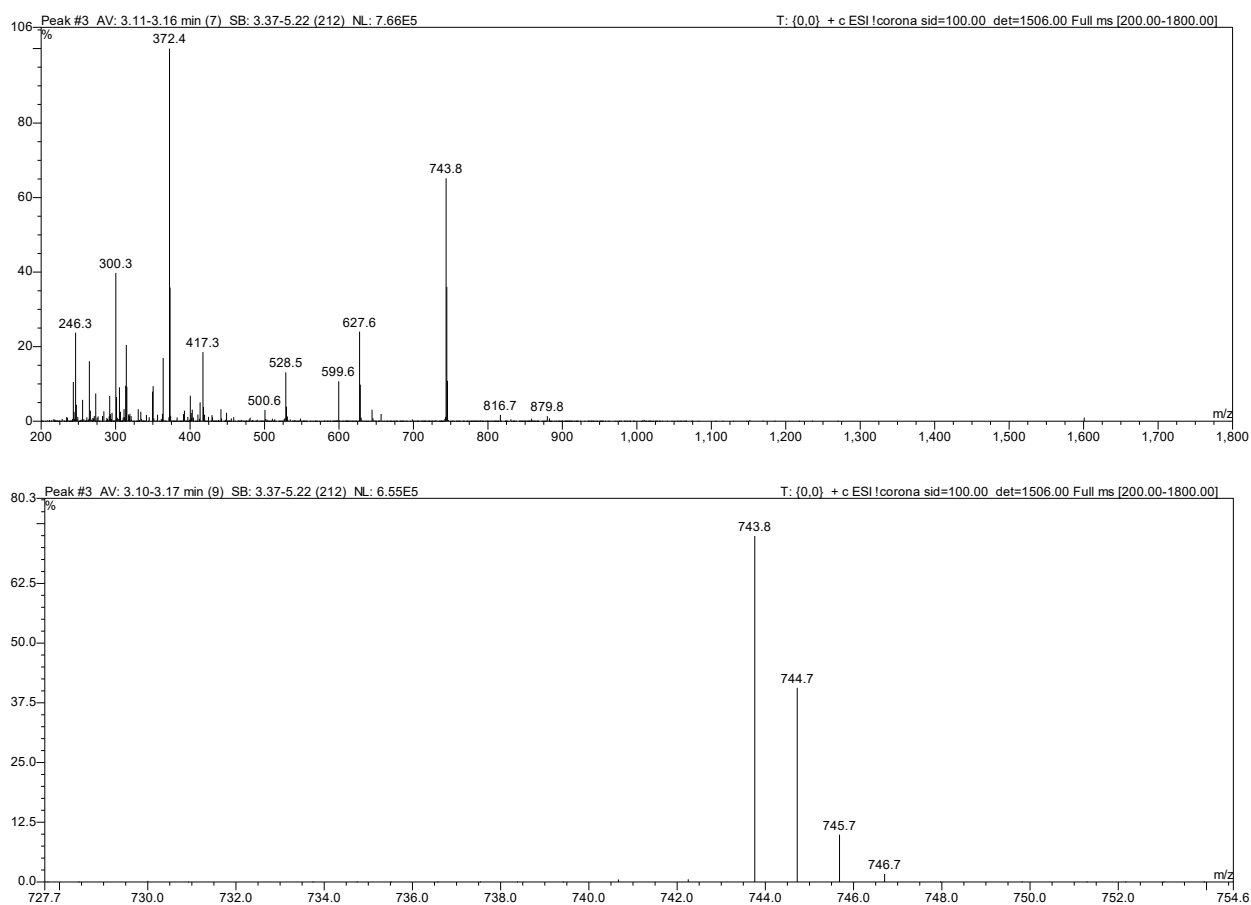
Figure SI 34. MS spectra of **17** of the peak 3.14 min (pure product). Zoom on the range 728-754 *m/z* was shown additionally.
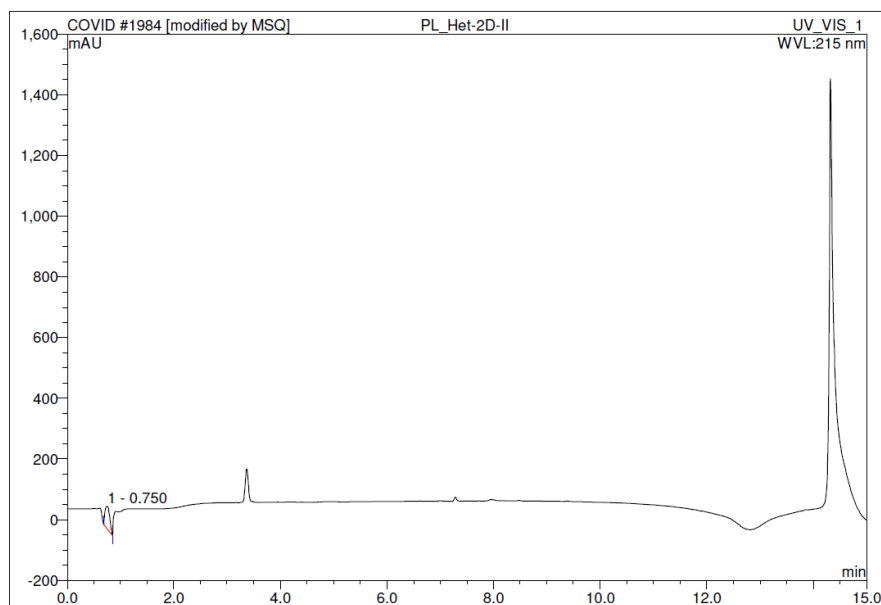
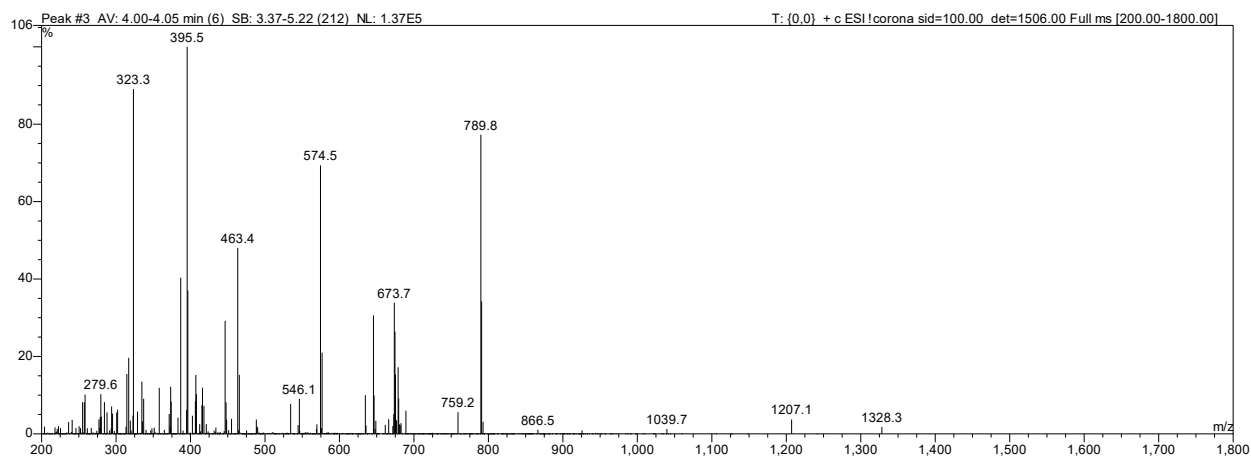**Figure SI 35.** Chromatogram of **18** (pure product).
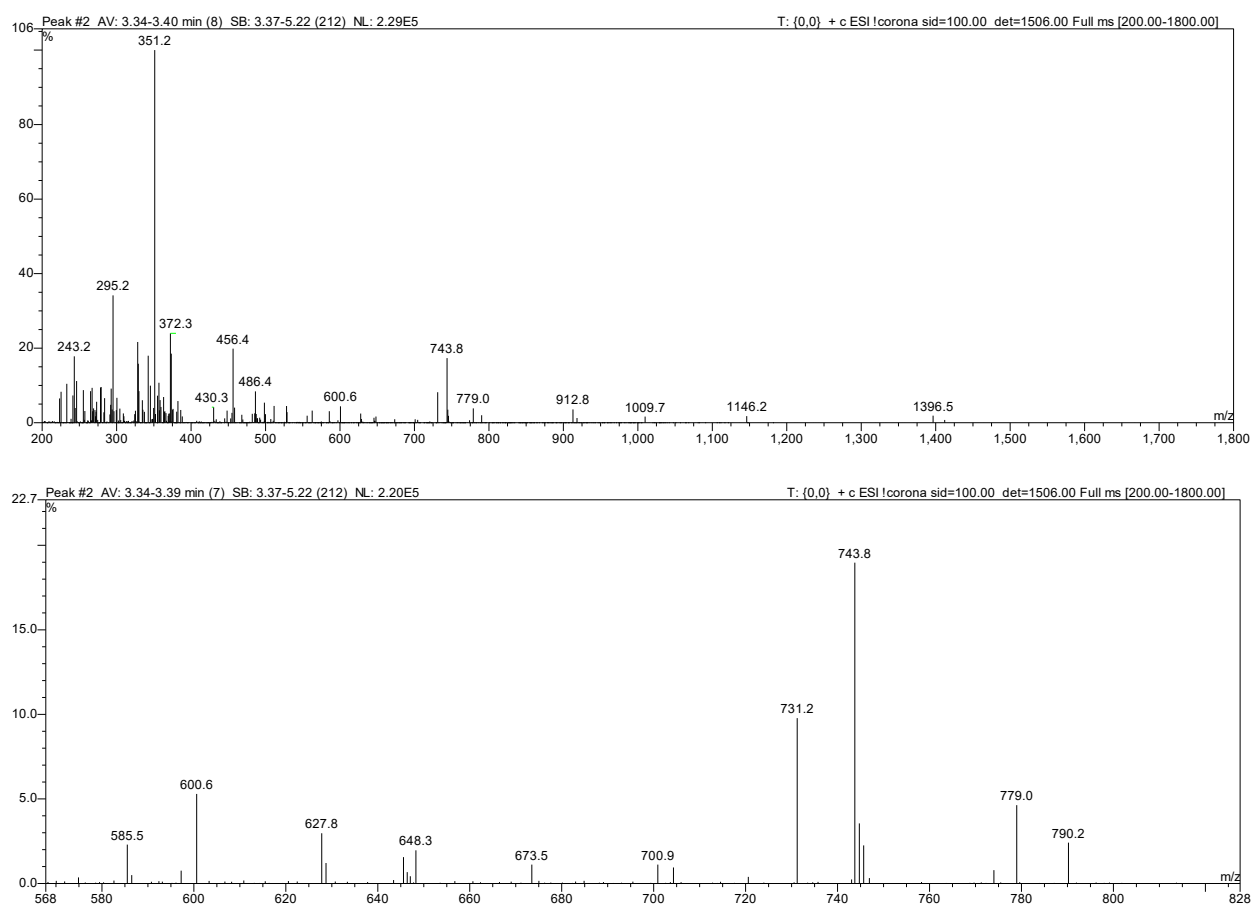
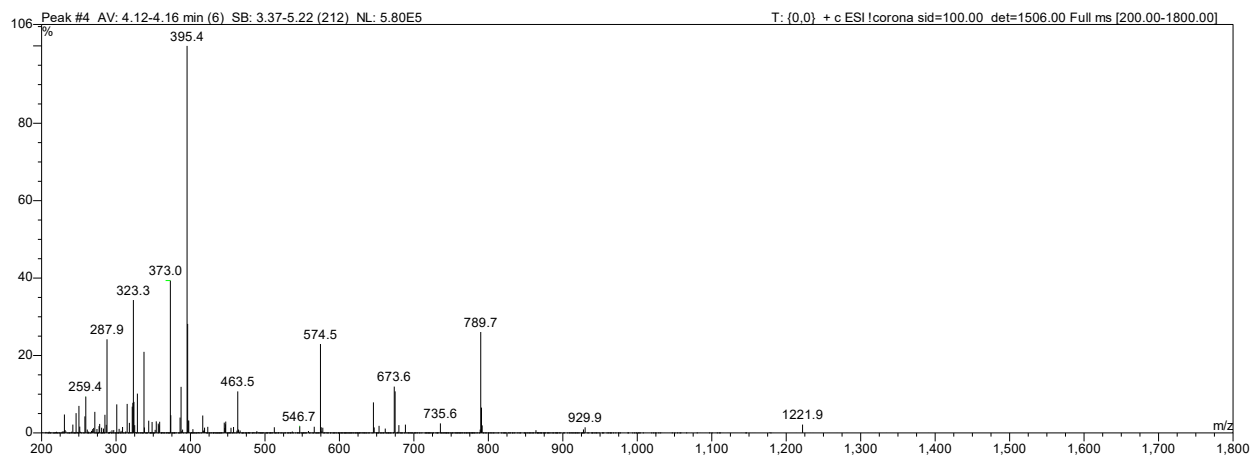**Figure SI 36.** MS spectra of **18** of the peak 3.37 min (pure product). Zoom on the range 568-828 *m/z* was shown additionally.
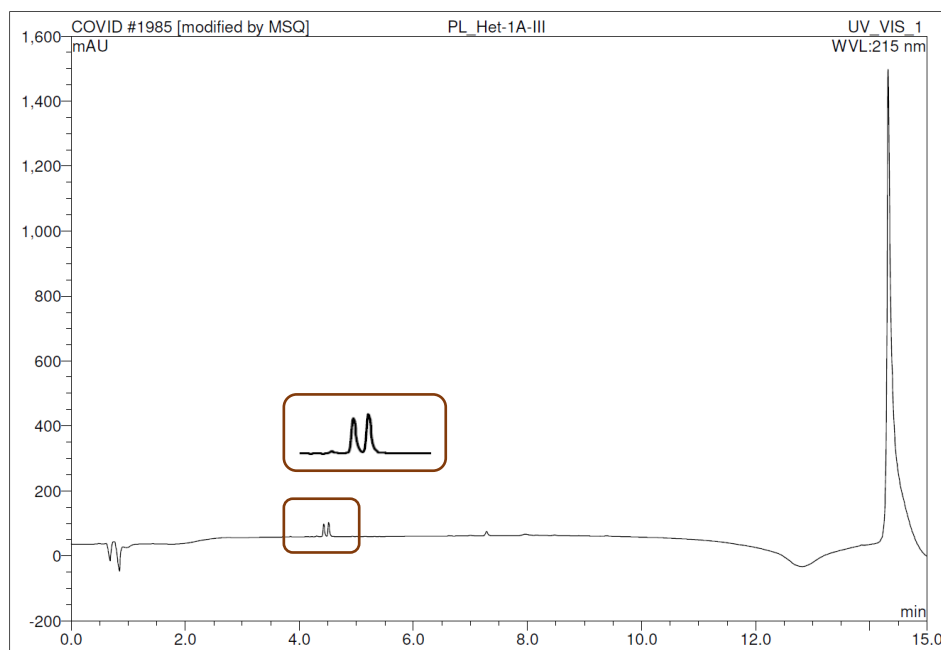
Figure SI 37. Chromatogram of **19** (pure product). Two separated peaks, with equal *m/z* value, are highlighted.
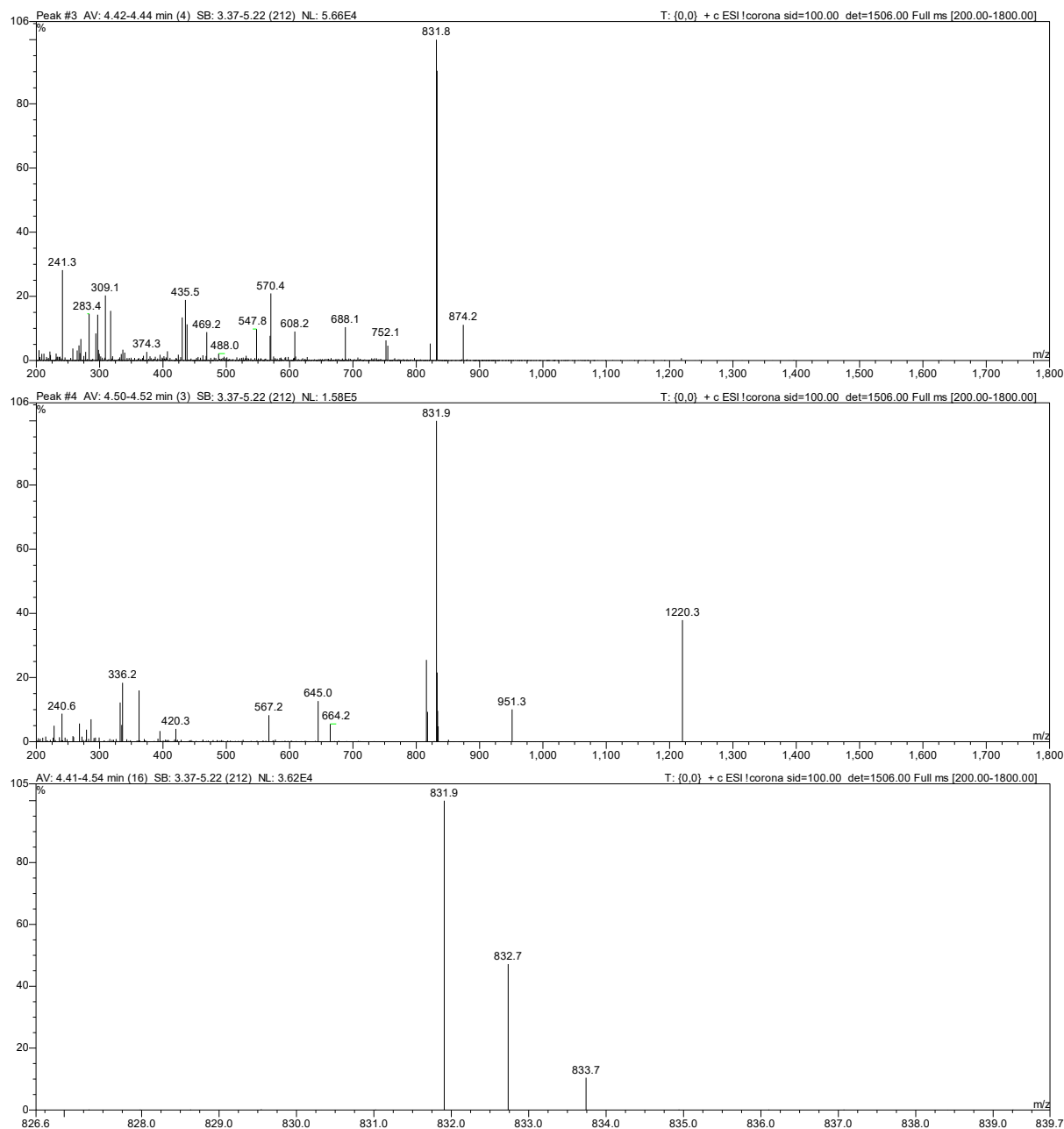
Figure SI 38. MS spectra of **19** of the peaks 4.42-4.44 (up) and 4.50-4.52 min (middle). Zoom on the range 826-840 *m/z* was shown additionally (down) (pure product).
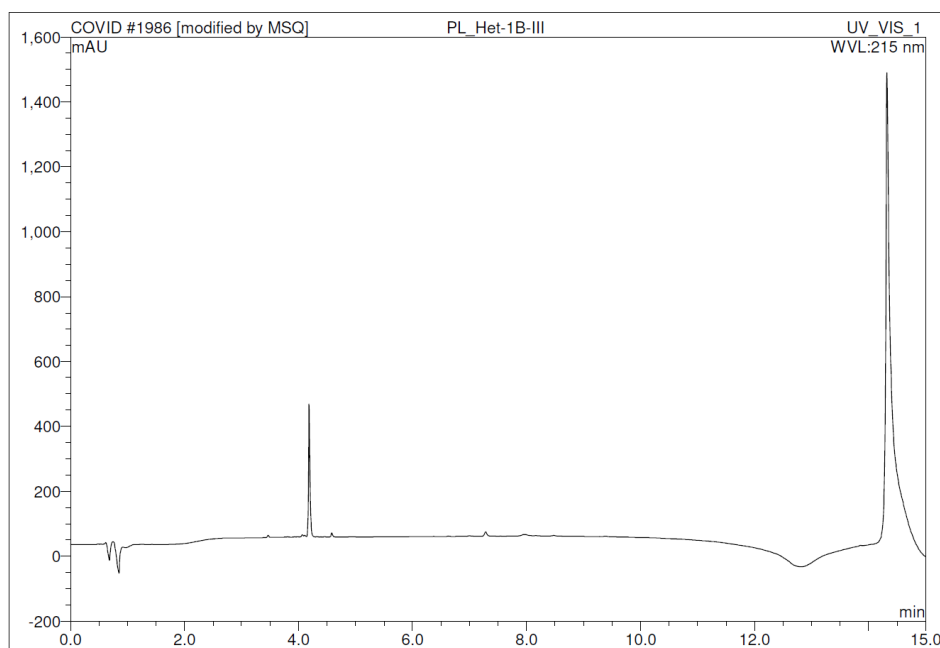
Figure SI 39. Chromatogram of **20** (pure product).
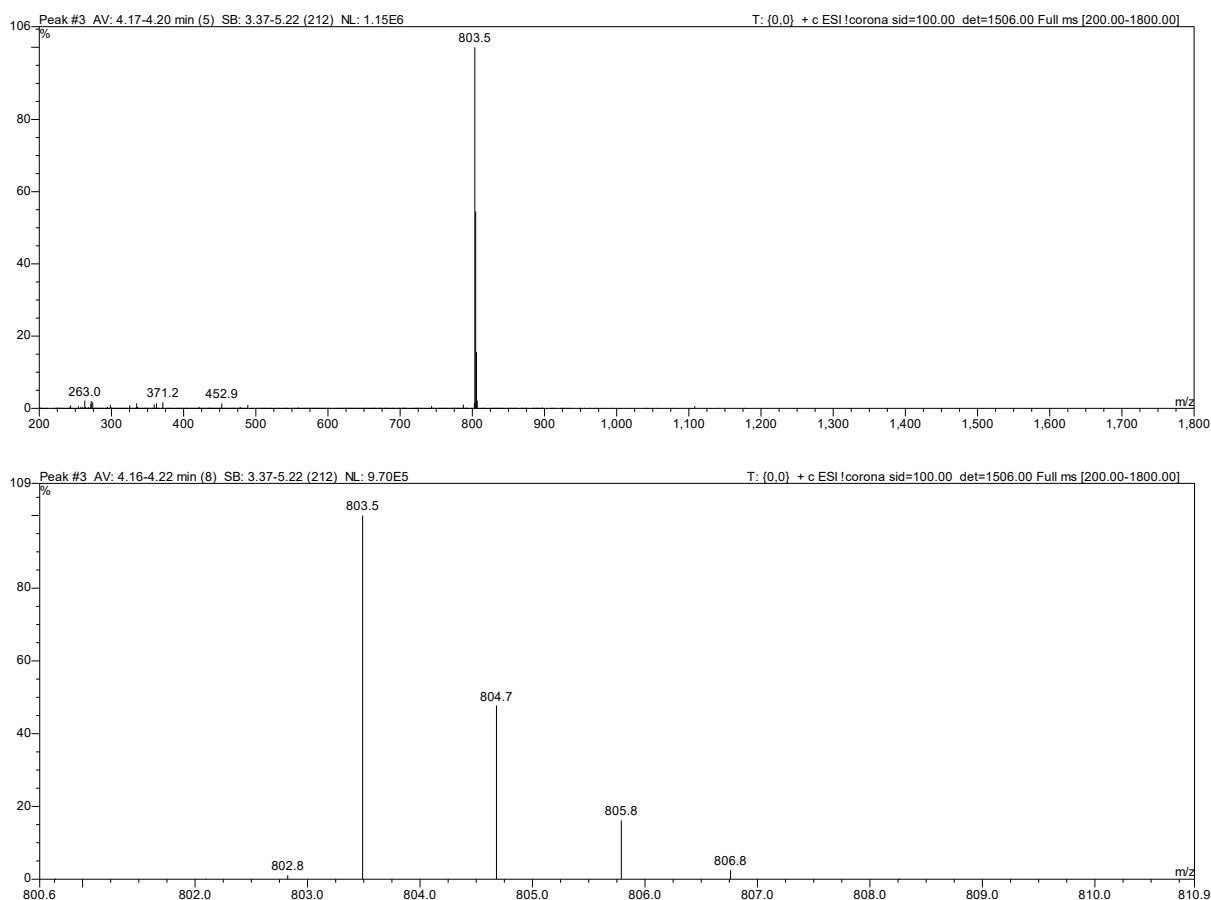
Figure SI 40. MS spectra of **20** of the peak 4.2 min (pure product). Zoom on the range 800-811 *m/z* was shown additionally.
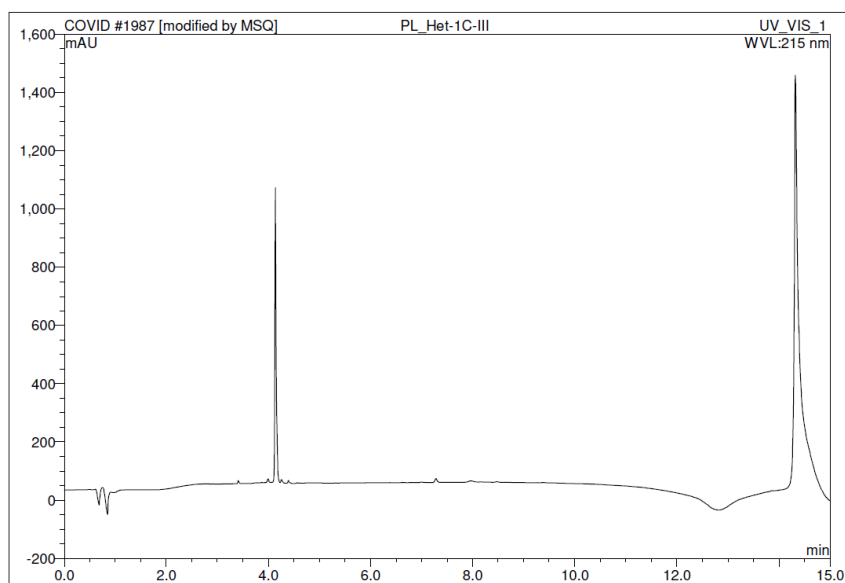
Figure SI 41. Chromatogram of **21** (pure product).
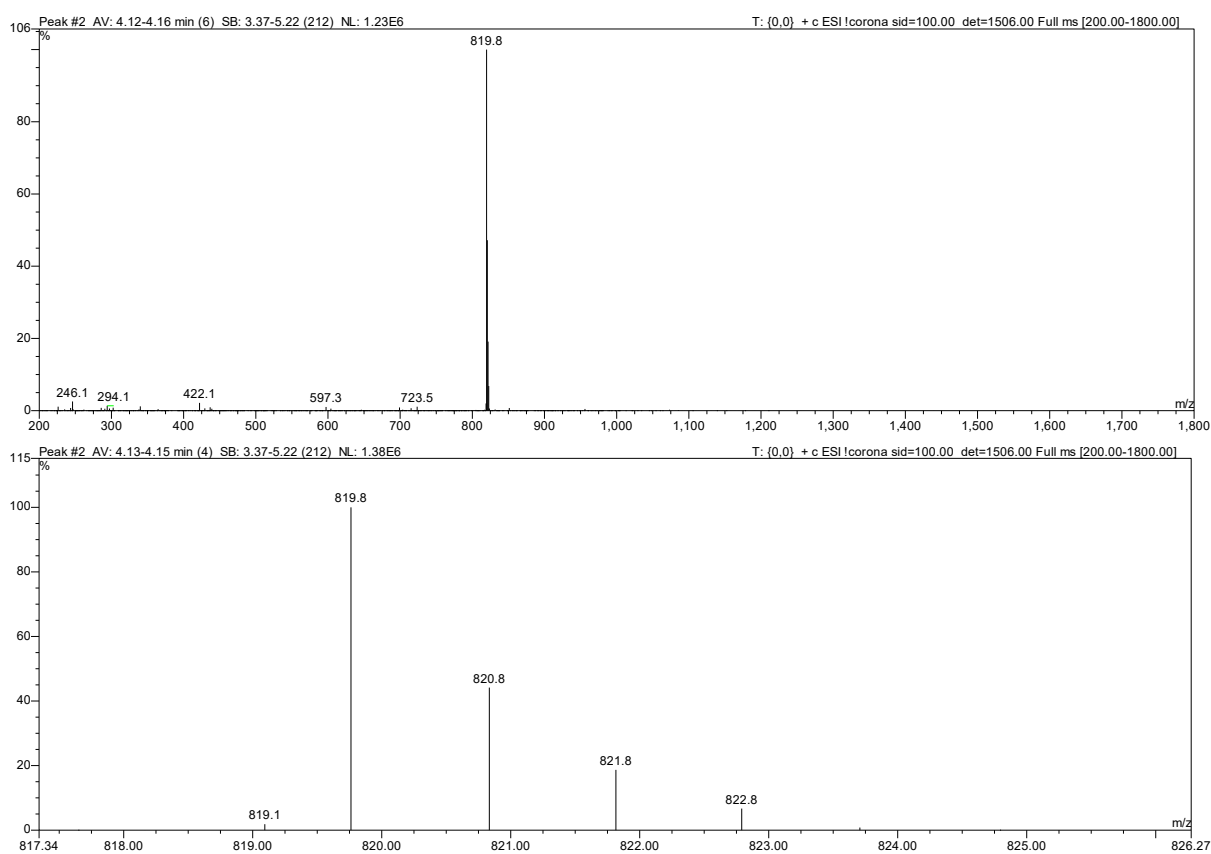
Figure SI 42. MS spectra of **21** of the peak 4.12-4.16 min (pure product). Zoom on the range 817-826 *m/z* was shown additionally.
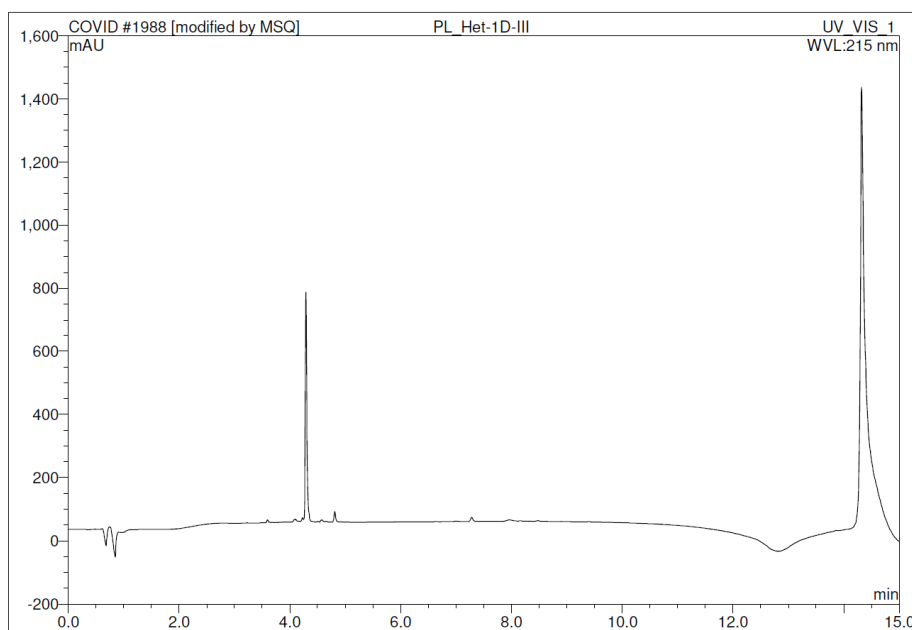
Figure SI 43. Chromatogram of **22** (pure product).
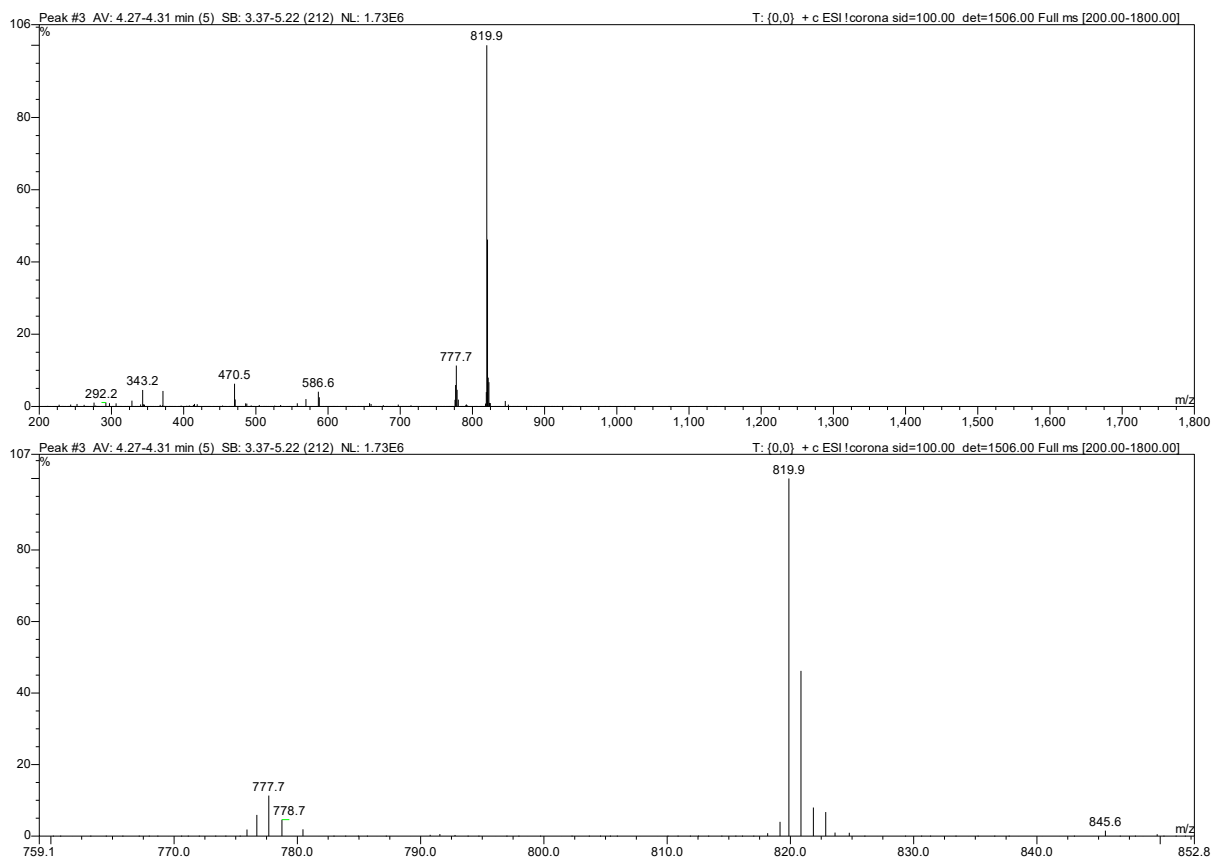
Figure SI 44. MS spectra of **22** of the peak 4.27-4.31 min (pure product). Zoom on the range 759-853 *m/z* was shown additionally.
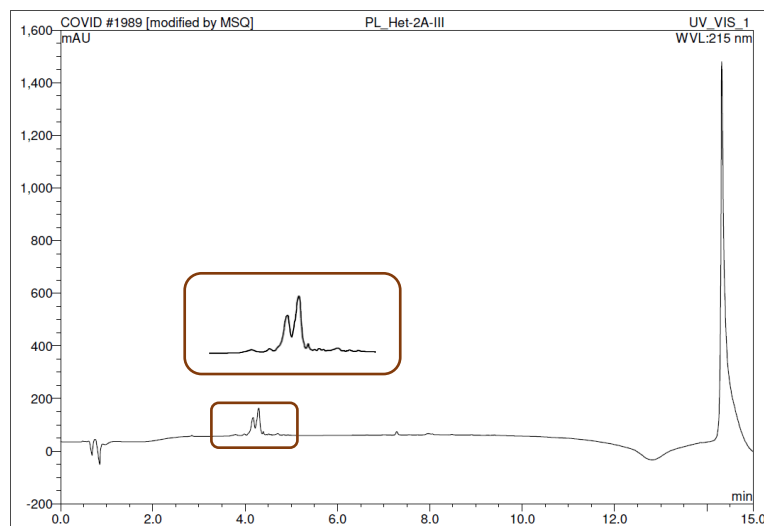
Figure SI 45. Chromatogram of **23** (pure product). Two separated peaks, with equal *m/z* value, are highlighted.
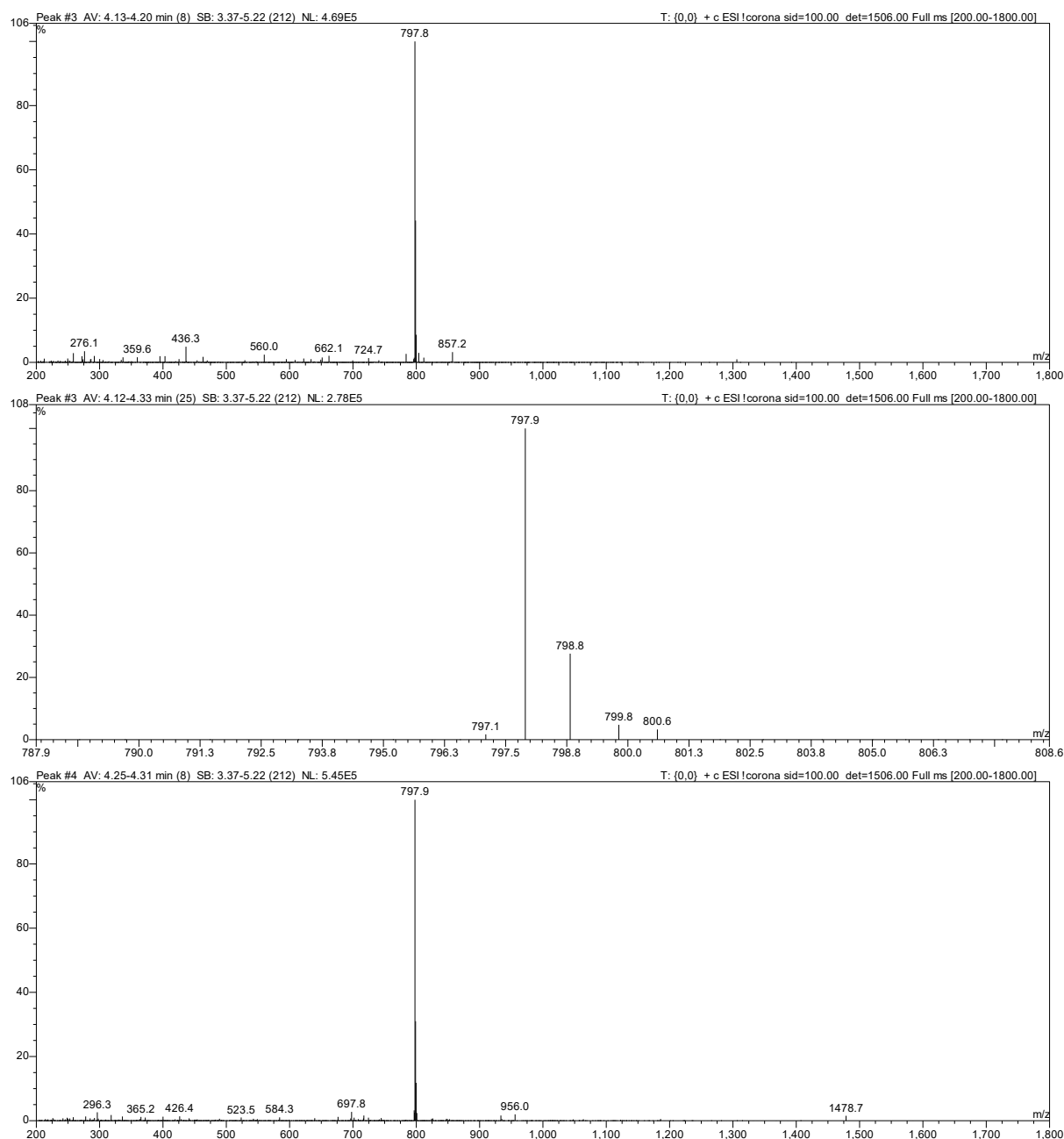
Figure SI 46. MS spectra of **23** of the peaks 4.13-4.20 (up) and 4.25-4.31 min (down) (pure product). Zoom on the range 788-809 *m/z* was shown additionally (middle).
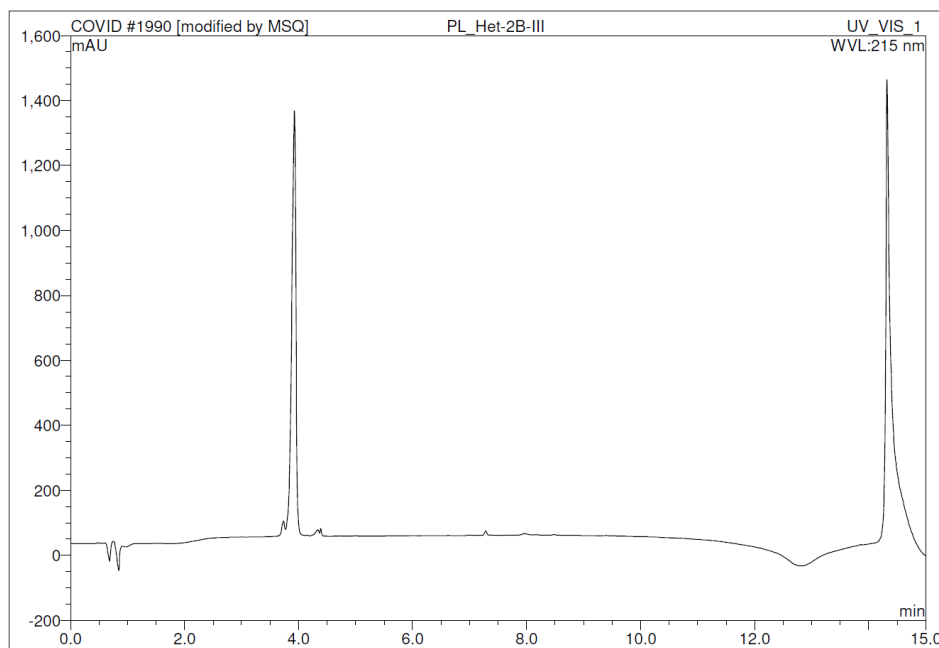
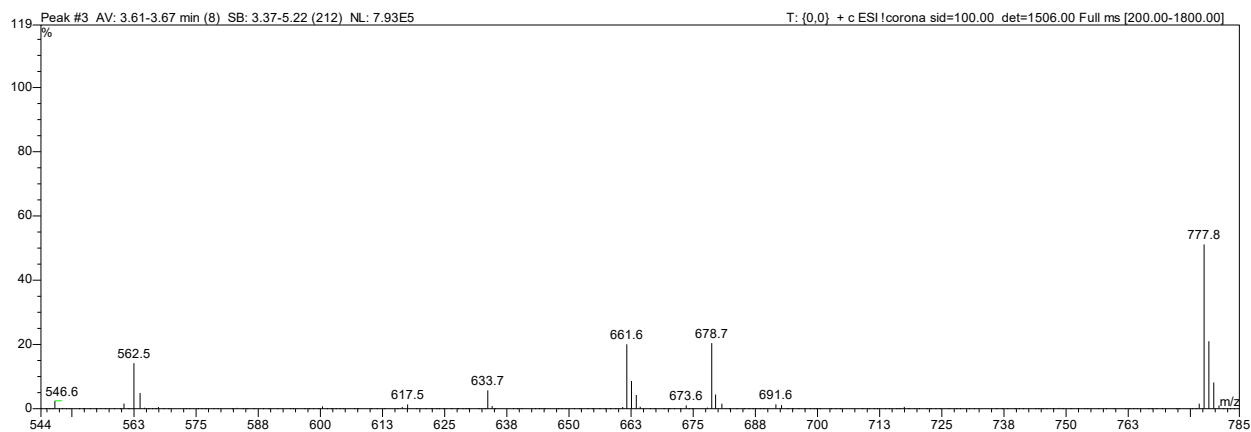**Figure SI 47.** Chromatogram of **24** (pure product).
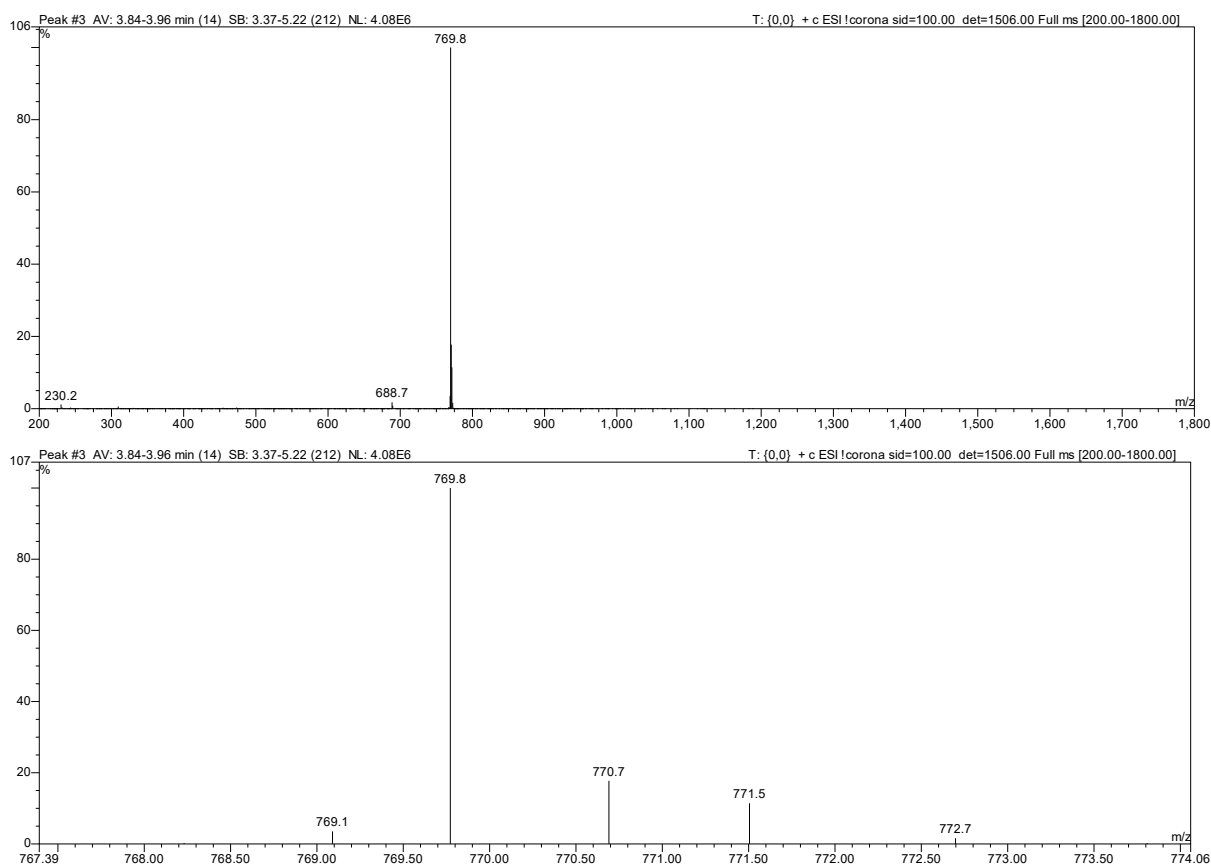
Figure SI 48. MS spectra of **24** of the peak 3.84-3.96 min (pure product). Zoom on the range 767-774 *m/z* was shown additionally.
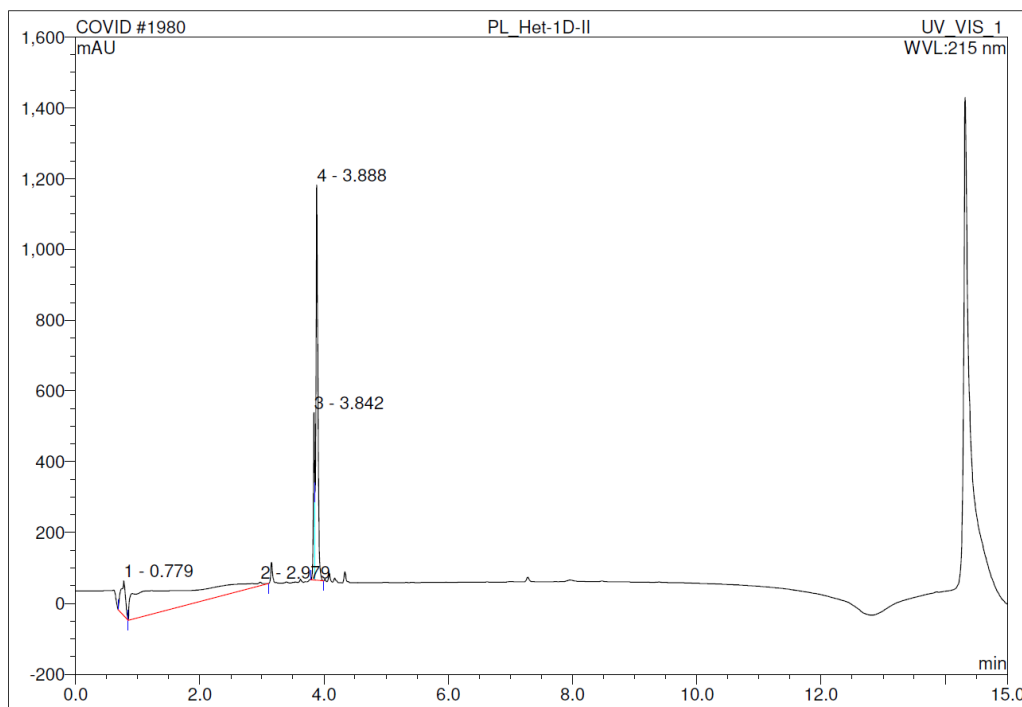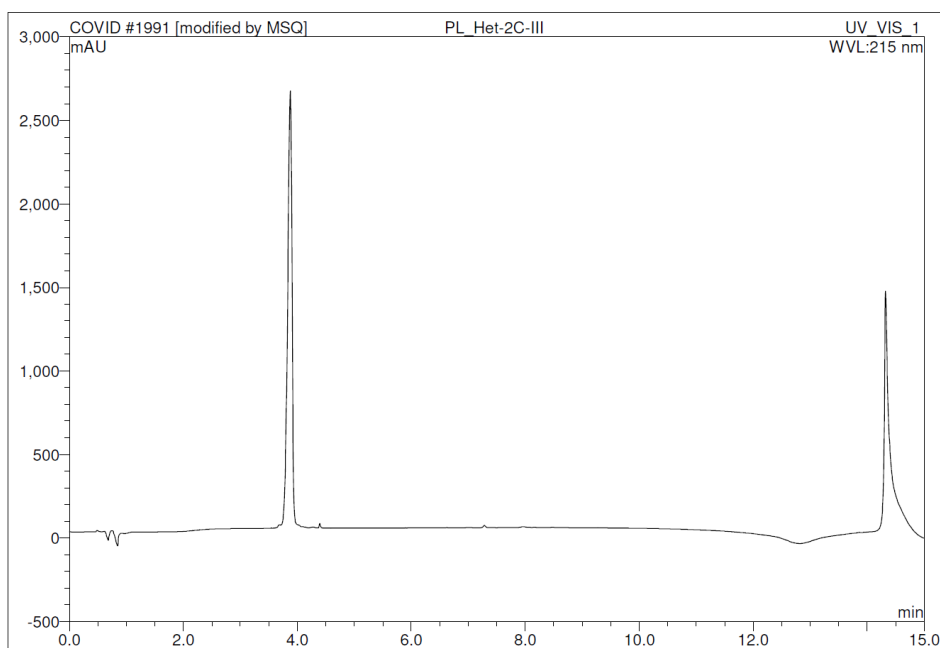
Figure SI 49. Chromatogram of **25** (pure product).
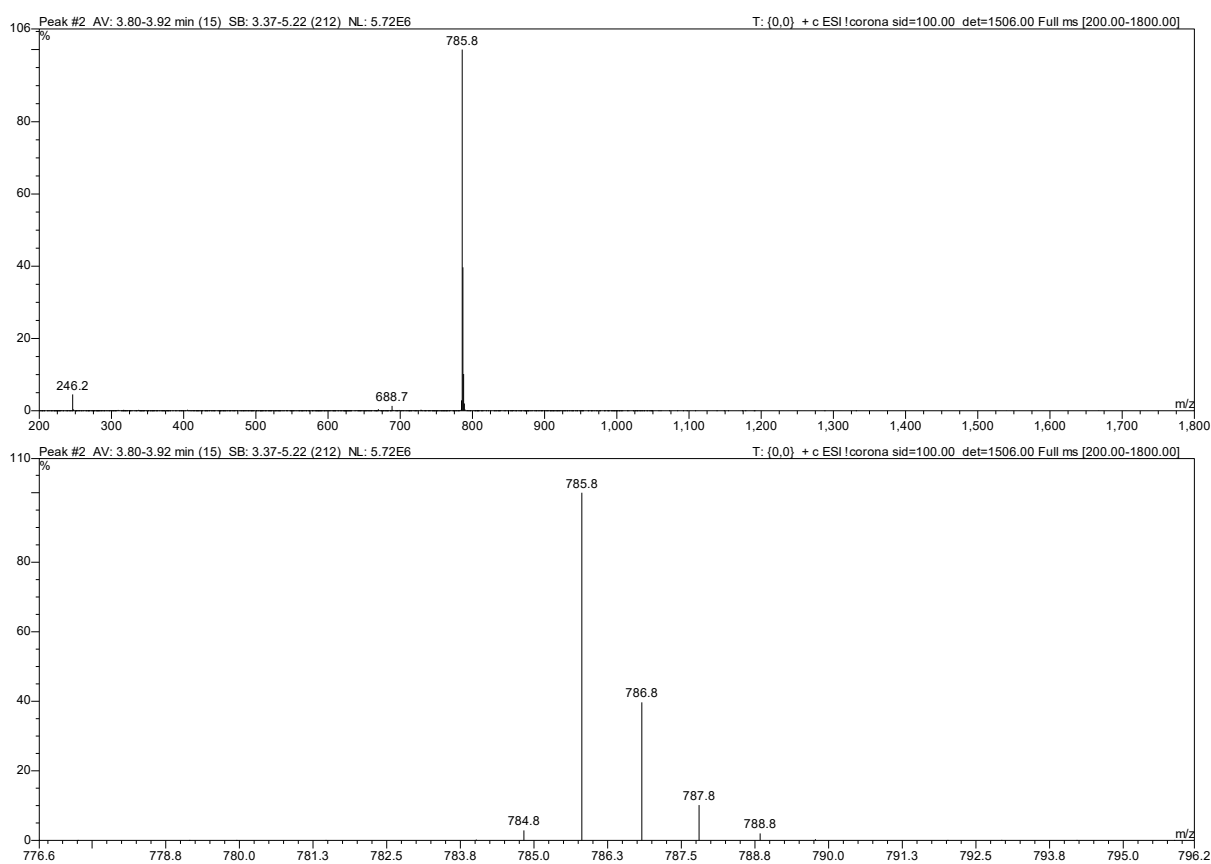
Figure SI 50. MS spectra of **25** of the peak 3.80-3.92 min (pure product). Zoom on the range 776-796 *m/z* was shown additionally.
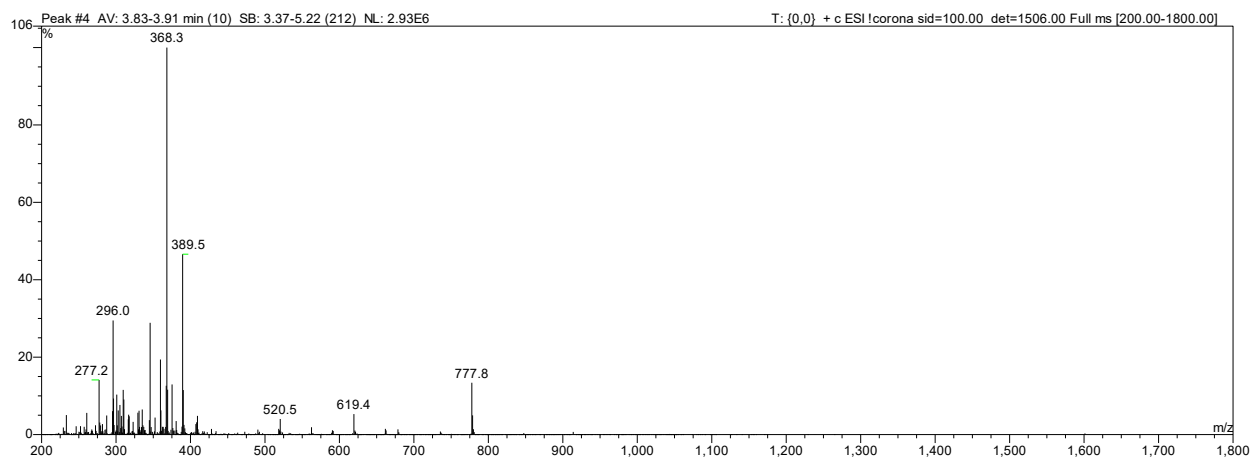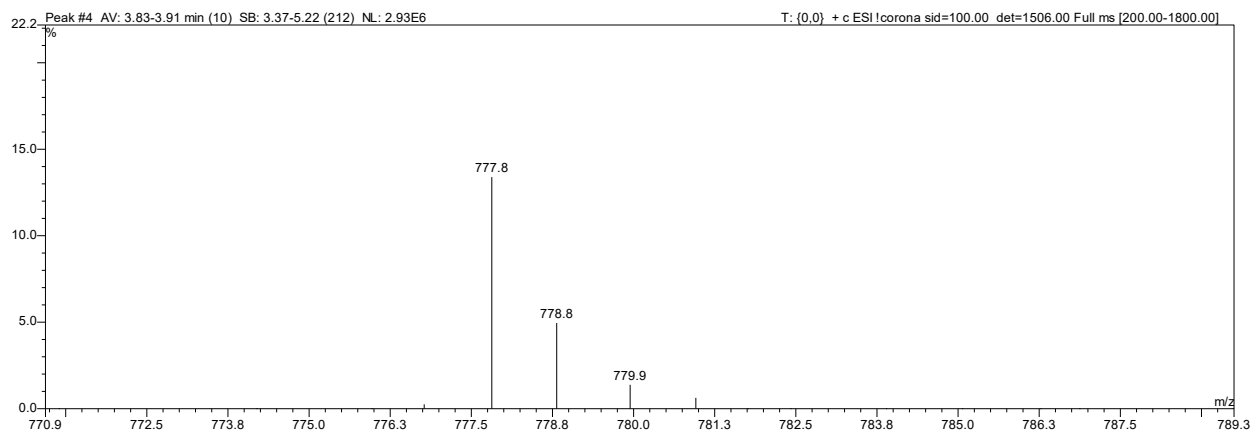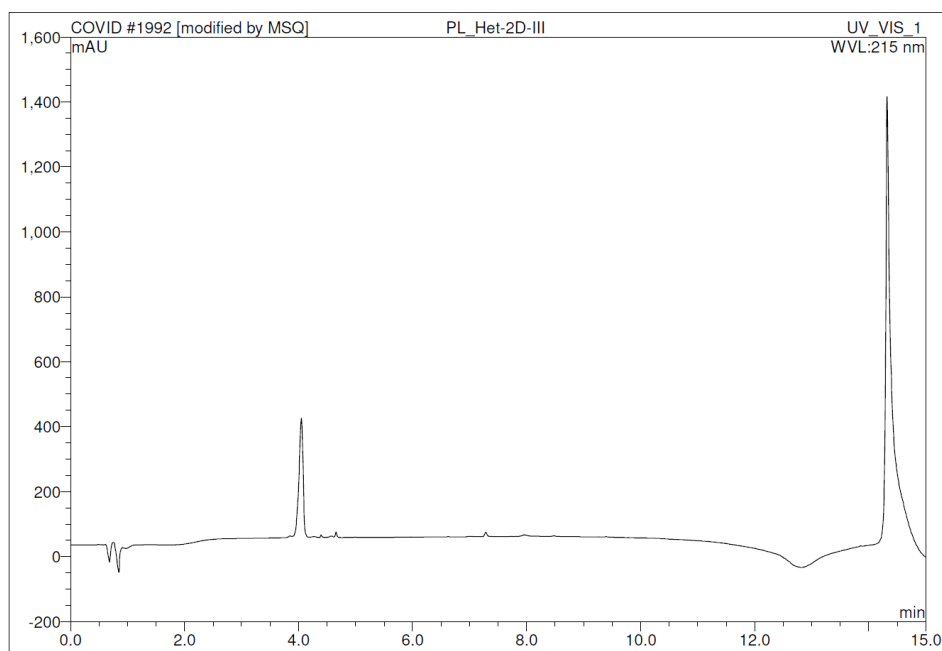
Figure SI 51. Chromatogram of **26** (pure product).
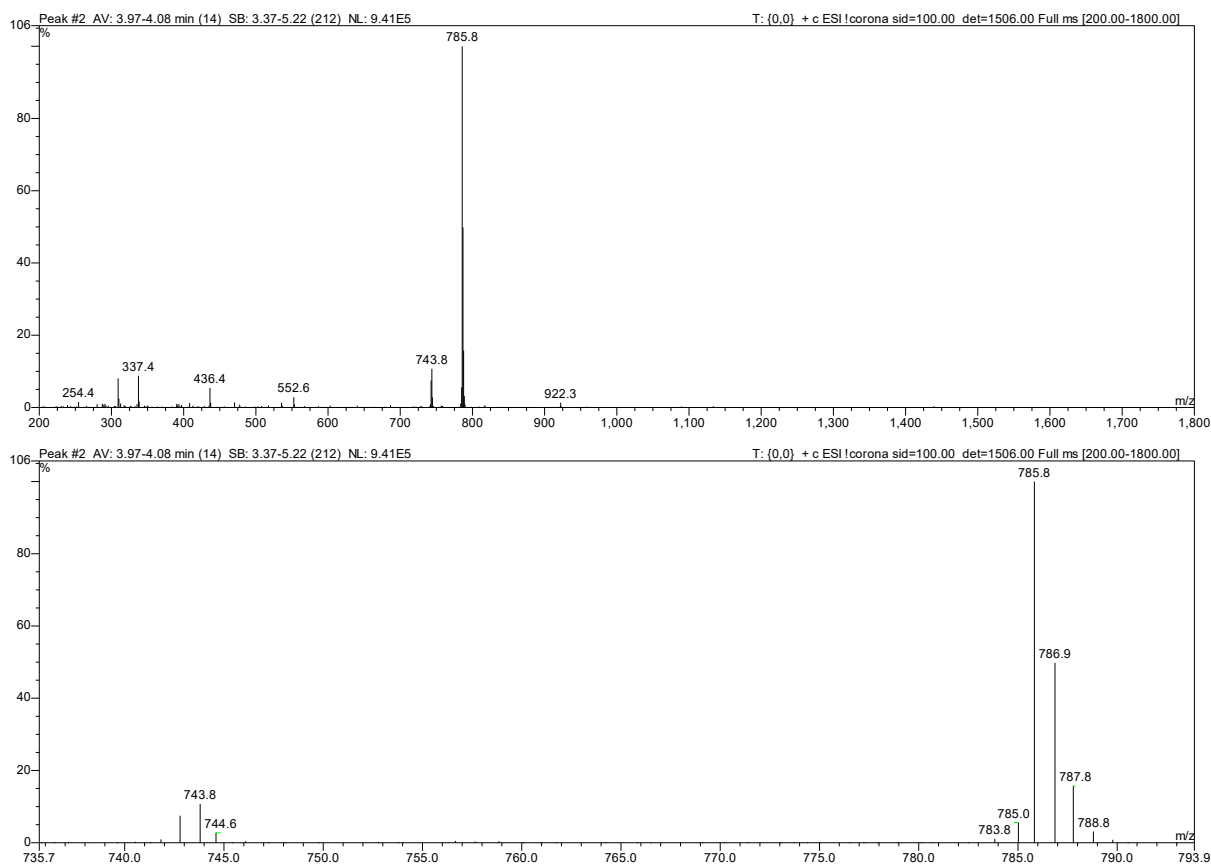
Figure SI 52. MS spectra of **26** of the peak 3.97-4.08 min (pure product). Zoom on the range 735-794 *m/z* was shown additionally.

1.2 Analyses of compounds 46-57
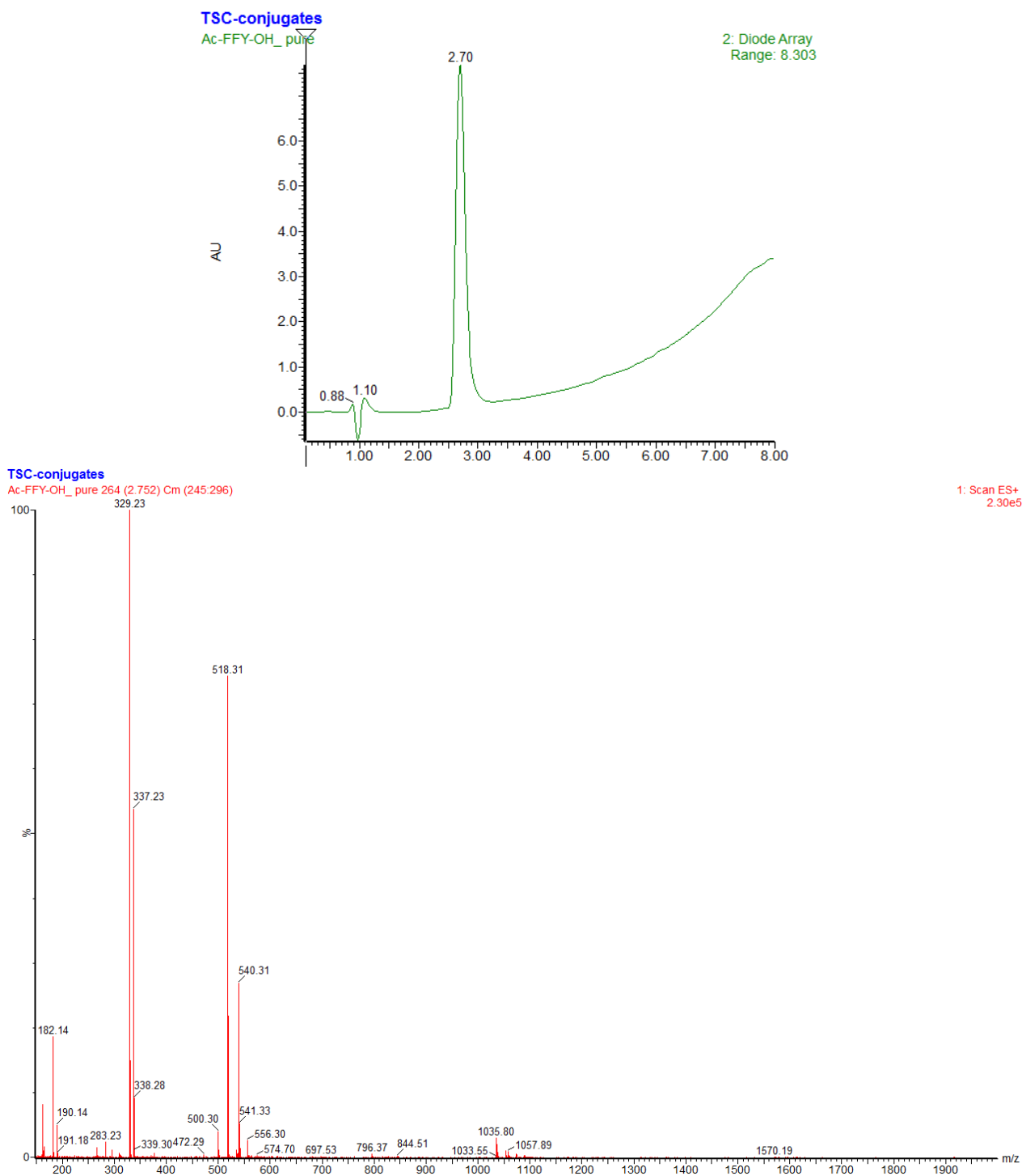
Figure SI 53. Chromatogram of **46** (Ac-FFY-OH) and MS spectra of the peak 2.7 min.
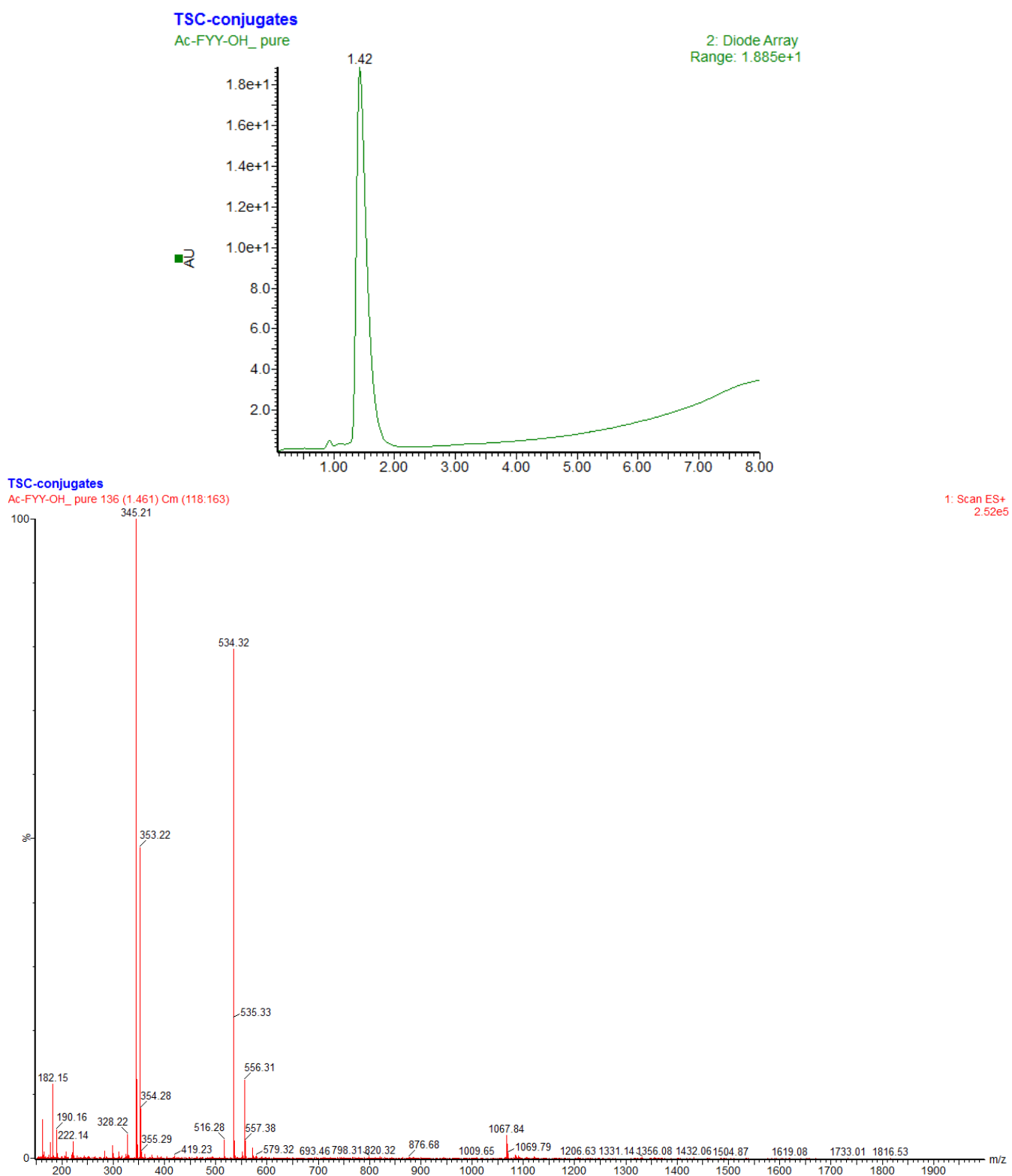
Figure SI 54. Chromatogram of **47** (Ac-FYY-OH) and MS spectra of the peak 1.4 min.
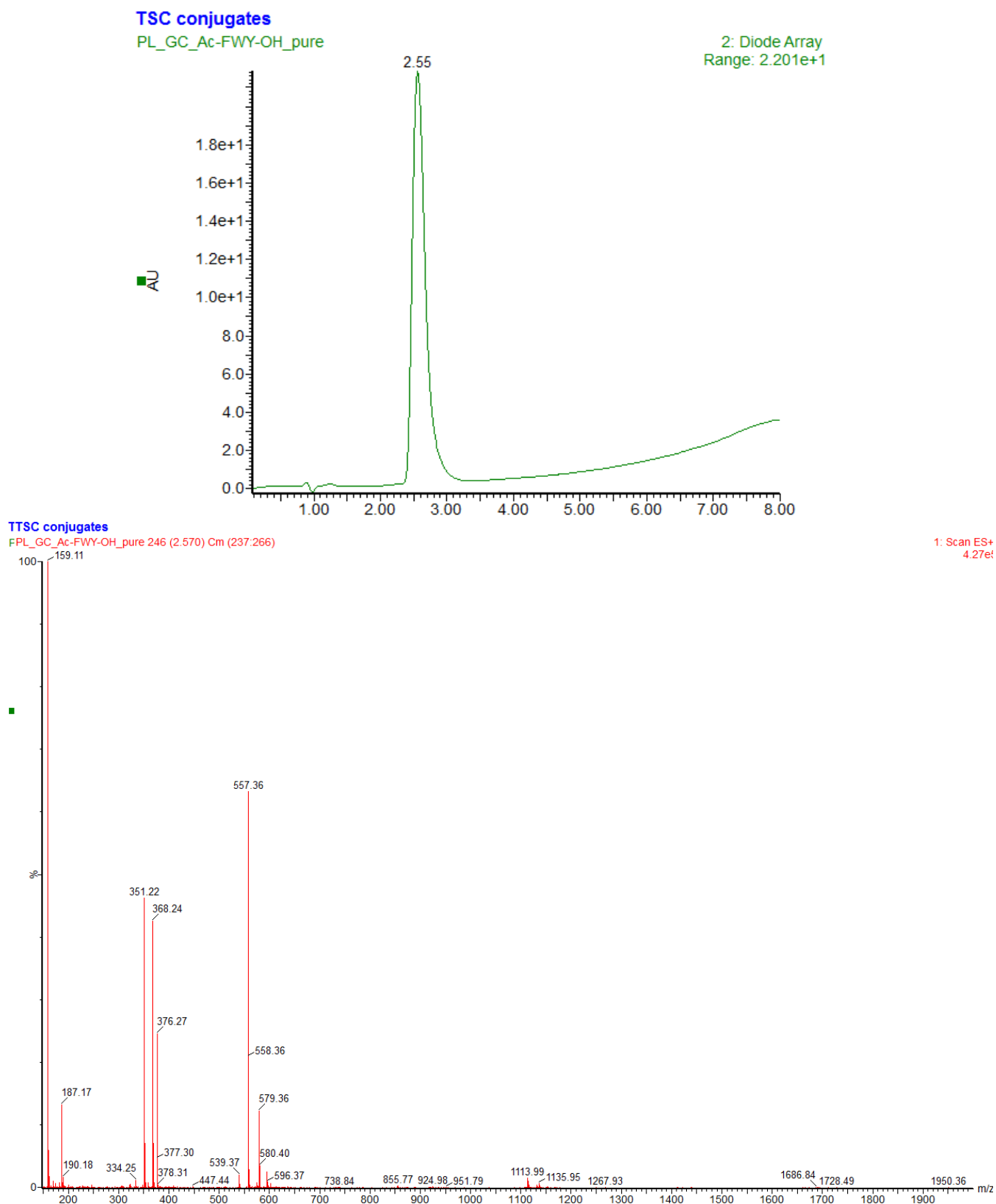
Figure SI 55. Chromatogram of **48** (Ac-FWY-OH) and MS spectra of the peak 2.5 min.

210616_epk1
PL_GC_TSC1-FFY-OH_pure

2: Diode Array
Range: 3.555
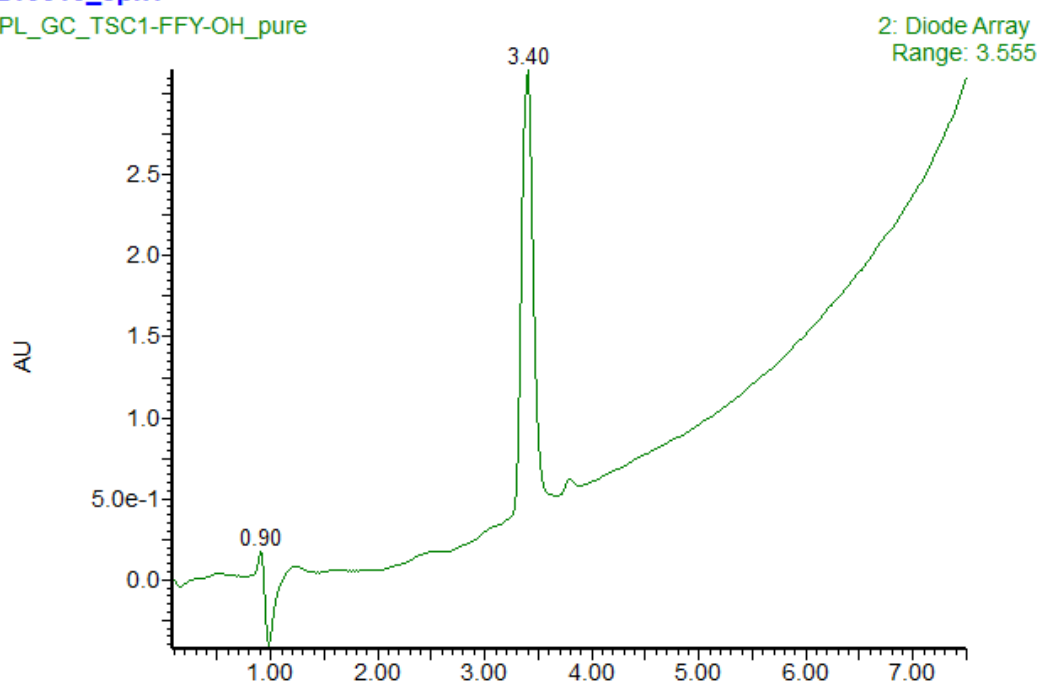
210616_epk1
PL_GC_TSC1-FFY-OH_pure 335 (3.468)

1: Scan ES+
1.02e5
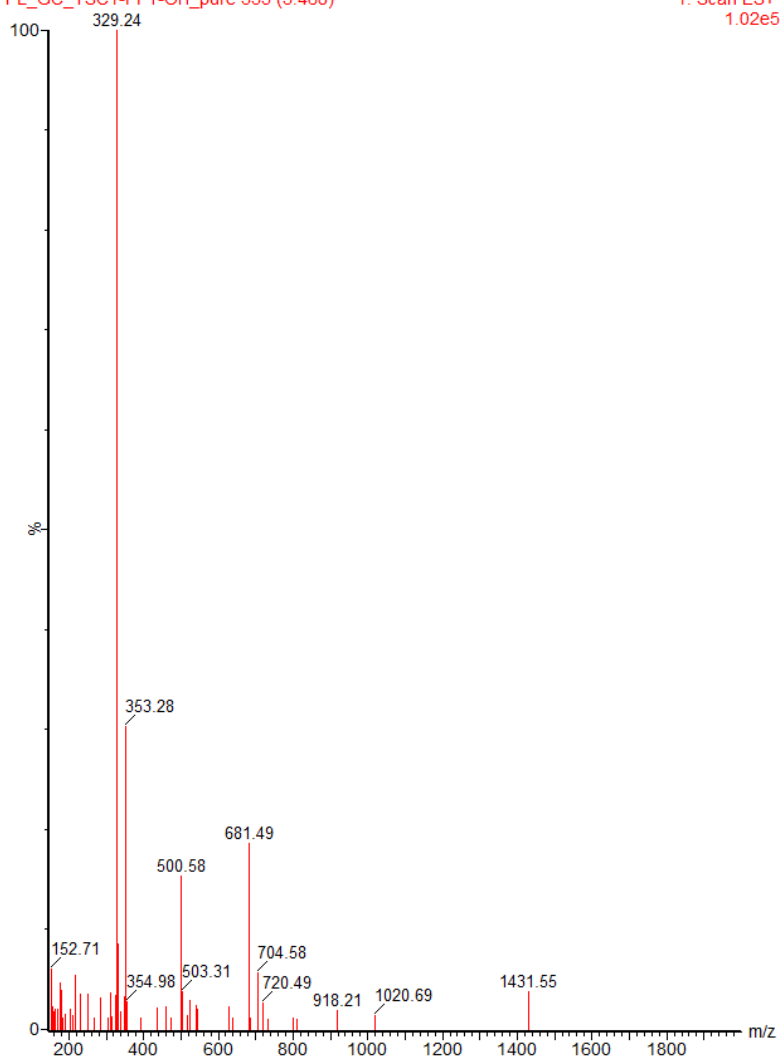
Figure SI 56. Chromatogram of **49** and MS spectra of the peak 3.4 min.
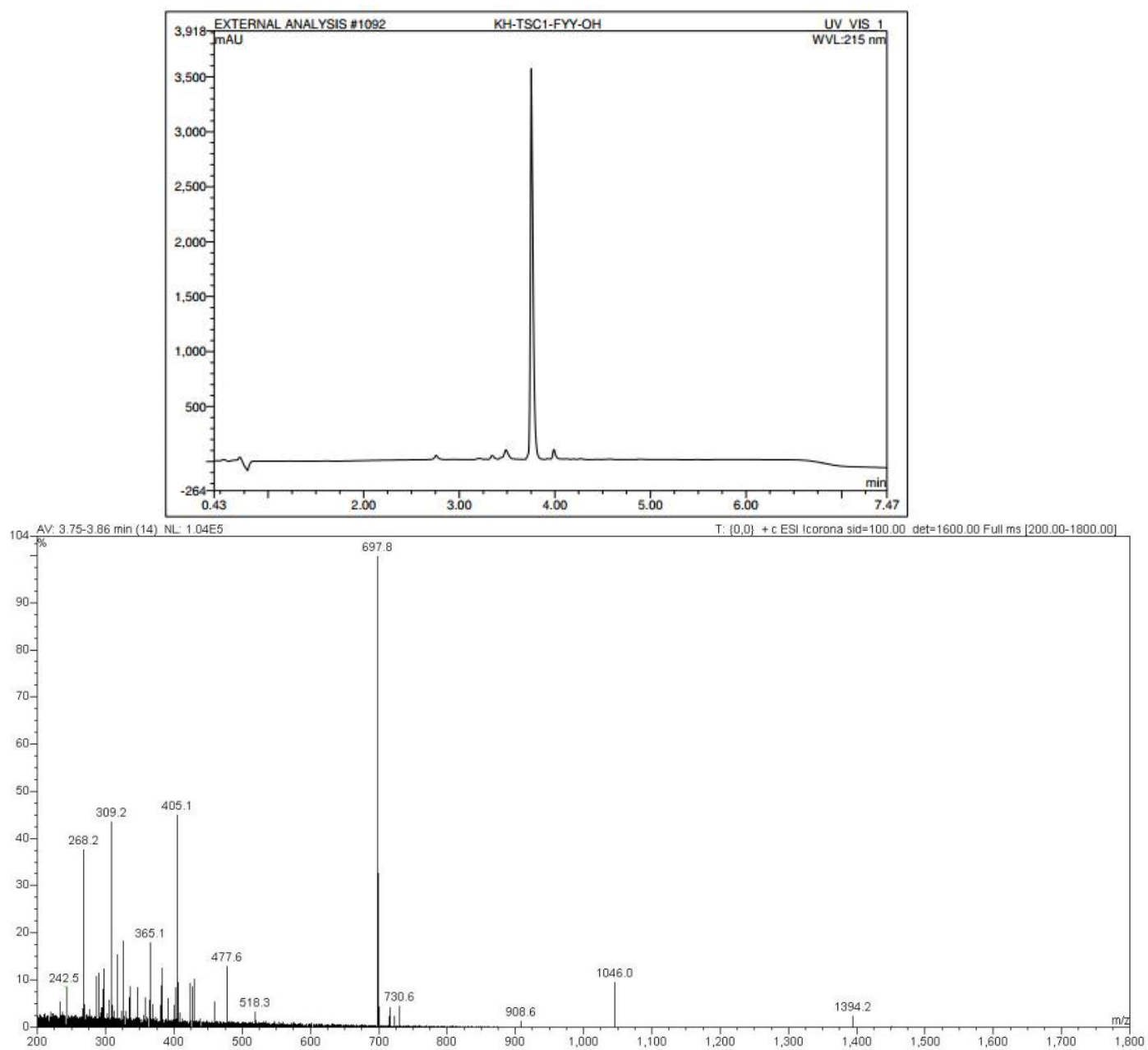
Figure SI 57. Chromatogram of **50** and MS spectra of the peak 3.8 min.

210616_epk1
PL_GC_TSC1-FWY-OH_pure

2: Diode Array
Range: 3.306

210616_epk1
PL_GC_TSC1-FWY-OH_pure 344 (3.558)
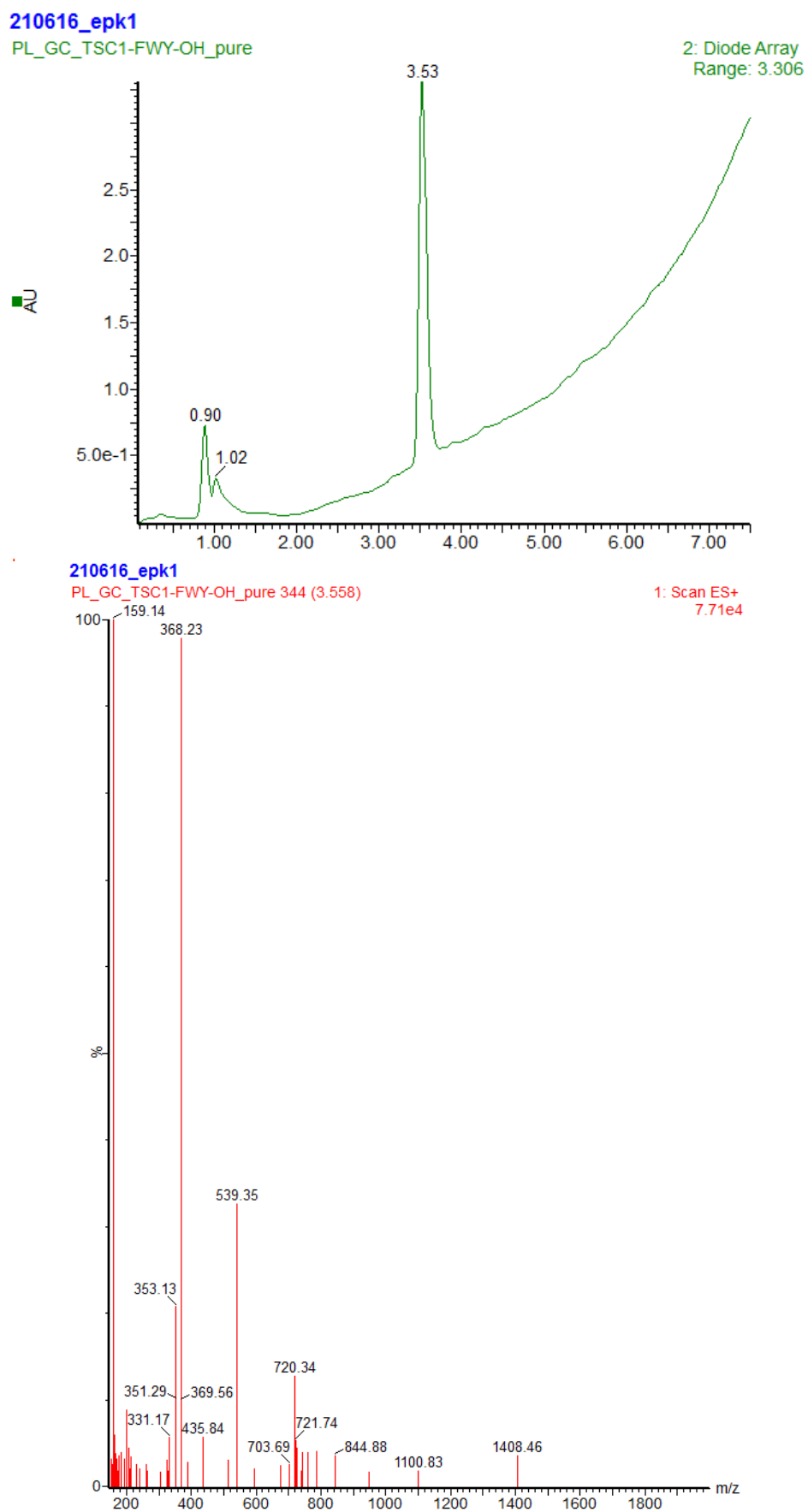
1: Scan ES+
7.71e4

Figure SI 58. Chromatogram of **51** and MS spectra of the peak 3.5 min.
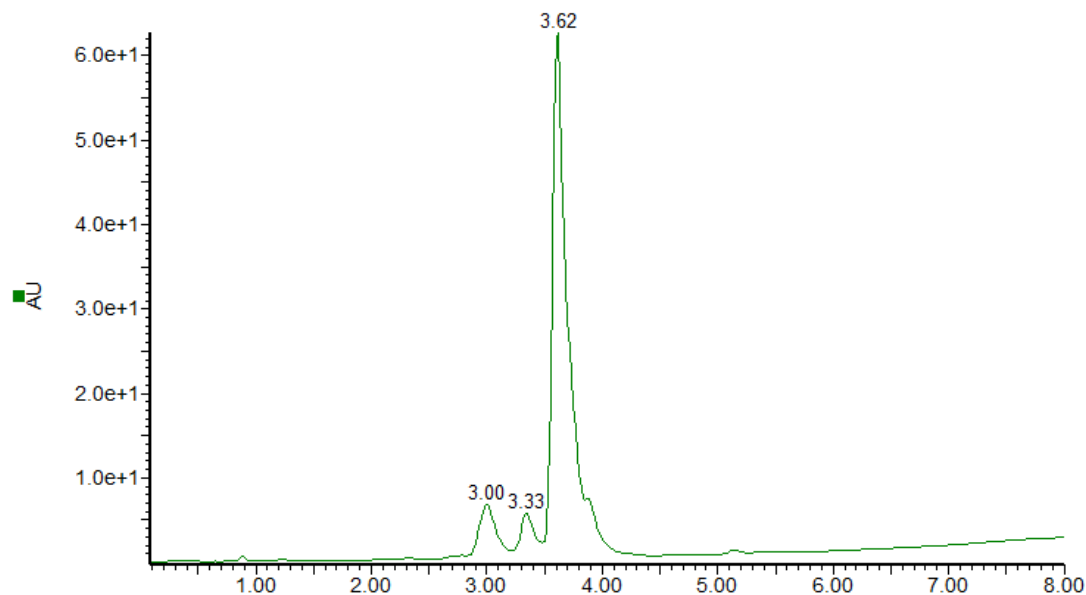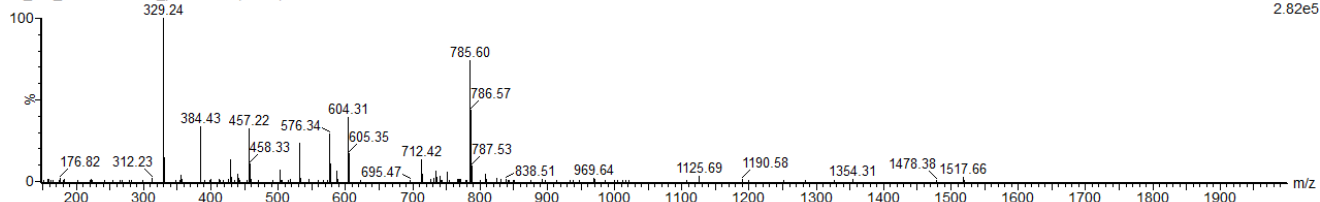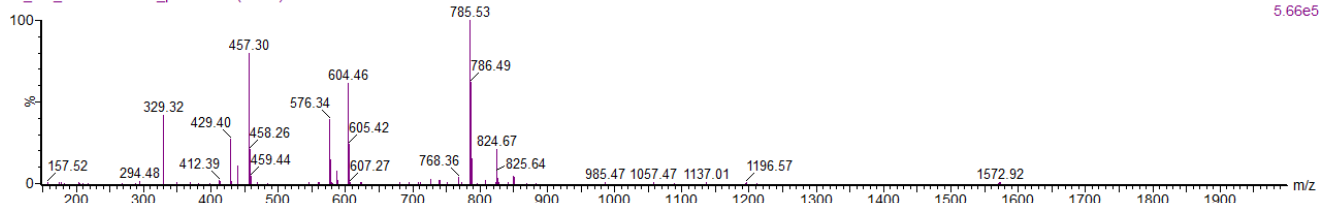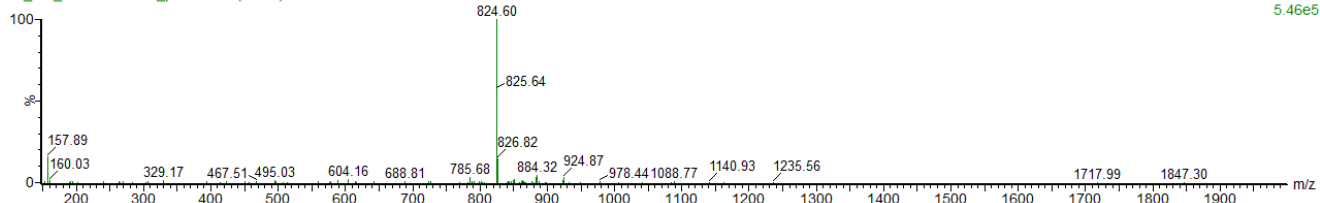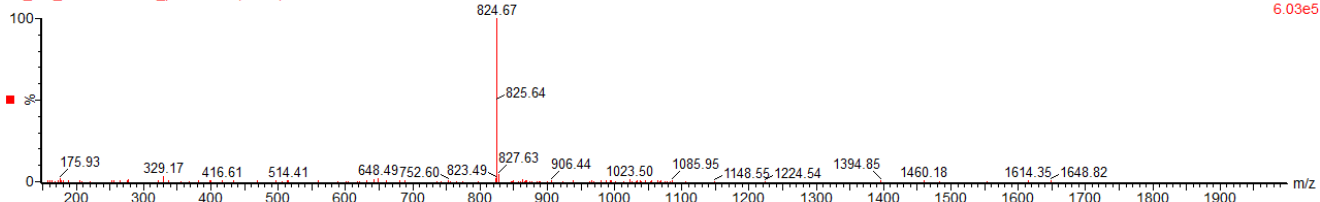
Figure SI 59. Chromatogram of **52** and MS spectra of the peaks found.
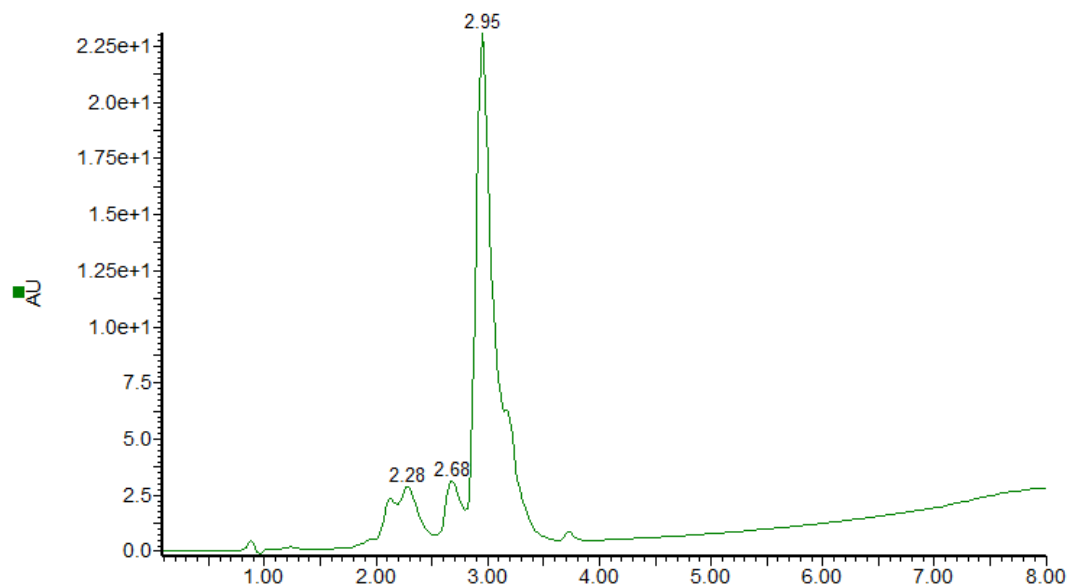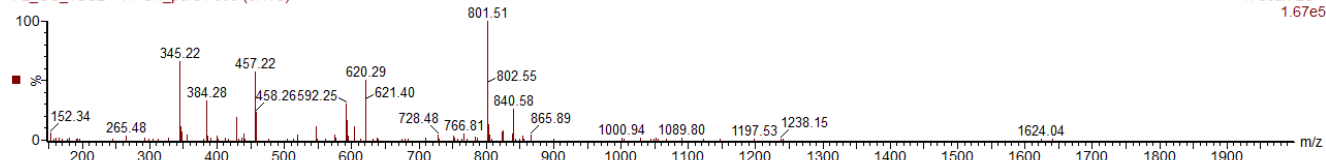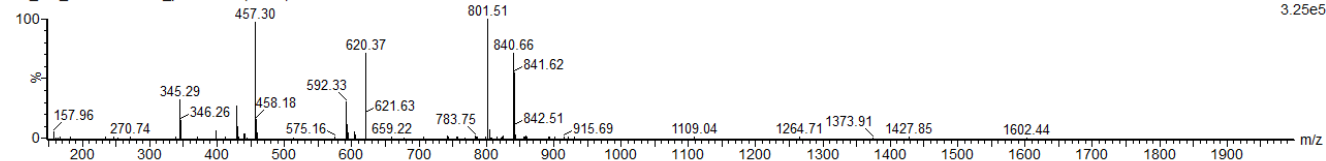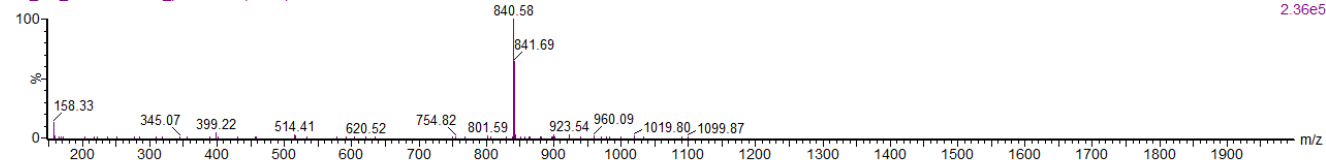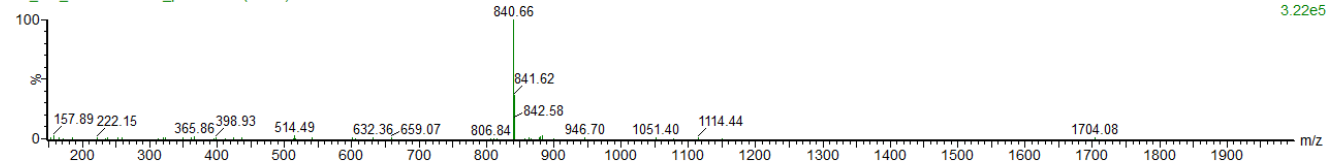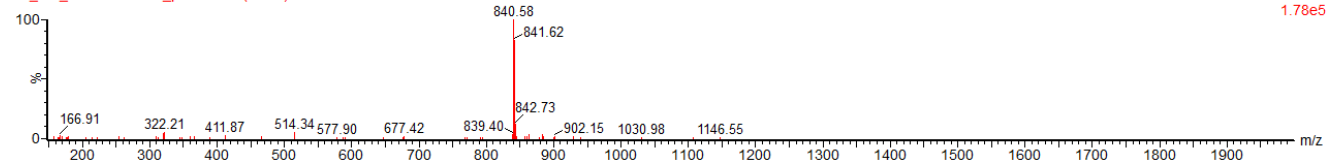
Figure SI 60. Chromatogram of **53** and MS spectra of the peaks found.
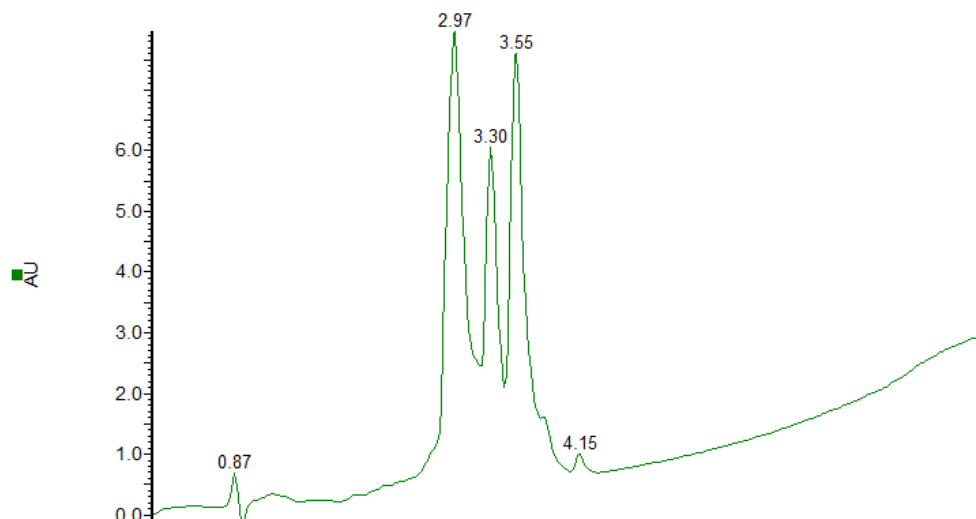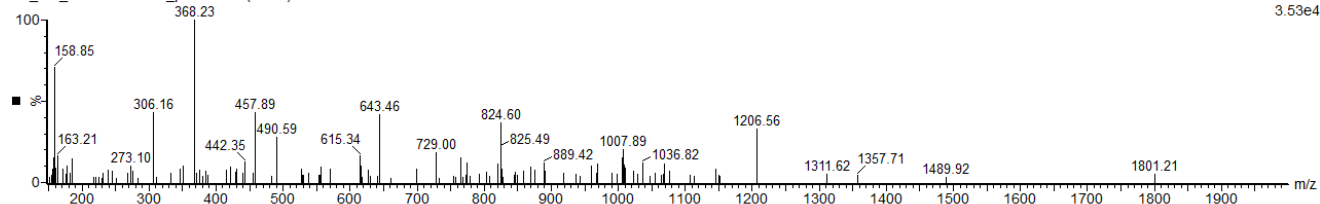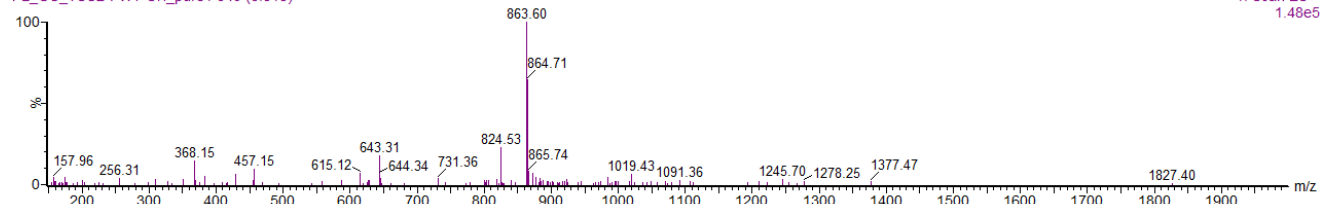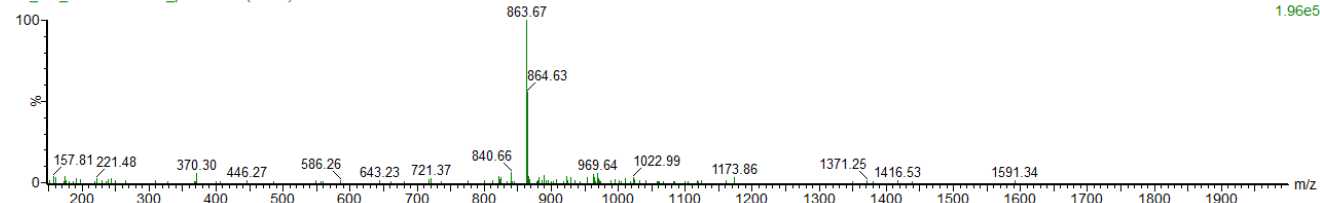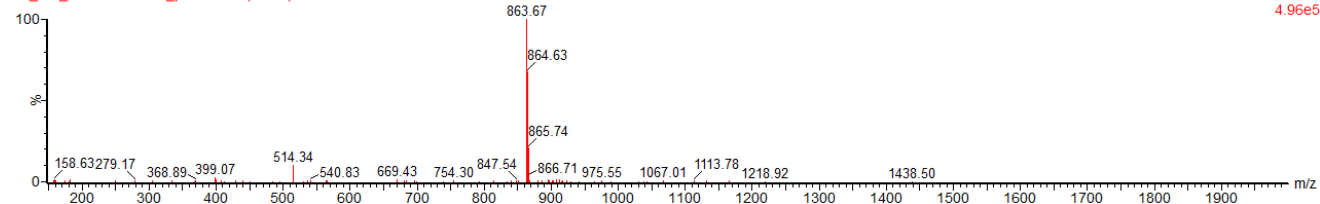
Figure SI 61. Chromatogram of **54** and MS spectra of the peaks found.
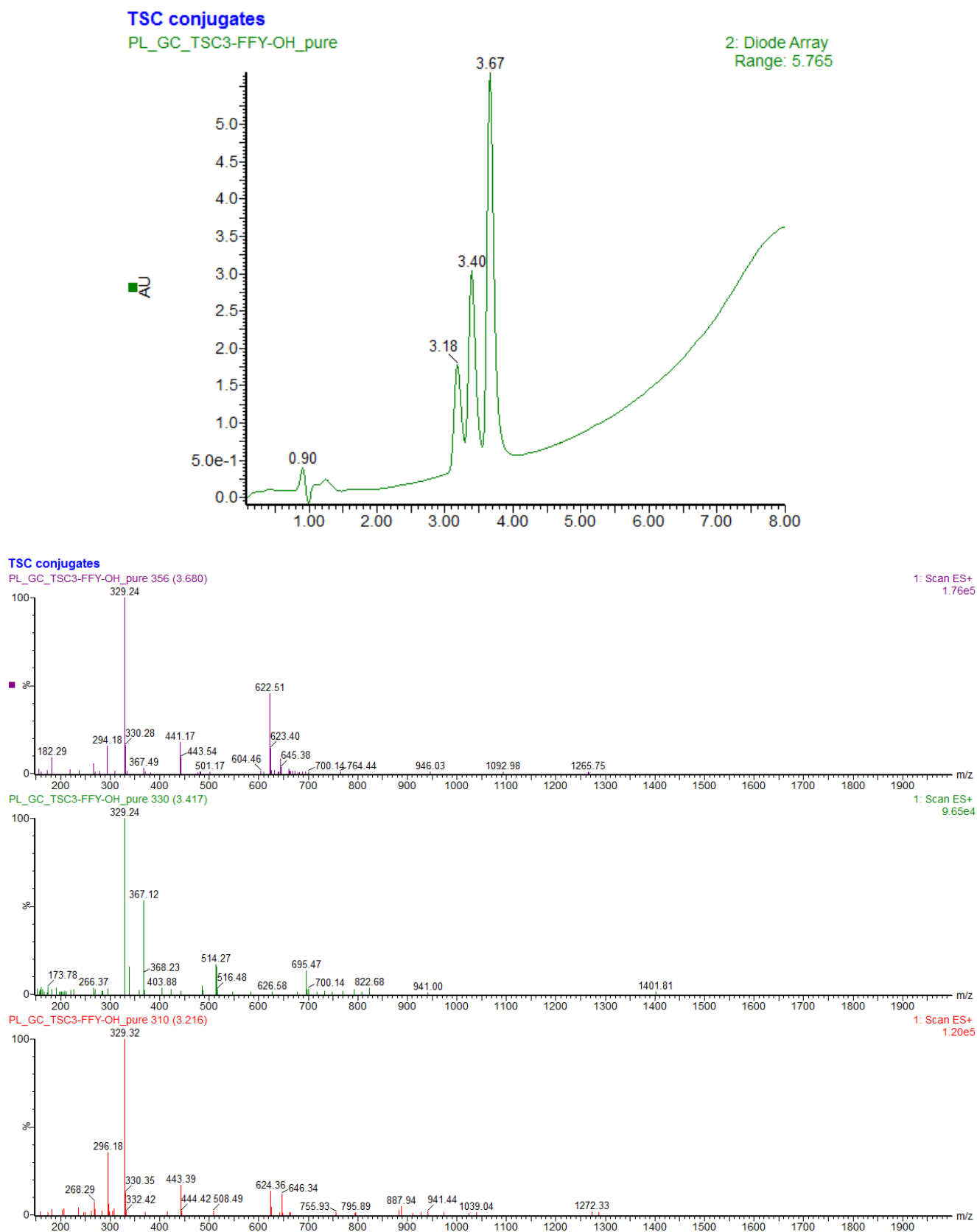
Figure SI 62. Chromatogram of **55** and MS spectra of the peaks found.
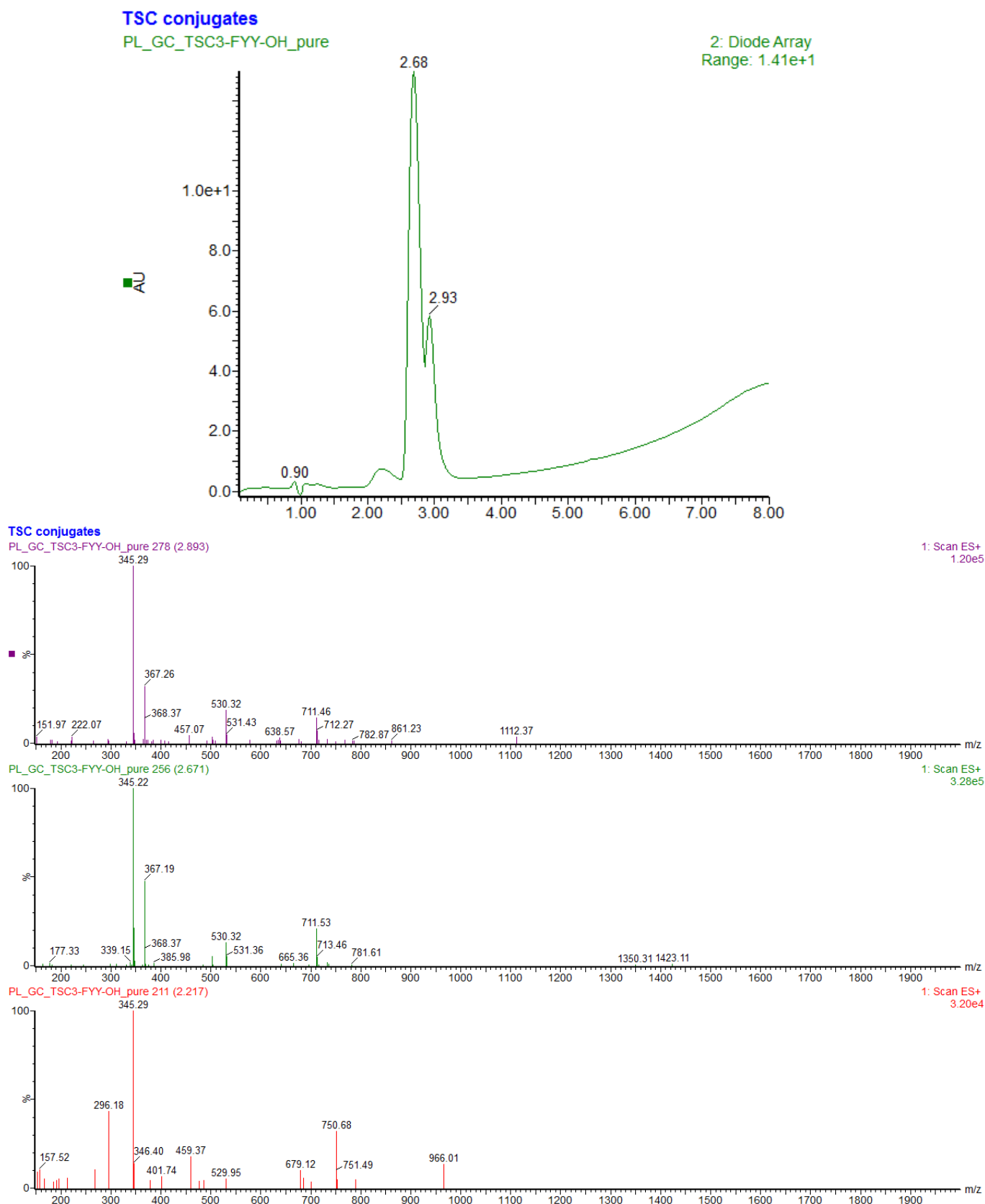
Figure SI 63. Chromatogram of **56** and MS spectra of the peaks found.

TSC-conjugates
TSC3-FWY-OH_ pure

2: Diode Array
Range: 6.135e+1
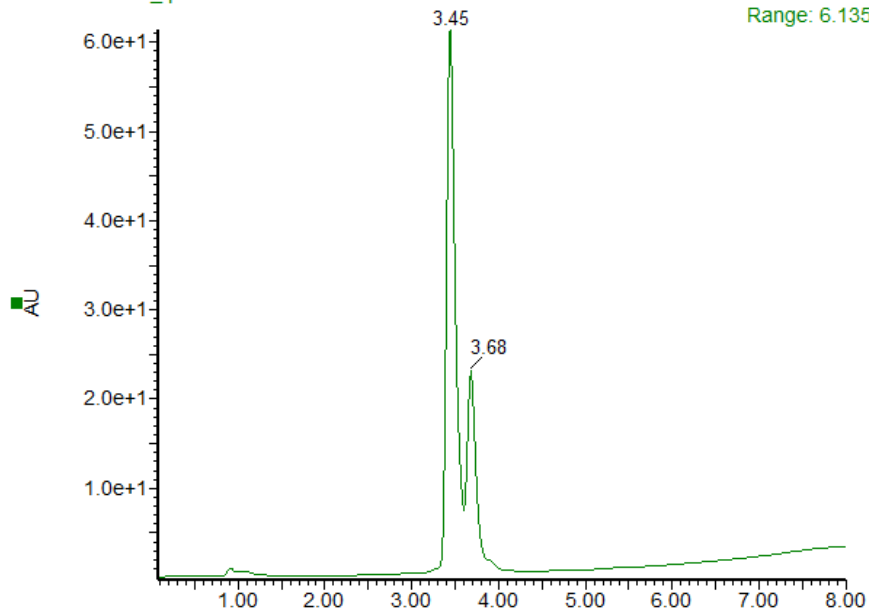
TSC-conjugates
TSC3-FWY-OH_ pure 354 (3.659)

1: Scan ES+
2.61e5
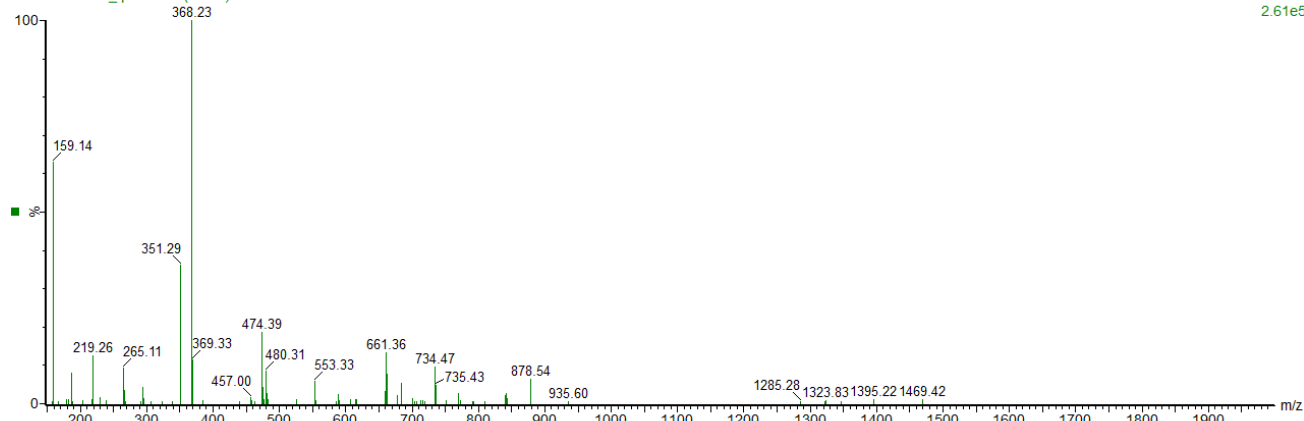
TSC3-FWY-OH_ pure 360 (3.720) Cm (330:368)

1: Scan ES+
3.03e5
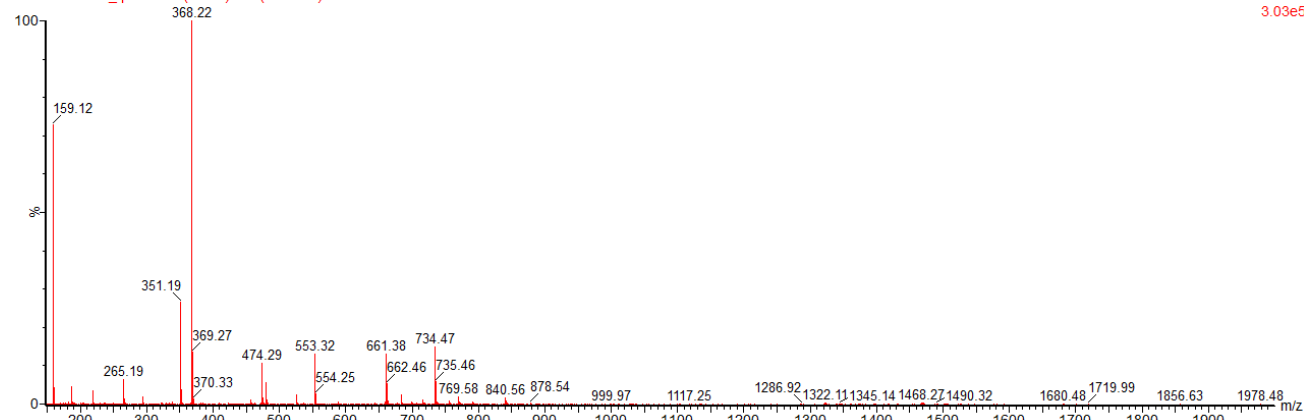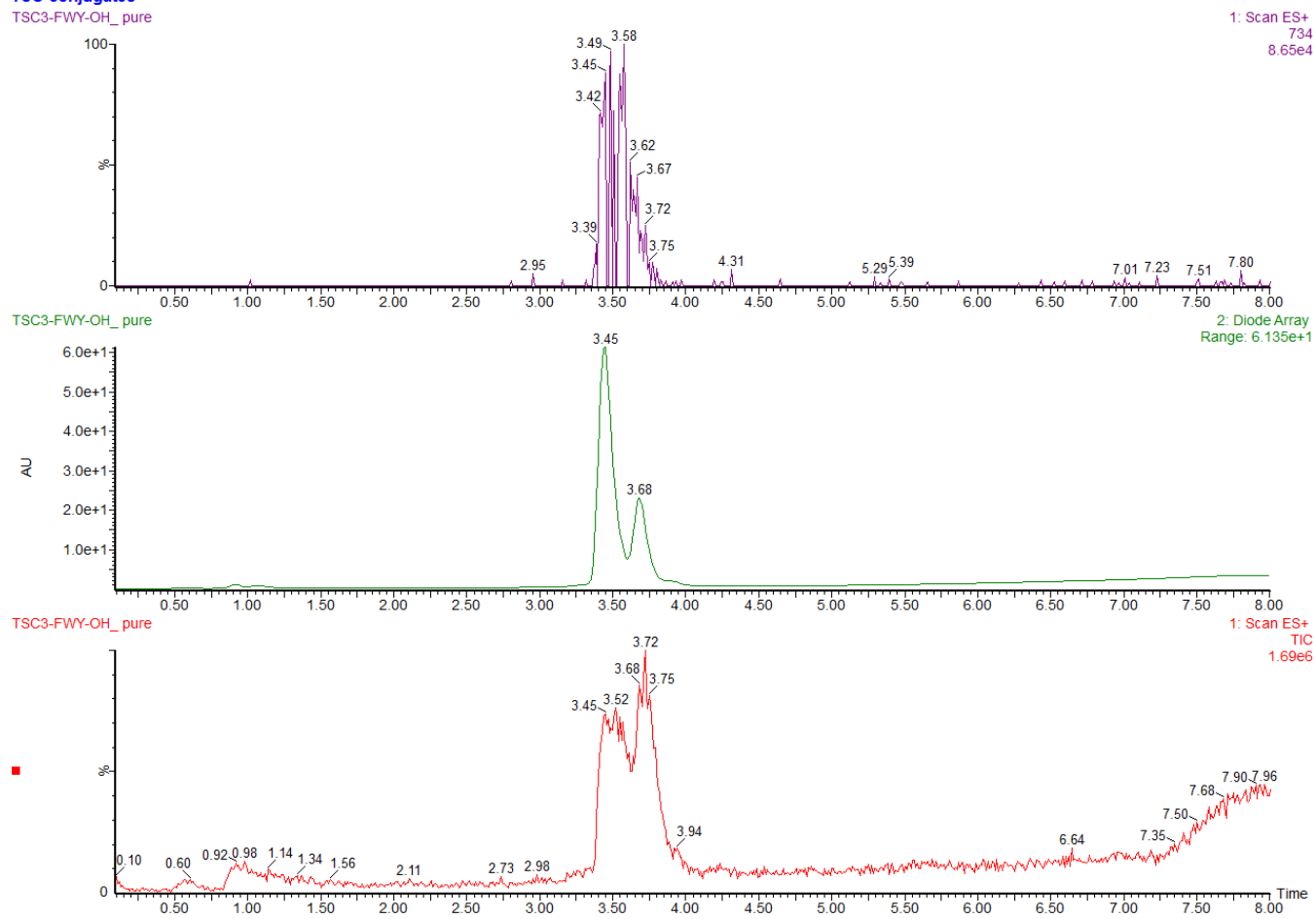
Figure SI 64. Chromatogram of **57** and MS spectra of the peaks found. The last set of spectra represents the search results of the signal *m/z*=734.

Chapter 2: Circular Dichroism (CD)

2.1   Analyses of compounds 8-9 and 11-26
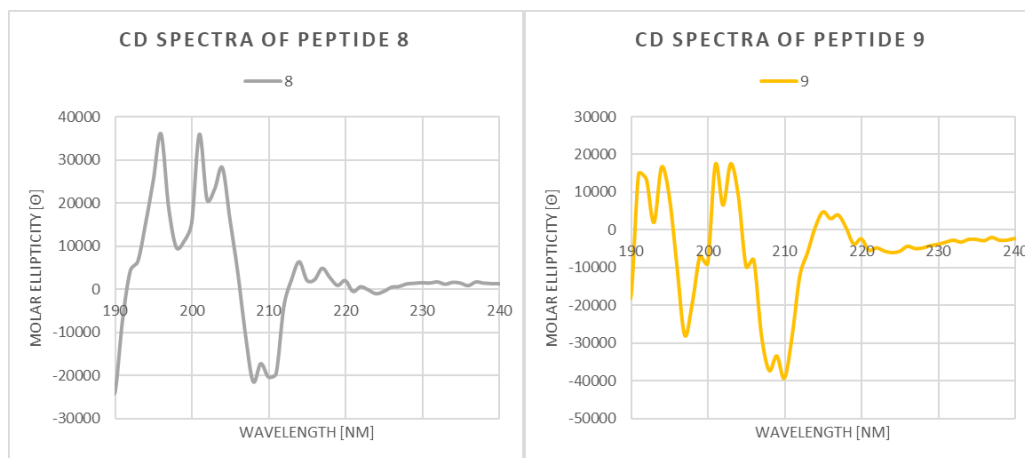
Figure SI 65. Single CD spectra registered for compounds **8** and **9**.
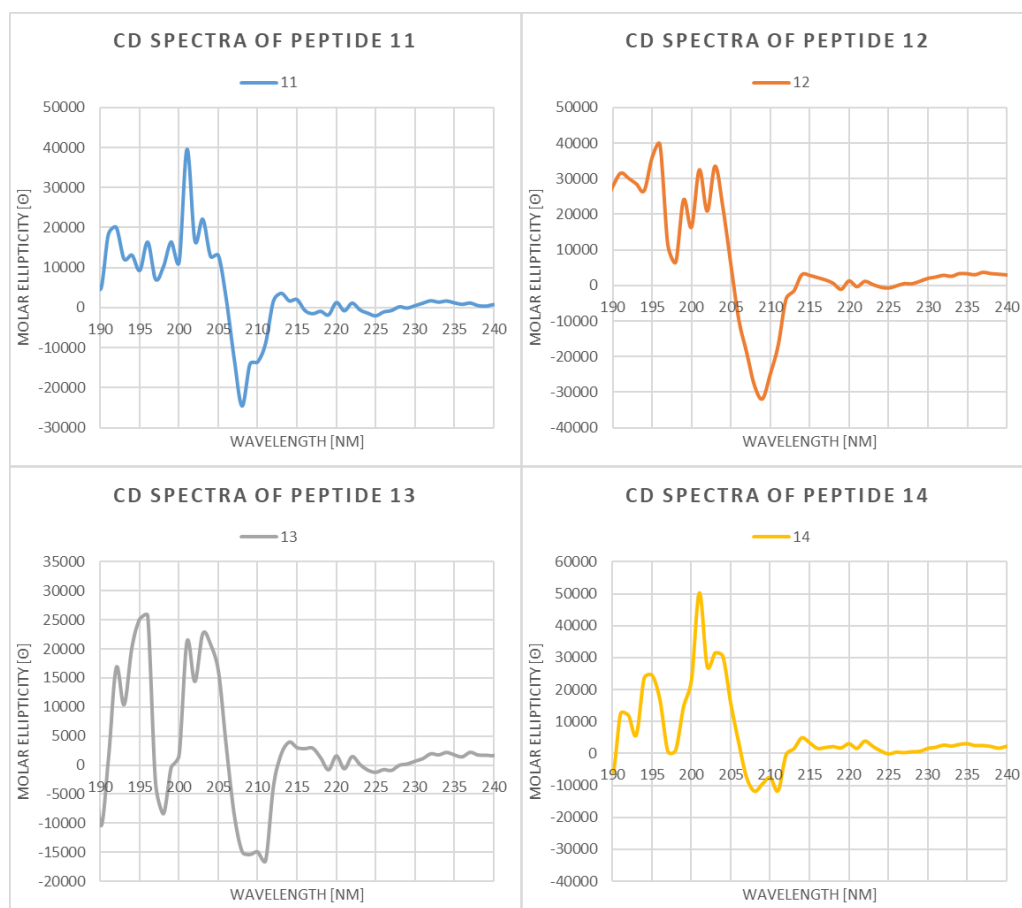
Figure SI 66. Single CD spectra registered for compounds **11-14**.
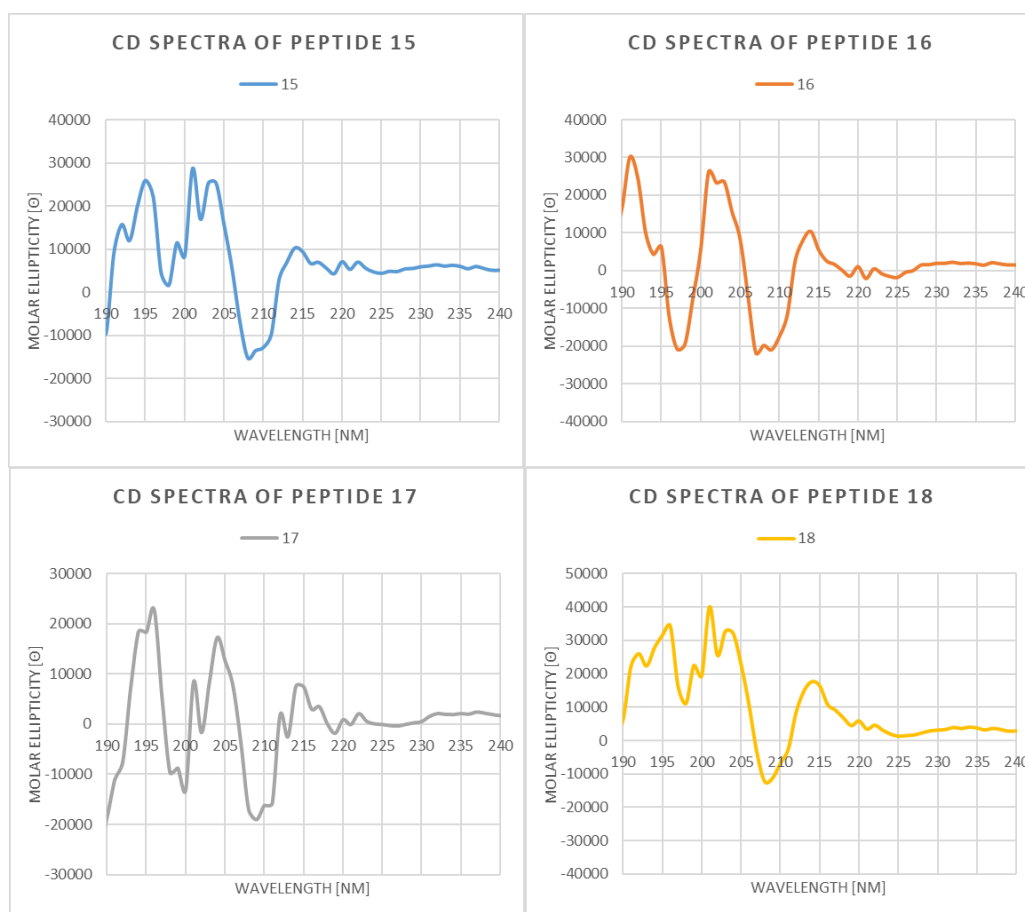
Figure SI 67. Single CD spectra registered for compounds **15-18**.
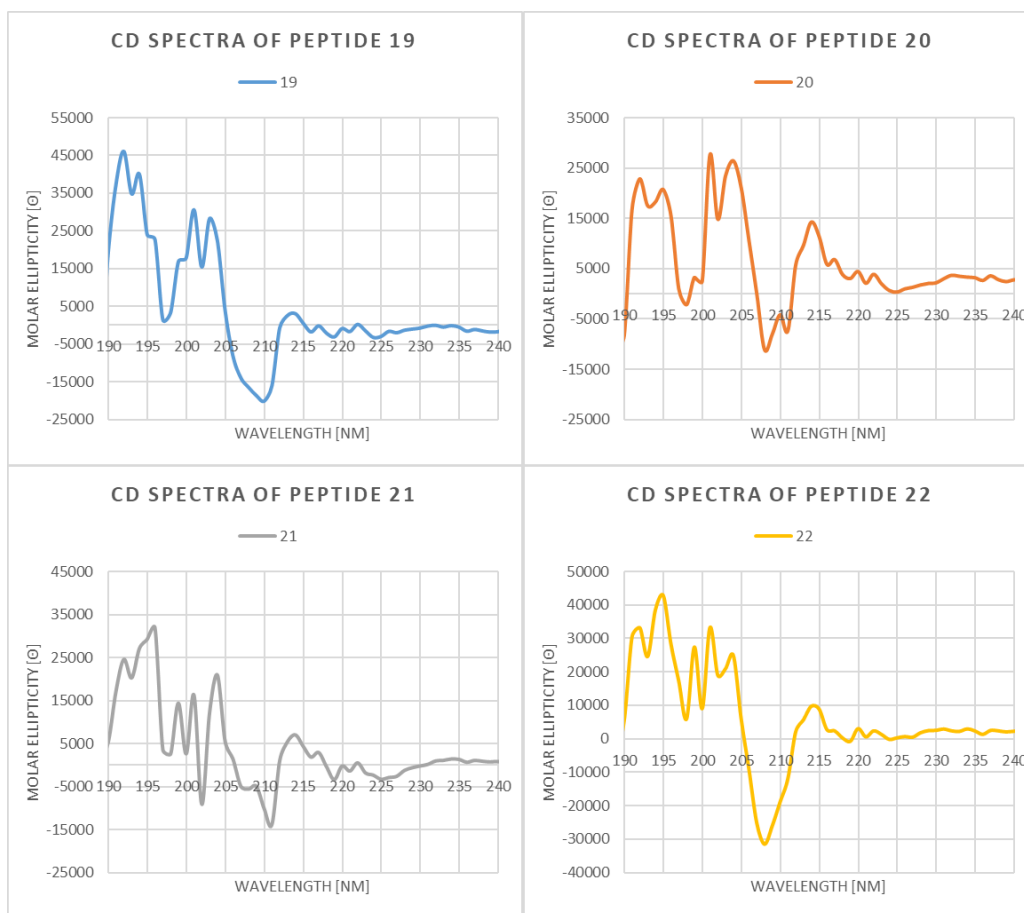
Figure SI 68. Single CD spectra registered for compounds **19-22**.
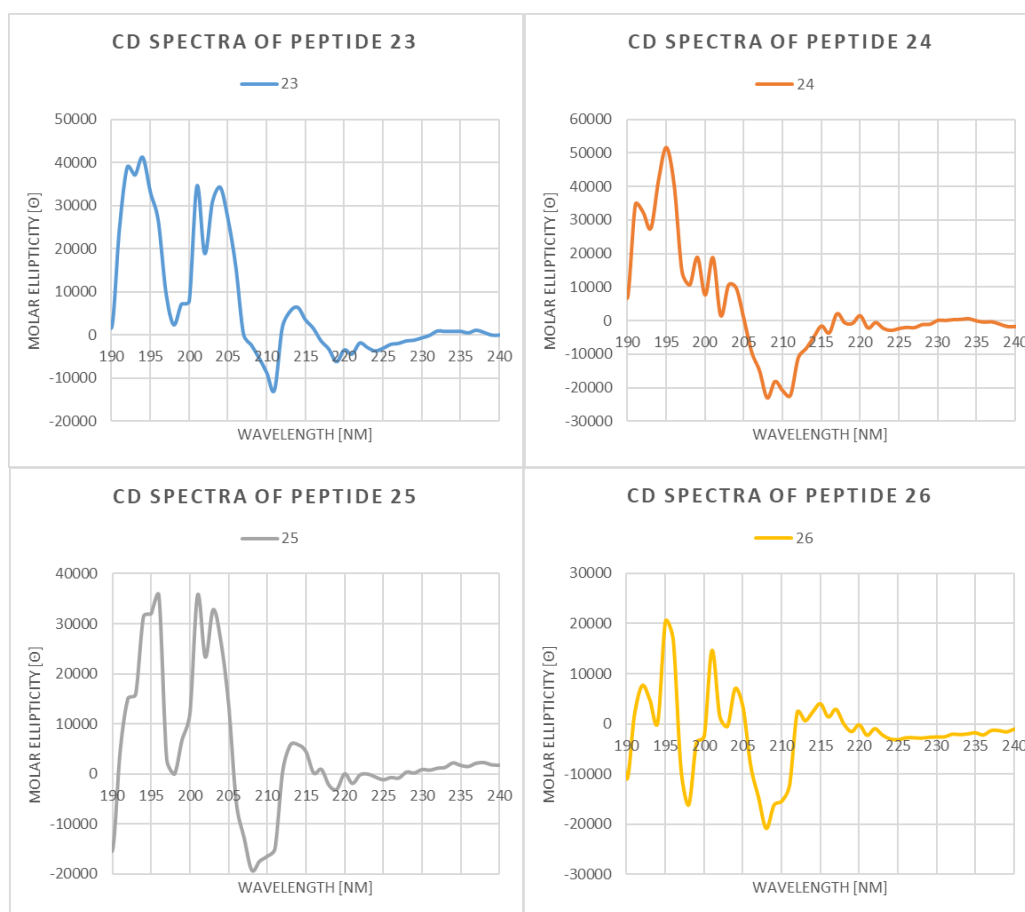
Figure SI 69. Single CD spectra registered for compounds **23-26**.

Chapter 3: Nuclear Magnetic Resonance (NMR)

3.1 ¹H-NMR of compound 3
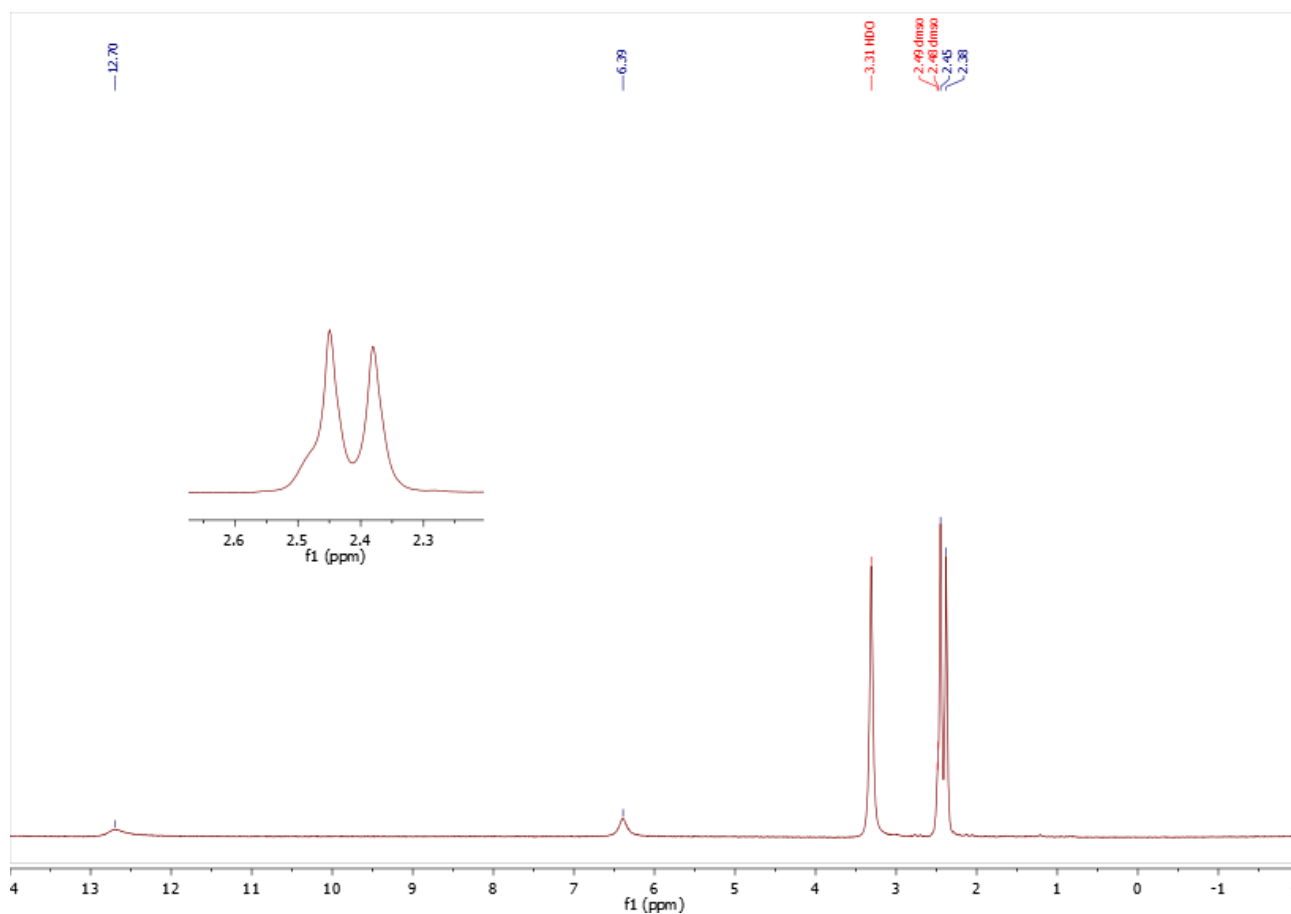
Figure SI 70. ¹H NMR spectra of 4,6-dimethylisoxazolo[3,4-*b*]pyridin-3(1*H*)-one **(3)** in DMSO-*d₆*.

Chemical shifts in ppm: δ=2.38 (s, 3H, CH₃), lit. 2.38; δ=2.45 (s, 3H, CH₃), lit. 2.45; δ=6.39 (s, 1H, CH), lit. 6.38; δ=12.70 (bs, 1H, NH), lit. 13.00. (b)s-(broad) singlet.

3.2 Chemical shifts values found in the spectra of compounds 4a-7a and 8-26

Table SI 1. Chemical shift values (ppm) from ^{1}H and ^{13}C spectra, assigned for building blocks **4a-7a.**

4a

	(C)H	(C)H2	(C)H3	C	C(H3	C(H)	C(H)2	C(H)3	COO(H)	Ca	Cb	Cc	Cd	Ce	Cg	H	Ha	Hb	Hc	Hd	He	Hg	NH(Het)
A	-	-	17.78	-	-	-	-	2.290	-	-	-	-	-	-	-	-	-	-	-	-	-	-	-
B	109.7	-	-	-	-	6.103	-	-	-	-	-	-	-	-	-	-	-	-	-	-	-	-	-
C	-	-	19.39	-	2.168	-	-	-	-	-	-	-	-	-	-	-	-	-	-	-	-	-	-
D	-	76.96	-	-	-	-	5.750	-	-	-	-	-	-	-	-	-	-	-	-	-	-	-	-
DMSO	-	-	-	39.45	-	-	-	-	-	-	-	-	-	-	2.501	-	-	-	-	-	-	-	-
E	-	72.32	-	-	-	-	5.771	-	-	-	-	-	-	-	-	-	-	-	-	-	-	-	-
F	-	64.37	-	-	-	-	3.655	-	-	-	-	-	-	-	-	-	-	-	-	-	-	-	-
Fmoc	46.42	65.36	-	-	-	4.219	4.279	-	-	125.1	126.9	127.4	120.0	-	-	-	7.718	7.331	7.422	7.896	-	-	-
L	28.18	-	-	-	-	1.791	-	-	-	-	-	-	-	-	-	-	-	-	-	-	-	-	-
Lys	-	-	-	-	-	-	-	-	8.207	38.07	28.19	-	30.20	53.58	22.74	-	3.204	1.613	-	1.727	3.853	1.438	7.627
M	-	-	20.21	-	-	-	-	0.9125	-	-	-	-	-	-	-	-	-	-	-	-	-	-	-

5a

	(C)H	(C)H2	(C)H3	C	C(H3	C(H)	C(H)2	C(H)3	C2	COO(H)	Ca	Cb	Cc	Cd	Ce	Cg	H	Ha	Hb	Hc	Hd	He	Hg	NH(Het)
A	-	-	17.75	-	-	-	-	2.277	-	-	-	-	-	-	-	-	-	-	-	-	-	-	-	-
B	110.0	-	-	-	-	6.104	-	-	-	-	-	-	-	-	-	-	-	-	-	-	-	-	-	-
C	-	-	19.40	-	2.160	-	-	2.180	-	-	-	-	-	-	-	-	-	-	-	-	-	-	-	-
D	-	74.01	-	-	-	-	5.876	-	-	-	-	-	-	-	-	-	-	-	-	-	-	-	-	-
DMSO	-	-	-	39.47	-	-	-	-	-	-	-	-	-	-	-	2.500	-	-	-	-	-	-	-	-
F	-	65.37	-	-	-	-	3.776	-	-	-	-	-	-	-	-	-	-	-	-	-	-	-	-	-
Fmoc	46.45	67.78	-	-	-	4.217	4.275	-	109.4	-	125.1	126.9	127.4	119.9	-	-	-	7.720	7.331	7.421	7.898	-	-	-
Lys	-	-	-	-	-	-	-	-	-	8.177	38.11	28.10	-	30.12	53.59	22.72	-	3.176	1.614	-	1.708	3.910	1.428	7.631

6a

	(C)H	(C)H2	(C)H3	C	C(H)	C(H)2	C(H)3	COO(H)	Ca	Cb	Cc	Cd	Ce	Cg	H	Ha	Hb	Hc	Hd	He	Hg	NH(Het)
A	-	-	17.77	-	-	-	2.296	-	-	-	-	-	-	-	-	-	-	-	-	-	-	-
B	110.4	-	-	-	6.152	-	-	-	-	-	-	-	-	-	-	-	-	-	-	-	-	-
C	-	-	19.44	-	-	-	2.195	-	-	-	-	-	-	-	-	-	-	-	-	-	-	-
D	-	75.98	-	-	-	5.854	-	-	-	-	-	-	-	-	-	-	-	-	-	-	-	-
DMSO	-	-	-	39.49	-	-	-	-	-	-	-	-	-	2.498	-	-	-	-	-	-	-	-
E	-	61.13	-	-	-	3.934	-	-	-	-	-	-	-	-	-	-	-	-	-	-	-	-
F	-	63.55	-	-	-	3.629	-	-	-	-	-	-	-	-	-	-	-	-	-	-	-	-
Fmoc	46.43	65.38	-	-	4.219	4.273	-	-	125.1	126.9	127.4	120.0	-	-	-	7.723	7.329	7.418	7.922	-	-	-
Lys	-	-	-	-	-	-	-	8.199	38.16	-	-	30.15	53.52	28.25	-	3.215	1.632	-	1.734	3.925	1.494	7.628

7a

	(C)H	(C)H2	(C)H3	C	C(H)	C(H)2	C(H)3	COO(H)	Ca	Cb	Cc	Cd	Ce	Cg	H	Ha	Hb	Hc	Hd	He	Hg	NH(Het)
A	-	-	17.72	-	-	-	2.327	-	-	-	-	-	-	-	-	-	-	-	-	-	-	-
B	109.6	-	-	-	6.074	-	-	-	-	-	-	-	-	-	-	-	-	-	-	-	-	-
C	-	-	19.23	-	-	-	2.143	-	-	-	-	-	-	-	-	-	-	-	-	-	-	-
D	-	69.33	-	-	-	5.761	-	-	-	-	-	-	-	-	-	-	-	-	-	-	-	-
DMSO	-	-	-	39.48	-	-	-	-	-	-	-	-	-	2.499	-	-	-	-	-	-	-	-
Fmoc	46.44	65.38	-	-	4.219	4.275	-	-	125.1	126.9	127.4	120.0	-	-	-	7.721	7.327	7.418	7.923	-	-	-
G	59.10	-	-	-	3.518	-	-	-	-	-	-	-	-	-	-	-	-	-	-	-	-	-
H+I	-	-	15.49	-	-	-	1.307	-	-	-	-	-	-	-	-	-	-	-	-	-	-	-
J	-	59.16	-	-	-	3.617	-	-	-	-	-	-	-	-	-	-	-	-	-	-	-	-
K	-	-	7.416	-	-	-	1.228	-	-	-	-	-	-	-	-	-	-	-	-	-	-	-
Lys	-	-	-	-	-	-	-	8.283	38.24	28.38	-	30.12	53.60	22.71	-	3.168	1.614	-	1.713	3.904	1.440	7.616

Table SI 2. Chemical shift values (ppm) from ^{1}H and ^{13}C spectra, assigned for unmodified peptides **8-9**.

8

	(C)OCH	-(C)H3	-C(H)3	C	C=O	CO(C)H	COCH3	CONH2a	CONH2b	Ca	Cb	Cd	Cg	H	Ha	Hb	Hb*	Hd	He	Hg	NH	NH2
DMSO	-	-	-	39.51	-	-	-	-	-	-	-	-	-	2.500	-	-	-	-	-	-	-	-
Gly	-	-	-	-	168.6	-	-	-	-	41.83	-	-	-	-	3.697	-	-	-	-	-	8.222	-
Lys	-	-	-	-	171.4	-	-	-	-	38.60	26.48	31.47	21.95	-	2.736	1.503	-	1.642	4.316	1.261	7.630	7.851
Met	169.9	14.52	2.029	-	171.8	22.36	1.854	-	-	52.15	31.16	-	29.47	-	4.255	1.798	1.900	-	-	2.469	8.143	-
Val	-	-	-	-	-	-	-	-	-	-	-	-	-	-	-	-	-	-	-	0.8288	-	-
Val1	-	-	-	-	171.2	-	-	-	-	57.92	29.93	-	18.90	-	4.135	1.995	-	-	-	-	7.913	-
Val2	-	-	-	-	172.7	-	-	7.036	7.350	57.30	30.34	-	18.00	-	4.096	1.939	-	-	-	-	7.585	-

9

	C	C=O	CO(C)H	COCH3	CONH2a	CONH2b	Ca	Cb	Cd	Ce	Cg	H	Ha	Hb	Hb*	Hd	Hd*	He	Hg	NH	NH2
DMSO	39.47	-	-	-	-	-	-	-	-	-	-	2.499	-	-	-	-	-	-	-	-	-
Gly	-	168.8	-	-	-	-	41.84	-	-	-	-	-	3.699	-	-	-	-	-	-	8.308	-
Lys	-	171.3	-	-	-	-	38.60	26.47	31.13	51.97	21.95	-	2.731	1.507	-	1.643	-	4.332	1.265	7.694	7.906
Pro	-	172.3	22.17	1.888	-	-	59.41	22.26	47.47	-	31.39	-	4.226	1.779	1.833	3.558	3.486	-	2.120	-	-
Val	-	-	-	-	-	-	-	-	-	-	-	-	-	-	-	-	-	-	0.8352	-	-
Val1	-	170.6	-	-	-	-	57.80	29.96	-	-	18.81	-	4.139	1.994	-	-	-	-	-	8.008	-
Val2	-	172.5	-	-	7.039	7.339	57.25	30.52	-	-	17.84	-	4.093	1.945	-	-	-	-	-	7.578	-

Table SI 3. Chemical shift values (ppm) from ^{1}H and ^{13}C spectra, assigned for modified peptide **10**.

10

	(C)H	(C)H2	(C)H3	C(H)	C(H)2	C(H)3	CON(H(	COO(H)	Ca	Cb	Cd	Ce	Cg	Ha	Hb	Hd	He	Hg	N(H)2	NH
A	-	-	17.65	-	-	2.399	-	-	-	-	-	-	-	-	-	-	-	-	-	-
B	111.9	-	-	6.188	-	-	-	-	-	-	-	-	-	-	-	-	-	-	-	-
C	-	-	19.78	-	-	2.280	-	-	-	-	-	-	-	-	-	-	-	-	-	-
D	-	72.54	-	-	5.789	-	-	-	-	-	-	-	-	-	-	-	-	-	-	-
Gly	-	-	-	-	-	-	-	-	42.24	-	-	-	-	3.908	-	-	-	-	-	8.525
Het	-	-	-	-	-	-	-	8.917	-	-	-	-	-	-	-	-	-	-	-	-
Lys	-	-	-	-	-	-	-	-	39.32	26.31	30.40	53.44	21.87	2.947	1.660	1.740	4.302	1.385	8.160	7.479
Pro	-	-	-	-	-	-	-	-	69.88	-	42.90	-	29.86	4.046	1.994	3.876	-	2.041	-	-
Val	-	-	-	-	-	-	-	-	-	29.88	-	-	-	-	1.988	-	-	0.9330	-	-
Val1	-	-	-	-	-	-	-	-	59.61	-	-	-	18.16	4.109	-	-	-	0.9090	-	8.279
Val2	-	-	-	-	-	-	7.098	-	59.37	-	-	-	17.72	4.029	-	-	-	0.8910	-	8.226

Table SI 4. Chemical shift values (ppm) from ^{1}H and ^{13}C spectra, assigned for modified peptides **11-14**.

11

	(C)H	(C)H2	(C)H3	(C)ONH	-(C)H3	-C(H)3	C(H)	C(H)2	C(H)3	C1	C2	C3	C4	C=O	CONH2	Ca	Cb	Cd	Ce	Cg	Ha	Hb	Hb*	Hd	He	Hg	NH	NH2
A	-	-	17.81	-	-	-	-	-	2.312	-	-	-	-	-	-	-	-	-	-	-	-	-	-	-	-	-	-	-
B	111.8	-	-	-	-	-	6.192	-	-	-	-	-	-	-	-	-	-	-	-	-	-	-	-	-	-	-	-	-
C	-	-	19.11	-	-	-	-	-	2.221	-	-	-	-	-	-	-	-	-	-	-	-	-	-	-	-	-	-	-
D	-	77.82	-	-	-	-	-	5.711	-	-	-	-	-	-	-	-	-	-	-	-	-	-	-	-	-	-	-	-
E	-	73.10	-	-	-	-	-	5.748	-	-	-	-	-	-	-	-	-	-	-	-	-	-	-	-	-	-	-	-
F	-	65.47	-	-	-	-	-	-	-	-	-	-	-	-	-	-	-	-	-	-	-	-	-	-	-	-	-	-
Gly	-	-	-	-	-	-	-	-	-	-	-	-	-	173.8	-	42.48	-	-	-	-	3.965	-	-	-	-	-	8.543	-
L	28.49	-	-	-	-	1.860	-	-	-	-	-	-	-	-	-	-	-	-	-	-	-	-	-	-	-	-	-	-
Lys	-	-	-	-	-	-	-	-	-	-	-	-	-	170.9	-	39.40	26.40	30.60	53.08	22.00	2.945	1.636	-	1.716	4.318	1.367	-	8.166
M	-	-	19.89	-	-	-	-	-	1.007	-	-	-	-	-	-	-	-	-	-	-	-	-	-	-	-	-	-	-
Met	-	-	-	-	14.05	2.104	-	-	-	-	-	-	-	166.3	-	-	26.72	-	-	29.26	-	1.805	1.859	-	-	2.658	8.951	-
Ring	-	-	-	-	-	-	-	-	-	109.7	144.1	154.2	155.4	-	-	-	-	-	-	-	-	-	-	-	-	-	-	-
Val	-	-	-	-	-	-	-	-	-	-	-	-	-	-	-	-	-	-	-	17.90	-	-	-	-	-	0.8978	-	-
Val1	-	-	-	-	-	-	-	-	-	-	-	-	-	173.5	-	59.65	30.22	-	-	-	4.094	2.171	-	-	-	-	8.238	-
Val2	-	-	-	175.7	-	-	-	-	-	-	-	-	-	-	7.090	59.41	29.89	-	-	17.85	4.045	2.014	-	-	-	-	7.623	-

12

	(C)H	(C)H2	(C)H3	(C)ONH	-(C)H3	-C(H)3	C(H)	C(H)2	C(H)3	C1	C2	C3	C4	C=O	CONH2	Ca	Cb	Cd	Ce	Cg	Ha	Hb	Hb*	Hd	He	Hg	NH	NH2
A	-	-	17.80	-	-	-	-	-	2.287	-	-	-	-	-	-	-	-	-	-	-	-	-	-	-	-	-	-	-
B	112.2	-	-	-	-	-	6.217	-	-	-	-	-	-	-	-	-	-	-	-	-	-	-	-	-	-	-	-	-
C	-	-	19.49	-	-	-	-	-	2.254	-	-	-	-	-	-	-	-	-	-	-	-	-	-	-	-	-	-	-
D	-	77.10	-	-	-	-	-	5.842	-	-	-	-	-	-	-	-	-	-	-	-	-	-	-	-	-	-	-	-
E	-	-	-	-	-	-	-	6.360	-	-	-	-	-	-	-	-	-	-	-	-	-	-	-	-	-	-	-	-
F	-	-	-	-	-	-	-	6.074	-	-	-	-	-	-	-	-	-	-	-	-	-	-	-	-	-	-	-	-
Gly	-	-	-	-	-	-	-	-	-	-	-	-	-	173.7	-	42.36	-	-	-	-	3.971	-	-	-	-	-	8.535	-
Lys	-	-	-	-	-	-	-	-	-	-	-	-	-	171.0	-	39.40	26.41	30.57	53.01	21.87	2.932	1.623	-	1.725	4.366	1.370	7.479	8.177
Met	-	-	-	-	14.13	2.122	-	-	-	-	-	-	-	166.5	-	64.16	30.41	-	-	29.24	3.862	2.048	2.373	-	-	2.676	8.949	-
Ring	-	-	-	-	-	-	-	-	-	109.8	144.2	155.1	155.8	-	-	-	-	-	-	-	-	-	-	-	-	-	-	-
Val	-	-	-	-	-	-	-	-	-	-	-	-	-	-	-	-	-	-	-	17.88	-	-	-	-	-	0.8792	-	-
Val1	-	-	-	-	-	-	-	-	-	-	-	-	-	173.7	-	59.66	30.21	-	-	18.37	4.079	2.101	-	-	-	-	8.230	-
Val2	-	-	-	175.8	-	-	-	-	-	-	-	-	-	-	7.083	59.41	29.96	-	-	17.88	4.029	1.991	-	-	-	-	7.615	-

13

	(C)H	(C)H2	(C)H3	(C)ONH	-(C)H3	-C(H)3	C(H)	C(H)2	C(H)3	C1	C2	C3	C4	C=O	CONH2	Ca	Cb	Cd	Ce	Cg	Ha	Hb	Hb*	Hd	He	Hg	NH	NH2
A	-	-	19.67	-	-	-	-	-	2.287	-	-	-	-	-	-	-	-	-	-	-	-	-	-	-	-	-	-	-
B	112.2	-	-	-	-	-	6.217	-	-	-	-	-	-	-	-	-	-	-	-	-	-	-	-	-	-	-	-	-
C	-	-	19.02	-	-	-	-	-	2.254	-	-	-	-	-	-	-	-	-	-	-	-	-	-	-	-	-	-	-
D	-	77.10	-	-	-	-	-	5.842	-	-	-	-	-	-	-	-	-	-	-	-	-	-	-	-	-	-	-	-
E	-	-	-	-	-	-	-	6.360	-	-	-	-	-	-	-	-	-	-	-	-	-	-	-	-	-	-	-	-
F	-	-	-	-	-	-	-	6.074	-	-	-	-	-	-	-	-	-	-	-	-	-	-	-	-	-	-	-	-
Gly	-	-	-	-	-	-	-	-	-	-	-	-	-	173.7	-	42.36	-	-	-	-	3.971	-	-	-	-	-	8.535	-
Lys	-	-	-	-	-	-	-	-	-	-	-	-	-	171.0	-	39.40	26.41	30.57	53.01	21.87	2.932	1.623	-	1.725	4.366	1.370	7.479	8.177
Met	-	-	-	-	14.13	2.122	-	-	-	-	-	-	-	166.5	-	64.16	30.41	-	-	29.24	3.862	2.048	2.373	-	-	2.676	8.949	-
Ring	-	-	-	-	-	-	-	-	-	109.8	144.2	155.1	155.8	-	-	-	-	-	-	-	-	-	-	-	-	-	-	-
Val	-	-	-	-	-	-	-	-	-	-	-	-	-	-	-	-	-	-	-	17.88	-	-	-	-	-	0.8792	-	-
Val1	-	-	-	-	-	-	-	-	-	-	-	-	-	173.7	-	59.66	30.21	-	-	18.37	4.079	2.101	-	-	-	-	8.230	-
Val2	-	-	-	175.8	-	-	-	-	-	-	-	-	-	-	7.083	59.41	29.96	-	-	17.88	4.029	1.991	-	-	-	-	7.615	-

14

	(C)H	(C)H2	(C)H3	C(H)	C(H)2	C(H)3	Ca	Cb	Cd	Ce	Cg	Ha	Hb	Hd	He	Hg	NH	NH2
A	-	-	-	-	-	2.303	-	-	-	-	-	-	-	-	-	-	-	-
B	111.6	-	-	6.174	-	-	-	-	-	-	-	-	-	-	-	-	-	-
D	-	70.27	-	-	5.720	-	-	-	-	-	-	-	-	-	-	-	-	-
G	60.36	-	-	3.582	-	-	-	-	-	-	-	-	-	-	-	-	-	-
Gly	-	-	-	-	-	-	42.41	-	-	-	-	3.952	-	-	-	-	8.549	-
H+I	-	-	15.53	-	-	1.372	-	-	-	-	-	-	-	-	-	-	-	-
J	-	60.37	-	-	3.711	-	-	-	-	-	-	-	-	-	-	-	-	-
K	-	-	7.262	-	-	1.290	-	-	-	-	-	-	-	-	-	-	-	-
Lys	-	-	-	-	-	-	39.40	26.27	30.56	53.42	21.96	2.935	1.628	1.720	4.310	1.354	7.492	8.159
Met	-	-	14.04	-	-	2.095	-	-	-	-	29.17	4.622	-	-	-	2.658	9.011	-
Val	-	-	-	-	-	-	-	-	-	-	17.80	-	-	-	-	0.9061	-	-
Val1	-	-	-	-	-	-	59.67	30.18	-	-	18.14	4.075	2.073	-	-	2.299	8.240	-
Val2	-	-	-	-	-	-	59.39	30.02	-	-	19.02	4.038	2.066	-	-	-	-	-

Table SI 5. Chemical shift values (ppm) from ^{1}H and ^{13}C spectra, assigned for modified peptides **15-18**.

15

	(C)H	(C)H2	(C)H3	C(H)	C(H)2	C(H)3	C2	C3	Ca	Cb	Cd	Ce	Cg	Ha	Hb	Hd	Hd*	He	Hg	NH	NH2
A	-	-	18.09	-	-	2.285	-	-	-	-	-	-	-	-	-	-	-	-	-	-	-
B	111.3	-	-	6.216	-	-	-	-	-	-	-	-	-	-	-	-	-	-	-	-	-
C	-	-	-	-	-	2.171	-	-	-	-	-	-	-	-	-	-	-	-	-	-	-
D	-	77.80	-	-	5.730	-	-	-	-	-	-	-	-	-	-	-	-	-	-	-	-
E	-	72.99	-	-	5.768	-	-	-	-	-	-	-	-	-	-	-	-	-	-	-	-
F	-	-	-	-	6.132	-	-	-	-	-	-	-	-	-	-	-	-	-	-	-	-
Gly	-	-	-	-	-	-	-	-	42.43	-	-	-	-	3.957	-	-	-	-	-	8.597	-
L	27.90	-	-	1.835	-	-	-	-	-	-	-	-	-	-	-	-	-	-	-	-	-
Lys	-	-	-	-	-	-	-	-	39.40	26.50	30.76	53.42	21.94	2.937	1.629	1.721	-	4.317	1.366	7.496	8.121
M	-	-	19.59	-	-	0.9980	-	-	-	-	-	-	-	-	-	-	-	-	-	-	-
Pro	-	-	-	-	-	-	-	-	60.86	24.34	48.49	-	29.86	4.400	1.971	3.522	3.449	-	2.373	-	-
Ring	-	-	-	-	-	-	143.5	152.6	-	-	-	-	-	-	-	-	-	-	-	-	-
Val	-	-	-	-	-	-	-	-	-	-	-	-	17.91	-	-	-	-	-	0.9063	-	-
Val1	-	-	-	-	-	-	-	-	59.59	30.02	-	-	-	4.092	2.018	-	-	-	-	8.270	-
Val2	-	-	-	-	-	-	-	-	59.35	-	-	-	-	4.043	2.006	-	-	-	-	-	-

16

	(C)H	(C)H2	(C)H3	C(H)	C(H)2	C(H)3	C2	C3	Ca	Cb	Cd	Ce	Cg	Ha	Hb	Hd	Hd*	He	Hg	NH	NH2
A	-	-	18.25	-	-	2.323	-	-	-	-	-	-	-	-	-	-	-	-	-	-	-
B	110.7	-	-	6.233	-	-	-	-	-	-	-	-	-	-	-	-	-	-	-	-	-
C	-	-	21.34	-	-	2.234	-	-	-	-	-	-	-	-	-	-	-	-	-	-	-
D	-	75.53	-	5.873	-	-	-	-	-	-	-	-	-	-	-	-	-	-	-	-	-
E	-	-	-	6.681	-	-	-	-	-	-	-	-	-	-	-	-	-	-	-	-	-
F	111.4	-	-	6.173	-	-	-	-	-	-	-	-	-	-	-	-	-	-	-	-	-
Gly	-	-	-	-	-	-	-	-	42.36	-	-	-	-	3.894	-	-	-	-	-	8.594	-
Lys	-	-	-	-	-	-	-	-	39.38	26.29	30.79	54.19	21.84	2.945	1.640	1.724	-	4.315	1.367	7.508	8.160
Pro	-	-	-	-	-	-	-	-	60.80	24.24	48.48	-	-	4.397	1.981	3.509	3.450	-	2.062	-	-
Ring	-	-	-	-	-	-	143.7	153.7	-	-	-	-	-	-	-	-	-	-	-	-	-
Val	-	-	-	-	-	-	-	-	-	-	-	-	17.88	-	-	-	-	-	0.8784	-	-
Val1	-	-	-	-	-	-	-	-	59.58	29.98	-	-	-	4.085	2.017	-	-	-	-	8.278	-
Val2	-	-	-	-	-	-	-	-	59.03	-	-	-	-	4.065	2.009	-	-	-	-	8.271	-

17

	(C)H	(C)H2	(C)H3	C(H)	C(H)2	C(H)3	C1	C2	C3	Ca	Cb	Cd	Cd*	Ce	Cg	Ha	Ha*	Hb	Hb*	Hd	Hd*	He	Hg	NH	NH2
A	-	-	17.95	-	-	2.317	-	-	-	-	-	-	-	-	-	-	-	-	-	-	-	-	-	-	-
B	111.5	-	-	6.258	-	-	-	-	-	-	-	-	-	-	-	-	-	-	-	-	-	-	-	-	-
C	-	-	18.30	-	-	2.186	-	-	-	-	-	-	-	-	-	-	-	-	-	-	-	-	-	-	-
D	-	76.70	-	-	5.889	-	-	-	-	-	-	-	-	-	-	-	-	-	-	-	-	-	-	-	-
E	-	-	-	6.264	6.252	-	-	-	-	-	-	-	-	-	-	-	-	-	-	-	-	-	-	-	-
F	-	-	-	6.179	-	-	-	-	-	-	-	-	-	-	-	-	-	-	-	-	-	-	-	-	-
Gly	-	-	-	-	-	-	-	-	-	42.24	-	-	-	-	-	3.994	3.956	-	-	-	-	-	-	8.593	-
Lys	-	-	-	-	-	-	-	-	-	39.40	26.28	30.57	-	53.36	21.97	2.938	-	1.622	-	1.724	-	4.297	1.358	7.495	8.156
Pro	-	-	-	-	-	-	-	-	-	61.42	24.16	46.19	47.59	-	29.86	4.406	-	1.967	1.905	3.624	3.579	-	2.116	-	-
Ring	-	-	-	-	-	-	110.8	143.7	153.1	-	-	-	-	-	-	-	-	-	-	-	-	-	-	-	-
Val	-	-	-	-	-	-	-	-	-	-	-	-	-	-	17.82	-	-	-	-	-	-	-	0.8984	-	-
Val1	-	-	-	-	-	-	-	-	-	59.68	30.26	-	-	-	18.31	4.080	-	2.022	-	-	-	-	-	8.266	-
Val2	-	-	-	-	-	-	-	-	-	59.46	29.95	-	-	-	17.96	4.032	-	2.004	-	-	-	-	-	-	-

18

	(C)H	(C)H2	(C)H3	C(H)	C(H)2	C(H)3	C2	C3	Ca	Cb	Cd	Ce	Cg	Ha	Hb	Hd	Hd*	He	Hg	NH	NH2
A	-	-	17.93	-	-	2.312	-	-	-	-	-	-	-	-	-	-	-	-	-	-	-
B	111.3	-	-	6.217	-	-	-	-	-	-	-	-	-	-	-	-	-	-	-	-	-
C	-	-	-	-	-	2.183	-	-	-	-	-	-	-	-	-	-	-	-	-	-	-
D	-	70.36	-	-	5.715	-	-	-	-	-	-	-	-	-	-	-	-	-	-	-	-
G	-	-	-	3.622	-	-	-	-	-	-	-	-	-	-	-	-	-	-	-	-	-
Gly	-	-	-	-	-	-	-	-	42.32	-	-	-	-	3.954	-	-	-	-	-	8.584	-
H+I	-	-	15.63	-	-	1.360	-	-	-	-	-	-	-	-	-	-	-	-	-	-	-
J	-	60.42	-	-	3.737	-	-	-	-	-	-	-	-	-	-	-	-	-	-	-	-
K	-	-	-	-	-	1.300	-	-	-	-	-	-	-	-	-	-	-	-	-	-	-
Lys	-	-	-	-	-	-	-	-	39.41	26.27	30.53	53.29	21.91	2.930	1.618	1.713	-	4.311	1.392	7.497	8.142
Pro	-	-	-	-	-	-	-	-	-	24.25	48.65	-	29.96	4.434	1.970	3.537	3.489	-	2.396	-	-
Ring	-	-	-	-	-	-	143.2	152.6	-	-	-	-	-	-	-	-	-	-	-	-	-
Val	-	-	-	-	-	-	-	-	-	-	-	-	18.10	-	-	-	-	-	0.8994	-	-
Val1	-	-	-	-	-	-	-	-	59.58	30.00	-	-	-	4.085	2.013	-	-	-	-	8.269	-
Val2	-	-	-	-	-	-	-	-	59.40	-	-	-	-	4.040	1.994	-	-	-	-	-	-

Table SI 6. Chemical shift values (ppm) from ^{1}H and ^{13}C spectra, assigned for modified peptides **19-22**.

19

	(C)H	(C)H2	(C)H3	C(H)	C(H)2	C(H)3	COCH3	Ca	Cb	Cd	Ce	Cg	Ha	Hb	Hd	He	Hg	NH	NH(Het)
A	-	-	18.37	-	-	2.290	-	-	-	-	-	-	-	-	-	-	-	-	-
B	-	-	-	6.164	-	-	-	-	-	-	-	-	-	-	-	-	-	-	-
C	-	-	19.05	-	-	2.196	-	-	-	-	-	-	-	-	-	-	-	-	-
D	-	77.87	-	-	5.700	-	-	-	-	-	-	-	-	-	-	-	-	-	-
E	-	73.08	-	-	5.757	-	-	-	-	-	-	-	-	-	-	-	-	-	-
F	-	65.38	-	-	3.638	-	-	-	-	-	-	-	-	-	-	-	-	-	-
Gly	-	-	-	-	-	-	-	65.75	-	-	-	-	3.599	-	-	-	-	8.557	-
L	28.42	-	-	1.860	-	-	-	-	-	-	-	-	-	-	-	-	-	-	-
Lys	-	-	-	-	-	-	-	39.60	27.83	30.70	53.61	22.33	3.315	1.593	1.790	4.353	1.391	8.503	8.367
M	-	-	20.09	-	-	0.9900	-	-	-	-	-	-	-	-	-	-	-	-	-
Met	-	-	14.32	-	-	2.037	1.967	42.78	-	-	-	29.50	3.813	2.037	-	-	2.571	8.489	-
Val	-	-	-	-	-	-	-	-	-	-	-	18.05	-	-	-	-	0.8998	-	-
Val1	-	-	-	-	-	-	-	59.78	30.14	-	-	-	4.065	2.030	-	-	-	8.211	-
Val2	-	-	-	-	-	-	-	59.59	-	-	-	-	4.086	1.992	-	-	-	8.168	-

20

	(C)H	(C)H2	(C)H3	C(H)	C(H)2	C(H)3	COCH3	CONH2	Ca	Cb	Cd	Ce	Cg	Ha	Hb	Hd	He	Hg	NH	NH(Het)
A	-	-	18.37	-	-	2.274	-	-	-	-	-	-	-	-	-	-	-	-	-	-
B	111.6	-	-	6.175	-	-	-	-	-	-	-	-	-	-	-	-	-	-	-	-
C	-	-	19.07	-	-	2.173	-	-	-	-	-	-	-	-	-	-	-	-	-	-
D	-	75.54	-	-	5.832	-	-	-	-	-	-	-	-	-	-	-	-	-	-	-
F	-	69.21	-	-	3.819	-	-	-	-	-	-	-	-	-	-	-	-	-	-	-
Gly	-	-	-	-	-	-	-	-	-	-	-	-	-	-	-	-	-	-	8.532	-
Lys	-	-	-	-	-	-	-	-	-	27.77	30.96	53.65	22.37	3.298	1.581	1.745	4.347	1.354	8.024	8.372
Met	-	-	14.37	-	-	2.055	1.965	-	42.84	-	-	-	29.55	3.898	2.036	-	-	2.582	8.497	-
Val	-	-	-	-	-	-	-	-	-	-	-	-	18.11	-	-	-	-	0.9088	-	-
Val1	-	-	-	-	-	-	-	-	59.91	30.33	-	-	-	4.061	2.007	-	-	-	8.217	-
Val2	-	-	-	-	-	-	-	7.692	59.64	-	-	-	-	4.093	-	-	-	-	8.178	-

21

	(C)H	(C)H2	(C)H3	(CH)2	C(H)	C(H)2	C(H)3	COCH3	CONH2	Ca	Cb	Cd	Ce	Cg	Ha	Hb	Hd	He	Hg	NH	NH(Het)
A	-	-	18.16	-	-	-	2.247	-	-	-	-	-	-	-	-	-	-	-	-	-	-
B	111.8	-	-	-	6.163	-	-	-	-	-	-	-	-	-	-	-	-	-	-	-	-
C	-	-	18.79	-	-	-	2.147	-	-	-	-	-	-	-	-	-	-	-	-	-	-
D	-	76.84	-	-	-	5.796	-	-	-	-	-	-	-	-	-	-	-	-	-	-	-
E	-	61.72	-	-	-	-	-	-	-	-	-	-	-	-	-	-	-	-	-	-	-
E(a)	-	-	-	3.964	-	-	-	-	-	-	-	-	-	-	-	-	-	-	-	-	-
E(b)	-	-	-	4.215	-	-	-	-	-	-	-	-	-	-	-	-	-	-	-	-	-
F	-	64.16	-	-	-	-	-	-	-	-	-	-	-	-	-	-	-	-	-	-	-
F(a)	-	-	-	3.665	-	-	-	-	-	-	-	-	-	-	-	-	-	-	-	-	-
F(b)	-	-	-	3.806	-	-	-	-	-	-	-	-	-	-	-	-	-	-	-	-	-
Gly	-	-	-	-	-	-	-	-	-	-	-	-	-	-	3.272	-	-	-	-	8.503	-
Lys	-	-	-	-	-	-	-	-	-	39.40	27.54	30.57	53.27	22.11	3.277	1.549	1.738	4.338	1.345	-	8.321
Met	-	-	14.08	-	-	-	2.005	1.969	-	42.57	-	-	-	29.13	3.849	2.002	-	-	2.520	8.444	-
Val	-	-	-	-	-	-	-	-	-	-	-	-	-	17.72	-	-	-	-	0.8675	-	-
Val1	-	-	-	-	-	-	-	-	-	59.73	30.03	-	-	-	4.012	1.976	-	-	-	8.169	-
Val2	-	-	-	-	-	-	-	-	7.978	59.36	-	-	-	-	4.044	1.972	-	-	-	8.127	-

22

	(C)H	(C)H2	(C)H3	C(H)	C(H)2	C(H)3	Ca	Cb	Cd	Ce	Cg	Ha	Hb	Hd	He	Hg	NH	NH(Het)
A	-	-	17.49	-	-	2.286	-	-	-	-	-	-	-	-	-	-	-	-
B	111.1	-	-	6.151	-	-	-	-	-	-	-	-	-	-	-	-	-	-
C	-	-	18.42	-	-	2.153	-	-	-	-	-	-	-	-	-	-	-	-
D	-	69.51	-	-	5.708	-	-	-	-	-	-	-	-	-	-	-	-	-
G	60.23	-	-	3.545	-	-	-	-	-	-	-	-	-	-	-	-	-	-
Gly	-	-	-	-	-	-	-	-	-	-	-	4.281	-	-	-	-	8.024	-
H+I	-	-	15.07	-	-	1.363	-	-	-	-	-	-	-	-	-	-	-	-
J	-	60.23	-	-	3.718	-	-	-	-	-	-	-	-	-	-	-	-	-
K	-	-	6.973	-	-	1.285	-	-	-	-	-	-	-	-	-	-	-	-
Lys	-	-	-	-	-	-	39.34	27.39	30.40	53.25	22.41	3.307	1.577	1.741	4.383	-	8.621	8.365
Met	-	-	-	-	-	1.993	42.36	-	-	-	29.09	3.913	-	-	-	2.578	8.491	-
Val	-	-	-	-	-	-	-	-	-	-	17.68	-	-	-	-	0.9463	-	-
Val1	-	-	-	-	-	-	-	29.76	-	-	-	4.032	-	-	-	-	8.213	-
Val2	-	-	-	-	-	-	59.28	-	-	-	-	4.084	-	-	-	-	8.166	-

Table SI 7. Chemical shift values (ppm) from ¹H and ¹³C spectra, assigned for modified peptides **23-26**.

23

	(C)H	(C)H2	(C)H3	C(H)	C(H)2	C(H)3	CO(C)H	COC(H)	CONH2	Ca	Cb	Cd	Ce	Cg	Ha	Hb	Hb*	Hd	He	Hg	NH	NH(Het)
A	-	-	17.60	-	-	2.269	-	-	-	-	-	-	-	-	-	-	-	-	-	-	-	-
B	111.2	-	-	6.147	-	-	-	-	-	-	-	-	-	-	-	-	-	-	-	-	-	-
C	-	-	18.84	-	-	2.187	-	-	-	-	-	-	-	-	-	-	-	-	-	-	-	-
D	-	77.42	-	-	5.675	-	-	-	-	-	-	-	-	-	-	-	-	-	-	-	-	-
E	-	72.67	-	-	5.708	-	-	-	-	-	-	-	-	-	-	-	-	-	-	-	-	-
F	-	65.02	-	-	3.584	-	-	-	-	-	-	-	-	-	-	-	-	-	-	-	-	-
Gly	-	-	-	-	-	-	-	-	-	42.56	-	-	-	-	3.747	-	-	-	-	-	8.192	-
L	28.09	-	-	1.771	-	-	-	-	-	-	-	-	-	-	-	-	-	-	-	-	-	-
Lys	-	-	-	-	-	-	-	-	-	39.34	27.57	30.87	54.90	22.35	3.299	1.575	-	1.675	4.107	1.331	8.525	7.657
M	-	-	19.61	-	-	0.9808	-	-	-	-	-	-	-	-	-	-	-	-	-	1.994	-	-
Pro	-	-	-	-	-	-	24.07	1.950	-	60.16	21.26	47.67	-	29.71	4.323	1.965	2.079	3.500	-	1.994	-	-
Val1	-	-	-	-	-	-	-	-	-	59.60	29.00	-	-	17.77	4.054	1.840	-	-	-	0.8803	8.055	-
Val2	-	-	-	-	-	-	-	-	7.722	59.32	29.54	-	-	16.38	4.021	1.917	-	-	-	0.9470	7.928	-

24

	(C)H	(C)H2	(C)H3	C(H)	C(H)2	C(H)3	CO(C)H	COC(H)	Ca	Cb	Cd	Ce	Cg	Ha	Hb	Hd	Hd*	He	Hg	NH
A	-	-	17.58	-	-	2.276	-	-	-	-	-	-	-	-	-	-	-	-	-	-
B	111.2	-	-	6.161	-	-	-	-	-	-	-	-	-	-	-	-	-	-	-	-
C	-	-	18.70	-	-	2.192	-	-	-	-	-	-	-	-	-	-	-	-	-	-
D	-	75.13	-	-	5.817	-	-	-	-	-	-	-	-	-	-	-	-	-	-	-
F	-	68.77	-	-	3.606	-	-	-	-	-	-	-	-	-	-	-	-	-	-	-
Gly	-	-	-	-	-	-	-	-	42.34	-	-	-	-	3.836	-	-	-	-	-	8.465
Lys	-	-	-	-	-	-	-	-	39.36	27.42	30.43	53.60	22.27	3.284	1.574	1.734	-	4.227	1.341	8.529
Pro	-	-	-	-	-	-	24.16	1.965	59.45	21.20	48.52	-	29.70	4.361	2.026	3.493	3.445	-	1.999	8.212
Val	-	-	-	-	-	-	-	-	-	29.62	-	-	-	-	1.933	-	-	-	-	-
Val1	-	-	-	-	-	-	-	-	59.23	-	-	-	18.15	4.081	1.987	-	-	-	0.9263	8.160
Val2	-	-	-	-	-	-	-	-	60.24	-	-	-	17.69	4.036	1.911	-	-	-	0.9400	7.969

25

	(C)H	(C)H2	(C)H3	C(H)	C(H)2	C(H)3	CO(C)H	COC(H)	Ca	Cb	Cd	Ce	Cg	Ha	Hb	Hd	He	Hg	NH
A	-	-	17.37	-	-	2.285	-	-	-	-	-	-	-	-	-	-	-	-	-
B	111.5	-	-	6.210	-	-	-	-	-	-	-	-	-	-	-	-	-	-	-
C	-	-	18.64	-	-	2.189	-	-	-	-	-	-	-	-	-	-	-	-	-
D	-	77.35	-	-	5.813	-	-	-	-	-	-	-	-	-	-	-	-	-	-
E	-	62.67	-	-	3.907	-	-	-	-	-	-	-	-	-	-	-	-	-	-
F	-	64.72	-	-	3.640	-	-	-	-	-	-	-	-	-	-	-	-	-	-
Gly	-	-	-	-	-	-	-	-	43.16	-	-	-	-	3.871	-	-	-	-	8.262
Lys	-	-	-	-	-	-	-	-	38.63	28.27	30.24	54.79	23.24	3.322	1.577	1.823	4.098	1.345	8.551
Pro	-	-	-	-	-	-	25.06	1.945	59.51	21.10	48.67	-	29.57	4.260	2.024	3.517	-	2.023	-
Val1	-	-	-	-	-	-	-	-	59.13	30.65	-	-	19.02	4.128	1.976	-	-	0.8760	-
Val2	-	-	-	-	-	-	-	-	60.05	30.39	-	-	17.45	4.032	1.915	-	-	0.9820	7.973

26

	(C)H	(C)H2	(C)H3	C(H)	C(H)2	C(H)3	CO(C)H	COC(H)	Ca	Cb	Cd	Ce	Cg	Ha	Hb	Hd	He	Hg	NH	NH(Het)
A	-	-	17.54	-	-	2.279	-	-	-	-	-	-	-	-	-	-	-	-	-	-
B	111.0	-	-	6.141	-	-	-	-	-	-	-	-	-	-	-	-	-	-	-	-
C	-	-	18.51	-	-	2.142	-	-	-	-	-	-	-	-	-	-	-	-	-	-
D	-	69.40	-	-	5.710	-	-	-	-	-	-	-	-	-	-	-	-	-	-	-
G	-	-	-	3.600	-	-	-	-	-	-	-	-	-	-	-	-	-	-	-	-
Gly	-	-	-	-	-	-	-	-	42.34	-	-	-	-	3.893	-	-	-	-	8.262	-
H+I	-	-	15.49	-	-	1.352	-	-	-	-	-	-	-	-	-	-	-	-	-	-
J	-	60.24	-	-	3.808	-	-	-	-	-	-	-	-	-	-	-	-	-	-	-
K	-	-	7.021	-	-	1.286	-	-	-	-	-	-	-	-	-	-	-	-	-	-
Lys	-	-	-	-	-	-	-	-	39.42	27.43	30.44	53.65	22.36	3.296	1.573	1.712	4.274	1.365	8.624	8.397
Pro	-	-	-	-	-	-	24.19	1.972	60.24	21.30	48.56	-	29.57	4.301	2.082	3.512	-	2.251	-	-
Val1	-	-	-	-	-	-	-	-	59.46	29.80	-	-	18.16	4.088	2.007	-	-	0.8692	-	-
Val2	-	-	-	-	-	-	-	-	59.23	29.63	-	-	17.70	4.038	1.899	-	-	0.9020	7.976	-

3.3 ¹H and ¹³C-NMR spectra of compounds 4a-7a and 8-26
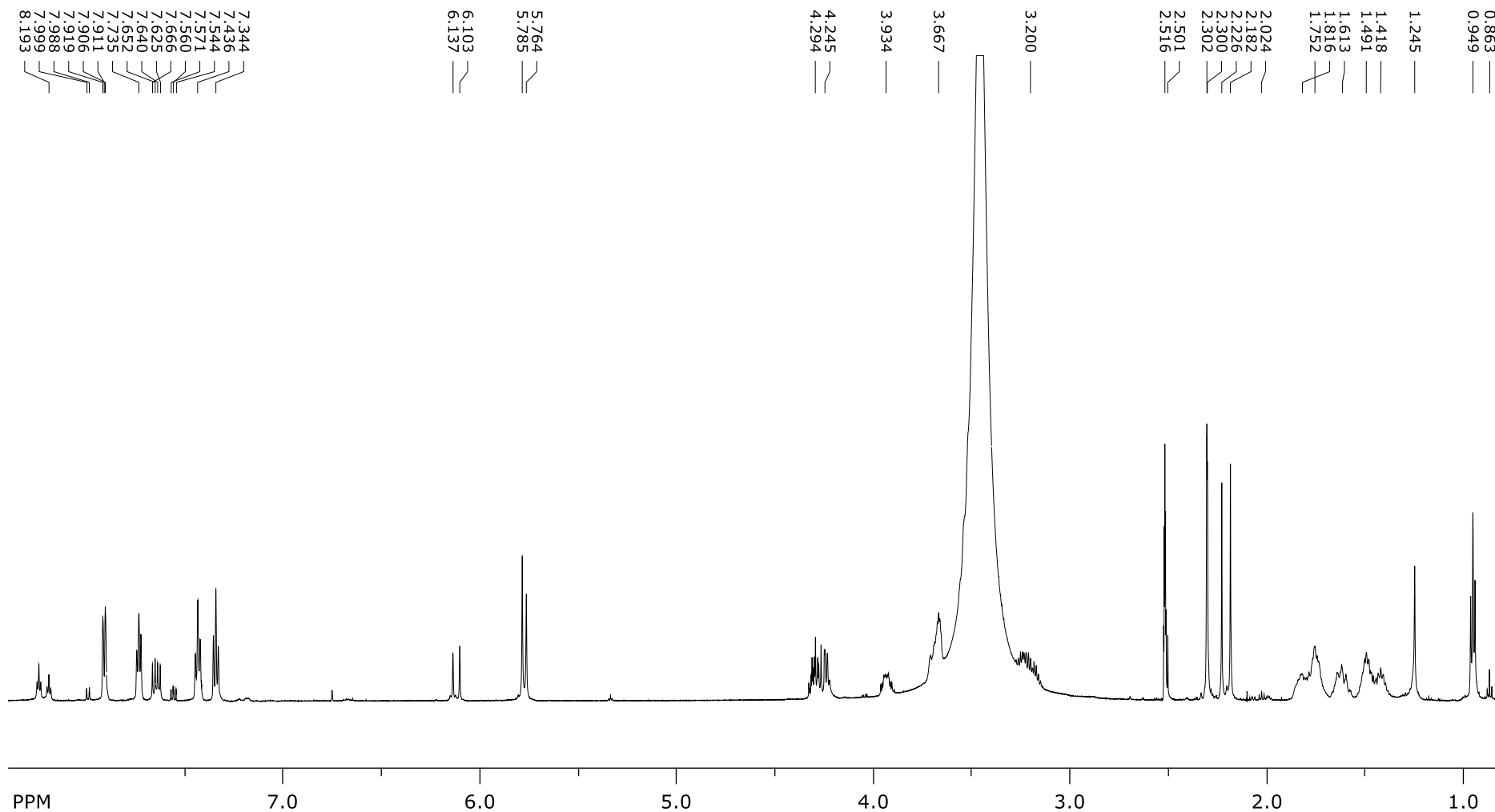
Figure SI 71. ¹H-NMR spectrum of **4a**.
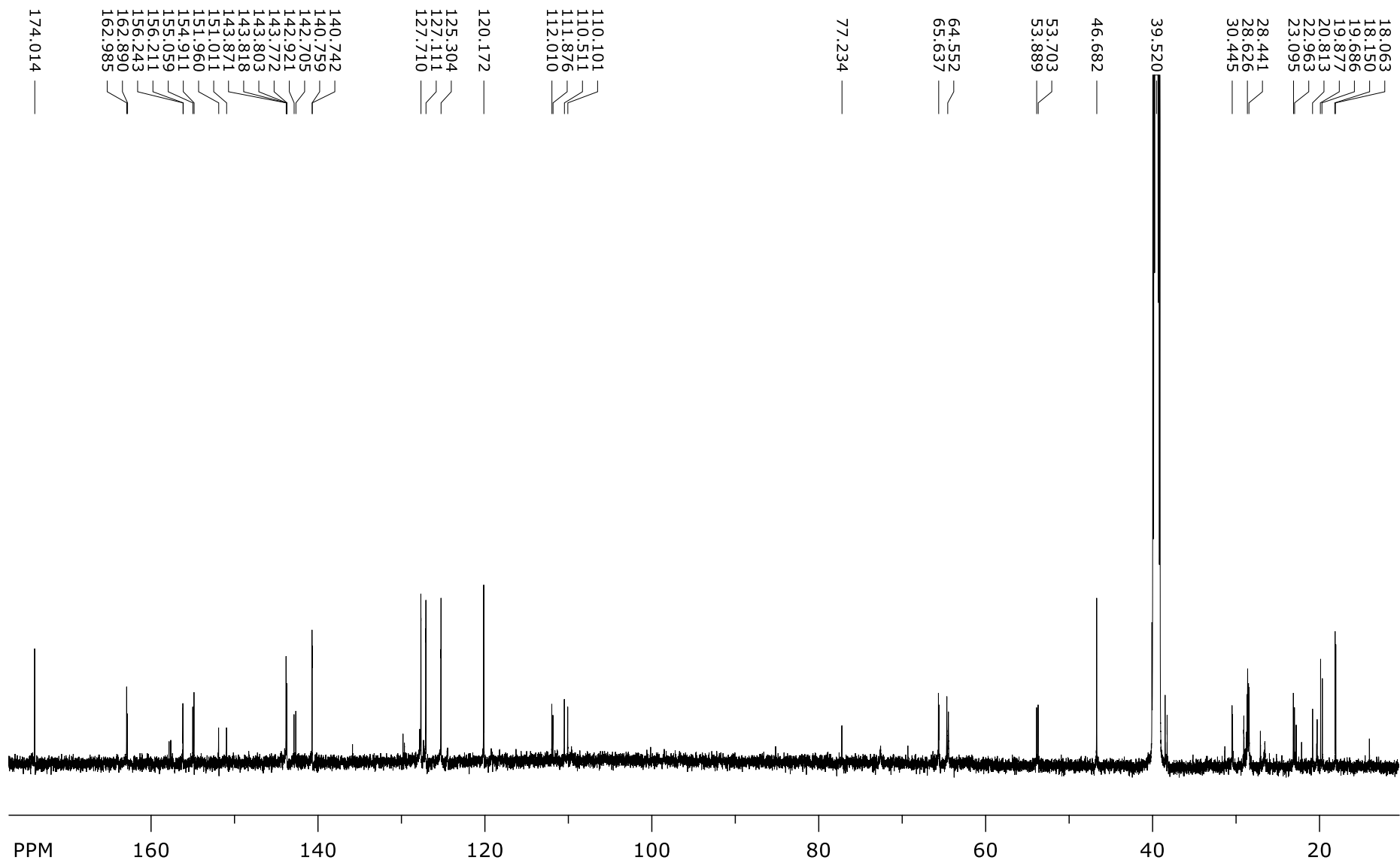
Figure SI 72. ^{13}C-NMR spectrum of **4a**.
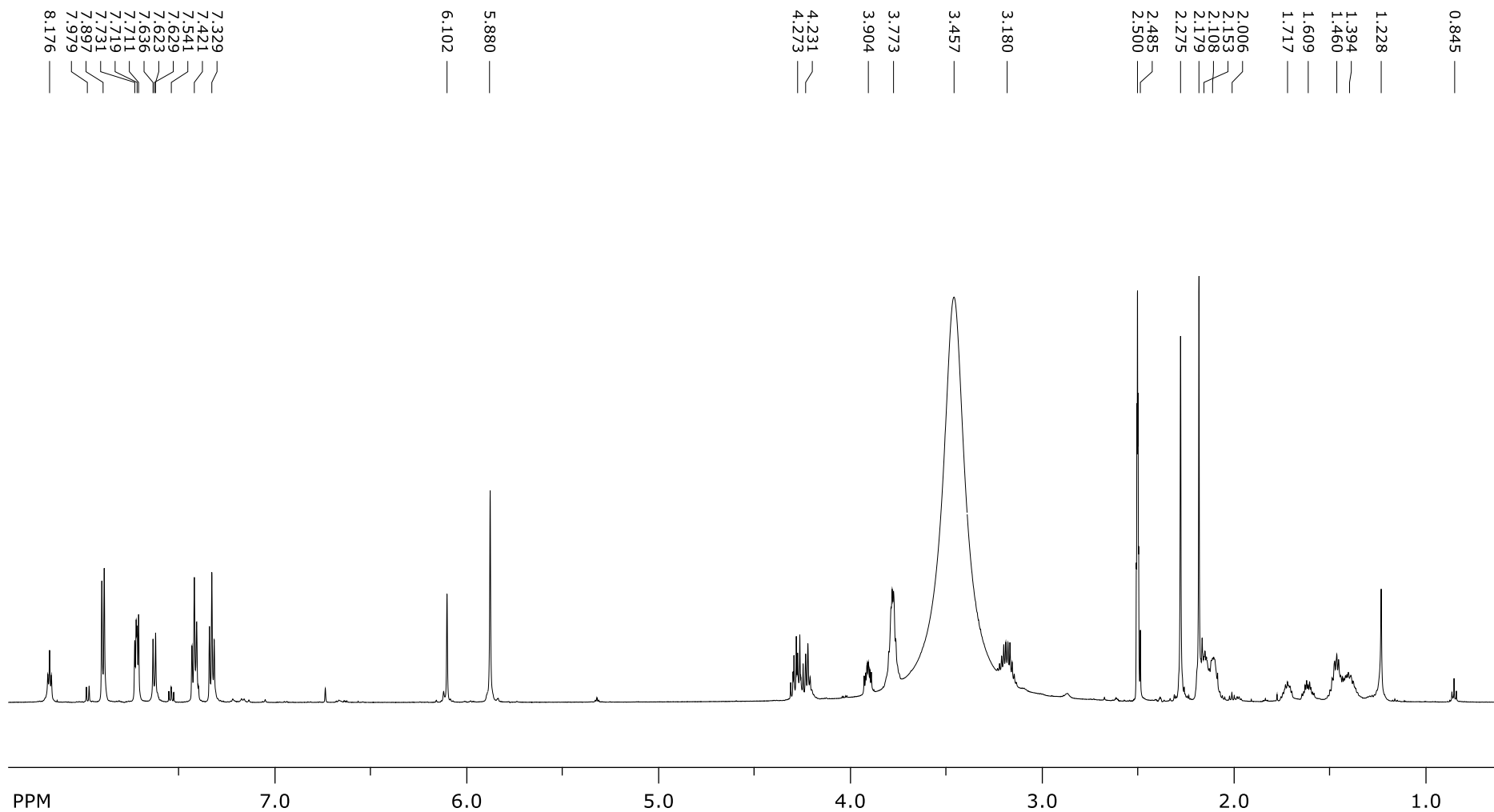
Figure SI 73. ^{1}H-NMR spectrum of **5a**.
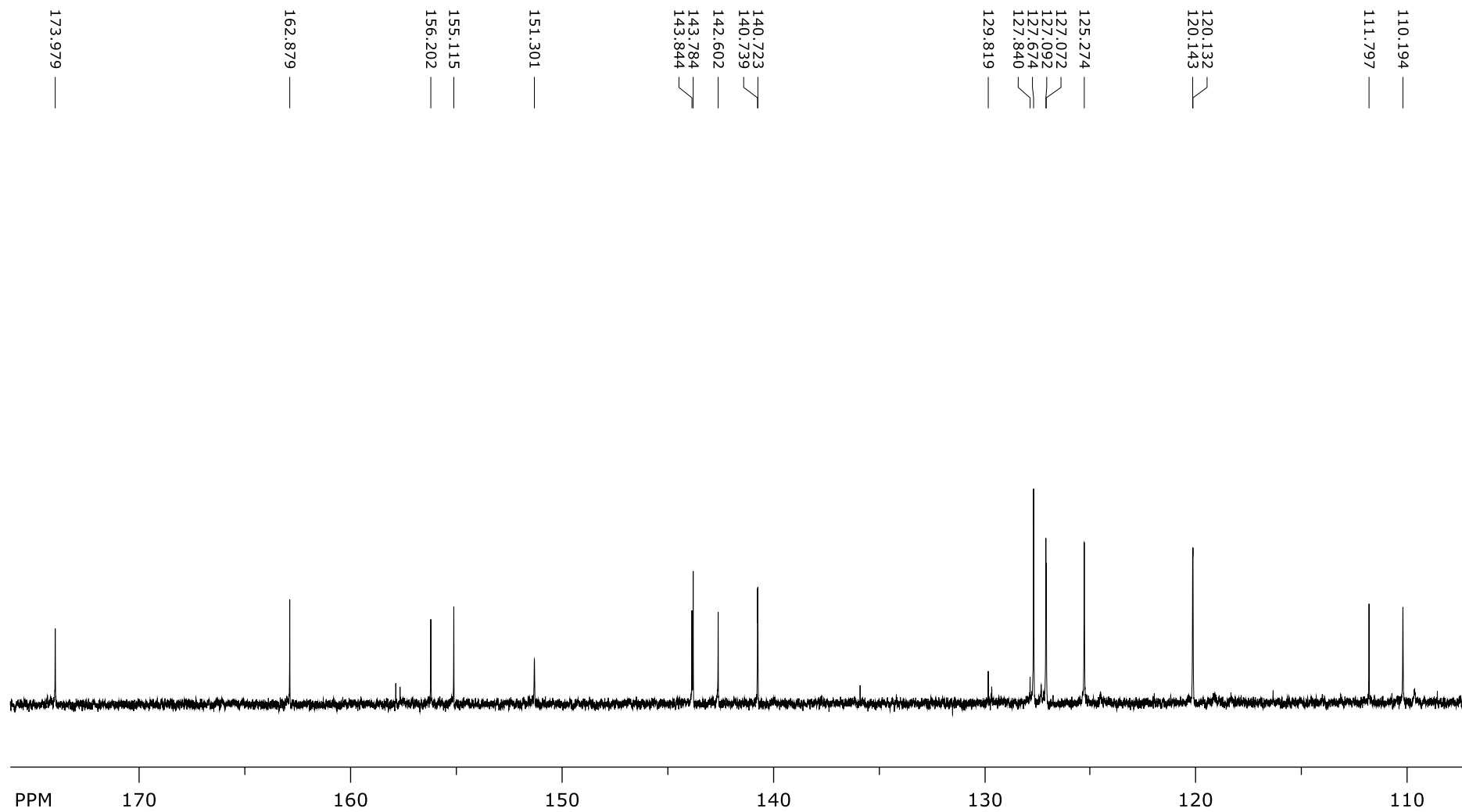
Figure SI 74. ^{13}C-NMR spectrum of **5a**.
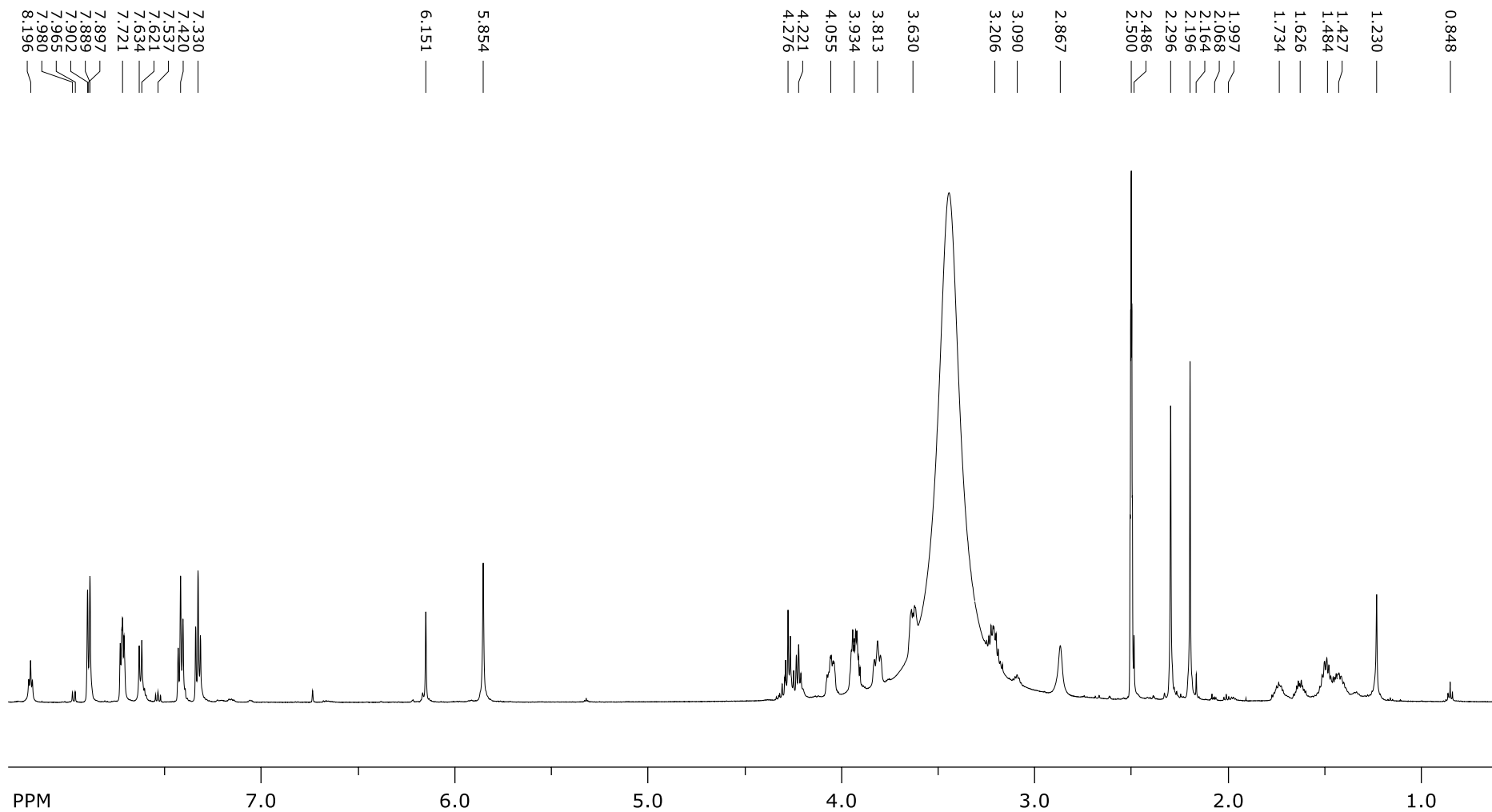
Figure SI 75. ^{1}H-NMR spectrum of **6a**.
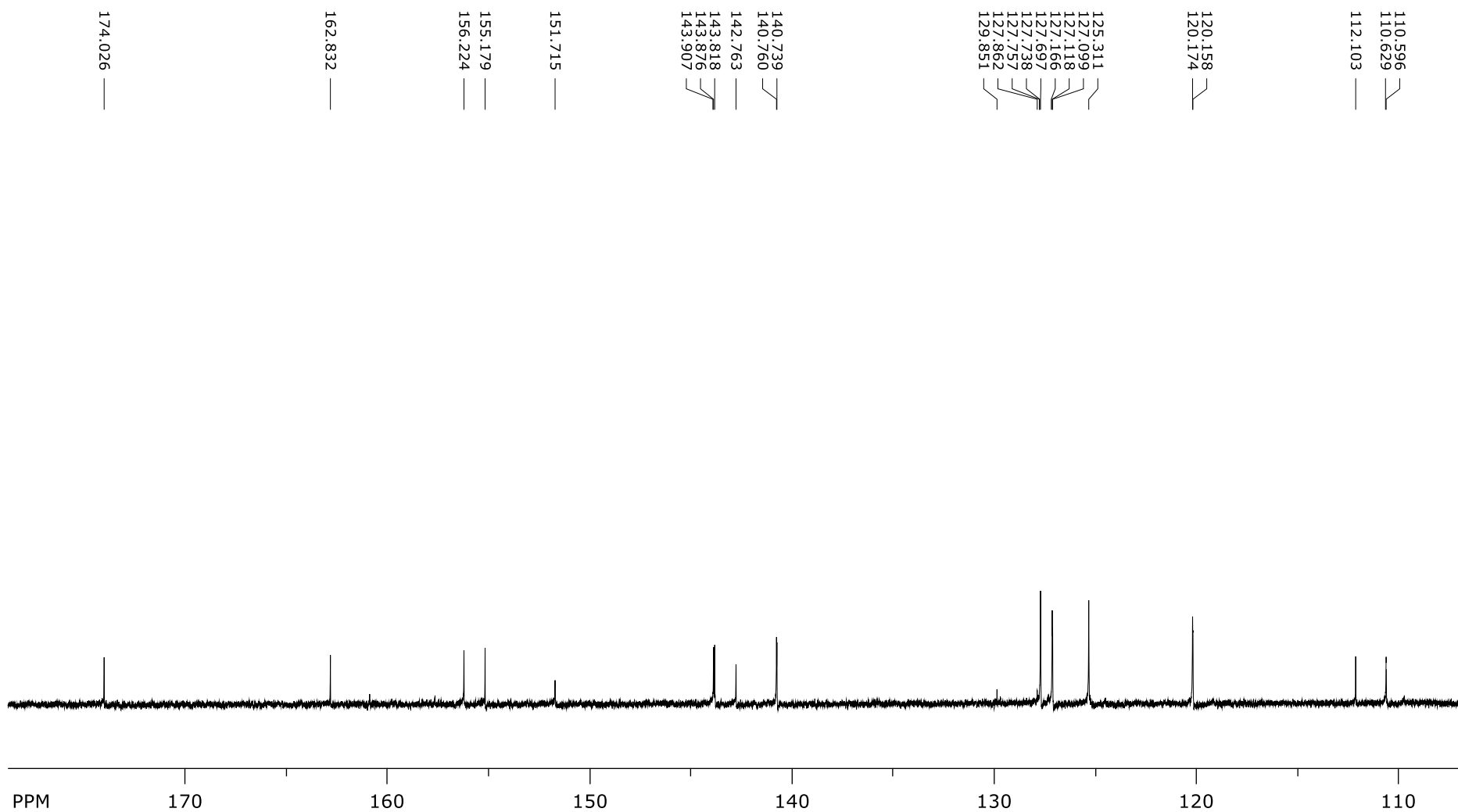
Figure SI 76. ^{13}C-NMR spectrum of **6a**.
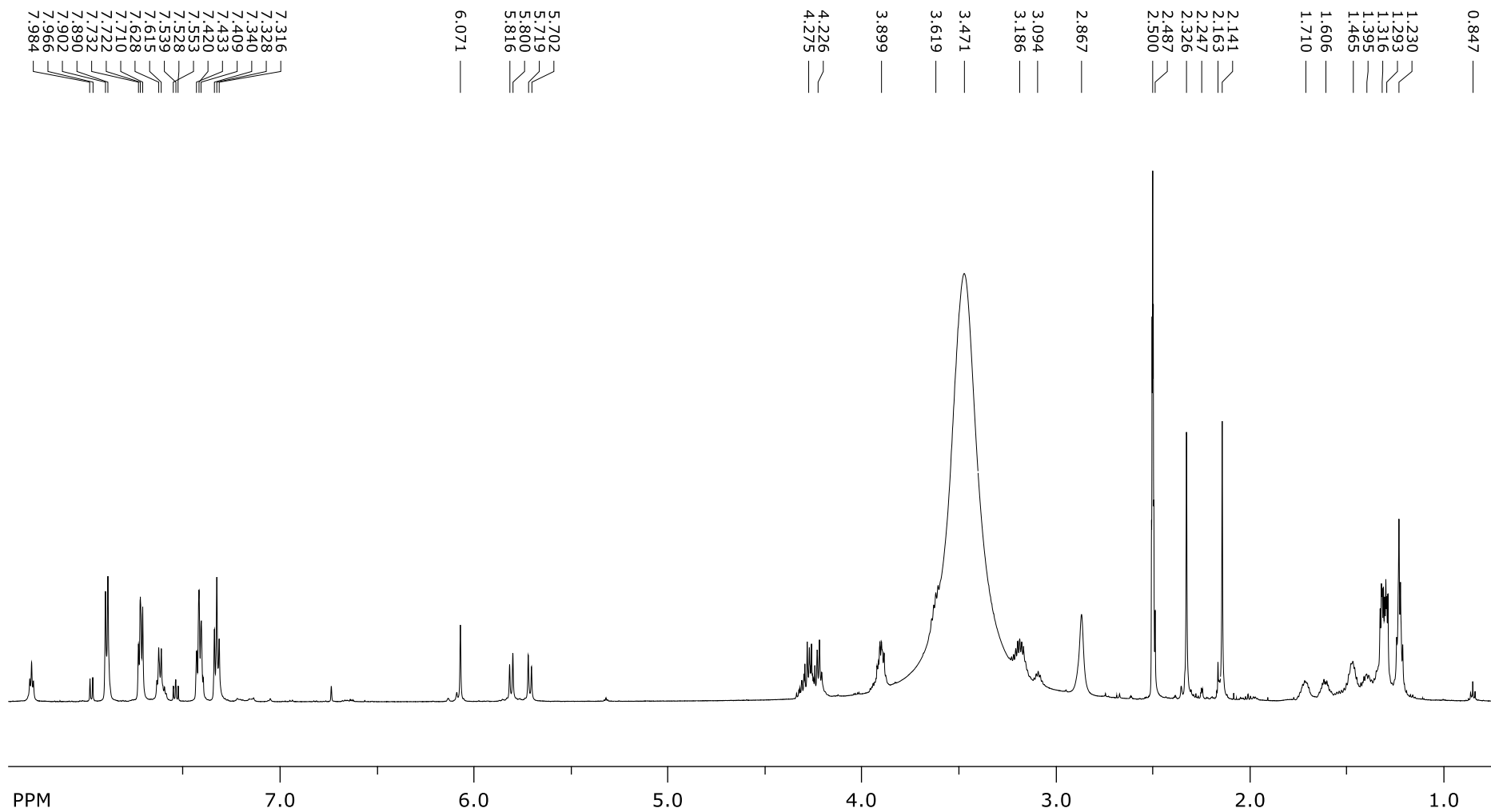
Figure SI 77. ^{1}H-NMR spectrum of **7a**.
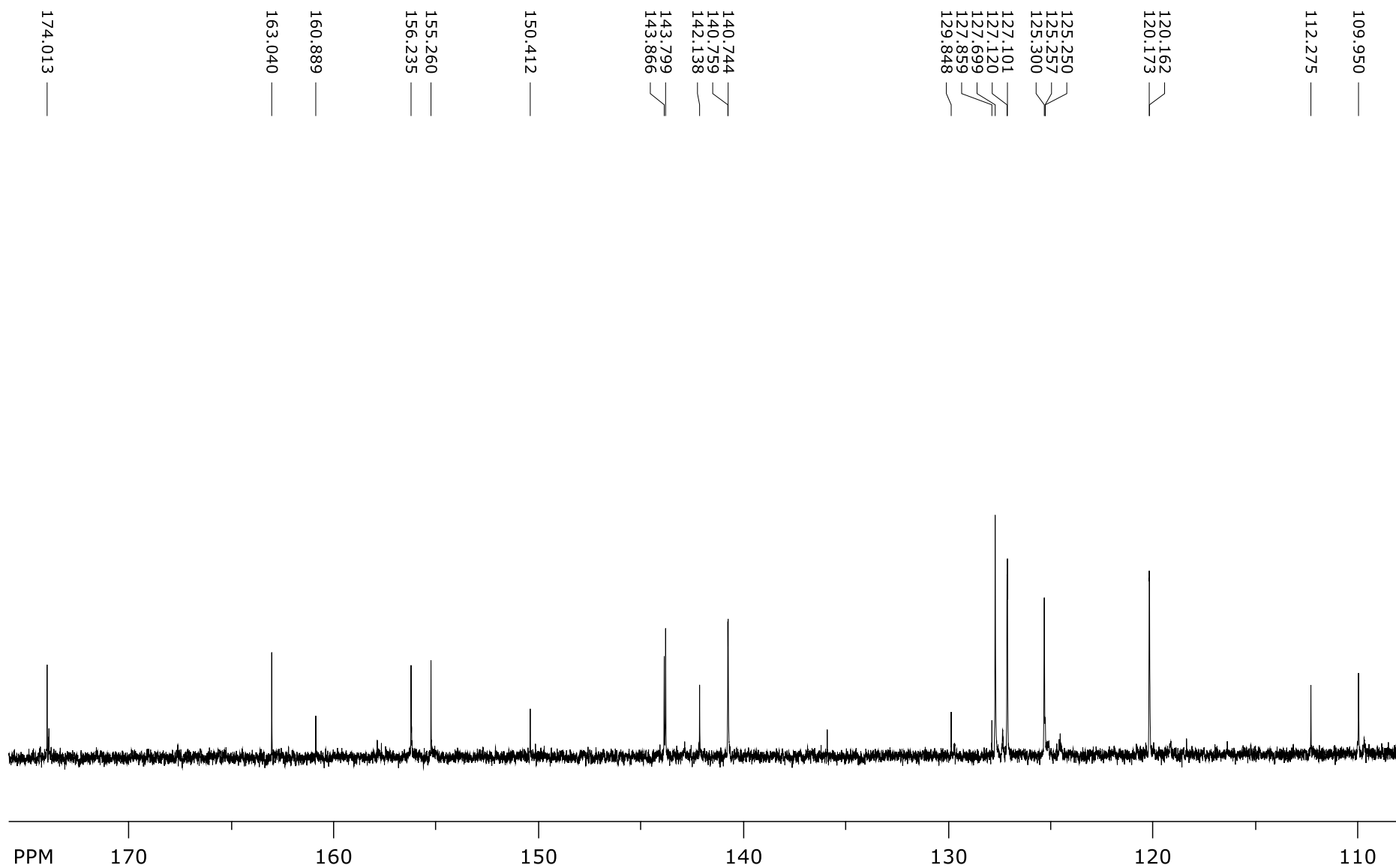
Figure SI 78. ^{13}C-NMR spectrum of **7a**.
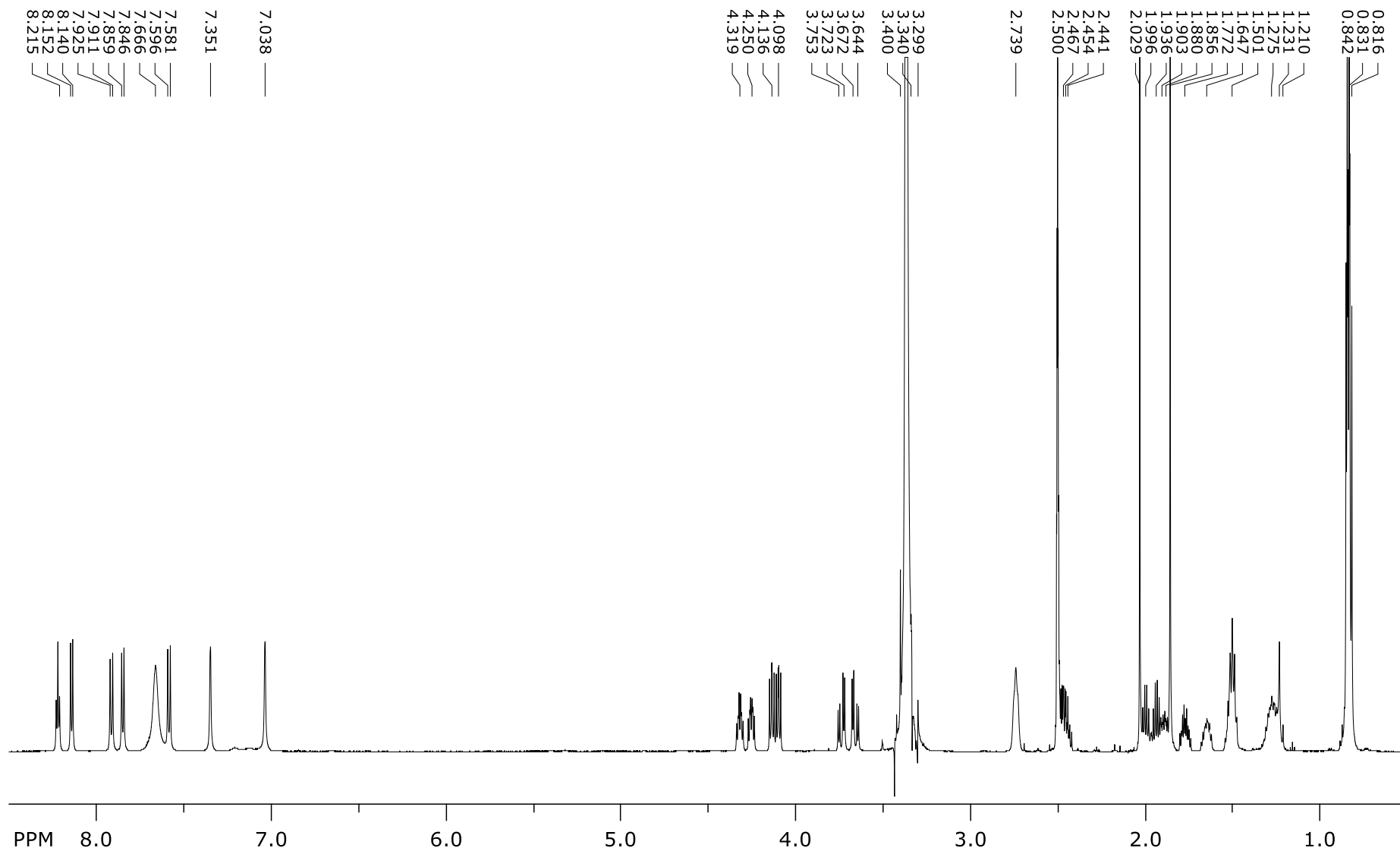
Figure SI 79. ^{1}H-NMR spectrum of **8**.
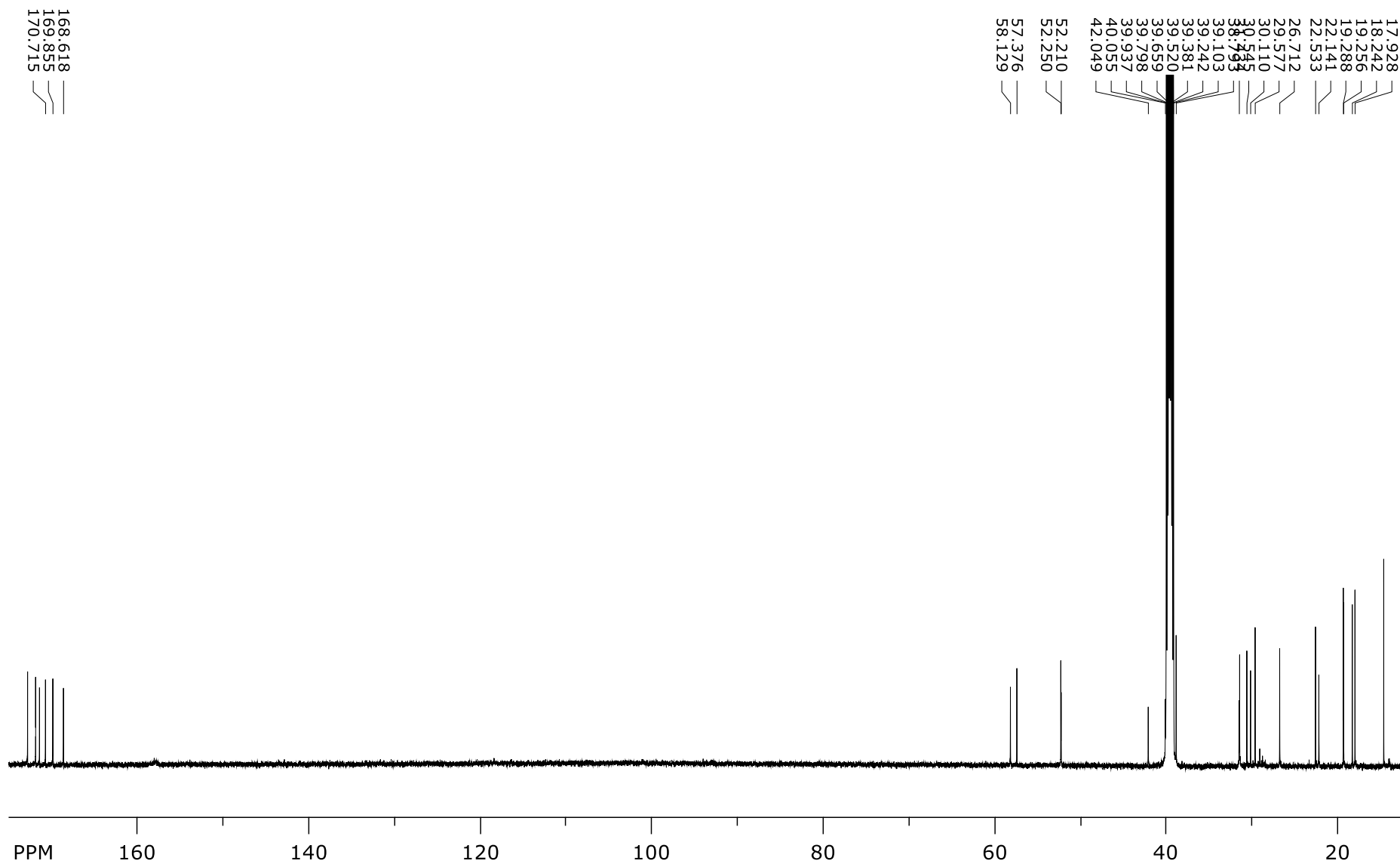
Figure SI 80. ^{13}C-NMR spectrum of **8**.
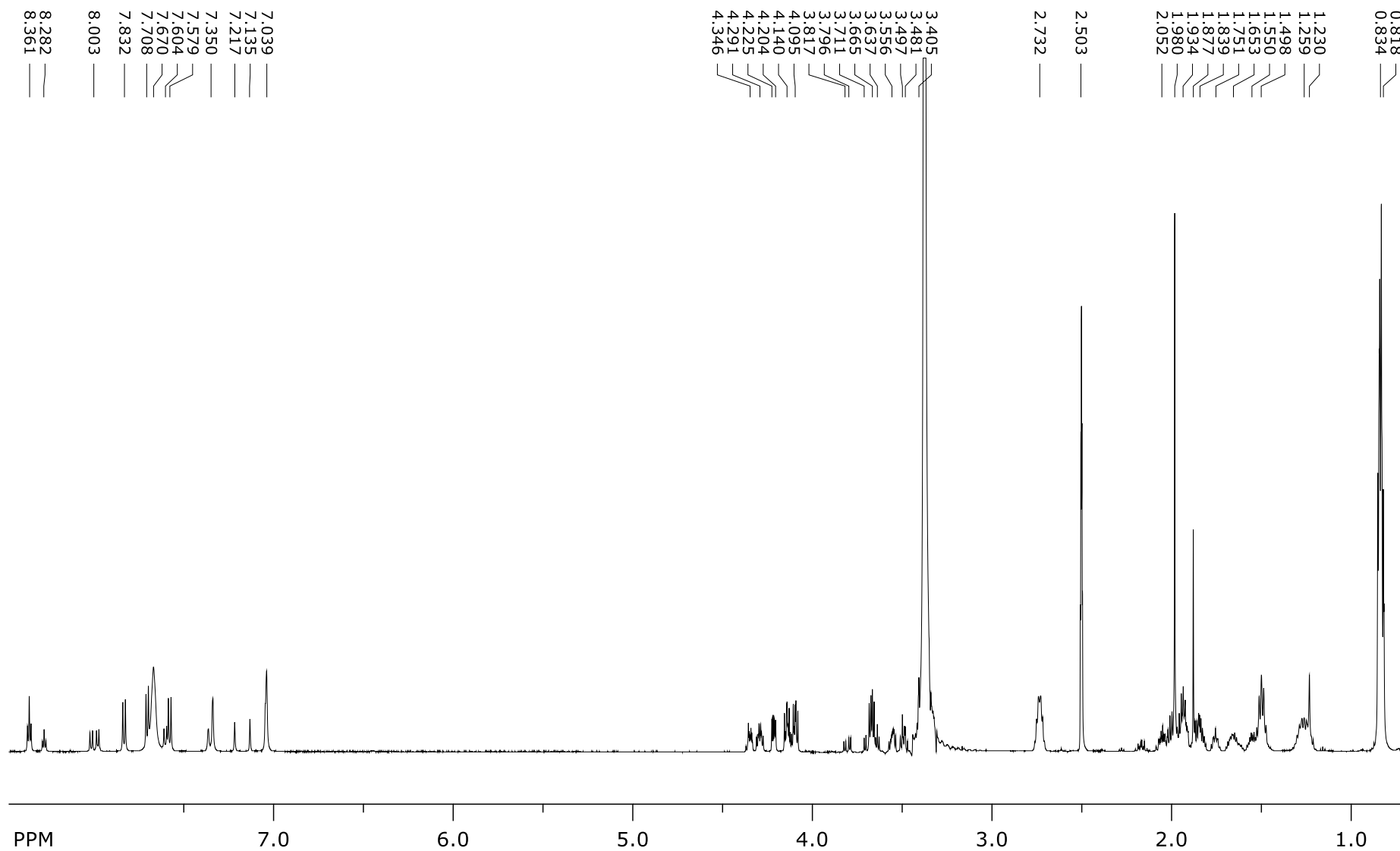
Figure SI 81. ^{1}H-NMR spectrum of **9**.
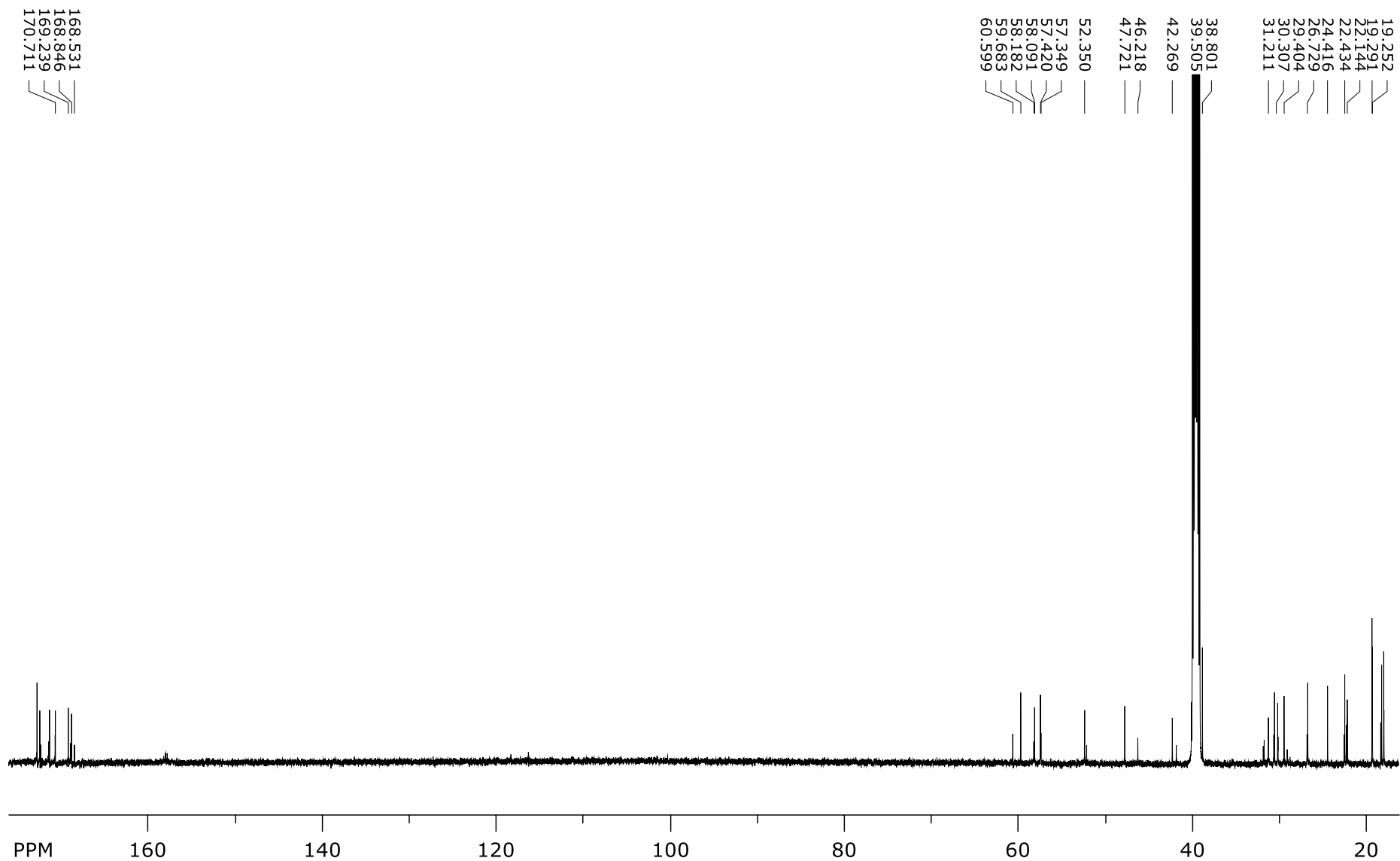
Figure SI 82. ^{13}C-NMR spectrum of **9**.
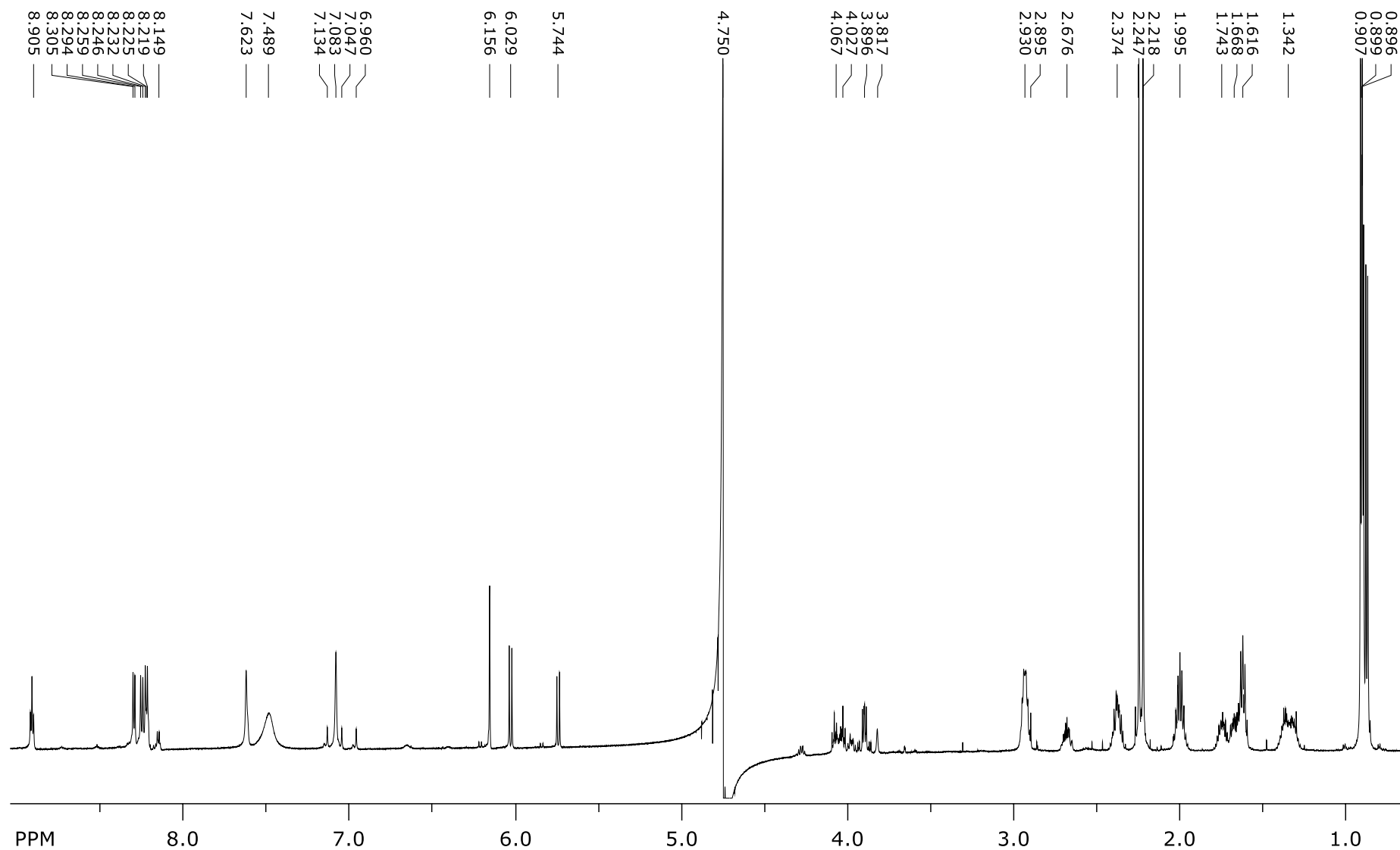
Figure SI 83. ^{1}H-NMR spectrum of **10**.
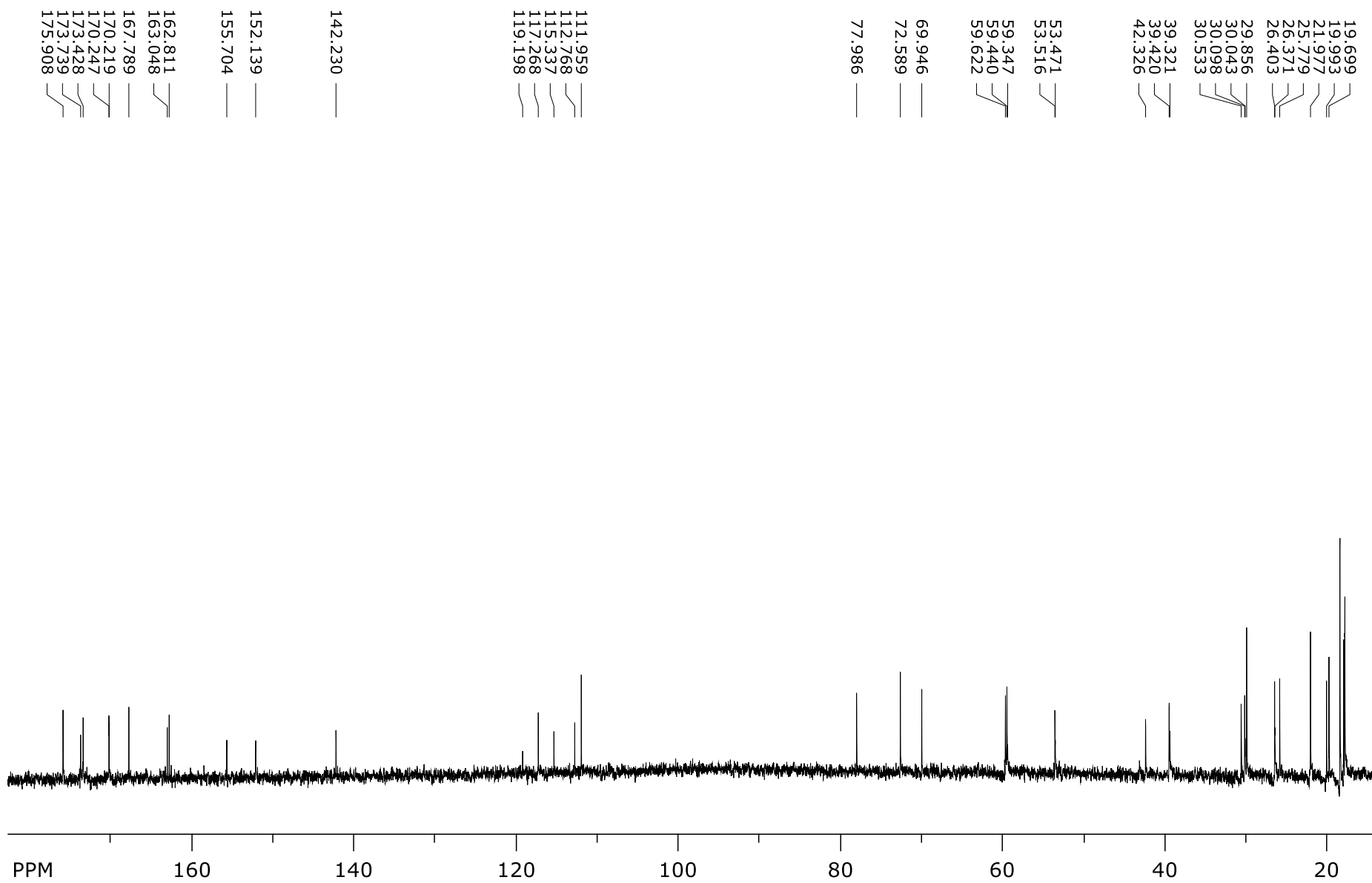
Figure SI 84. ^{13}C-NMR spectrum of **10**.
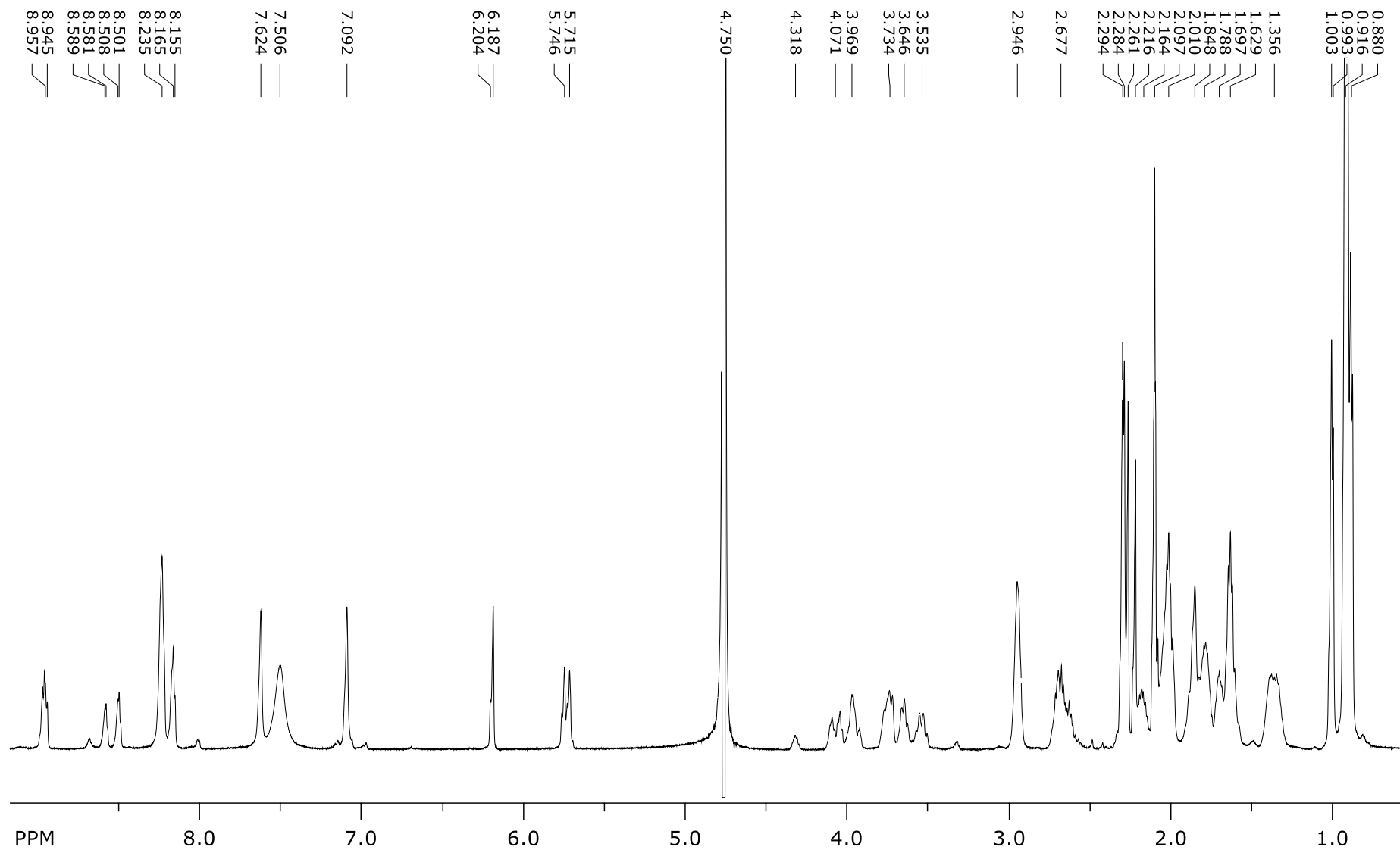
Figure SI 85. ^{1}H-NMR spectrum of **11**.
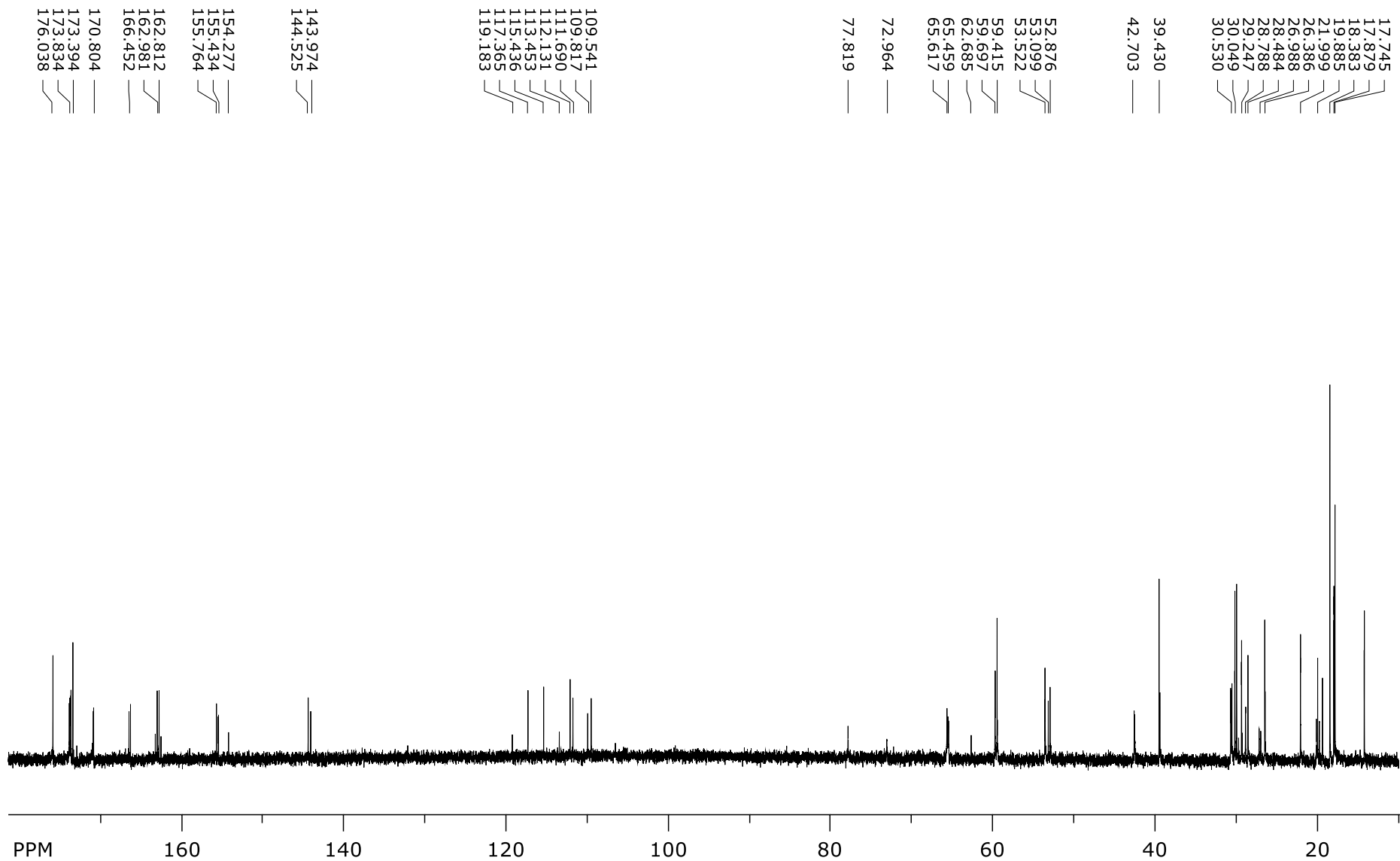
Figure SI 86. ^{13}C-NMR spectrum of **11**.
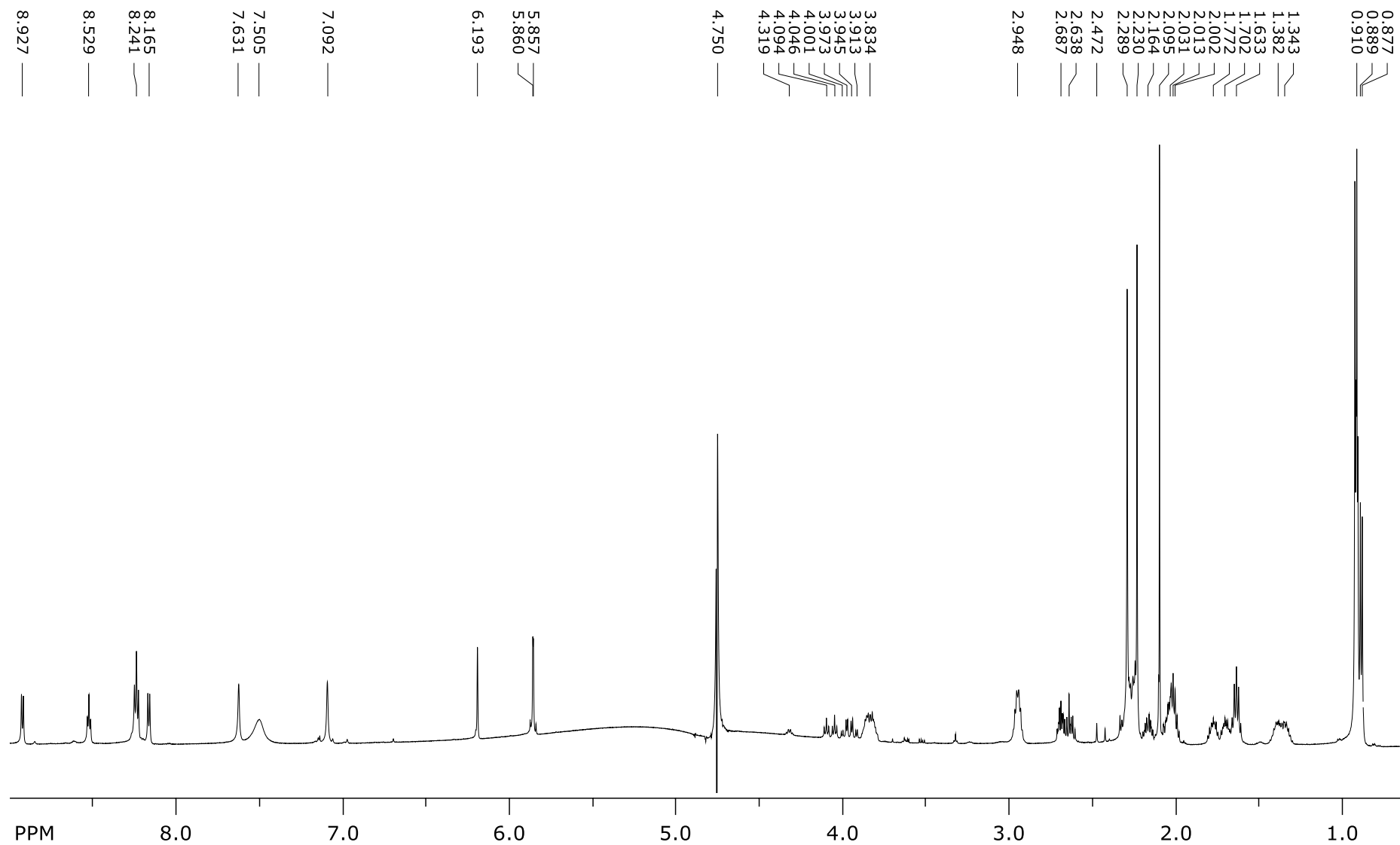
Figure SI 87. ¹H-NMR spectrum of **12**.
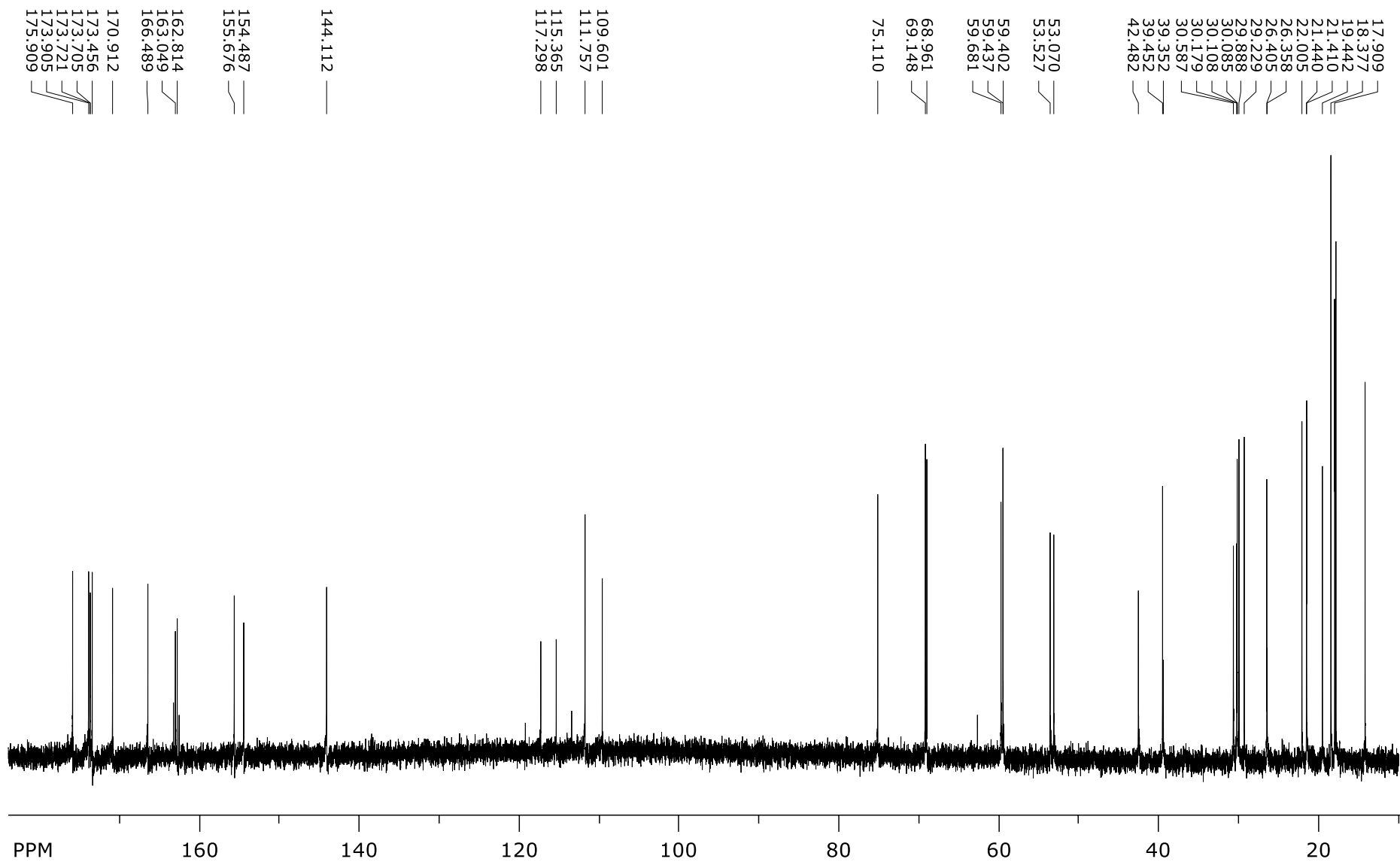
Figure SI 88. ^{13}C-NMR spectrum of **12**.
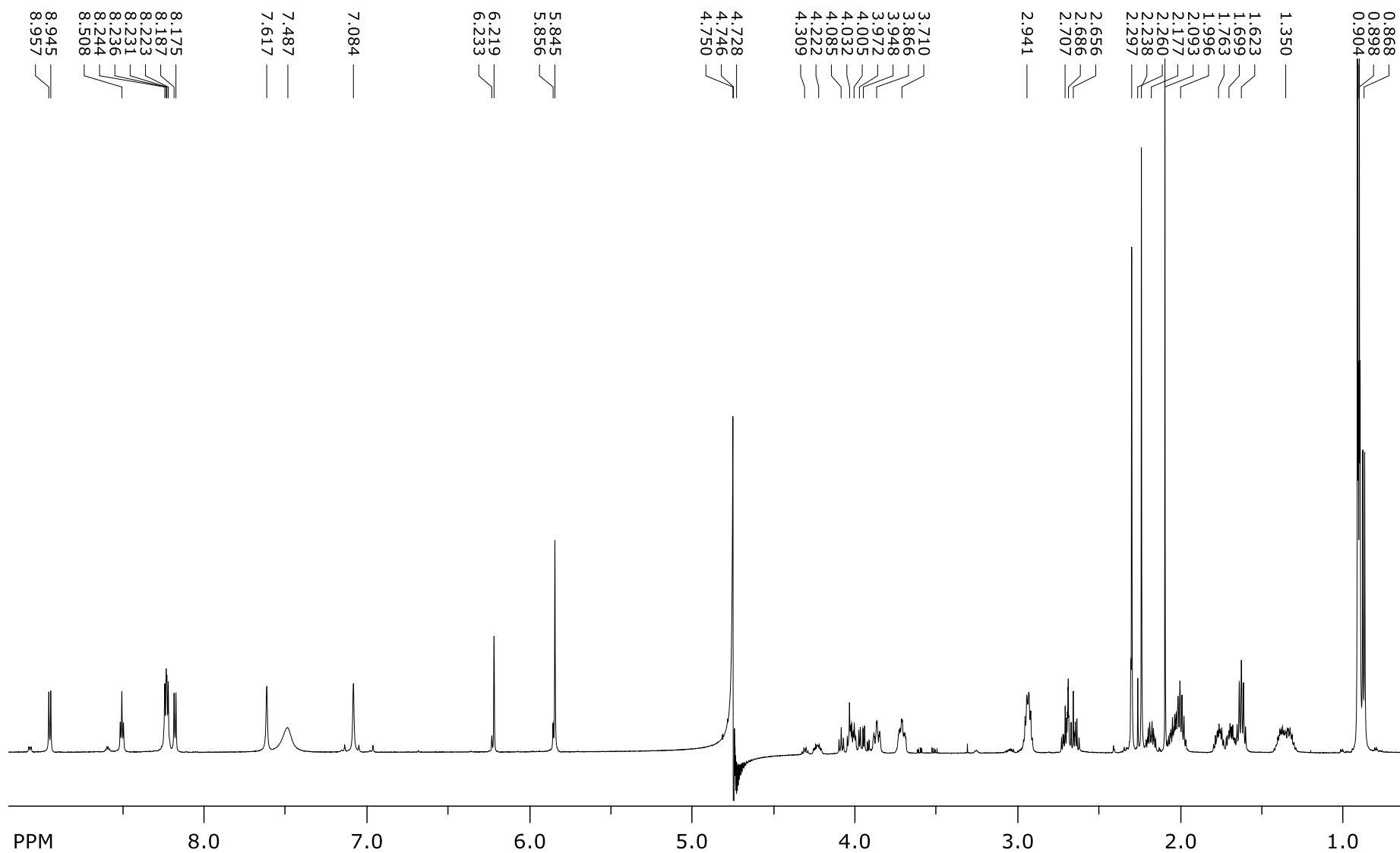
Figure SI 89. ^{1}H-NMR spectrum of **13**.
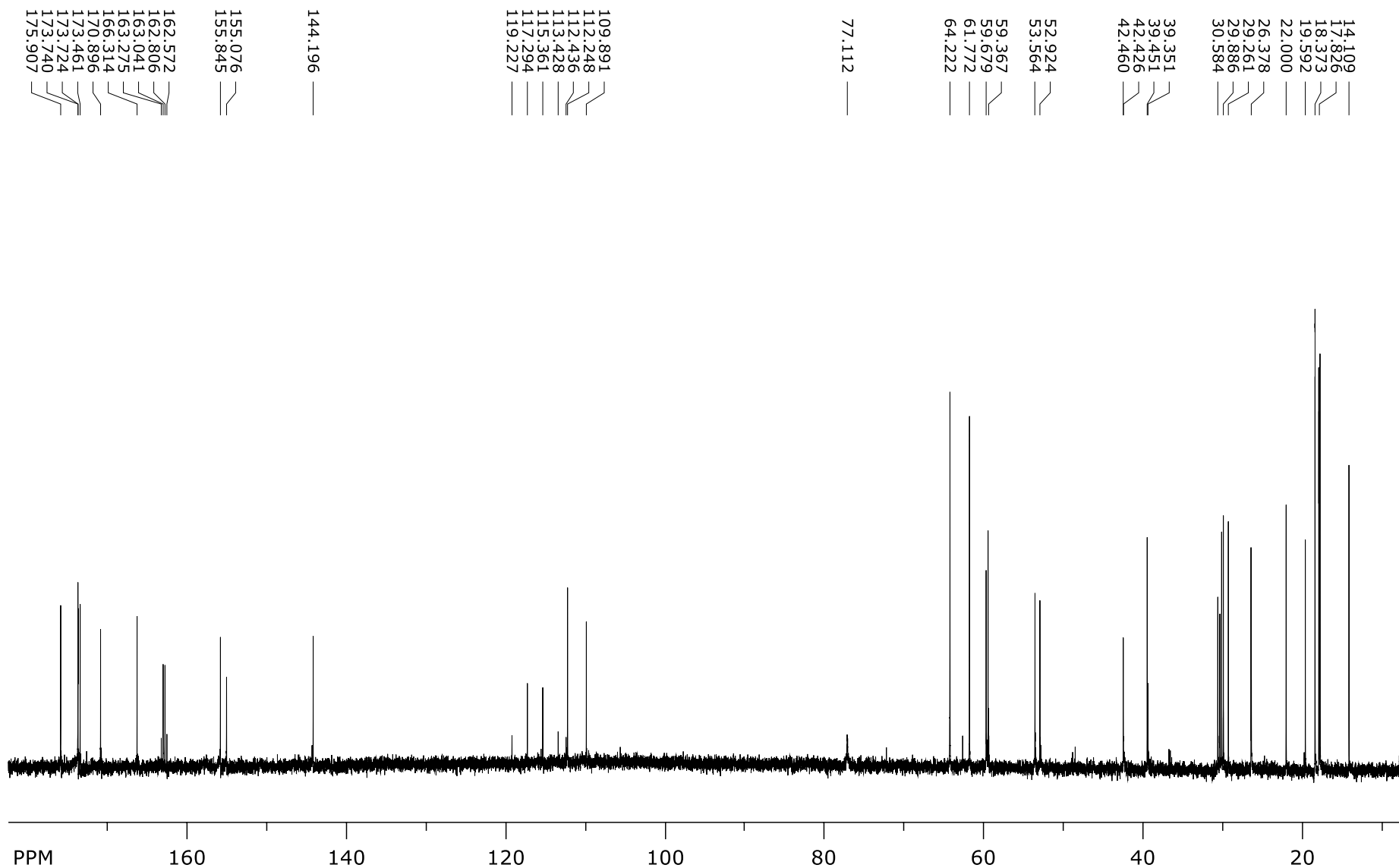
Figure SI 90. ^{13}C-NMR spectrum of **13**.
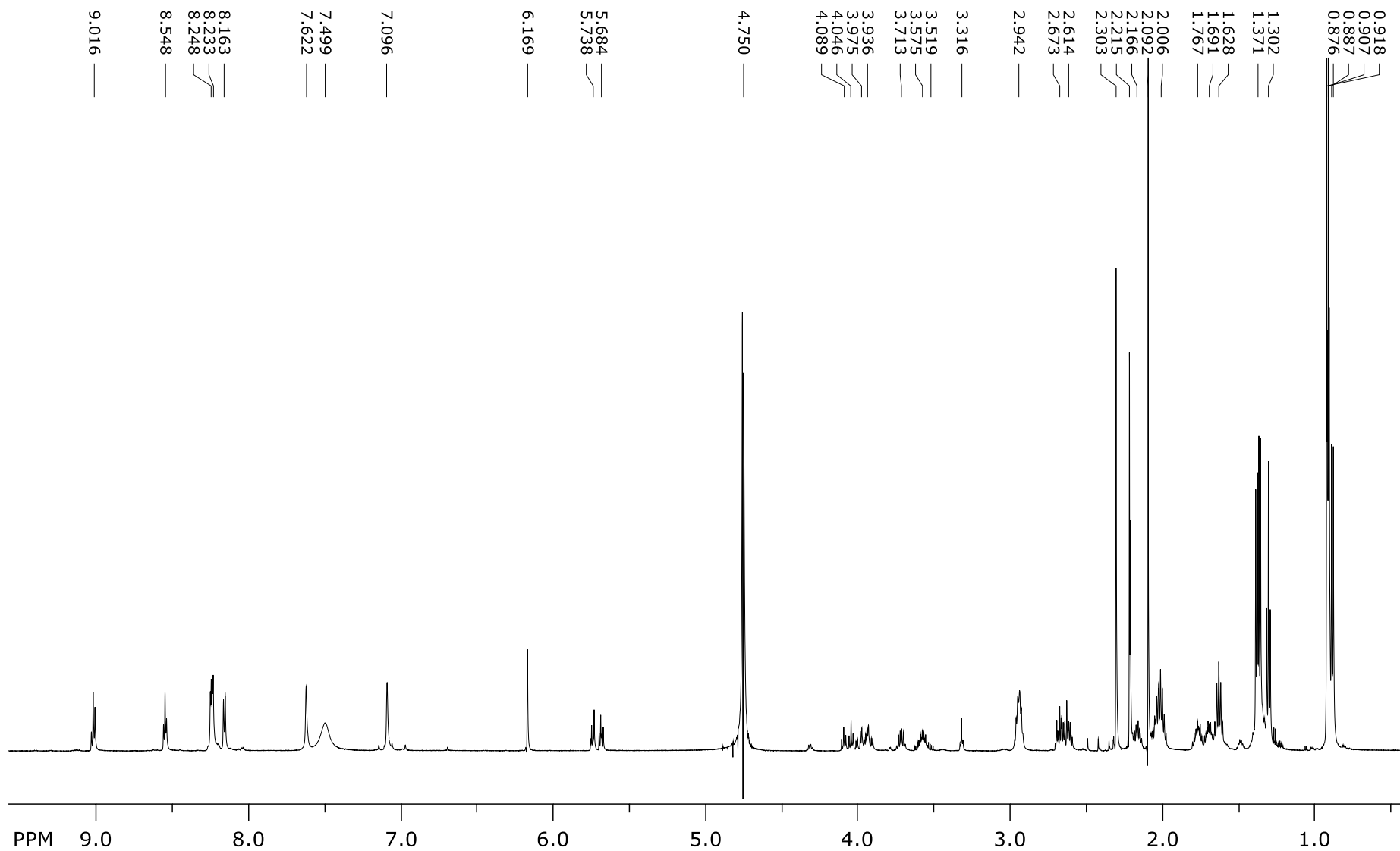
Figure SI 91. ^{1}H-NMR spectrum of **14**.
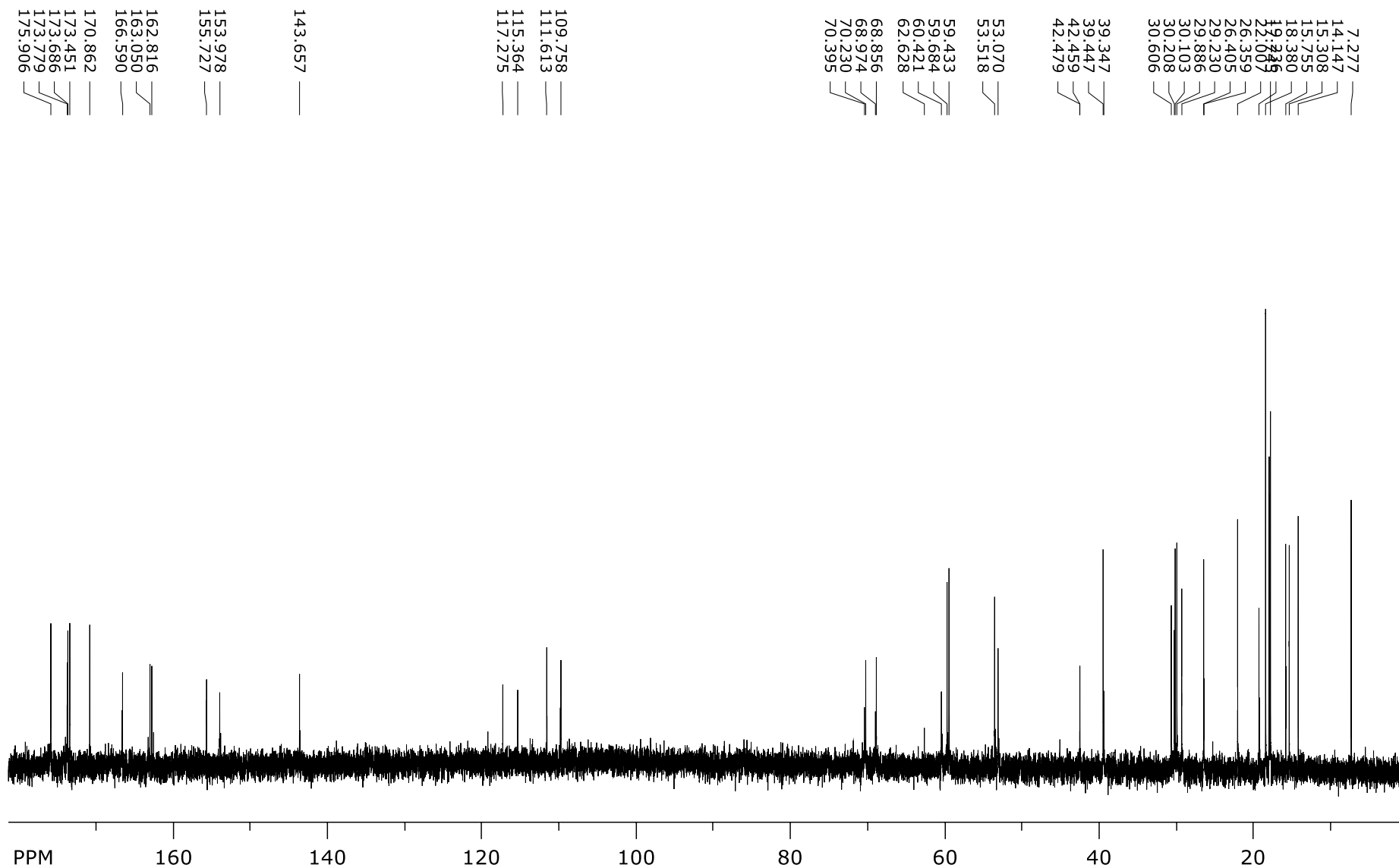
Figure SI 92. ^{13}C-NMR spectrum of **14**.
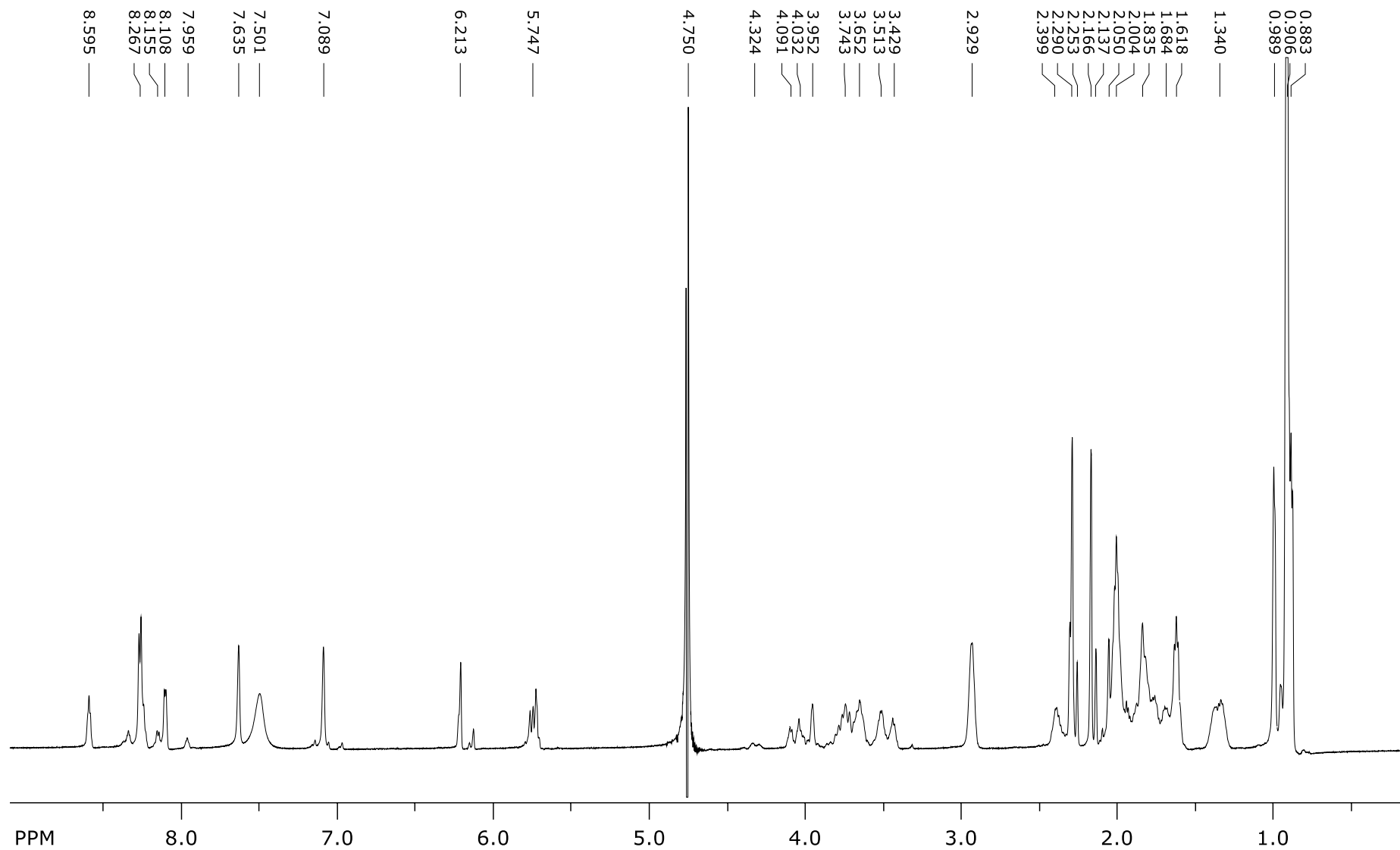
Figure SI 93. ^{1}H-NMR spectrum of **15**.
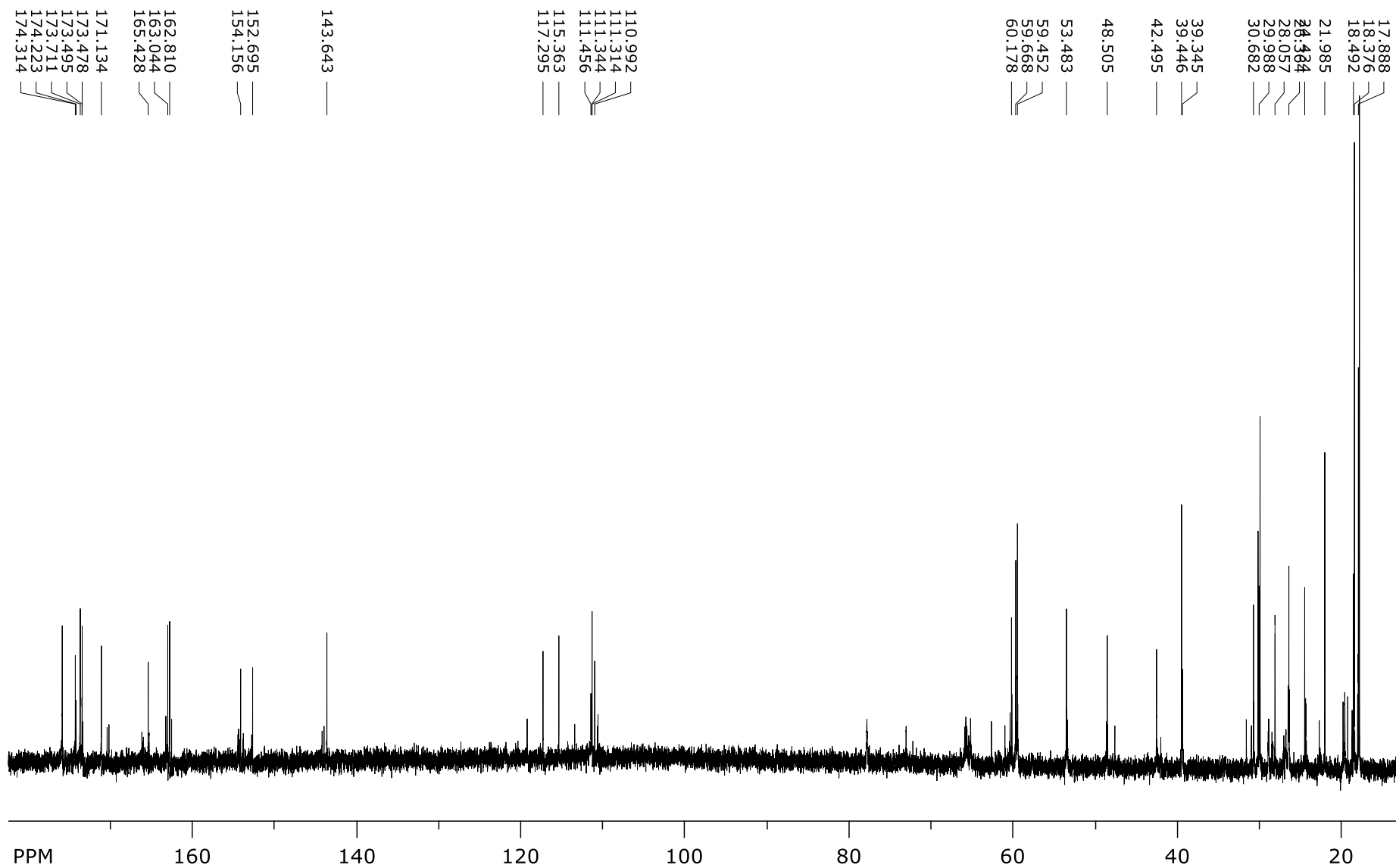
Figure SI 94. ^{13}C-NMR spectrum of **15**.
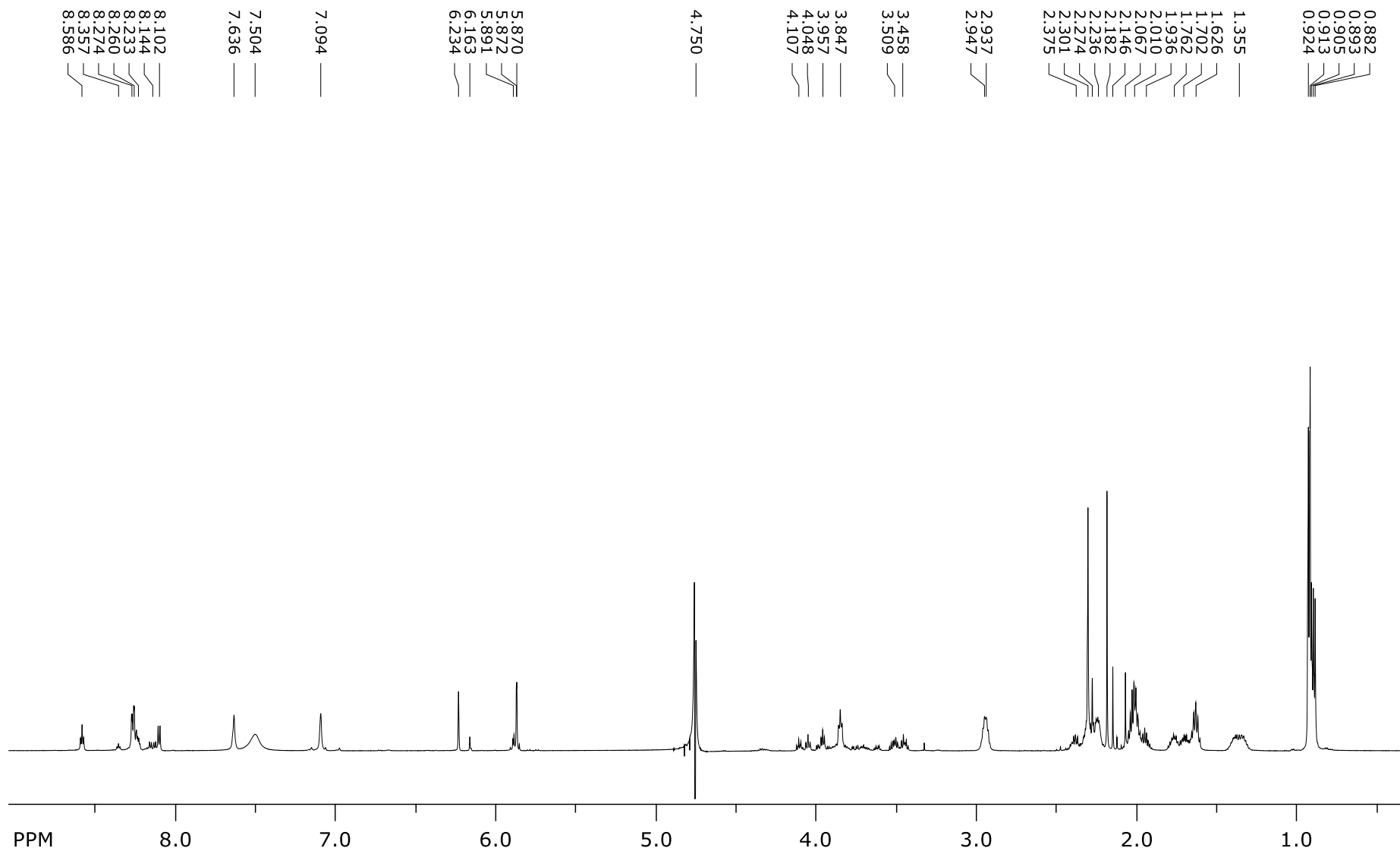
Figure SI 95. ^{1}H-NMR spectrum of **16**.
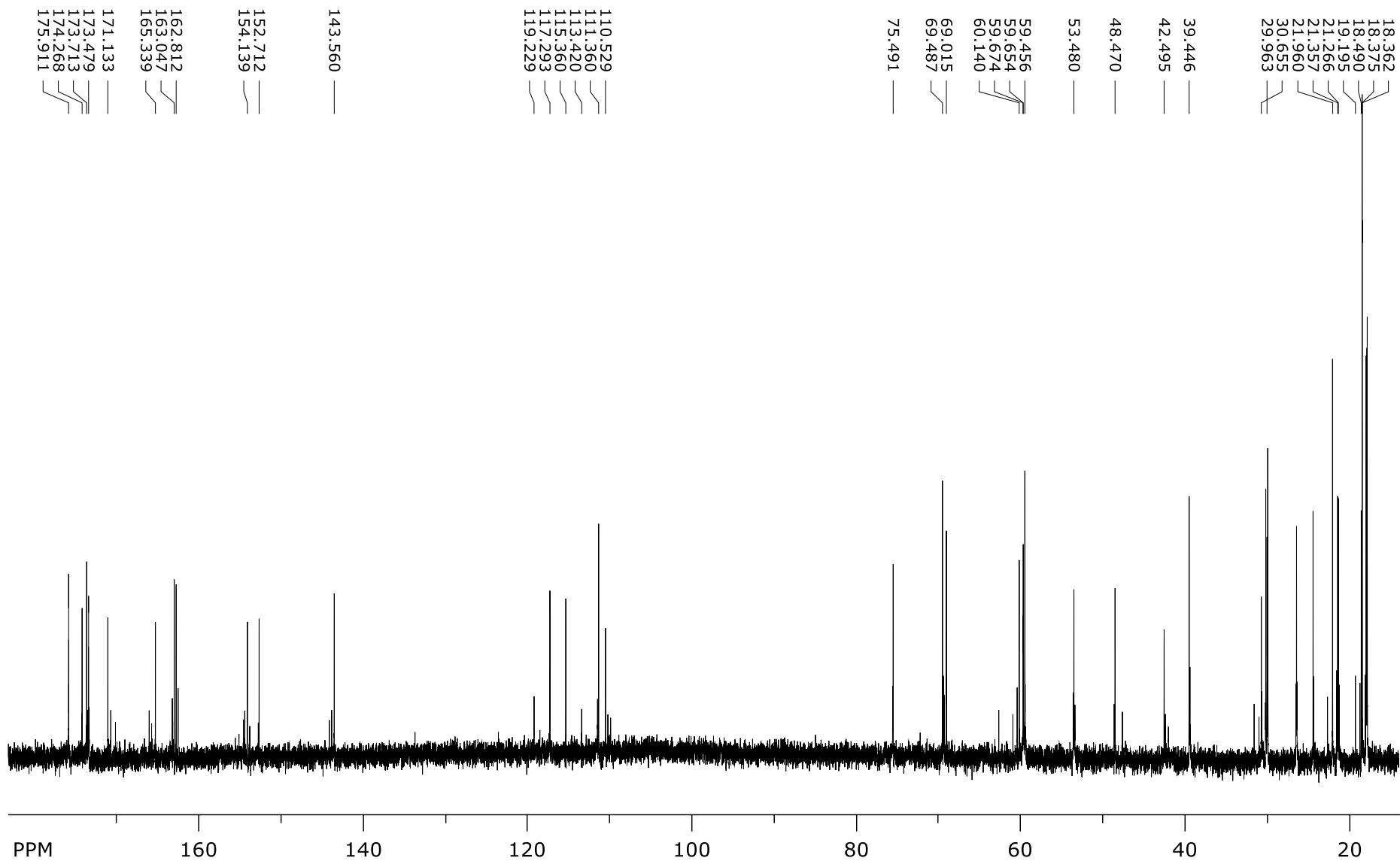
Figure SI 96. ^{13}C-NMR spectrum of **16**.
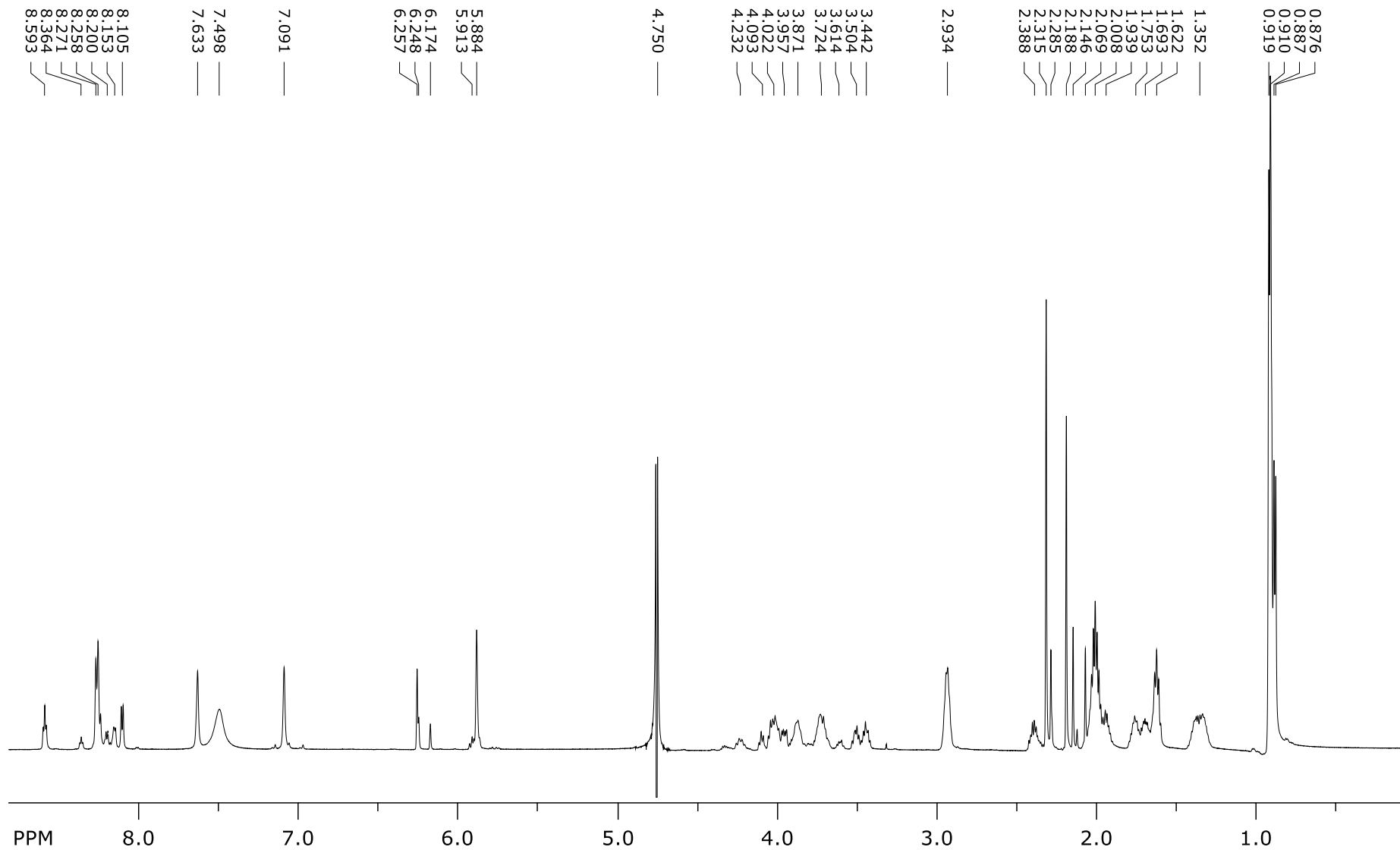
Figure SI 97. ^{1}H-NMR spectrum of **17**.
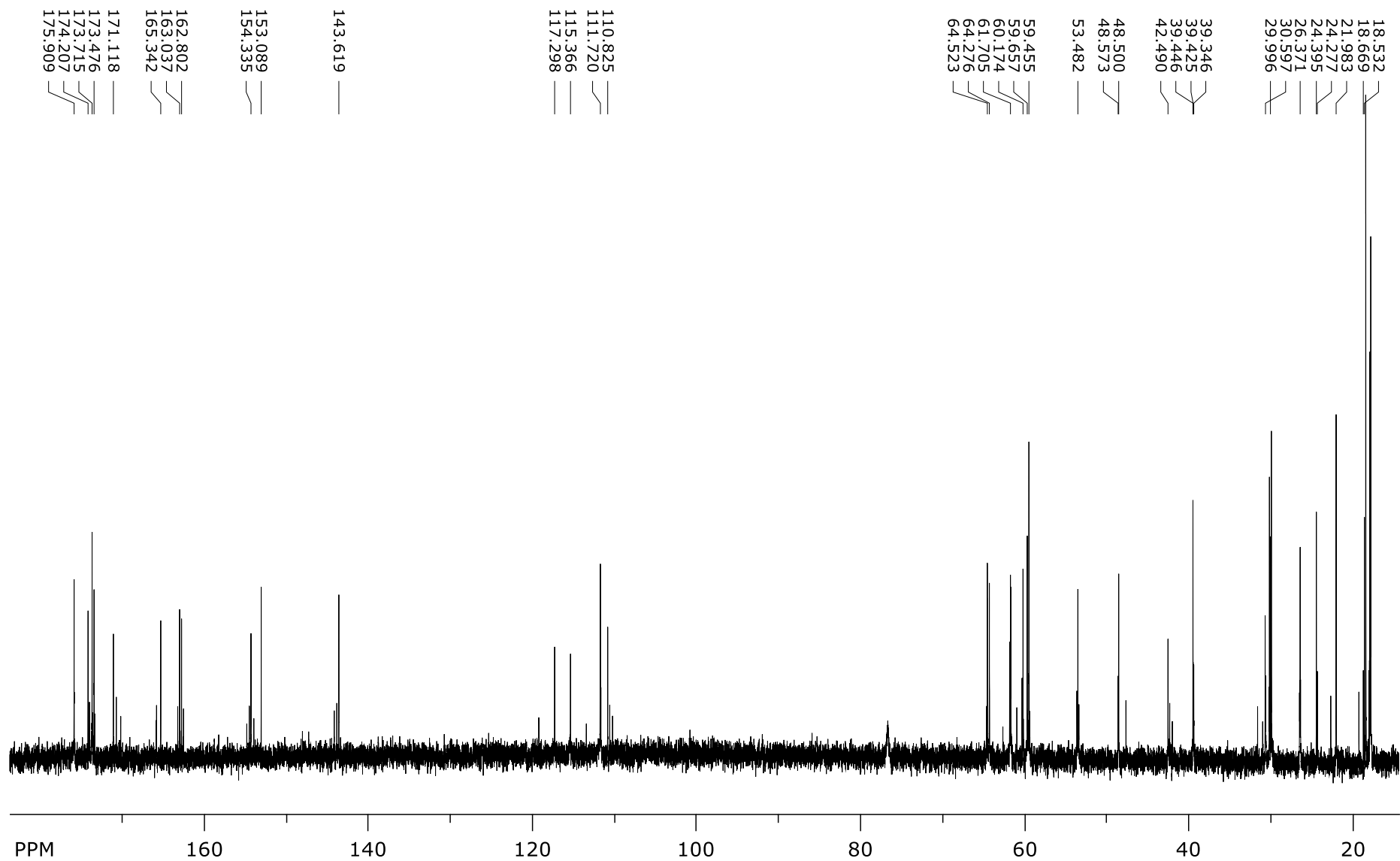
Figure SI 98. ^{13}C-NMR spectrum of **17**.
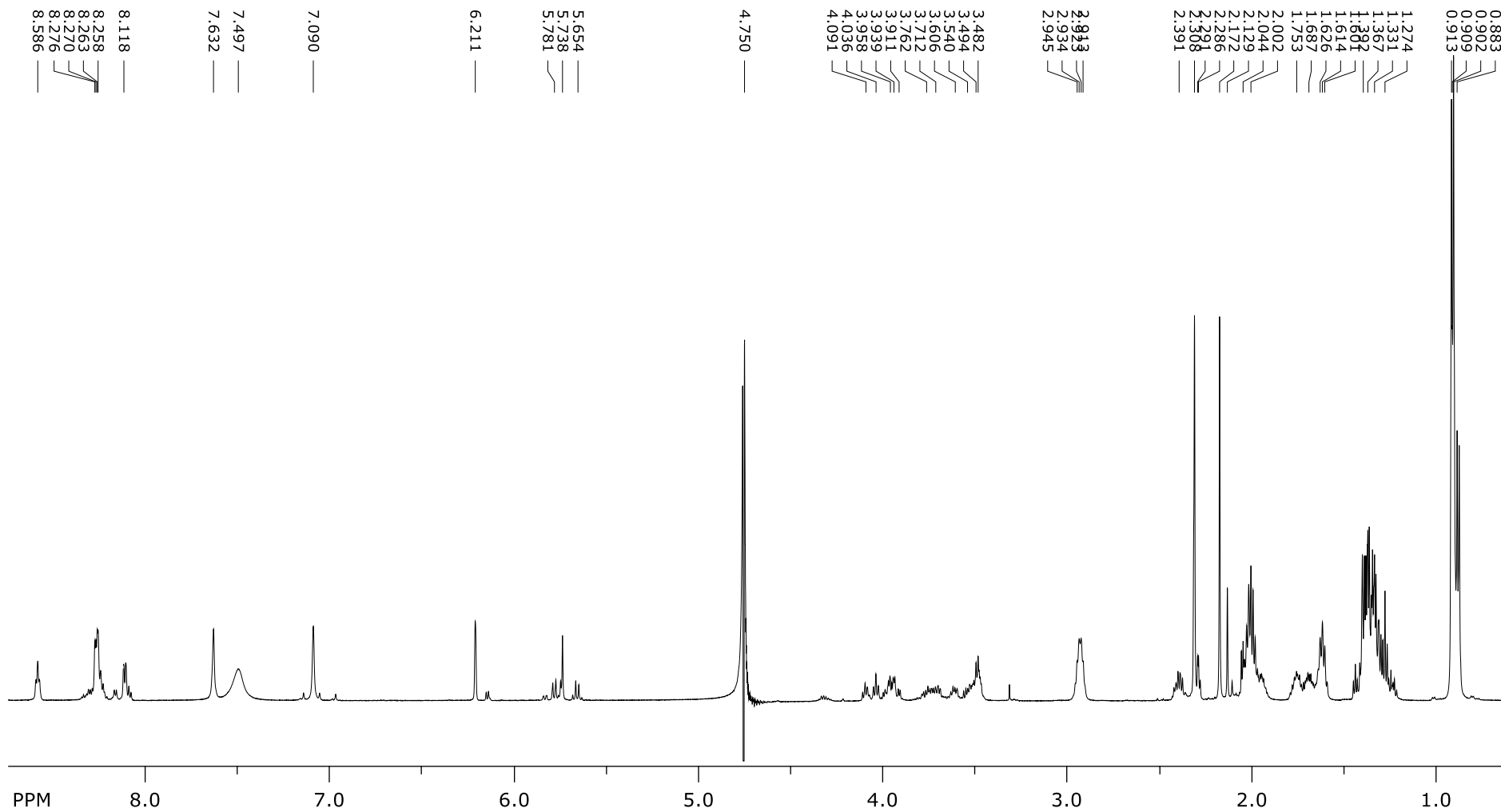
Figure SI 99. ^{1}H-NMR spectrum of **18**.
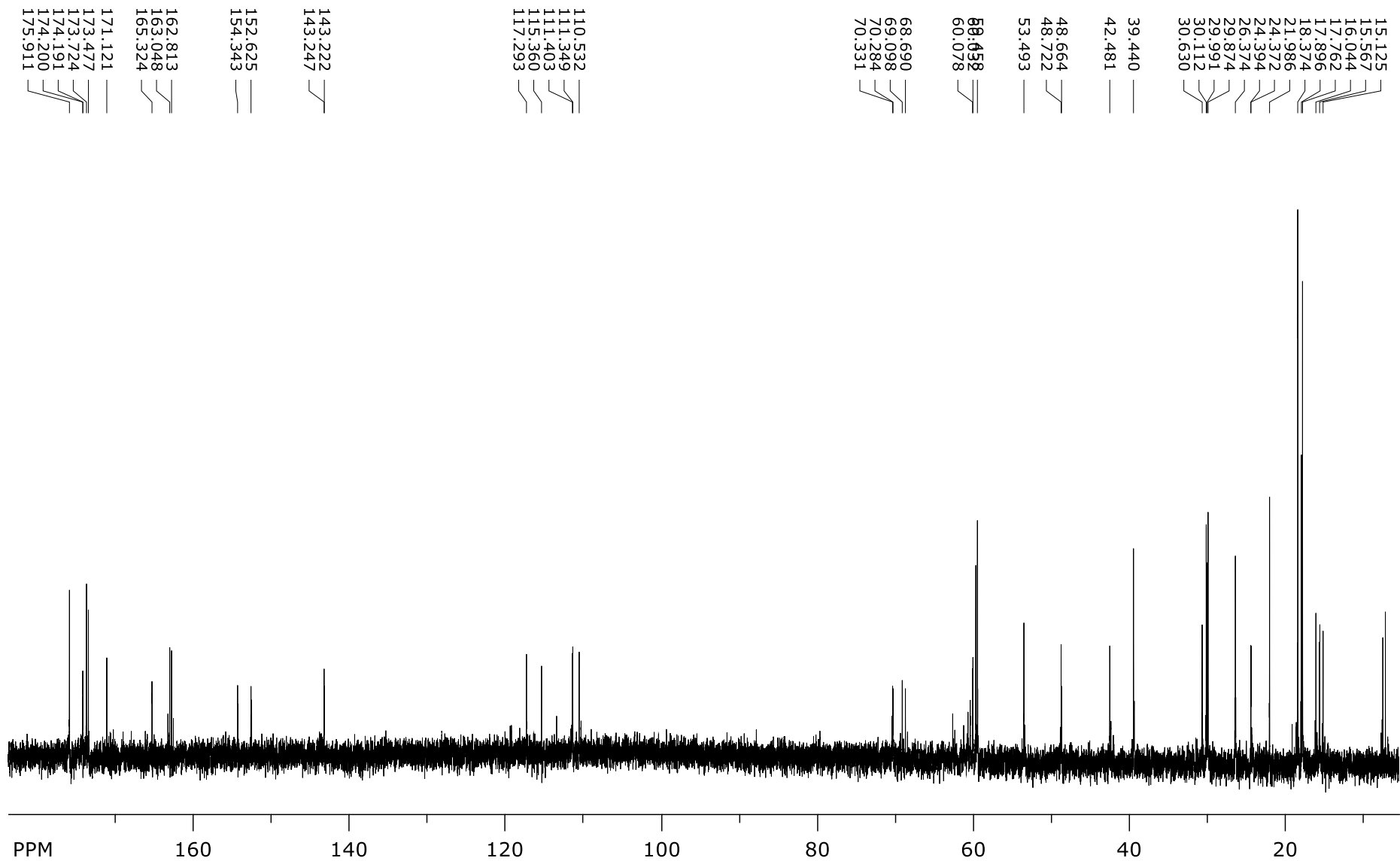
Figure SI 100. ^{13}C-NMR spectrum of **18**.
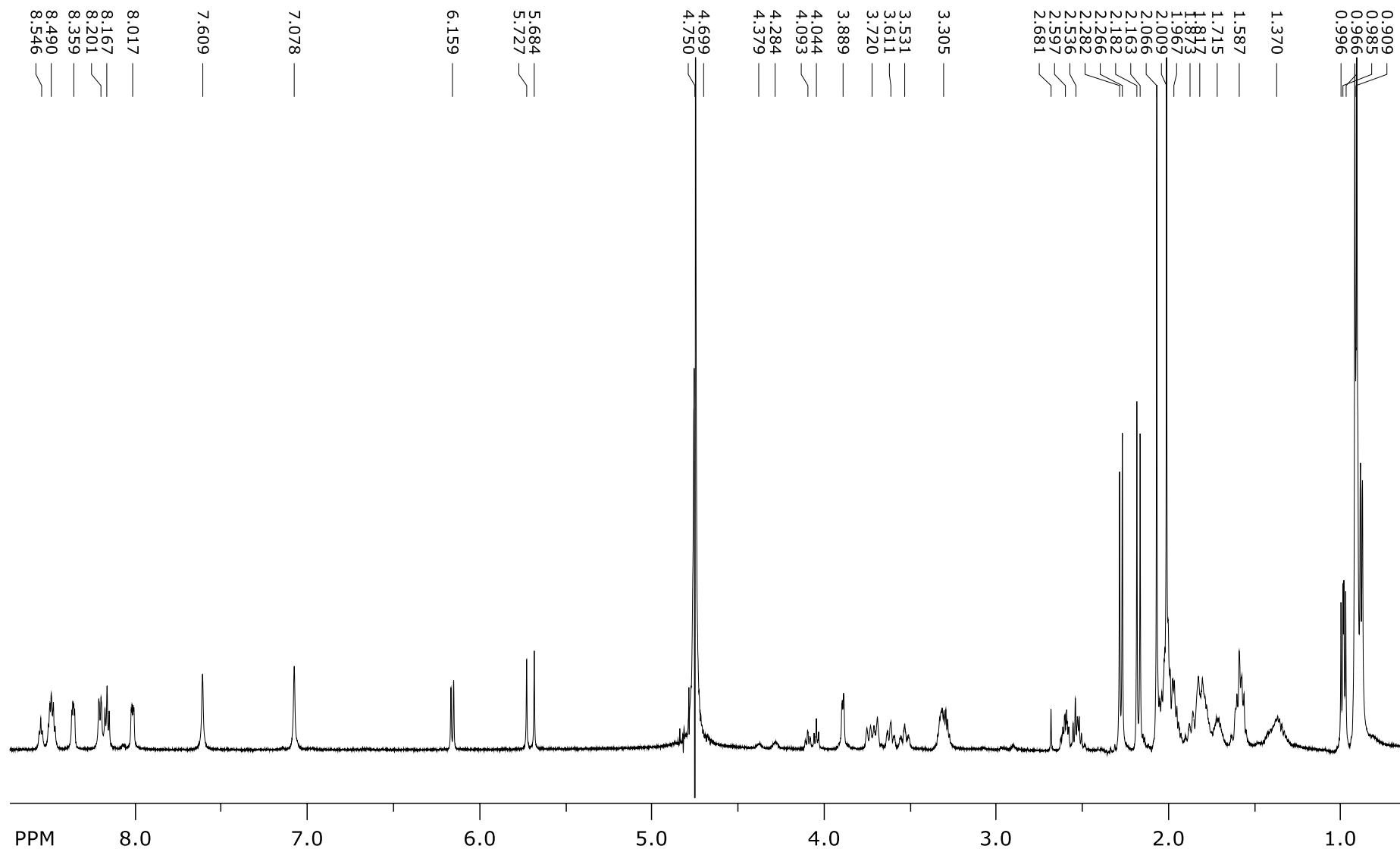
Figure SI 101. ^{1}H-NMR spectrum of **19**.
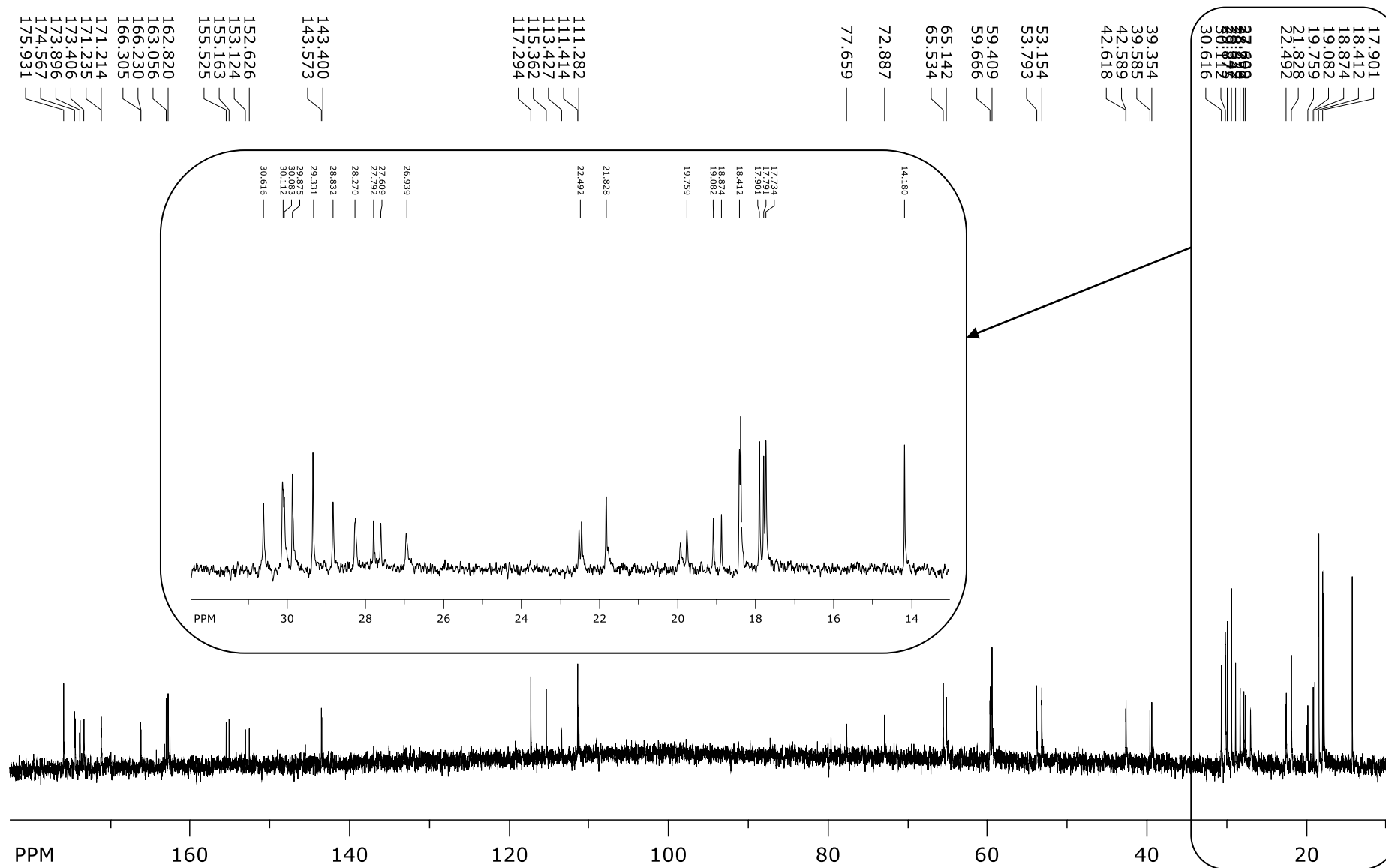
Figure SI 102. ^{13}C-NMR spectrum of **19**. Zoom on the fragment 15-32 ppm was added.
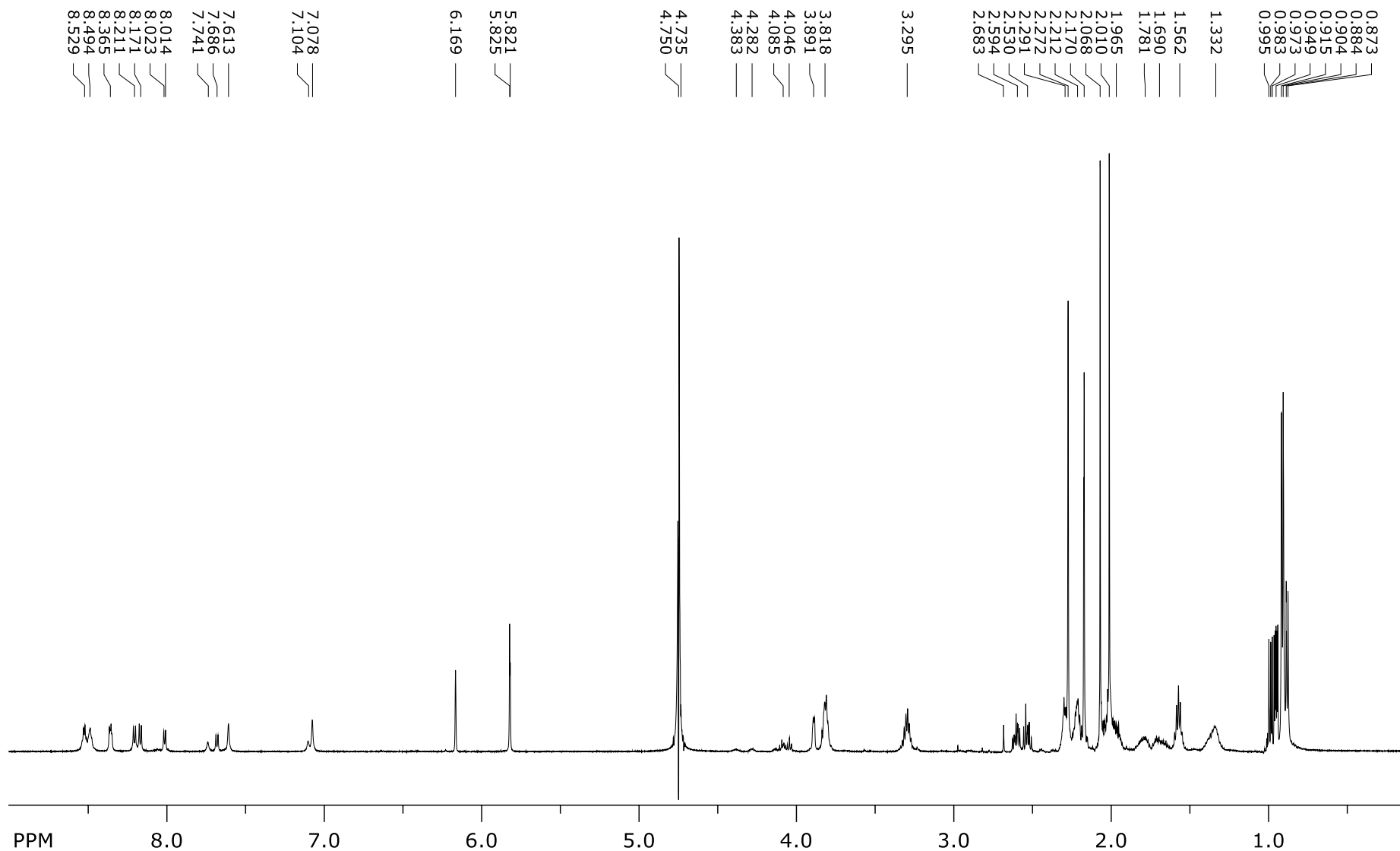
Figure SI 103. ^{1}H-NMR spectrum of **20**.
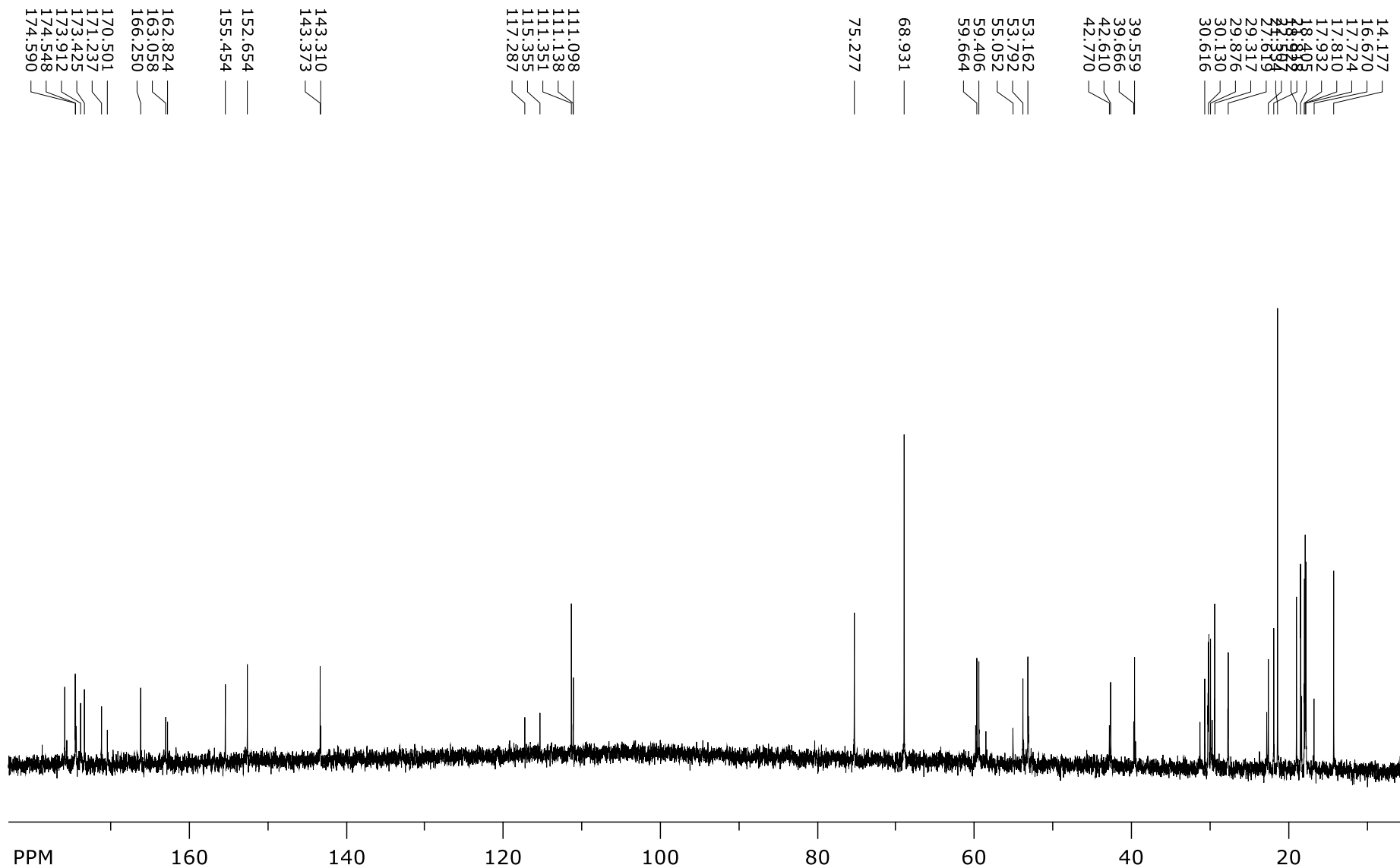
Figure SI 104. ^{13}C-NMR spectrum of **20**.
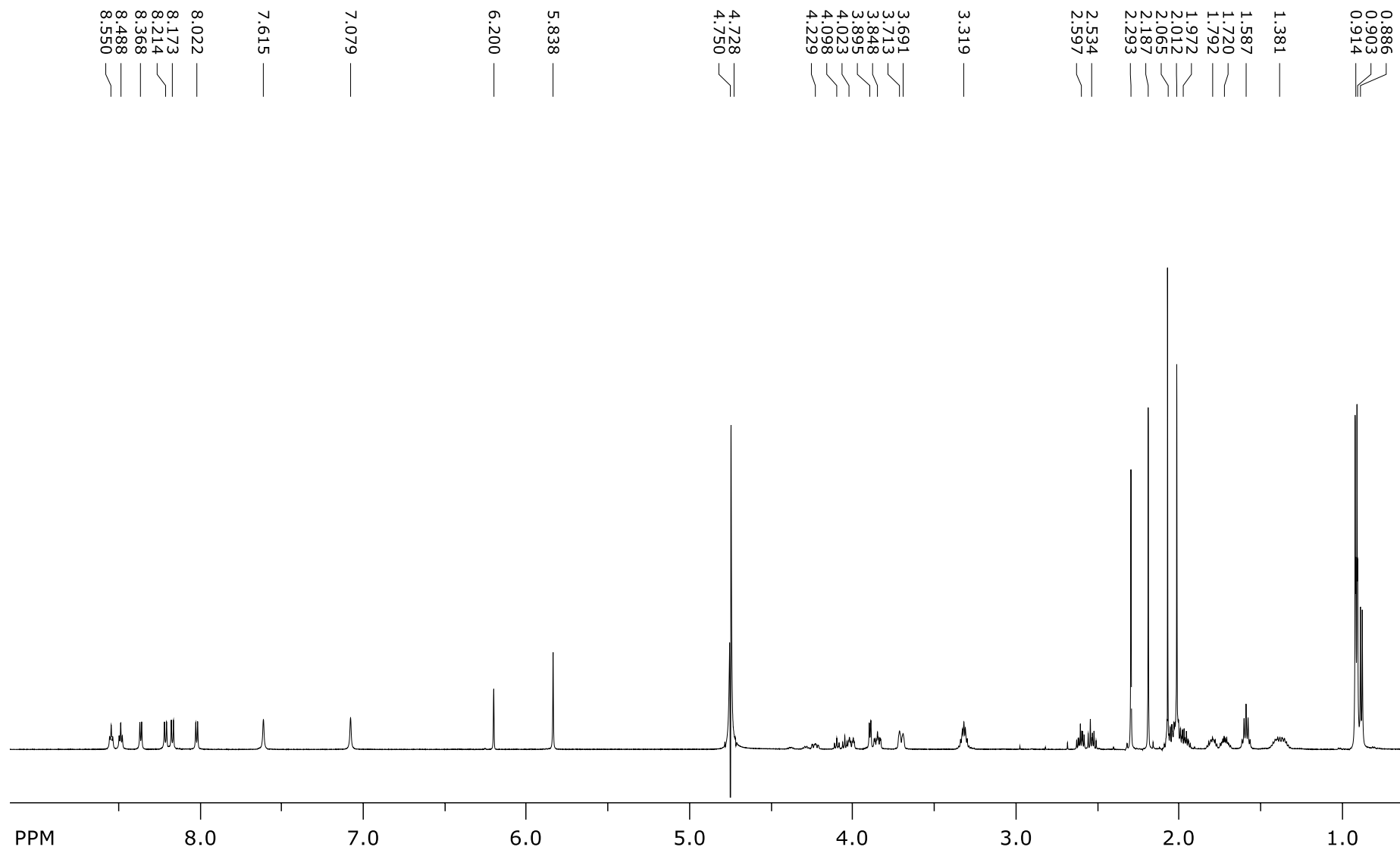
Figure SI 105. ^{1}H-NMR spectrum of **21.**
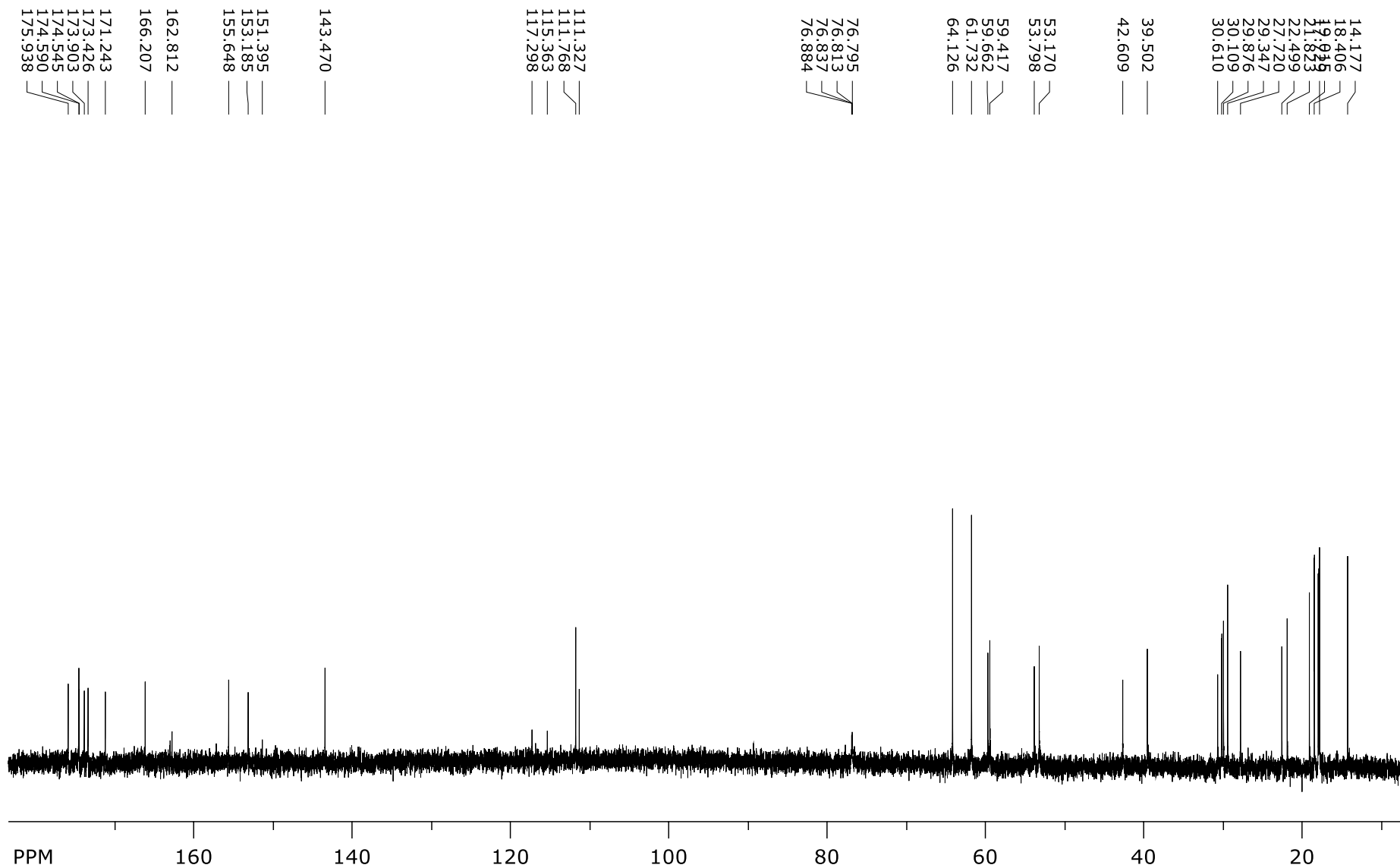
Figure SI 106. ^{13}C-NMR spectrum of **21**.
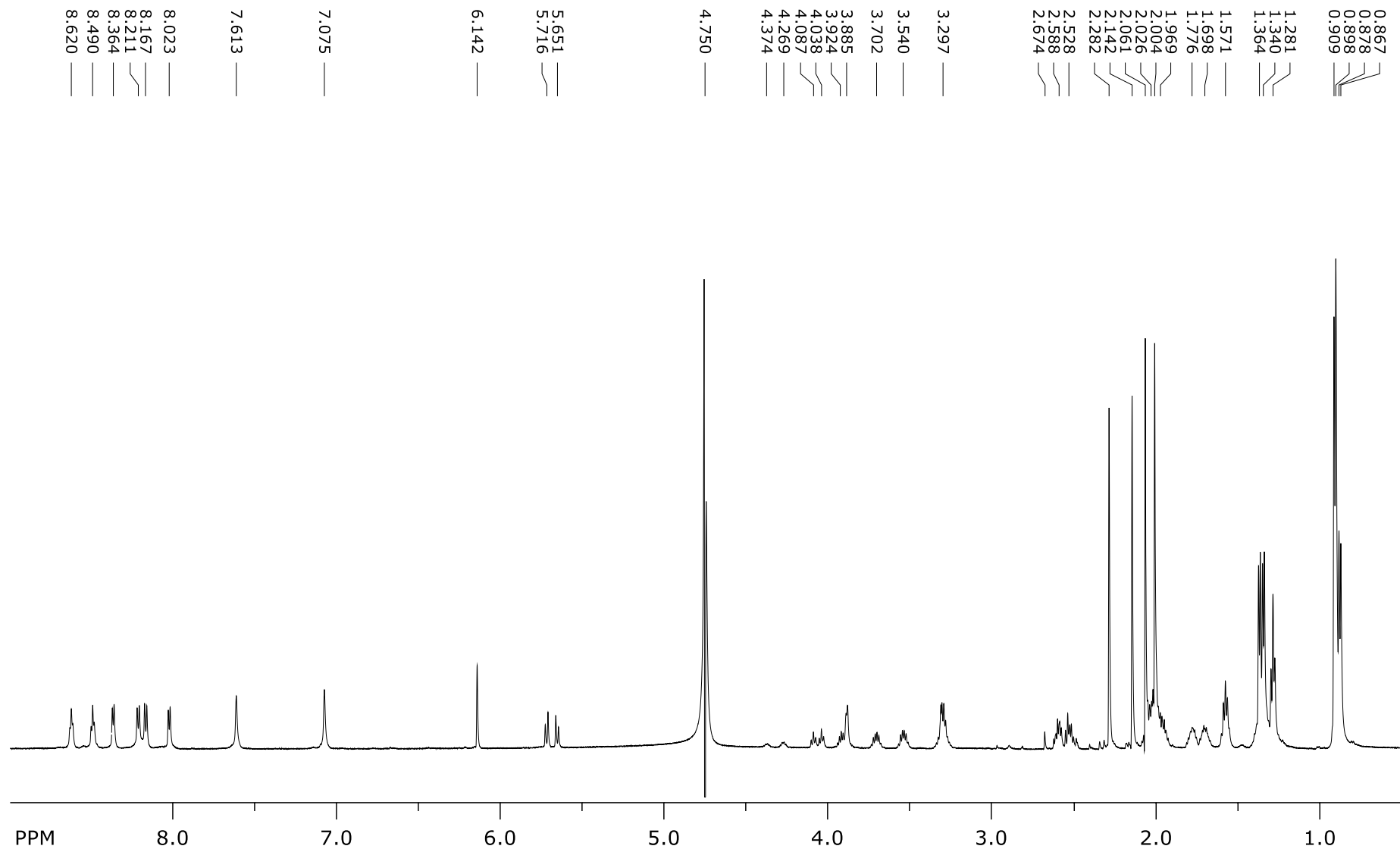
Figure SI 107. ^{1}H-NMR spectrum of **22**.
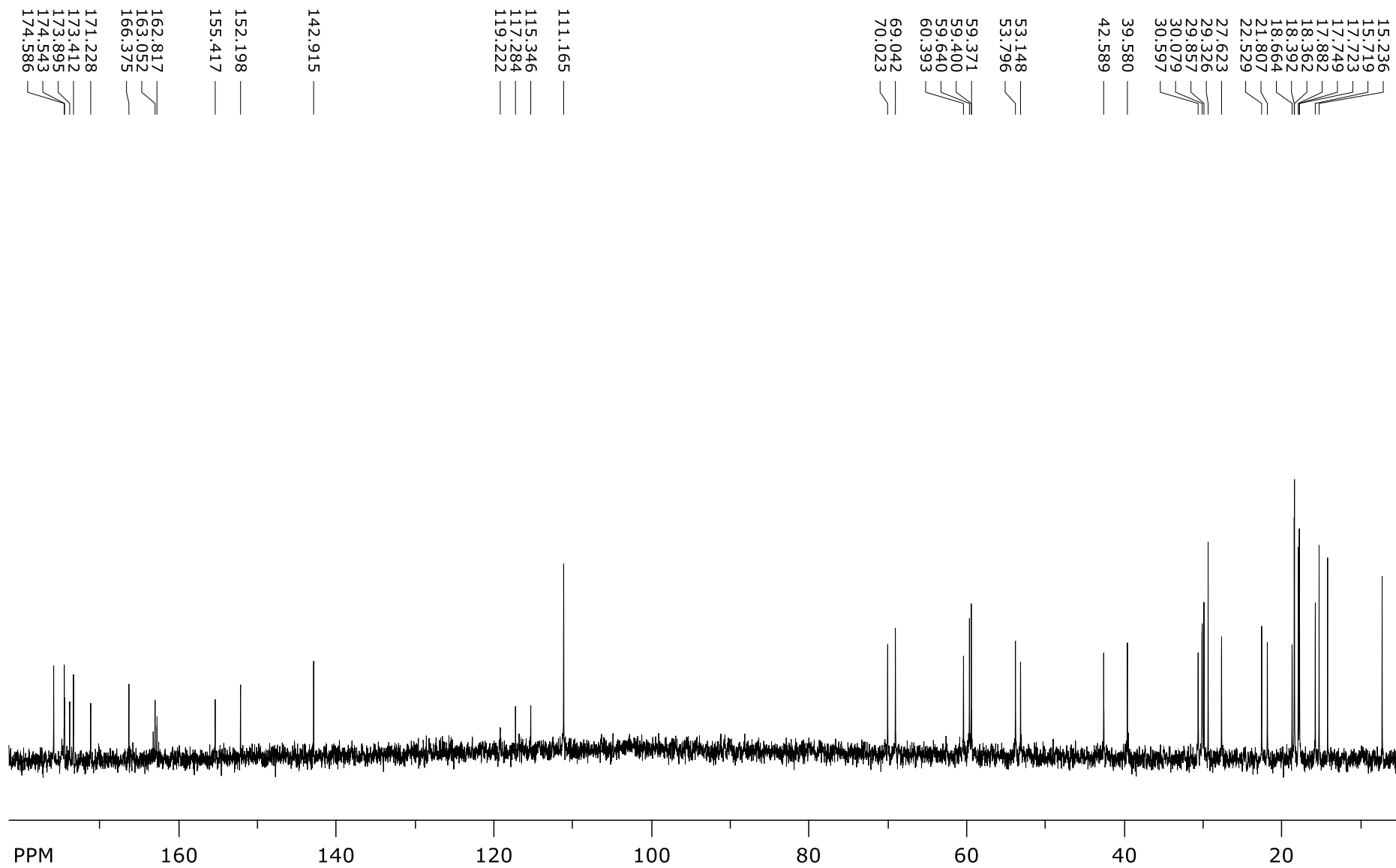
Figure SI 108. ^{13}C-NMR spectrum of **22**.
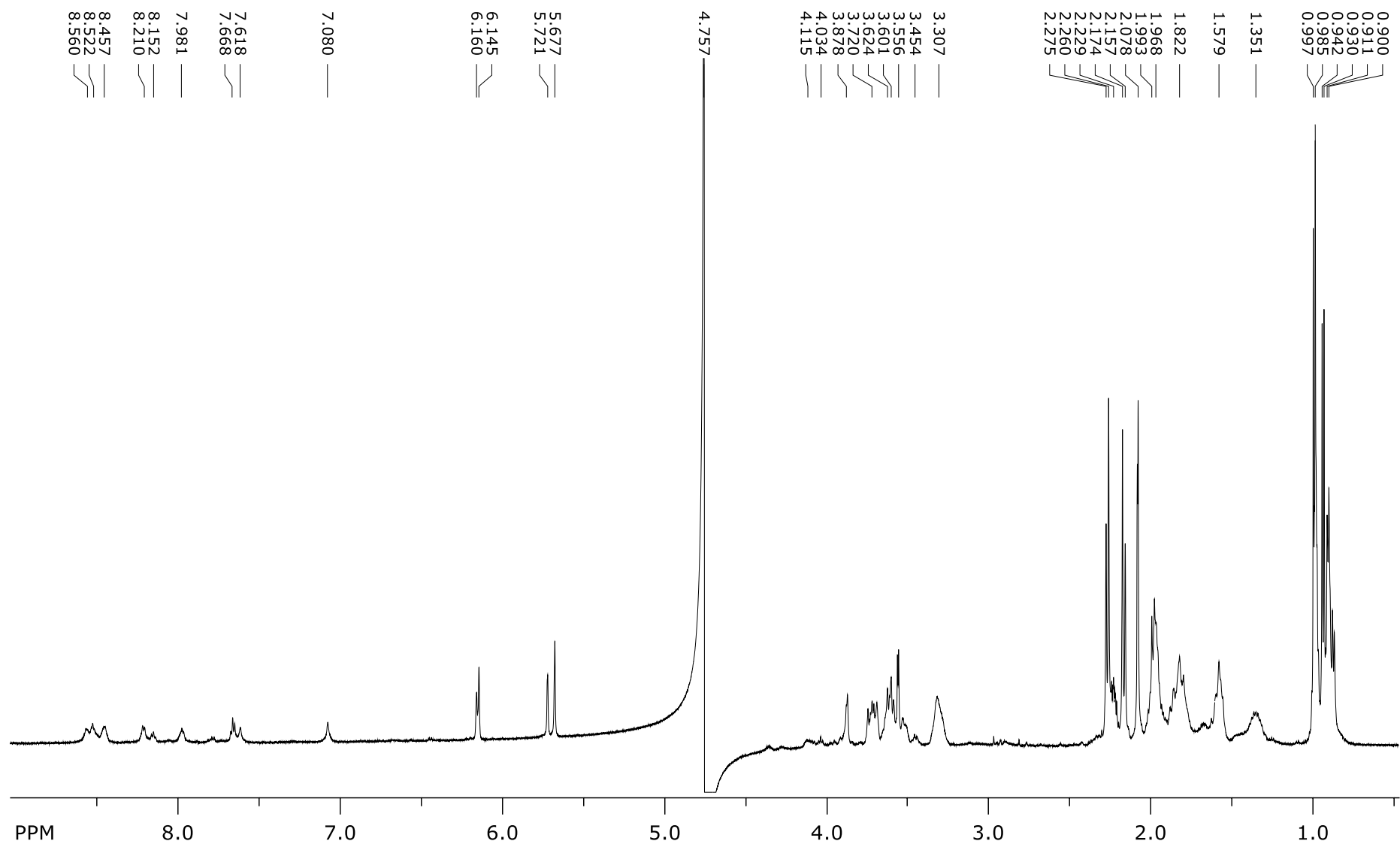
Figure SI 109. ^{1}H-NMR spectrum of **23**.
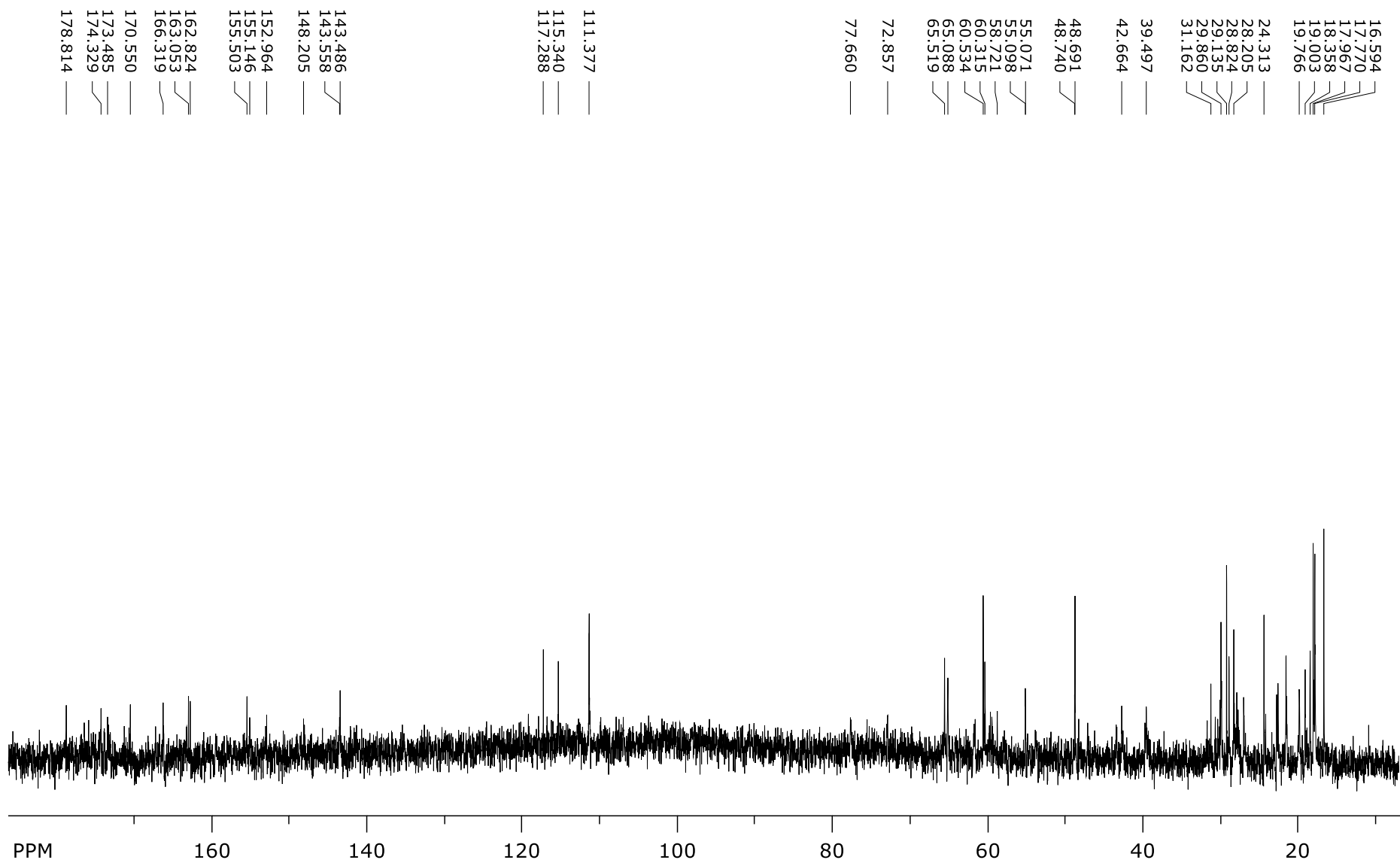
Figure SI 110. ^{13}C-NMR spectrum of **23**.
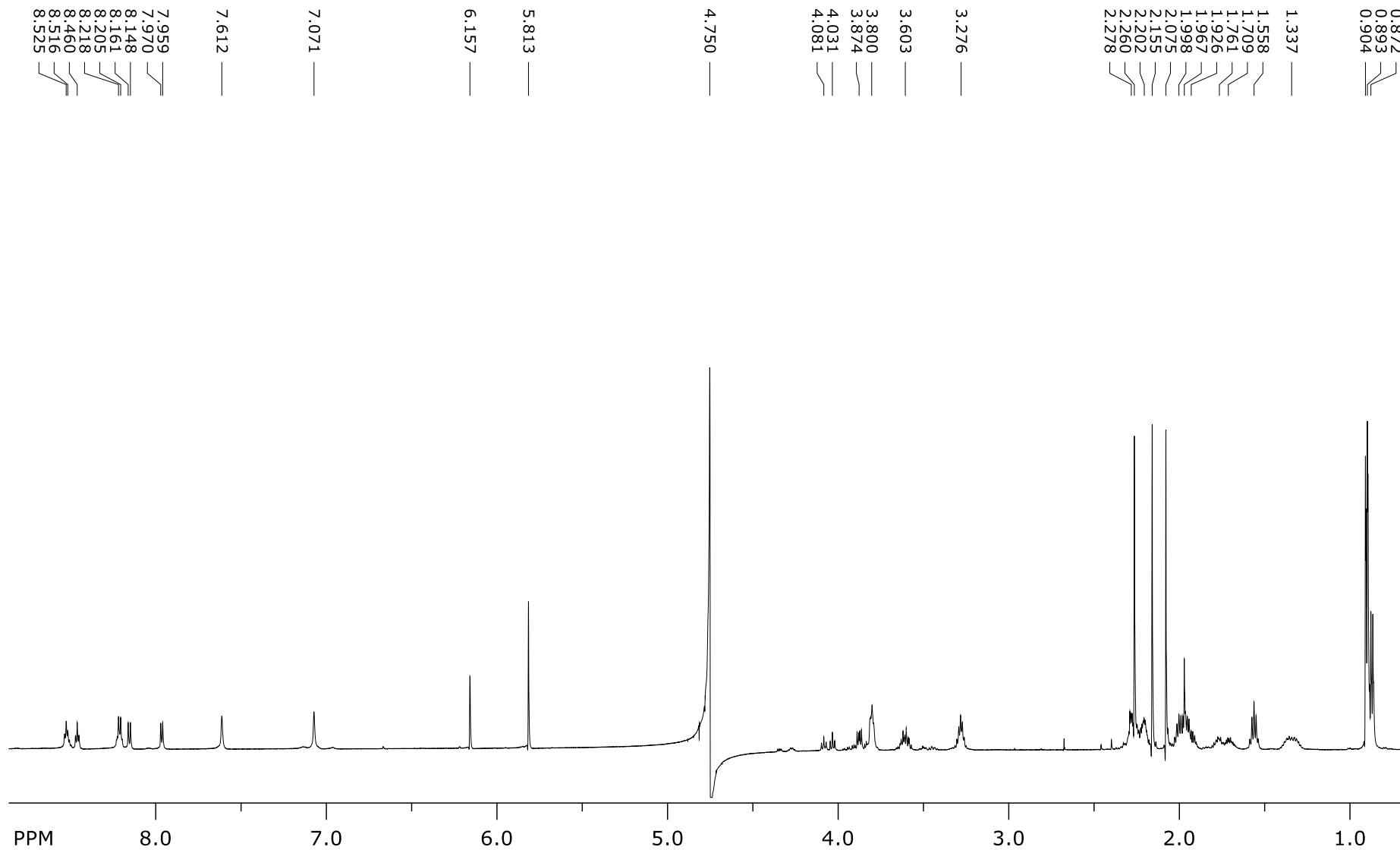
Figure SI 111. ^{1}H-NMR spectrum of **24**.
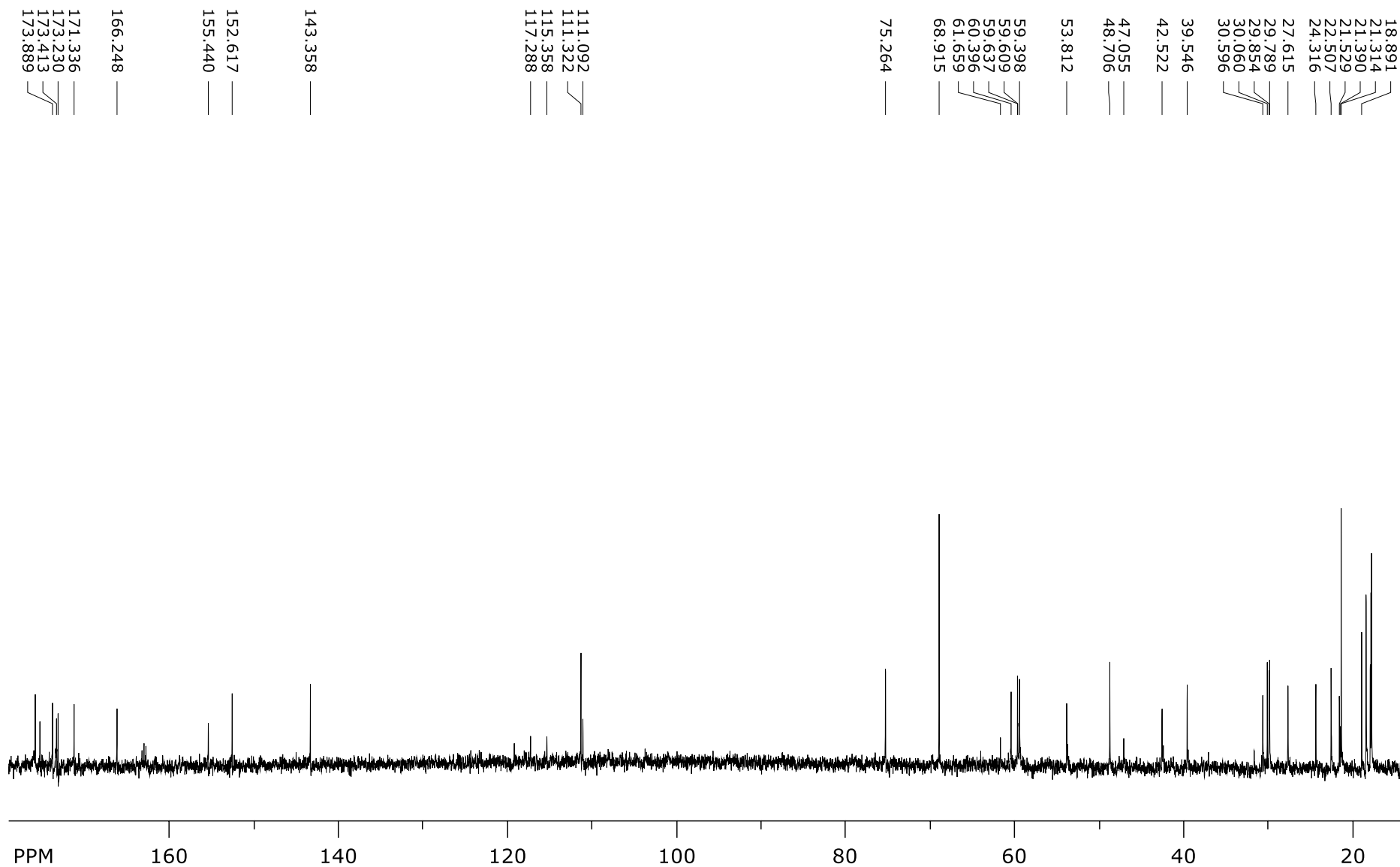
Figure SI 112. ^{13}C-NMR spectrum of **24**.
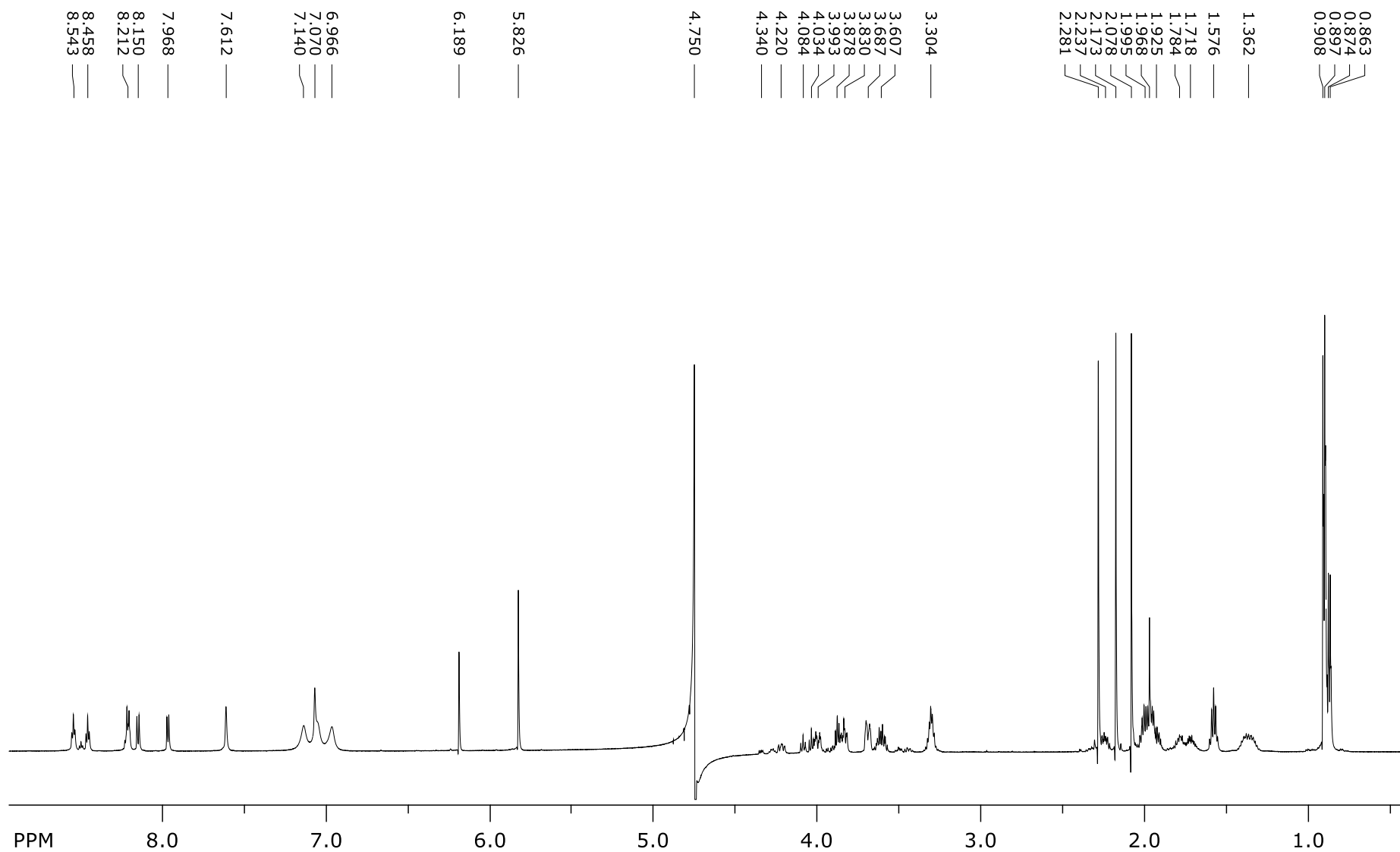
Figure SI 113. ^{1}H-NMR spectrum of **25**.
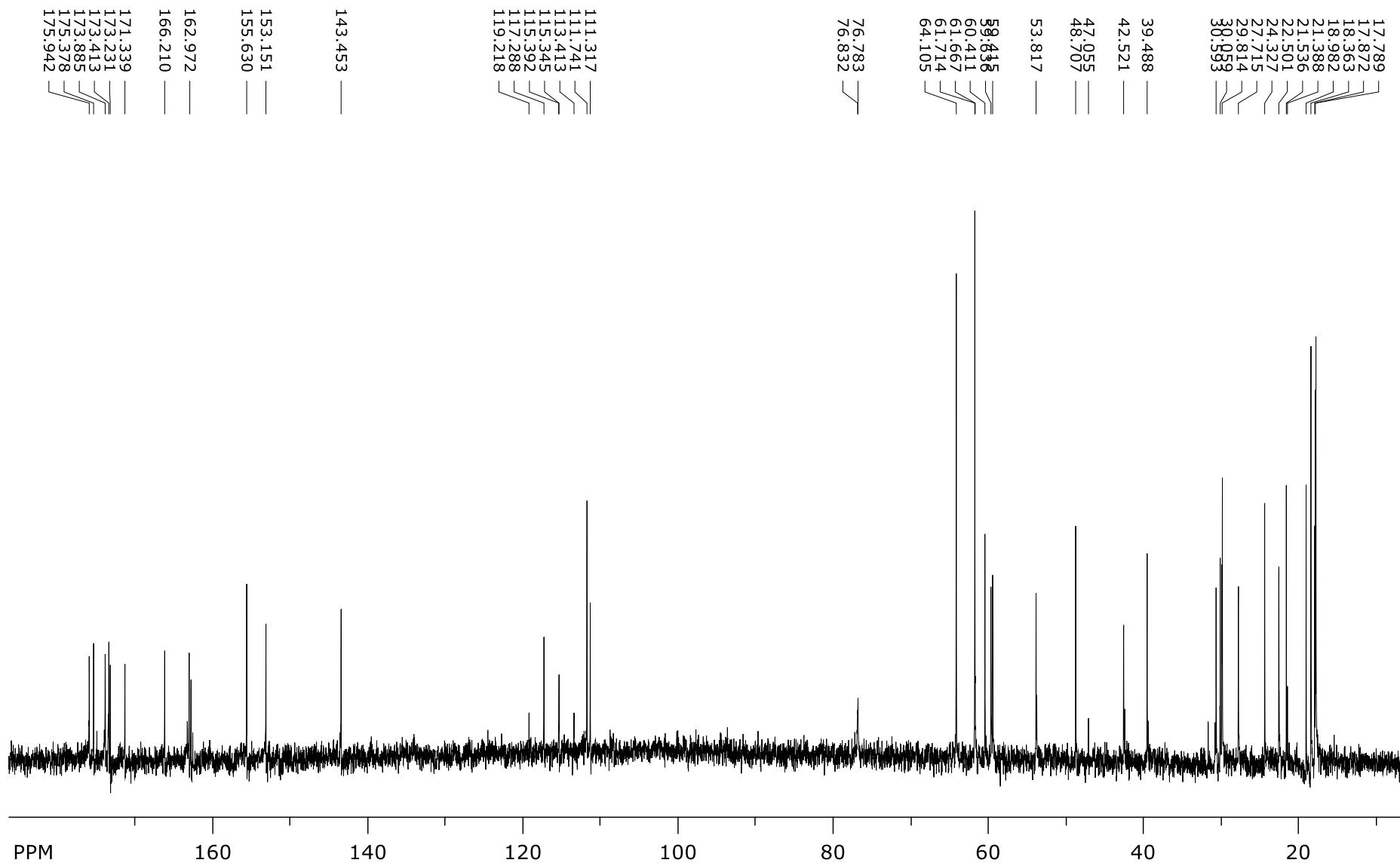
Figure SI 114. ^{13}C-NMR spectrum of **25**.
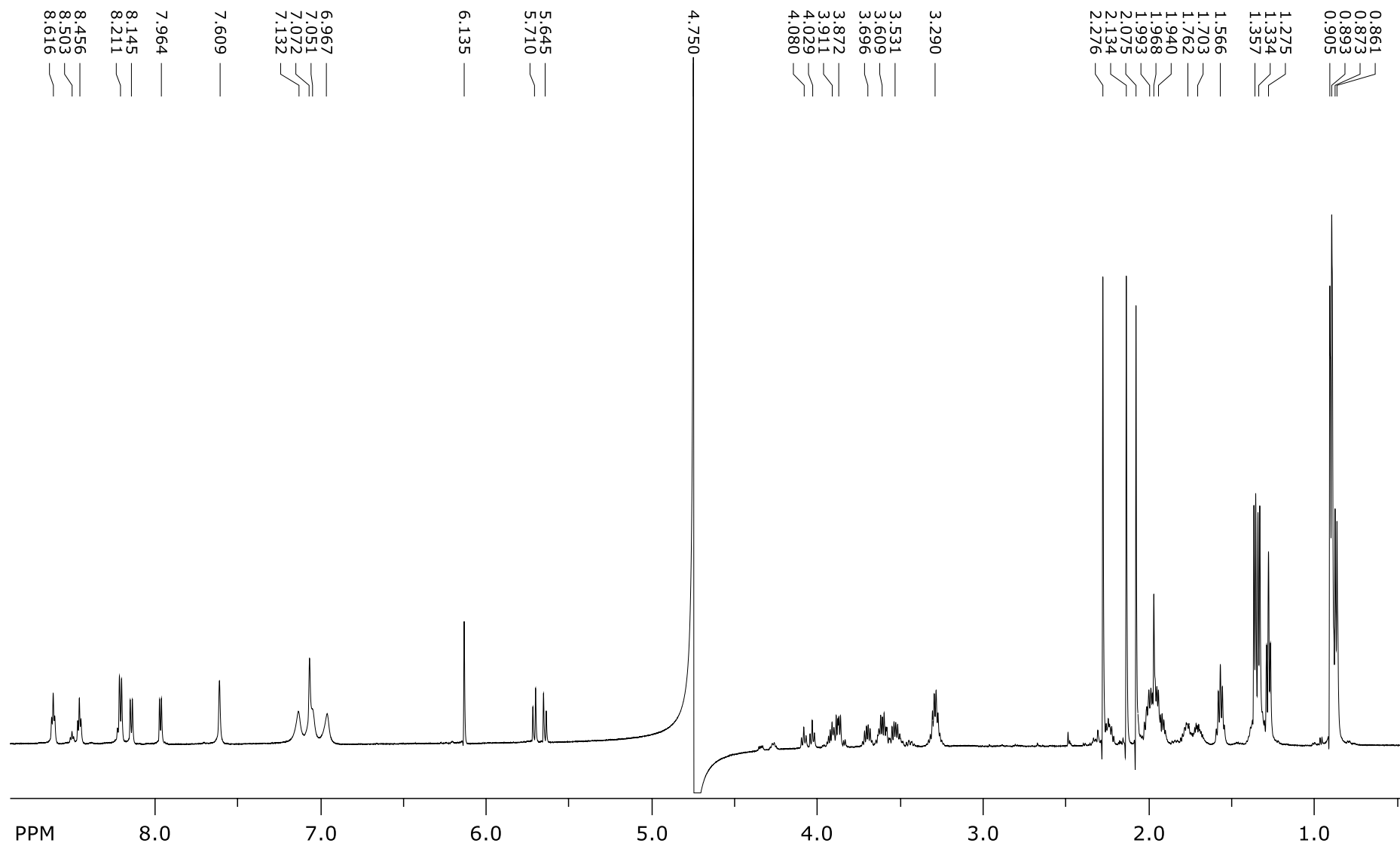
Figure SI 115. ^{1}H-NMR spectrum of **26**.
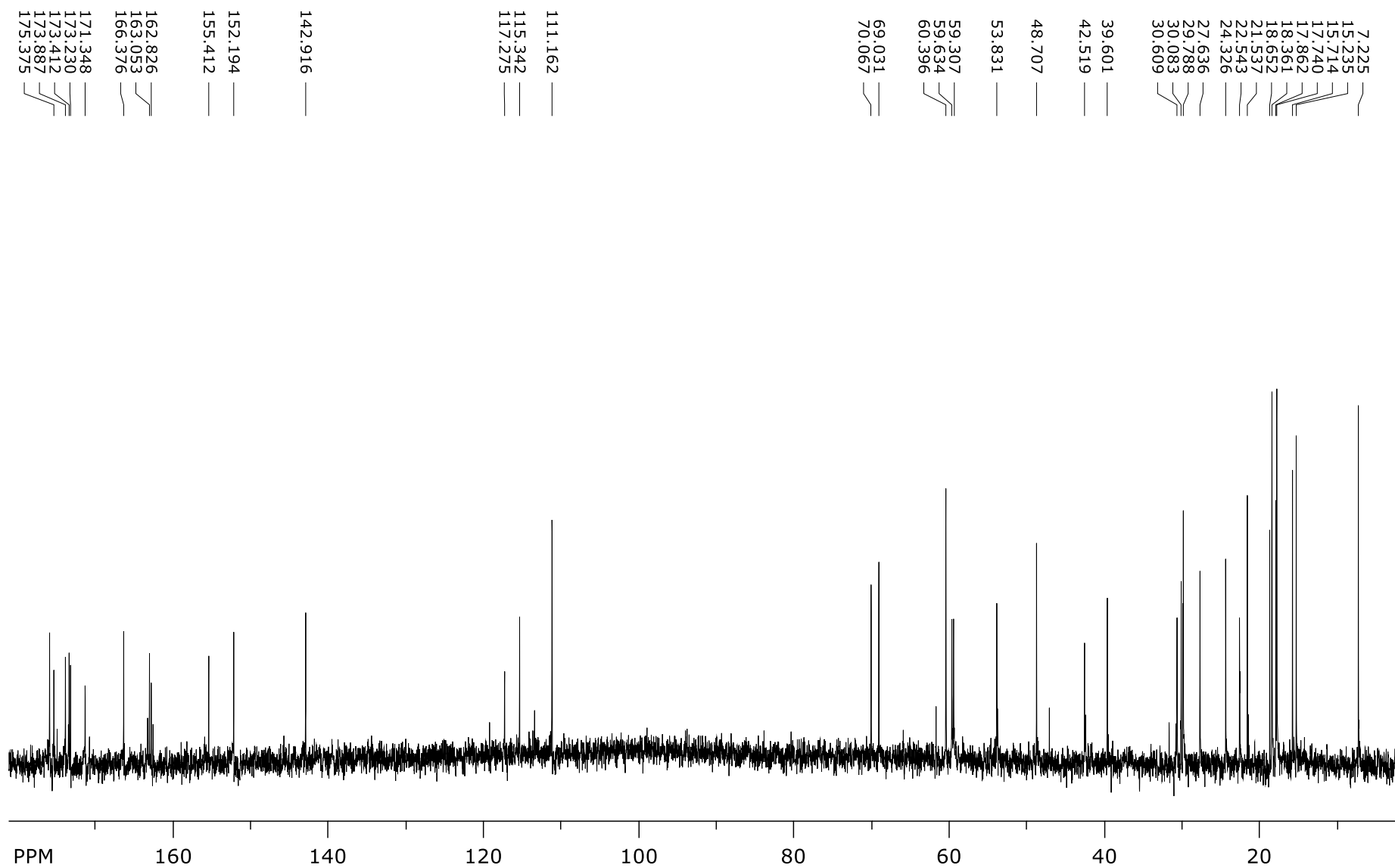
Figure SI 116. ^{13}C-NMR spectrum of **26**.